



Keele
University

This work is protected by copyright and other intellectual property rights and duplication or sale of all or part is not permitted, except that material may be duplicated by you for research, private study, criticism/review or educational purposes. Electronic or print copies are for your own personal, non-commercial use and shall not be passed to any other individual. No quotation may be published without proper acknowledgement. For any other use, or to quote extensively from the work, permission must be obtained from the copyright holder/s.

An *in vitro* study of the chondrogenic and immunomodulatory properties of mesenchymal stem cells from the osteoarthritic joint

John K Garcia

Submitted for the degree of Doctorate of Philosophy

June 2017

Keele University

Abstract

Osteoarthritis (OA) is a debilitating joint disease characterised by pain and progressive destruction of elements such as articular cartilage. Autologous chondrocyte implantation is a cellular therapy developed to regenerate damaged cartilage and delay or negate the need for a total joint replacement. The use of mesenchymal stem cells (MSCs) provides an alternative to harvesting healthy cartilage in order to obtain chondrocytes for transplantation. In this thesis, the chondrogenic and immunomodulatory properties of human bone marrow (BM-MSCs), infrapatellar fat pad (FP-MSCs), subcutaneous fat (SCF-MSCs) and synovial fluid (SF-MSCs) derived mesenchymal stem/stromal cells were characterised to determine their suitability for cartilage repair. Synovial inflammation and the prevalence of macrophage subsets were determined in the synovium and infrapatellar fat pad from patients with and without OA.

FP-MSCs and SF-MSCs from the same donor differed with regards to *in vitro* proliferation and their response to a proinflammatory stimulus. None of the MSC populations examined displayed levels of chondrogenic potency that were akin to their matched chondrocyte counterparts, although BM-MSCs and FP-MSCs did show a more enhanced ability to undergo chondrogenesis than SCF-MSCs and SF-MSCs. Additionally, the expression of certain surface markers commonly associated with chondrogenic potency in chondrocytes, such as CD44, were not indicative of the chondrogenic propensity of MSCs. Analyses of the phenotype of macrophages in human synovium and FP showed a co-existence of pro- (M1) and anti-inflammatory (M2) cells in both tissues. However, cell surface markers employed in the study did not permit a clear distinction between M1 and M2 cells. Image analyses revealed that the obesity related hypertrophy observed in adipocytes from subcutaneous fat,

does not occur in adipocytes in the FP. To conclude, the results presented in this thesis adds to current knowledge of joint derived stem cells and immune cells.

Contents

Abstract	ii
Contents	iv
List of Figures	viii
List of Tables	xi
Abbreviations	xiii
Dissemination	xviii
Acknowledgements	xx

Chapter 1: Introduction

1	Introduction.....	2
1.1	Articular Cartilage: Structure and Function.....	3
1.2	The Chondrocyte.....	6
1.3	The Extracellular Matrix.....	8
1.3.1	Collagens.....	8
1.3.2	Proteoglycans.....	10
1.3.3	Cell-Matrix Interactions and Mechanotransduction.....	14
1.4	Cartilage Development and Remodelling.....	14
1.5	Articular Cartilage Pathologies.....	17
1.5.1	Cartilage injury.....	17
1.5.2	Osteoarthritis (OA).....	19
1.5.3	Inflammation in OA.....	25
1.5.4	Risk factors in OA progression: age, gender, previous trauma obesity.....	31
1.6	General management of OA.....	33
1.7	Autologous Chondrocyte Implantation (ACI) for Cartilage Repair.....	35
1.7.1	Introduction to cell based therapies.....	35
1.7.2	History of ACI.....	36
1.7.3	Clinical outcomes of ACI.....	37
1.8	Optimisation of ACI.....	40
1.8.1	Cell-Matrix combinations.....	40
1.8.2	Alternative cell based strategies for cartilage repair and osteoarthritis.....	40
1.8.3	Combination of chondrocytes and stem cells.....	46
1.8.4	Hypoxic conditions for cell expansion.....	47

1.9	Aims of PhD Project	48
Chapter 2: Materials and Methods.....		50
2.1	Cell isolation, culture and maintenance techniques.....	51
2.1.1	Isolation of BM-MSCs	51
2.1.2	Isolation of MSCs from adipose tissues	53
2.1.3	Isolation of SF-MSCs	53
2.1.4	Isolation of chondrocytes.....	55
2.1.5	Passaging of cells in monolayer culture	55
2.1.6	Mycoplasma testing of cells	56
2.1.7	Cryopreservation and thawing of cells	57
2.2	Phenotyping of cells.....	58
2.2.1	Growth Kinetics.....	58
2.2.2	Trilineage Differentiation of MSCs.....	58
2.2.3	Cell surface marker detection by flow cytometry.....	66
2.2.4	Stimulation of MSCs with IFN- γ	71
2.2.4.1	Characterisation of co-stimulatory and Major Histocompatibility Complex class II markers after stimulation with IFN- γ	73
2.2.4.2	Detection of immunomodulatory markers.....	73
2.2.5	Differentiation of cells in hypoxic conditions	75
2.2.5.1	Measuring oxygen levels in culture medium.....	77
2.2.5.2	Differentiation of cells in hypoxia.....	77
2.3	Histology of the infrapatellar fat pad and synovium.....	78
2.3.1	Tissue fixation and wax embedding	78
2.3.2	Sectioning of tissues	79
2.3.3	Haematoxylin and Eosin staining	79
2.4	RNA extraction and quantitative real-time polymerase chain reaction (RT-qPCR).80	
2.4.1	Extraction of mRNA from cells.....	80
2.4.2	Generation of cDNA from mRNA.....	81
2.4.3	Assessing gene expression via RT-qPCR.....	81
2.5	Characterisation of macrophages in synovium and fat pad: <i>in situ</i> and freshly isolated	85
2.5.1	Immunohistochemical characterisation of macrophages in the synovium and infrapatellar fat pad	85
2.5.2	Ranking the positivity of macrophage markers in stained tissues.....	88

2.5.3	Synovitis score.....	90
2.5.4	Stimulation of fat pad explants with Triamcinolone acetonide (TA).....	90
2.5.5	Extraction of the macrophages from synovium and fat pad tissues or explants.....	92
2.5.6	Evaluation of macrophage phenotype by flow cytometry.....	92
2.5.7	Measuring the size of adipocytes in adipose tissues.....	94
2.6	Statistical analysis.....	97
Chapter 3: Results.		98
3.1	Introduction and aim.....	99
3.2	Experimental design.....	100
3.3	Results.....	101
3.3.1	Macroscopic and histological features of the FP.....	101
3.3.2	Cell morphology and Growth kinetics.....	104
3.3.3	MSC immunoprofile.....	108
3.3.4	Multipotency.....	110
3.3.5	Immunogenic and immunomodulatory properties of FP- and SF-MSCs in a pro-inflammatory environment.....	112
3.4	Discussion.....	115
3.5	Conclusion.....	120
Chapter 4: Results.		122
4.1	Introduction and aim.....	123
4.2	Experimental design-1.....	124
4.3	Experimental design-2.....	126
4.4	Results: Comparing the chondrogenic induction of donor matched chondrocytes and MSCs.....	129
4.4.1	Measurement of oxygen levels in culture media.....	129
4.4.2	Comparison of the formation of chondrogenic pellets in hypoxia and normoxia.....	129
4.4.3	Immunoprofiling of cells for MSC and chondrogenic markers.....	132
4.4.4	Gene expression prior to chondrogenic differentiation.....	136
4.4.5	Assessment of GAG production and pellet sizes after chondrogenic differentiation.....	139
4.4.6	Association between surface markers or gene expression and GAG production.....	144
4.5	Results: Predictive analysis of the chondrogenic potential of SF-MSCs.....	146

4.5.1	Immunoprofiling SF-MSCs for MSC and chondropotency markers	146
4.5.2	Expression of chondrogenic and hypertrophic genes in SF-MSCs	146
4.5.3	Assessment of GAG production in SF-MSCs after chondrogenic differentiation	148
4.5.4	Correlation between surface markers, gene expression and donor demographics compared to the production of GAG/DNA and histological outcome after chondrogenic differentiation.....	150
4.6	Discussion	153
4.7	Conclusion	160
Chapter 5: Result.....		163
5.1	Introduction and aim	164
5.2	Experimental design-1	165
5.3	Experimental design-2	165
5.4	Results: Characterisation of macrophages from synovium and FP	168
5.4.1	General histological features of synovium and FP	168
5.4.2	Immunohistochemical characterisation of macrophages in synovium, sub- synovial stroma and FP	171
5.4.3	Correlation between synovitis score and macrophage score	179
5.4.4	Flow cytometric assessment of macrophages from matched synovium and FP	181
5.4.5	The influence of anti-inflammatory stimuli on the polarisation of macrophages from FP explant cultures	186
5.4.6	Association between donor BMI and adipocyte size.....	189
5.5	Discussion	192
5.6	Conclusion	200
Chapter 6: General Discussion.....		202
6.1	General Discussion	203
6.2	Conclusions and future work	207

List of Figures

Figure 1.1: Schematic representation of the morphology and spatial distribution of chondrocytes in articular cartilage.	5
Figure 1.2: Illustration of the progressive assembly of collagen fibres.	9
Figure 1.3: Schematic of the tetrasaccharide and poly-N-acetyllactosamine bond that exists between core proteins.	11
Figure 1.4: Illustration of the aggrecan "bottlebrush" structure.	12
Figure 1.5: Histological observation of cartilage fibrillation and chondrocyte clusters.	21
Figure 1.6: Immunohistochemical representation of normal human synovium.	28
Figure 1.7: Illustration of the isolation and multiple cell lineages into which MSCs have been shown to differentiate.	42
Figure 2.1: Isolation of mononuclear cells from bone marrow.	52
Figure 2.2: Representative images of synovium and FP tissues from an end-stage OA donor.	54
Figure 2.3: Distribution of fluorochrome conjugated antibodies (Abs) in tubes for flow cytometry.	70
Figure 2.4: Example of flow cytometry analysis to determine the positivity of a surface marker.	72
Figure 2.5: HypoxyCOOL™ and Sci-tive.	76
Figure 2.6: Example of a PCR amplification plot.	84
Figure 2.7: Illustration of the different regions that were ranked for each macrophage marker following immunohistochemistry.	89

Figure 2.8: Examples of flow cytometry analyses to determine double positivity of M1 and M2 markers on macrophages.	95
Figure 2.9: Identification of adipocytes using the Adiposoft plugin in Fiji.....	96
Figure 3.1: Histology of a FP.....	103
Figure 3.2: Microscopic photographs of FP- and SF-MSCs.....	105
Figure 3.3: Growth kinetics for FP- and SF-MSCs..	106
Figure 3.4: MSC immunoprofile of FP and SF-MSCs (flow cytometry)	109
Figure 3.5: Trilineage differentiation of FP and SF-MSCs.	111
Figure 3.6: Immunogenic properties of FP and SF-MSCs after stimulation with IFN- γ ...	113
Figure 3.7: Immunomodulatory properties of FP and SF-MSCs after stimulation with IFN- γ	114
Figure 4.1: Workflow of experiments to compare the chondrogenic potential of donor matched chondrocytes and MSCs.	127
Figure 4.2: Measurement of oxygen levels in culture media in various conditions.	130
Figure 4.3: Pellets formed in hypoxic and normoxic conditions	131
Figure 4.4: Immunoprofiles for putative chondrogenic potency markers on culture expanded cells prior to chondrogenic induction	135
Figure 4.5: The expression of chondrogenic and hypertrophic genes in monolayer cell populations prior to chondrogenic induction	137
Figure 4.6: Assessments of chondrogenic differentiation in pellet cultures for individual donor	142
Figure 4.7: Chondrogenic assessments of pellet cultures across cell types for all donors combined	143

Figure 4.8: The production of GAG by SF-MSCs.....	149
Figure 5.1: General observations of synovium and FP from H&E stain	169
Figure 5.2: Assessment of synovitis	170
Figure 5.3: Immunohistochemical analysis of CD68 in normal and representative OA synovium and FP.....	173
Figure 5.4: Immunohistochemical analysis of CD86 in normal and representative OA synovium and FP.....	174
Figure 5.5: Immunohistochemical analysis of CD11c in normal and representative OA synovium and FP.....	175
Figure 5.6: Immunohistochemical analysis of Arginase-1 (Arg-1) in normal and representative OA synovium and FP.....	176
Figure 5.7: Immunohistochemical analysis of CD206 in normal and representative OA synovium and FP.....	177
Figure 5.8: Spearman’s rank correlation analysis of macrophage staining between tissue layers	178
Figure 5.9: Immunopositivity of macrophage markers in cells from donor matched synovium and FP.....	182
Figure 5.10: Flow cytometry analysis of the co-positivity of M1 and M2 markers	185
Figure 5.11: The effect of triamcinolone on explant cultured macrophages from the FP .	187
Figure 5.12: Scatter plots illustrating the influence of triamcinolone (72 hours treatment) on the co-expression of CD86 and CD163 markers on macrophages from FP explant cultures.	188
Figure 5.13: Representative images of H&E stained cryosections of adipose tissue derived from the FP and SCF of non-obese and obese donors.....	190
Figure 5.14: Relationship between BMI and adipocyte size.	191

List of Tables

Table 1.1: Classification of cartilage injury according to the International Cartilage Research Society.....	18
Table 2.1: Modified Bern Score used to assess chondrogenic pellets stained with toluidine blue.....	63
Table 2.2: Fluorochrome-conjugated antibodies used to identify MSC and chondrogenic potency surface markers.	69
Table 2.3: Primers used for qRT-PCR.....	82
Table 2.4: Markers used in immunohistochemistry to identify macrophages in synovium and FP.....	87
Table 2.5: Criteria for the grading of synovitis.....	91
Table 2.6: Panel of surface markers used to investigate macrophage polarisation via multicolour flow cytometry.....	93
Table 3.1: Demographics of donors from which samples were sourced.....	102
Table 3.2: Results of the Multilevel modelling of the influence of cell source, passage number and donor on doubling time of matched FP- and SF-MSCs.	Error! Bookmark not defined.
Table 4.1: Demographics of patients used in experimental design 1.....	125
Table 4.2: Demographics of patients used in experimental design 2.....	128
Table 4.3: Immunoprofiles for MSC markers on cell culture expanded cells prior to chondrogenic differentiation.....	133
Table 4.4: Pearson's correlation analysis matrix comparing genes which may be predictive of chondrogenic potential. Significant values are highlighted.	138
Table 4.5: Multilevel modelling of how gene expression and surface markers relate to chondrogenic outcome.....	145

Table 4.6: The immunoprofile of SF-MSCs for surface markers prior to chondrogenic differentiation.	147
Table 4.7: The expression of chondrogenic genes relative to reference genes prior to chondrogenic differentiation by SF-MSCs.....	147
Table 4.8: Correlation between the positivity of surface markers before chondrogenic induction with the production of GAG and histological score after chondrogenic differentiation of SF-MSCs.	152
Table 5.1: Demographics of donors used in the immunohistochemical characterisation of macrophages in synovium and FP.....	166
Table 5.2: Demographic information and categorisation for obese and non-obese donors	167
Table 5.3: Spearman’s correlation analysis of the association between the synovitis score and macrophage rank in the synovium, stroma and FP	180
Table 5. 4: Comparison of M1 and M2 markers in CD14 positive macrophages from matched synovium and FP	183

Abbreviations

α ROR2	alpha receptor tyrosine kinase like orphan receptor 2
ACI	Autologous Chondrocyte Implantation
ADAMTS	Aggrecanases or disintegrin and metalloproteinases with thrombospondin motifs
ADAMTS4	Aggrecanases or disintegrin and metalloproteinases with thrombospondin motifs 4
ADAMTS5	Aggrecanases or disintegrin and metalloproteinases with thrombospondin motifs 5
AGES	Advanced glycation end products
ASCs	Adipose Derived Mesenchymal Stem Cells
B2M	Beta-2 Microglobulin
BCA	Bicinchoninic acid
BCL-2	B cell lymphoma-2
BM-MSCs	Bone Marrow- Mesenchymal Stem Cells
BMI	Body Mass Index
BSA	Bovine Serum Albumin
BV421	Brilliant Violet 421
cDNA	Complementary DNA
COMP	Cartilage Oligomeric Matrix Protein
CS	Chondroitin sulphate
DAMPs	Damage Associated Molecular Patterns
DMEM/F12	Dulbecco's Modified Eagle's Medium/F-12
DMMB	1,9-Dimethyl-methylene Blue
DMSO	Dimethyl Sulfoxide
DT	Doubling Time

ECM	Extracellular Matrix
EDTA	Ethylenediaminetetraacetic acid
ESCs	Embryonic Stem Cells
FAK	focal adhesion kinases
FCS	Foetal Calf Serum
FDA	Food and Drug Administration
FGFR3	Fibroblast growth factor receptor 3
FITC	Flourescein isothyocyanate
FP	Fat pad
FP-MSCs	Fat Pad Derived Mesenchymal Stem Cells
GAGs	Glycosaminoglycans
GDF5	Growth differentiation factor 5
GMP	Good Manufacturing Practice
GPR22	G protein-coupled receptor 22
GWAS	Genome Wide Association Studies
H & E	Haematoxylin and Eosin
HA	Hyaluronan
HBP1	HMG-box transcription factor 1
HGF	Hepatocyte Growth Factor
HIF-1 α	Hypoxia Inducible Factor-1 α
HLA-DR	Human Leukocyte Antigen-antigen D Related
HLA-G	Human Leukocyte Antigen- G
HPTR1	Hypoxanthine Phosphoribosyltransferase 1
ICRS	The International Cartilage Repair Society
IDO	Indoleamine 2,3-dioxygenase

IFN- γ	Interferon- γ
IGD	Inter-globular domain
IL-1 β	Interleukin-1 β
IMS	Industrial Methylated Spirit
IPA	Isopropanol
iPSCs	Induced Pluripotent Stem Cells
ISCT	International Society for Cell Therapy
ITS	Insulin Transferrin Selenium X
KS	Keratin Sulphate
LP	link Proteins
LPS	Lipopolysaccharide
MACI	Matrix Assisted Chondrocyte Implantation
MACT	Matrix Assisted Chondrocyte Transplantation
MHC	Major Histocompatibility Complex
MMP3	Collagenase 3
MMPs	Matrix Metalloproteinases
MRI	Magnetic Resonance Imaging
mRNA	Messenger RNA
MSCs	Mesenchymal Stem Cells
N-CAM	Neural Cell Adhesion Molecule
NBF	Neutral Buffered Formalin
NICE	National Institute of Health and Care Excellence
NO	Nitric Oxide
OA	Osteoarthritis
OCD	Osteochondritis dissecans

P/S	Penicillin/ Streptomycin
PBS	Phosphate Buffered Saline
PCR	Polymerase Chain Reaction
PE	Phycoerythrin
PercP-Cy5.5	Peridinin-chlorophyll-protein-Cyanine5.5
PPIA	Peptidylprolyl Isomerase A
PTHrP	Parathyroid Hormone-Related Protein
RA	Rheumatoid Arthritis
RT-qPCR	Quantitative Real-Time Polymerase Chain Reaction
RUNX2	Runt-Related Transcription Factor 2
S100	S100 Calcium Binding Protein
SCF	Subcutaneous Fat
SCF-MSCs	Subcutaneous Fat-Mesenchymal Stem Cells
SF	Synovial Fluid
SF-MSCs	Synovial Fluid- Mesenchymal Stem Cells
SLRPs	Small leucine-rich proteoglycans
SM-MSCs	Synovium- Mesenchymal Stem Cells
SNP	Single Nucleotide Polymorphism
Sox9	Sex-Determining Region Y-Box 9 Transcription Factor
SPSS	Statistical Package for the Social Sciences
TA	Triamcinolone acetamide
TBE	TRIS-borate ethylenediaminetetraacetic acid
TGF- β	Transforming Growth Factor Beta
TIMPS	Tissue Inhibitors of Metalloproteinases
TKR	Total Knee Replacement

TLRs	Toll-like receptors
TNF	Tumour Necrosis Factor
US	United States
VDR	Vitamin D receptor
SEM	Standard Error of the Mean
SD	Standard Deviation
UC-MSCs	Umbilical Cord- Mesenchymal Stem Cells

Dissemination

Publications related to this thesis:

1. **Garcia J**, Mennan C, McCarthy HS, Roberts S, Richardson JB, Wright KT, Garcia J, Mennan C, McCarthy HS, Roberts S, Richardson JB, Wright KT. Chondrogenic Potency Analyses of Donor-Matched Chondrocytes and Mesenchymal Stem Cells Derived from Bone Marrow, Infrapatellar Fat Pad, and Subcutaneous Fat. *Stem Cells Int.* 2016;2016:1-11. doi:10.1155/2016/6969726.
2. **Garcia J**, Wright K, Roberts S, Kuiper JH, Mangham C, Richardson J, Mennan C. Characterisation of synovial fluid and infrapatellar fat pad derived mesenchymal stromal cells: The influence of tissue source and inflammatory stimulus. *Sci Rep.* 2016;6(April):24295. doi:10.1038/srep24295.
3. de Jong, A; Klein-Wieringa, I.R.; Andersen, S; Kwekkeboom, J.C.; Herb-van Toorn, L; de Lange - Brokaar, B; van Delft, Danny; **Garcia, J**; Wei, W; van der Heide, H; Bastiaansen-Jenniskens, Y; van Osch, G; Zuijmond, A; Susulic, V; Nelissen, R; Toes, R; Kloppenburg, M; Ioan-Facsinay, A: Lack of obesity-related changes in adipocytes and inflammatory cells in the infrapatellar fat pad (IFP): a different type of fat? (submitted)
4. Mennan C, **Garcia J**, McCarthy H, Wilson E, Wright K, Banerjee R, Richardson J, Roberts S: Human articular chondrocytes retain their phenotype in sustained hypoxia whilst normoxia promotes their immunomodulatory capacity. (manuscript in preparation)

Published abstracts:

1. **Garcia J**, C. Mennan, J. Richardson, K. Wright, S. Roberts, Cells isolated from fat pad and synovial fluid. Are they suitable for cartilage repair? *Osteoarthr. Cartil.* 22 (2014) S445. doi:10.1016/j.joca.2014.02.843.
2. **Garcia J**, C. Mennan, J. Richardson, S. Roberts, K. & Wright. Comparison of the chondrogenic potential of human donor-matched chondrocytes, bone marrow and adipose derived mesenchymal stem cells from arthritic joints. *Int. J. Exp. Pathol.* 92, A18 (2015).

Podium Presentation and prizes:

- **Tissue Engineering Centre meeting for Arthritis Research UK (York, 2013):** Investigations towards the optimisation of autologous therapies for cartilage repair
- **Doctoral Training Centre Conference 2014:** Investigations towards the optimisation of autologous therapies for cartilage repair. (1st prize for best oral presentation)

- **Robert Jones and Agnes Hunt Orthopaedic Hospital Research Day (Oswestry 2015):** Investigations towards the optimisation of autologous therapies for cartilage repair. (1st prize for best oral presentation)
- **Future Investigators of Regenerative Medicine Symposium (Girona, 2014):** Characterisation of Donor Matched Infrapatellar Fat Pad and Synovial Fluid Cells.

Poster Presentations

- MERCIA Stem Cell Alliance Meeting (Keele, 2013)
- British Society for Matrix Biology Conference (Bristol, 2014)
- Robert Jones Agnes Hunt Orthopaedic Hospital Research Day (Oswestry, 2014)
- Osteoarthritis Research Society International (Paris, 2014)
- MERCIA Stem Cell Alliance Meeting (Liverpool, 2014)
- International cartilage repair society (Chicago, 2015)
- British Society for Matrix Biology Conference (Chester, 2016)
- Osteoarthritis Research Society International (Amsterdam, 2016)

Acknowledgements

I would like to express my sincere thanks to all the members of the Spinal Studies group at the Robert Jones and Agnes Hunt Orthopaedic Hospital for their support over the past 3 years. In particular, I would like to express my gratitude to my supervisors Dr Karina Wright, Dr Claire Mennan and Professor Sally Roberts for their guidance and mentoring during my Ph.D. I thank the members of the Orthopaedic Research department at the ERASMUS Medical Center (Rotterdam, Netherlands), notably Dr Yvonne Bastiaansen-Jenniskens, Dr Wu Wei and Professor Gerjo van Osch, for the privilege offered to me to work in their lab.

I would like to dedicate this thesis to my mother, Sophia Cenac-Michel, for her constant support and encouragement during my studies.

Chapter 1: Introduction

1 Introduction

Cartilage lesions caused by injury or osteoarthritis (OA) are a serious clinical concern due to their limited reparative capacity. Current surgical techniques including debridement, mosaicplasty and microfracture, although routinely used, do present some drawbacks. Indeed, these methods of treatment can be costly and may not be suitable for certain patients depending on certain demographics such as age, body mass index and surgical history¹⁻⁵. As a result, new approaches to treat cartilage defects are being considered in the interests of patients, clinicians and health care services. The advent of tissue engineering and cellular therapies has provided innovative means of treating cartilage degeneration^{6,7}. Autologous chondrocyte implantation (ACI) has emerged as an interesting alternative to traditional surgeries for the repair of full thickness chondral lesions. Despite the new hope offered by such regenerative techniques, a tremendous amount of research is still required to address the many unanswered questions with regard to the basic biology of articular cartilage, the characterisation of degenerative joint diseases and the long term clinical benefits of novel repair techniques. Clinicians, researchers and bioengineers will need to unite their expertise if any meaningful progress is to be made.

The aim of this thesis introductory chapter is to describe the current scientific knowledge of articular cartilage biology and degeneration and to discuss cell based therapies for cartilage repair. Special focus will be given to OA as a joint disease, while the future perspectives of cell based therapies for cartilage repair will be reviewed. Finally, a brief description of the aims of the PhD research project will be provided.

1.1 Anatomy of the Knee Joint

The human knee is comprised of an intricate articulation between three bones: the tibia, femur and patella (Figure 1.1). This joint is stabilised by ligaments that attach the bones to each other, and is enclosed by a fibrous capsule. The interior of the knee is lined with a single layer of cells called the synovium, and is lubricated by the synovial fluid to facilitate joint movements. Two crescent-shaped fibrocartilaginous structures (Figure 1.1), called menisci, are located between the femur and tibia to help disperse forces within the joint. The structural elements in the knee work together to maintain the mechanical stability of the joint, but can also be subject to various pathologies.

1.2 Articular Cartilage: Structure and Function

Cartilage is a tissue that varies in structure according to its location and function in the body. Hyaline cartilage is located at the articulating surface of joints and is structurally adapted to its biomechanical functions of load bearing and force distribution. Macroscopically, the articular surface in a healthy joint appears smooth and polished⁸⁻¹⁰ which contributes to free, low friction movements. The thickness of this cartilage ranges from 1-3mm and is divided into a superficial zone, a transitional zone, and a deep zone (Figure 1.2), and is separated from the calcified cartilage by one or more tidemarks^{11,12}. This calcified region attaches cartilage to bone and helps limit the progression of subchondral bone while supporting endochondral ossification¹³⁻¹⁵.

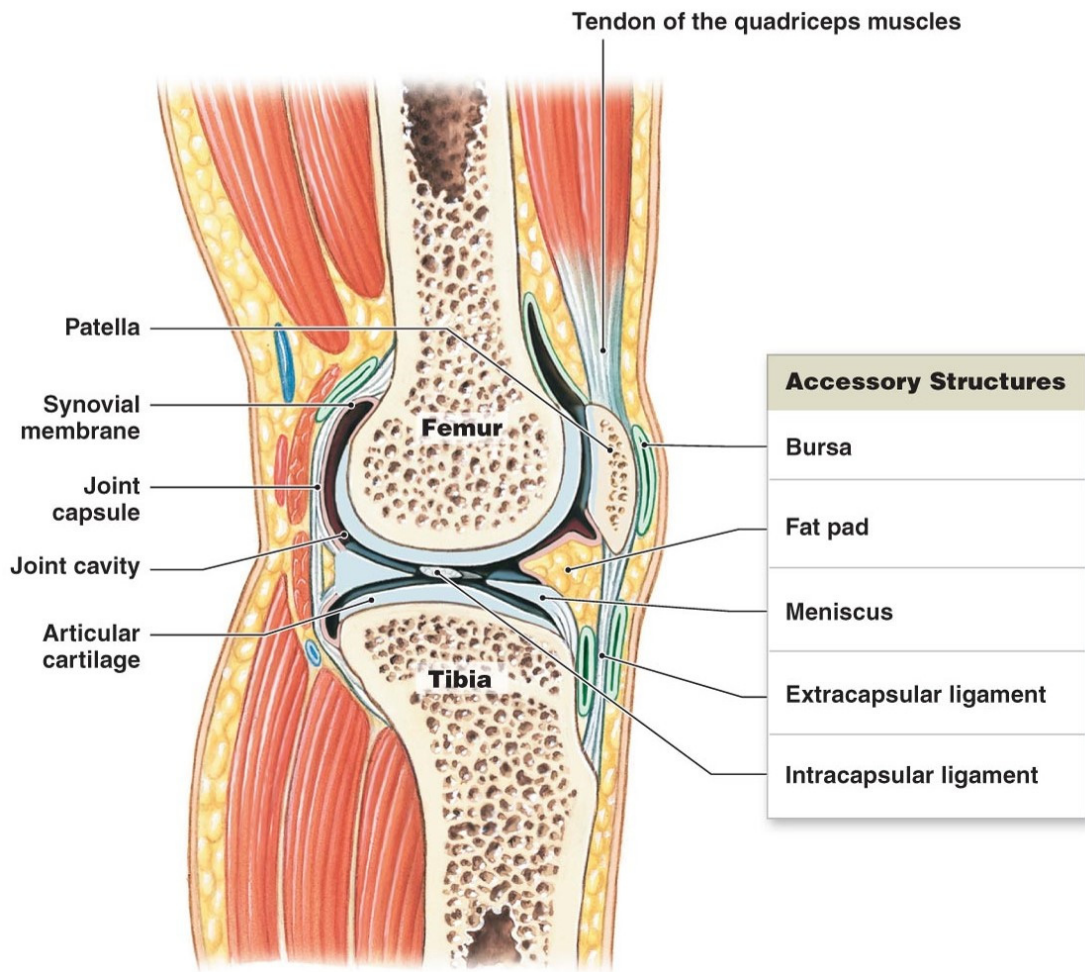


Figure 1.1: Anatomy of the human knee joint.

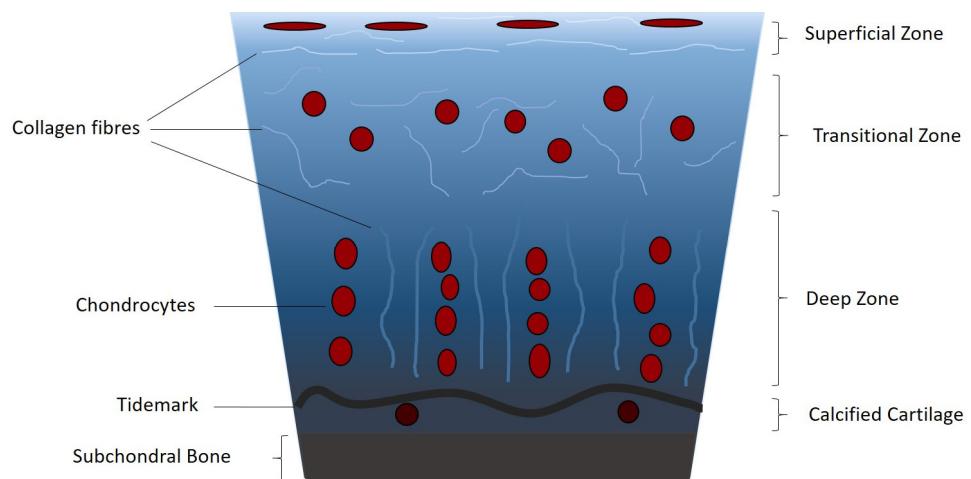


Figure 1.2: Schematic representation of articular cartilage. Chondrocytes are arranged perpendicular to the joint surface in the deep zone, disorganised in the transitional (middle) zone, and aligned parallel to the joint surface in the superficial zone. The orientation of collagen fibres mirrors the organisation of chondrocytes in articular cartilage.

Together, these stacked layers form a solid yet elastic structure capable of resisting compressive and shear forces to allow optimal joint movements. The physical properties of articular cartilage are also largely attributed to the complex nature of the extracellular matrix (ECM). Chondrocytes are specialised cells that occupy this matrix and are responsible for its development and maintenance. Alterations to the function of these cells or degradation of the ECM can be the cause of cartilage pathologies. Another key feature of articular cartilage is a lack of vascularisation and innervation^{16,17}, the significance of which will be discussed later. Additionally, low oxygen levels have been noted in articular cartilage. This hypoxic state is often attributed to the lack of blood supply in this tissue and it is believed that the chondrocytes adjust to these conditions by adapting their cellular activity through hypoxia induced signalling pathways¹⁸. Hypoxia inducible factor-1 α (HIF-1 α) is produced by articular chondrocytes and controls the factors involved in cartilage maintenance, in particular Sex-Determining Region Y-Box 9 transcription factor (Sox9) and the cartilage matrix components under its regulation¹⁹. *In vivo* developmental studies have demonstrated that rats lacking expression of HIF-1 α show cell death in regions cartilaginous limbs growth deprived of oxygen²⁰.

1.3 The Chondrocyte

Chondrocytes are the lone resident cells of cartilage tissue with a peculiar spatial distribution. Early studies by Stockwell indicate an overall low density of cells (as low as 19 cells per mm³) within mature human cartilage tissue; cell numbers tend to decrease from the superficial zone down to the deep zone. There is also a decrease in cell density from infancy to adolescence, but a constant cell density during adulthood^{21,22}. Cells in the superficial layer appear elongated and lie parallel to the articular surface. In the transitional zone (or middle zone), cells appear bigger with a more rounded morphology in either clusters or more

frequently as dispersed single cells. Finally, chondrocytes in the deep zone are elliptical in morphology and may be arranged in columns perpendicular to the articular surface²³. The calcified region contains hypertrophic cells (terminally differentiated) that can express collagen type-X and alkaline phosphatase²⁴⁻²⁶. When enzymatically isolated and placed in tissue culture flasks chondrocytes adhere to culture plastic, adopt a round/cubical shape in early passages and shift to a more elongated fibroblastic morphology as passage number increases^{27,28}.

The biological activities of chondrocytes are vital to the maintenance of articular cartilage structure. The functions of chondrocytes are often detailed as: a) production of the components of the ECM, b) remodelling of the ECM and c) detection and response to external physical signals through mechanotransduction. Collagens and proteoglycans are secreted by chondrocytes¹⁶ and are incorporated into the architecture of the surrounding matrix. The pericellular matrix of mature human chondrocytes incorporates collagens, hyaluronan, sulphated proteoglycans, fibronectin and glycoproteins in an encapsulating ring-like structure²⁹⁻³¹. The chondrocyte together with this pericellular matrix form what is known as a chondron, a functional unit believed to have a dual role of resisting compressive forces and metabolising matrix components³⁰. In response to a host of stimuli (both mechanical and biochemical), chondrocytes secrete a number of enzymes and catabolic factors that facilitate the remodelling of the matrix by breaking down its protein components³²⁻³⁶.

1.4 The Extracellular Matrix

1.4.1 Collagens

Collagen is the most abundant protein in articular cartilage accounting for approximately 60% of its dry mass. These structural proteins occur as triple α -helices coiled around each other to form a collagen molecule (Figure 1.3). These in turn organise into collagen fibrils and then fibres. To date, 28 collagen proteins have been characterised of which collagen type II, IX and XI are the most represented in articular cartilage^{37,38}. In mature articular cartilage collagen type II is estimated to comprise $\geq 90\%$ of the total collagen whereas types IX and XI are 1% and 3% respectively. The cross-linking of these collagen types is crucial to the microarchitecture of cartilage³⁹⁻⁴¹. Collagen fibres form a robust network that helps to maintain the general structure of the ECM by resisting the swelling pressure caused by the interactions between glycosaminoglycans (GAGs) and water (to be discussed in section 1.3.2). It is also worth noting the size, distribution and orientation of collagen fibres in the different zones of articular cartilage mentioned previously. In the superficial zone, the fibres (60-90 nm diameter) appear oriented parallel to the articular surface. A random organisation of fibres is observed in the transitional zone, with a smaller variation of fibre diameters (60-80nm), while bigger fibres (80-100nm) oriented perpendicularly to the articular surface appear in the deep zone^{42,43}. This fibrillar organisation mirrors the distribution of chondrocytes described earlier, which suggests an interaction between the ECM and the phenotypes of the cells residing in each zone.

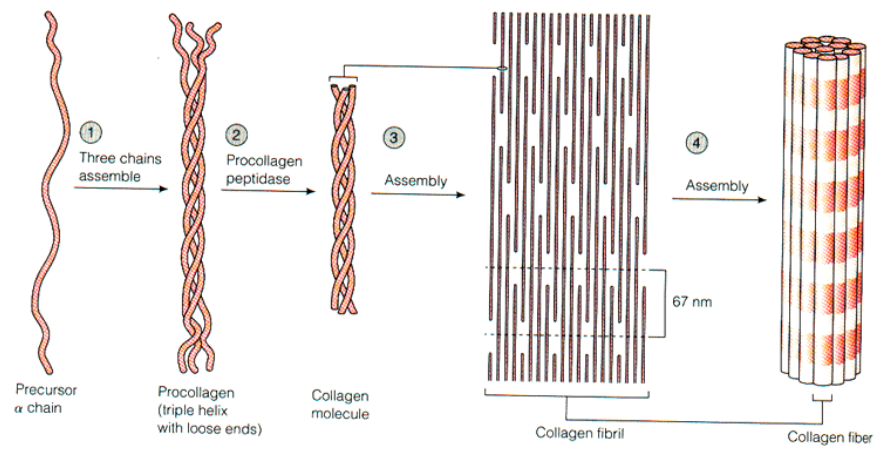


Figure 1.3: Illustration of the progressive assembly of collagen fibres. Image modified from Biology (8th Edition)⁴⁴.

1.4.2 Proteoglycans

Proteoglycans, like collagens, constitute an essential part of articular cartilage by contributing to its biomechanical properties. The basic structure of proteoglycans comprises of a core protein to which a series of unbranched sulphated GAGs attach⁴⁵. Chondroitin sulphate (CS) and keratan sulphate (KS) are the main GAGs that attached to these proteins (Figure 1.4).

Aggrecan is the most common proteoglycan in articular cartilage (35% of the dry weight of cartilage proteins) and can attach as many as 100 CS chains⁴⁶. Furthermore, numerous aggrecan molecules will bind to link proteins (LP) and “aggregate” on hyaluronan (HA) to form a bottlebrush structure (Figure 1.5).

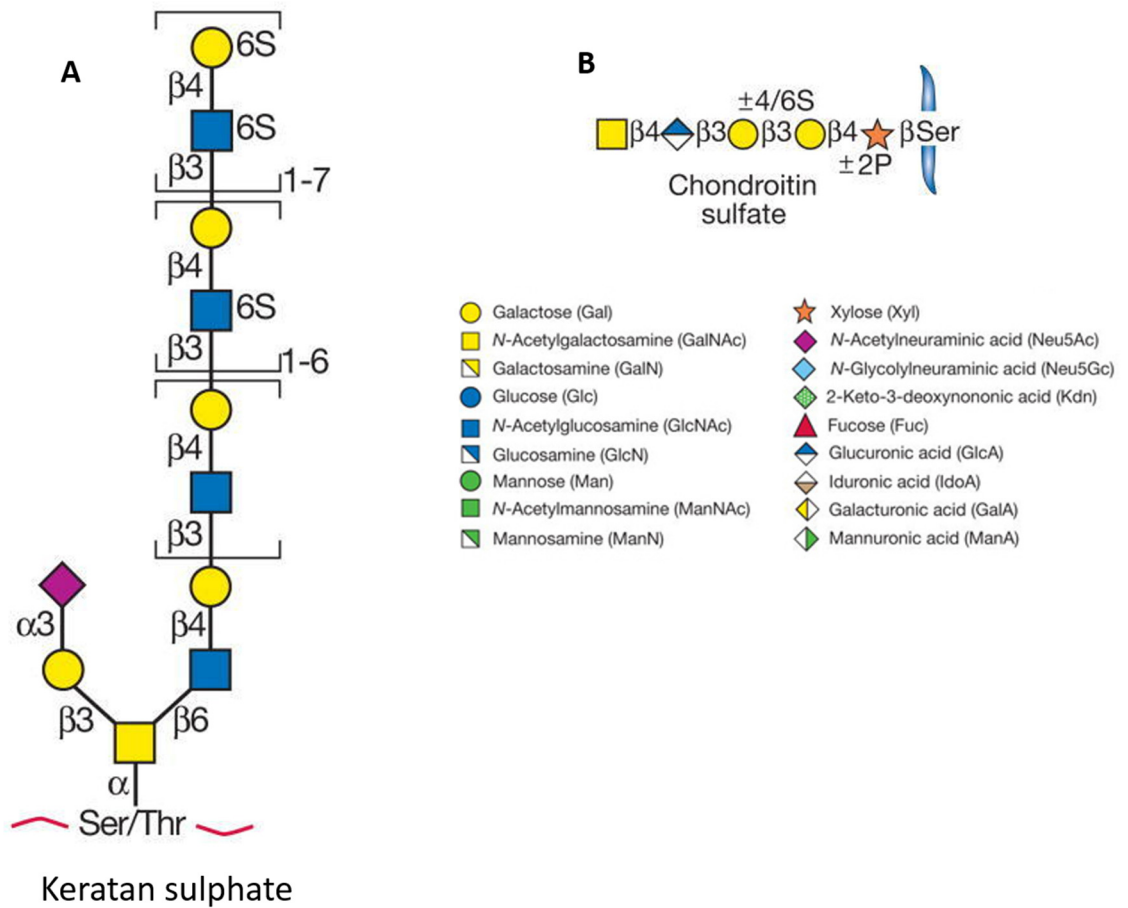


Figure 1.4: Schematic of the tetrasaccharide and poly-N-acetyllactosamine bond that exists between core proteins and A) chondroitin sulphate or, B) keratan sulphate side chains in proteoglycans. Image modified from Essentials of Glycobiology⁴⁵.

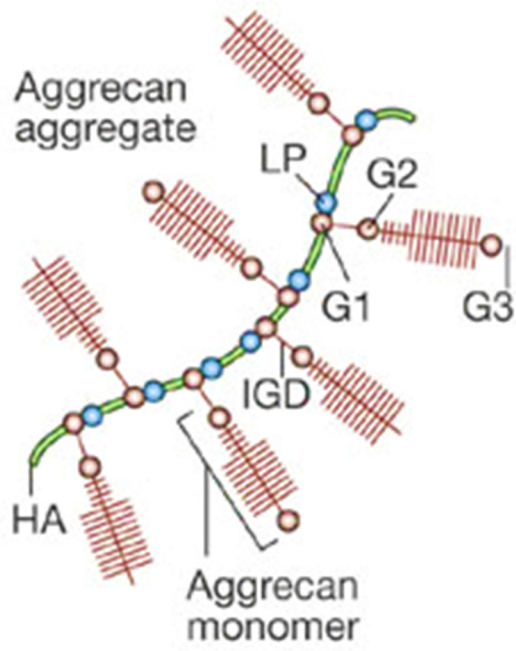


Figure 1.5: Illustration of the aggrecan "bottlebrush" structure (HA =hyaluronan ,LP= link protein, IGD= inter-globular domain, G1+G2+G3= globular domains). Image modified from Fosang *et al*⁴⁷

In addition to aggrecan, small leucine-rich proteoglycans (SLRPs) are distributed throughout the cartilage matrix. This subfamily of proteoglycans is characterised by multiple protein domains linked by a common leucine-rich motif and includes decorin, biglycan, fibromodulin and lumican. An intricate interaction between the core proteins of SLRPs and collagen fibres not only contributes to the organisation of the cartilage matrix, but also helps to protect collagen from catabolic enzymes^{48,49}. Studies in SLRP knockout mice revealed a lack of, or faulty development of the musculoskeletal system⁵⁰⁻⁵².

Lubricin is 345-KDa proteoglycan that occupies the superficial layer of articular cartilage and is believed to play a role in joint lubrication by creating low friction conditions for articulating surfaces⁵³⁻⁵⁵. The proteoglycan 4 gene (*PRG4*) codes for lubricin and is highly expressed by synovial cells and chondrocytes residing in the superficial zone of articular cartilage⁵³.

The negative charge found on the sulphated groups of GAGs causes an attraction of cations (such as Na⁺) which in turn engenders an influx of water molecules into the cartilage matrix in an attempt to maintain an electrolytic balance^{45,56}. This water accounts for ~70% of the wet weight of cartilage. Swelling caused by this water uptake is restricted by the collagen network as discussed previously. The maintenance of physicochemical conditions, such as osmolarity and pH within the cartilage tissue, is heavily dependent on these hydrostatic events^{57,58}. In addition, the anaerobic conditions in the articular joint promote an acidic environment that chondrocytes appear to buffer efficiently with Na⁺/H⁺ exchanger molecules⁵⁹.

1.4.3 Cell-Matrix Interactions and Mechanotransduction

Mechanotransduction is the complex process by which cells detect and respond to physical stimuli from their surrounding microenvironment. To accomplish this, cells are usually attached to their ECM by means of specific binding proteins that form a continuum of interconnected structures from the matrix components to the cell nucleus^{60,61}. Although some aspects of these cell-matrix interactions are still being researched, it is clear that cells, especially in load bearing tissues, are conditioned by the physical forces that they are exposed to. In the case of articular cartilage, integrins play a pivotal role in the connection between chondrocytes and their matrix. Cyclic loading by physical activity deforms the matrix which in turn exerts physical forces on the cells themselves; this activates a cascade of intracellular reactions catalysed by various enzymes. Focal adhesion proteins such as focal adhesion kinases (FAK) are important molecular mediators of these processes. This chain reaction ultimately leads to the up or down regulation of specific genes to elaborate a cell response. For example, Millard-Sadler *et al.* demonstrated that signal transduction through integrins resulted in the upregulation of aggrecan and metalloproteinases in chondrocytes from arthritic patients³⁴. This observation not only confirms the ability of cells to respond to mechanical signals, but also highlights the role of physical stimuli in the remodelling of cartilage tissue.

1.5 Cartilage Development and Remodelling

An understanding of the embryonic events that lead to *in vivo* chondrogenesis could provide important concepts for developing new therapies for cartilage repair. Embryonic formation of the skeletal system commences with the early appearance of cartilaginous condensations, also called anlage, in specific blastema⁶². Experiments using chick embryo models revealed a highly organised process where mesenchymal cells migrate from the mesoderm and neural crest to designated areas, forming condensed structures^{63,64}. This process is thought to be

mediated by cell adhesion molecules such as neural-cell adhesion molecule (N-CAM) and N-cadherin⁶⁵⁻⁶⁹. These mesenchymal cells then adopt a chondrocyte phenotype which is confirmed by a shift in the composition of the ECM secreted by the cells. Hence, these chondrocytes now produce more collagen type II and proteoglycans while the expression of collagen type I is downregulated⁷⁰⁻⁷².

Cartilaginous condensation is a crucial phase in skeletal development; it serves as a template for endochondral ossification which eventually leads to the formation of the majority of bones in the axial skeleton and limbs^{73,74}. This process involves the secretion of collagen type X by hypertrophic chondrocytes, followed by the invasion of the cartilage template by blood vessels, osteoblasts and haematopoietic cells^{75,76}. In the case of long bone formation, the osteoblasts continue to produce more calcified matrix starting from the primary centre of ossification (diaphysis), leaving behind only small non-mineralised regions in the epiphyses destined to become articular cartilage^{76,77}.

Pattern formation during embryonic chondrogenesis is controlled by an interplay between a host of transcription factors and growth factors⁷⁶. For example, Sox9 is recognized as a major regulator of chondrogenesis during skeletal development by activating the enhancer of the collagen type II gene^{78,79}. In fact, anomalies in the expression of Sox9 are known to be the main cause of the rare cartilage disease campomelic dysplasia⁸⁰. Polypeptides of the transforming growth factor beta (TGF- β) class, notably TGF- β 1 and TGF- β 3, have been shown to promote the production of GAGs and prevent terminal differentiation of chondrocytes^{81,82}. In addition, bone morphogenic proteins, which are also part of the TGF superfamily, play an essential role in the initiation of embryonic chondrogenesis^{83,84}. Other factors, notably parathyroid hormone-related peptides, Wnt family proteins and fibroblast growth factors have been shown to be crucial in skeletal development, but are thought to be under the direct or indirect influence of Sox9⁷⁶.

Although chondrocytes in mature cartilage have a low proliferative activity, it is generally accepted that they remodel their environment *in vivo* by secreting components of the ECM, as well as enzymes which can break down matrix molecules. Like many other tissues, it is assumed that a fine balance is maintained between the degradation and production of structural entities in articular cartilage. The rate of cartilage matrix turnover is relatively slow, with molecules such as aggrecan and collagen having half-lives of 3-24 years and 117 years respectively^{85,86}. Collagenases or matrix metalloproteinases (MMPs) and aggrecanases or disintegrin and metalloproteinases with thrombospondin motifs (ADAMTS), are the main enzymes involved in cartilage degradation. Collagenase 3 (MMP-13) for example, is a well-known zinc dependent proteinase capable of cleaving the helical structure of collagen II⁸⁷⁻⁸⁹. Similarly, aggrecanase-1 (ADAMTS-4) and aggrecanase-2 (ADAMTS-5) cleave specific motifs between the globular domains, G1 and G2, of aggrecan to release GAGs^{90,91}. To counterbalance the degradative effects of these enzymes, particularly MMPs, special tissue inhibitors of metalloproteinases (TIMPs) are also produced by chondrocytes and a low or a lack of synthesis of these inhibitors has been related to several cartilage pathologies⁹²⁻⁹⁴.

Historically, it was believed that mature articular cartilage, once injured, does not heal⁸. However, a growing body of evidence now suggest that in some cases articular cartilage does spontaneously repair without intervention^{95,96}. For instance, in a longitudinal MRI based study investigating the factors that predict the progression of OA, the investigators observed that certain large cartilage defects had improved over the course of a two year period⁹⁵. It has also been shown that defect in younger patients tend to improve more than in patient with OA⁹⁷. Although the exact cellular mechanisms involved in this natural repair remains largely unknown, it is believed that the series of molecular and cellular events occurs after and acute joint injury, namely the inflammatory followed by and anabolic/catabolic

phase and finally a matrix formation phase⁹⁸. Understanding these events could offer essential insight and open new avenues of research into treating cartilage defects.

1.6 Articular Cartilage Pathologies

1.6.1 Cartilage injury

Treating injuries to articular cartilage is one of the major challenges facing clinicians and scientists in orthopaedic care and research. Chondral defects can develop as a result of acute traumatic impact and normal or abnormal joint loading. It is estimated that 63% of patients observed in arthroscopy present some form of cartilage defect⁹⁹. The International Cartilage Repair Society (ICRS) has classified chondral defects into five categories according to the depth and size of the injury¹⁰⁰ (Table 1.1).

Table 1.1: Classification of cartilage injury according to the International Cartilage Research Society. Table adapted from Brittberg and Winalski ¹⁰⁰.

Grade	Description
Grade 0	Normal cartilage with no apparent defect
Grade I	Intact cartilage with slight fibrillation and, or softening. Lacerations and fissures may be present.
Grade II	Defects extending to $\leq 50\%$ of the cartilage thickness
Grade III	Defects extending to $\geq 50\%$ of the cartilage thickness but not down to the subchondral bone.
Grade IV	Full thickness cartilage lesion that extends to the subchondral bone.

In addition to trauma-induced cartilage defects, several osteochondral pathologies also present a clinical burden. One such disease is osteochondritis dissecans (OCD), which occurs predominantly in young males and is characterised as an initial lesion of the subchondral bone, caused by a lack of blood supply, that may progressively lead to the fragmentation and or collapse of articular cartilage¹⁰¹⁻¹⁰³. OA however is the most prevalent degenerative joint disease and will be the focus of the following sub-sections.

1.6.2 Osteoarthritis (OA)

1.6.2.1 Introduction

OA is a degenerative joint disease that compromises the integrity of articular cartilage but also affects other elements of the joints including the synovium and bone. Although not life threatening, OA affects the quality of life of patients causing joint pain, swelling and reduced range of motion. Over 8.5 million people suffer from OA in the United Kingdom (the majority being over 40 years old), and as such significant financial investment is required for its direct and indirect treatment^{104,105}. In 2010, the total cost of arthroscopy, total hip and knee replacements for OA in the United Kingdom was estimated at £851.3 million, which was increased to £3.2 billion when indirect costs including work days lost and disability allowances were factored into the calculation¹⁰⁴.

Women tend to be more frequently affected by OA, while obesity and genetic predisposition have also been identified as risk factors¹⁰⁶⁻¹¹⁰. The pathogenesis of this condition remains largely unclear, however an imbalance in the homeostatic state of articular cartilage combined with the risk factors mentioned above could help to explain the onset risk and progression of this disease.

1.6.2.2 Articular cartilage in OA

An understanding of the physiological changes that occur in articular cartilage during OA is key to the development of new therapies and targets. Cartilage softening and fibrillation (Figure 1.6) are some of the earliest visible events used to characterise the onset of OA. Small clefts appear along the surface of the cartilage and progressively increase in depth until the degradation of the previously solid structure becomes visible. This process is believed to be accentuated with repeated mechanical loading on the joint, leading to further ulceration of the articular surface and ultimately contributing to the reduction in cartilage thickness¹¹¹.

1.6.2.3 Chondrocyte activity in OA

Injury to articular cartilage affects the architecture of the ECM and the phenotype of resident chondrocytes. The loss of the characteristic phenotype of chondrocytes can, in part, be accounted for by the downregulation of the transcription factor Sox9, which is the principal regulator of chondrogenesis^{112,113}. Studies have shown that chondrocytes from arthritic joints enter a hypertrophic state that is defined by increased proliferation and apoptosis, the downregulation of factors promoting cartilage matrix formation and the upregulation of matrix degrading proteinases and osteogenic factors^{114,115}. Histological observation of arthritic cartilage indicates clustering of chondrocytes adjacent to the site of fissure (Figure 1.6)^{116,117}. It is not clear whether this is due to an increase in chondrocyte proliferation within their local pericellular matrix or an aggregation of cells following tissue migration. However, mitotic assays appear to support the former^{118,119}.

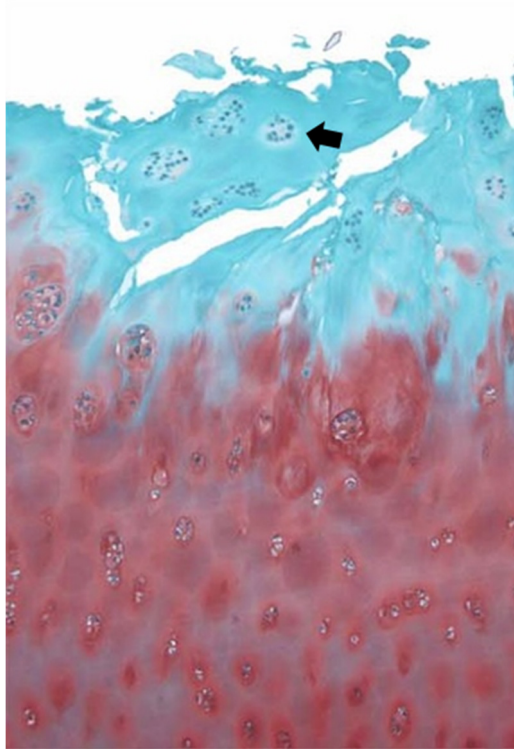


Figure 1.6: Histological observation of cartilage fibrillation and chondrocyte clusters (black arrow) in a Grade III cartilage lesion. Image adapted from Pritzker *et al.*¹¹⁷

Although there is an age related decrease in the gene expression of collagen type II, chondrocytes from OA patients have been shown to increase the production of the protein^{120–122}, possibly in an attempt to restore the disrupted cartilage matrix. Previous immunolocalisation and gene analysis assays have revealed increased expression of collagen type X as an indicator of the change in phenotype of OA chondrocytes^{123–125}, although this is not a universally established observation in OA¹¹⁵.

The abnormal secretion of matrix degrading enzymes by chondrocytes is well documented and is an important factor in the progression of OA^{126,127}. Quantitative gene analysis by Kevorkian *et al.* strongly correlated OA progression with the upregulation of MMP13, MMP28, MMP9, MMP16, ADAMTS16, ADAMTS2, and ADAMTS14¹²⁸. The role of TIMPs in OA is not fully understood, but the increased expression of TIMP-1 and TIMP-3 reported by Su *et al.* does not appear to be sufficient to temper the deleterious effects of MMPs¹²⁹. As mentioned above, another indicator of chondrocyte hypertrophy is the production of molecules involved in tissue calcification, notably osteocalcin, osteonectin, osteopontin, and alkaline phosphatase^{130–134} and the expression of the osteogenic transcription factor runt-related transcription factor 2 (Runx2)^{135,136}. In addition, several studies have proven that a higher percentage of apoptotic cells reside in OA cartilage compared to normal cartilage^{137,138}. These cells show positive expression for the pro-apoptotic factors, β cell lymphoma-2 (Bcl-2), Fas and annexin V, while a significant amount of DNA fragmentation has also been detected^{137,138}.

1.6.2.4 Modifications to the ECM in OA

Changes that occur in the phenotype of articular chondrocytes will inevitably affect the composition and architecture of the cartilage ECM. As a result, proteinases secreted by

chondrocytes coupled with the insufficient production of matrix components facilitate the overall breakdown of cartilage in OA. The implication of collagenase-mediated denaturation of type II collagen fibres has also been demonstrated, while aggrecan degradation is well documented in OA subjects^{91,122,127,139–141}. Histological observations indicate a progressive loss of GAGs in human cartilage during OA¹¹⁷.

Furthermore, an age related accumulation of advanced glycation end products (AGEs) prompts the excessive crosslinking of collagen fibres in articular cartilage^{142,143}. This process leads to increased stiffness of the cartilage matrix, which makes the tissue more brittle and prone to breakages and lesions^{144,145}.

1.6.2.5 Involvement of the subchondral bone in OA

In addition to the changes that occur in the articular cartilage, several studies have highlighted the contribution of the subchondral bone in the pathogenesis of OA. Cysts present in the subchondral bone are a common radiographic feature that has been correlated to OA and eventually knee replacement in a longitudinal study^{146,147}. While there is no consensus in the literature regarding the exact mechanism through which these cysts are formed, it is believed that they interact with the articular cartilage via small fractures, the implications of which remain unclear¹⁴⁷.

Vascular invasion of the calcified zone from the subchondral bone causes the tidemark to drift, leading to cartilage thinning and an incorrect dissipation of forces during cyclic joint loading¹⁴. Radiographic analyses confirm an increase in cortical bone thickness of the subchondral plate associated with increased tissue remodelling¹⁴⁸. Here again, the mechanical properties of the articular unit are altered due to the inefficient mineralisation of bone during high turnover rates^{149,150}. Proliferation and terminal hypertrophic differentiation

of periosteal cells at the cartilage-bone interface engenders osseous outgrowths on the periphery of the joint. These structures are known as osteophytes and represent another key feature for the diagnosis of OA¹⁵¹.

1.6.2.6 Influence of Genetics in OA

The genetics of OA is a subject of much debate. No single gene alteration has been identified as solely responsible for the onset and progression of OA. In addition, Mendelian inheritance does not support the appearance of OA, which suggests the improbable transmission of the disease from parent to child. Genome wide association studies (GWAS) in hip, knee and hand arthritic patients have recognised a number of susceptible loci on chromosomes 2,3,4,6,7,11 and 16. A Single nucleotide polymorphism (SNP) was observed on the chromosome 7q22 locus in a GWAS including 1341 Dutch subjects¹⁵². The genes implicated in this polymorphism include those coding for G protein-coupled receptor 22 (*GPR22*) and HMG-box transcription factor 1 (*HBPI*). The recent UK based GWAS project, arcOGEN, analysed 7410 subjects identifying six OA linked loci¹⁵³. The authors noted a high association linkage on chromosome 3, related to a SNP in guanine nucleotide-binding protein-like 3 gene. However these loci do not represent strict OA determinants, but operate as predisposing regions that promote the development of the disease. Factors such as physical activity tend to be shared within family cohorts and could indirectly influence OA clustering by affecting susceptible genes.

As discussed before, the structural elements of the cartilage ECM are important in maintaining the tissue's integrity. Mutations or alterations in the expression of the genes coding for these elements could thus result in the production of defective proteins or no proteins at all. The type II collagen α -chain (*COL2A1*) has been linked to the onset of OA,

with the arginine to cysteine codon substitution known to be associated with chondrodysplasia-induced OA¹⁵⁴. There appears to be some contradictory results in the literature with regard to the role of the vitamin D receptor (VDR) gene in OA. In one study, the investigators used molecular haplotyping in 846 samples to show that an overexpression of VDR resulted in a 2.27 fold increase in the risk of knee OA by facilitating the appearance of osteophytes¹⁵⁵. However, Loughlin *et al.* were unable to make an association between VDR and OA¹⁵⁶. In another study, microarray analyses demonstrated a significant over representation of the asporin gene in radiographic OA that reduced the expression of aggrecan and type II collagen¹⁵⁷. Similar associations have been made for other proteins such as growth differentiation factor 5 (GDF5) and frizzled-related protein (FRZB)^{158–160}. To conclude, while there is sufficient evidence to support the participation of certain genes in the pathogenesis of OA, a definitive hereditary description of the disease is yet to be detailed. In addition, it appears that a genetic predisposition to OA is significantly influenced by a number of demographic features which further underscores its multifactorial origin.

1.6.3 Inflammation in OA

As mentioned previously, the destruction of articular cartilage is the primary characteristic of OA. An extensive amount of research now points to the secondary involvement of pro-inflammatory processes in the pathogenesis of OA. Although the historical characterisation of inflammation (redness, heat, swelling and pain) may reflect some of the symptoms of OA, this definition needs to be extended to integrate the cellular and molecular events that initiate and promote the degradation of cartilage¹⁶¹. It must be mentioned that OA-related inflammation is not as pronounced as in rheumatoid arthritis (RA) which is an autoimmune disease with systemic inflammation^{162,163}.

1.6.3.1 Pro-inflammatory molecules in the joint

The cytokines interleukin-1 β (IL-1 β) and tumour necrosis factor (TNF) are considered the main participants in driving joint inflammation¹⁶⁴. IL-1 β binds to its specific receptor (IL-1 receptor type 1)¹⁶⁵ and triggers the inhibition of the production of key components of articular cartilage matrix, such as collagen type 2 and aggrecan by chondrocytes^{166,167}. TNF- α has a similar suppressive effect on the synthesis of the link protein of proteoglycans and collagen type II by downregulating their respective genes expression in articular chondrocytes^{168,169}. Additionally, IL-1- β and TNF- α induce the upregulation of genes of catalytic enzymes such as MMP-1, MMP-3, MMP-13 and ADAMTS-4 in chondrocytes^{90,170,171}. Studies have also shown that chondrocytes exposed to IL-1 β and TNF- α increase their secretion of other pro-inflammatory molecules, notably IL-6, IL-8 and monocyte chemoattractant protein 1¹⁷²⁻¹⁷⁴. Not only are IL-1- β and TNF- α elevated in the synovial fluid (SF) of OA patient, but the expression of the receptors for these cytokines are also increased in OA synovial fibroblasts and chondrocytes^{175,176}.

1.6.3.2 Damage-associated inflammation

The causes of inflammation in the OA joint are continually being revealed. One established mechanism is the damage-associated molecular patterns (DAMP) pathway which is initiated as a result of tissue and cellular damage in the articular joint. Whether it be through trauma or progressive wearing of the joint, small particles and by-products of degeneration are released from tissues, such as cartilage and bone. These products represent DAMPs resulting in an innate immune response from the host, which in turn generates an increase in local pro-inflammatory conditions. This process is known as sterile inflammation. HA, cartilage oligomeric matrix protein (COMP) and fibronectin are among the molecules derived from the breakdown of cartilage ECM known to initiate this immune response¹⁷⁷⁻¹⁷⁹.

DAMPs are detected by specific cell surface molecules, of which toll-like receptors (TLRs) are the best characterised. For example, one study has shown that TLR-4 is necessary for the HA induced immune response provoked by sterile inflammation in a mouse model of OA¹⁷⁹. The activation of the TLR pathways (TLR-2 and TLR-4) leads to the release of catabolic factors within the joint by cells such as chondrocytes and macrophages (discussed below in section 1.6.3.4)¹⁸⁰⁻¹⁸².

1.6.3.3 The role of the synovium and synovitis in joint inflammation

The synovium can be described as the soft tissue that lines the inside of the articular joint. In healthy individuals (no indication of joint pathology), the synovium is comprised of a single continuous layer of lining cells (intima) and a fibrous underlying subsynovial stromal tissue (subintima) (Figure 1.7)¹⁸³. The synovial lining cells are divided into macrophages (type A cells) and fibroblasts (type B cells or fibroblast-like synoviocytes), which are the most abundant of the two cell types. The subsynovial stroma contains fibroblasts and, to a lesser extent, immune cells such as macrophages, T cells and mast cells¹⁸⁴. Under healthy conditions, the synovium maintains the composition of the synovial fluid, secretes lubricin which is needed for the lubrication of the joint, and produces nutrients for joint cartilage¹⁸³.

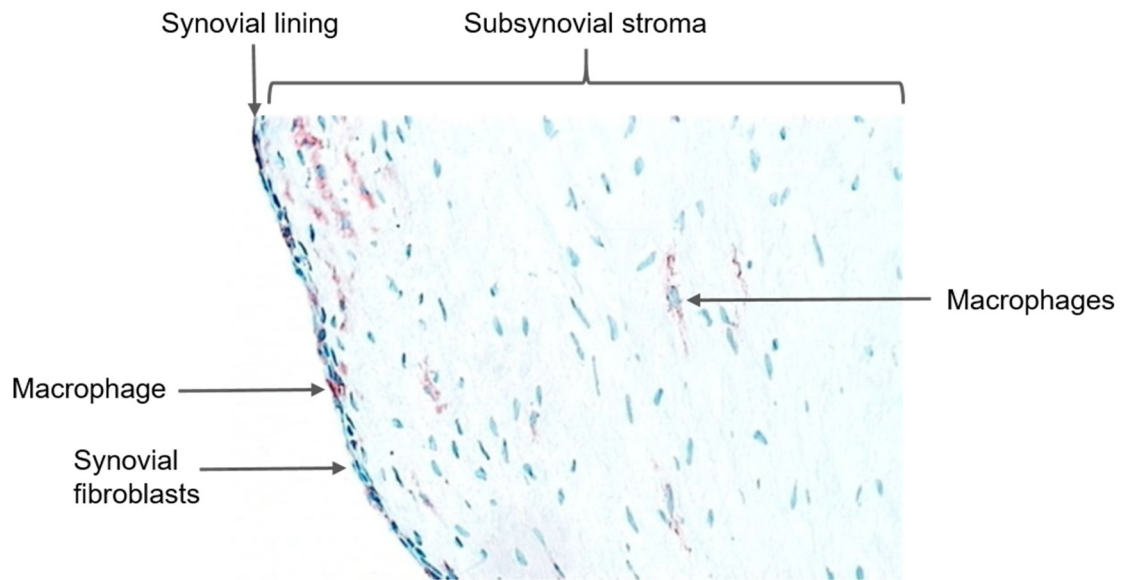


Figure 1.7: Immunohistochemical representation of normal human synovium. Red staining indicates CD68 positive macrophages. Image taken from Smith *et al.*,¹⁸³.

In a diseased joint (OA and RA), the synovium often becomes inflamed; a condition known as synovitis. From a histological perspective, synovitis is generally characterised by hyperplasia of the synovial lining cells (increase in the number of cells), increased cellularity of the subsynovial stroma and infiltration of immune cells from blood vessels¹⁸⁵. Synovitis can be found in early or late stages of OA, but does not affect the entire synovium (patchy) and is not as severe as in RA^{185,186}. Nevertheless, synovitis is believed to play a pivotal role in the progression of OA by increasing the inflammatory and catabolic environment in the joint. Indeed, immune cells are more abundant in an inflamed synovium and thus the pro-inflammatory molecules they secrete also becomes elevated¹⁸⁷. A longitudinal study has correlated an increase in radiographic synovitis with the deterioration of cartilage and increased joint pain¹⁸⁸.

The exact mechanism which results in the onset of synovitis is still unknown. The synovial tissue appears to be responsive to the presence of fragments of damaged joint tissues and chronic haemorrhage. Loose bodies of cartilage and crystal structures, such as those found in the bone, are known to induce inflammatory processes in the synovium; a process believed to be mediated by IL-1¹⁸⁹⁻¹⁹¹. Taken together, it can be theorised that joint degeneration may be one of the initiators of synovitis, which coincides with the general consensus that inflammation is a secondary attribute of OA and not the cause of the disease^{192,193}.

1.6.3.4 Macrophages as key mediators of joint immunomodulation

Originally characterised for their phagocytic activity, macrophages are immune cells involved in tissue development and inflammation¹⁹⁴. While a pool of tissue resident macrophages exist around the human body, monocytes (precursors to macrophages) circulating in peripheral blood can be recruited into a given tissue where they become

specialised macrophages according to the biochemical composition of the local microenvironment¹⁹⁵. A variety of surface and intracellular receptors and sensors allow macrophages to detect signals (DAMP, metabolic and physicochemical changes) in tissues to then become activated towards specific phenotypes in order to restore homeostasis¹⁹⁵.

Historically, macrophages were believed to undergo two activation states, classical and alternative activation. Macrophages stimulated with any two of interferon- γ (IFN- γ), lipopolysaccharide (LPS) or TNF produce classically activated cells with a pro-inflammatory phenotype also known as the M1 polarisation state¹⁹⁶. These cells are characterised by their propensity (when activated) to upregulate genes involved in inflammatory cytokine signalling (such as *STAT-1*), and the secretion of pro-inflammatory molecules IL-1, TNF- α , IFN- γ , IL-12, IL-23 and nitric oxide (NO)^{196,197}. The alternatively activated macrophages, in the M2 polarisation state, are generated following stimulation with IL-4 and IL-13, resulting in cells that secrete anti-inflammatory molecules such as IL-10 and IL-1RA (an antagonist of IL-1)^{196,197}. However, a significant number of recent studies now suggest that macrophages exist on a spectrum of different phenotypes, as opposed to a strict dichotomous model of M1 and M2^{197,198}. This is supported by the discovery of M2 macrophage subsets that include parasite clearing (M2a), immune regulatory (M2b) and wound healing (M2c) macrophages¹⁹⁷⁻¹⁹⁹. This tremendous plasticity of macrophages has attracted significant research interest, however, the exact functional role of the various macrophage subsets in OA still remains unclear.

In the arthritic joint, much of the available literature is focused on macrophage activity in RA. Although studies have investigated the presence of macrophages in the degenerative OA joint, few investigations to date have explored the different macrophage subsets and how they are potentially involved in the disease^{200,201}. It has been shown that both M1 and M2 macrophages are present in human synovium and that M1 macrophages were more

responsive to alarmins S100 calcium binding protein (S100) A9 and S100A8 (danger signals that are functionally similar to DAMPs) by secreting higher amounts of IL-1, IL-6, TNF- α and expressing higher levels of MMP-1, MMP-3 and MMP-9 than M2 macrophages²⁰⁰.

1.6.3.5 Role of the infrapatellar fat pad in joint inflammation

The infrapatellar fat pad (FP) is a depot of fat tissue located beneath the patellar, forming a continuous structure with the patellar tendon. Although the FP is inside the joint capsule, it resides outside of the synovial cavity. The precise mechanical function of this adipose tissue remains elusive, but recent evidence points to a possible contribution to the inflammatory environment in the knee joint. Explant cultures of FP generated significantly higher quantities of IL-6 compared to subcutaneous fat²⁰², and conditioned media from FP tissues was able to induce fibrosis (measured by the production of total collagen) in synoviocytes, which is a common observation in OA synovium²⁰³. FP derived cells secrete a host of other molecules (both pro- and anti-inflammatory) *in vitro*, however it is still unknown whether these molecules are produced and to what extent *in vivo*^{204,205}, or to what degree this affects the joint at the various stages of OA.

1.6.4 Risk factors in OA progression: age, gender, previous trauma obesity

1.6.4.1 Age

Often referred to as an age-related disease, OA is significantly prevalent in individuals over the age of 50 years²⁰⁶. The natural course of aging and loading leads to progressive wearing of the joint, which is characteristic of OA. On a cellular level, the hallmarks of aging include telomere shortening (engendering genetic instability), reduced anabolism and intracellular trafficking, senescence and the depletion of stem cell populations²⁰⁷. These processes have

been extensively studied in chondrocytes but are believed to also affect the cells in other joint tissues. In addition, these cellular modifications contribute to an age-related inflammation, or inflammaging, that accelerates joint destruction^{192,207–209}.

1.6.4.2 Gender

Radiographic studies of OA patients, have revealed that women have significantly reduced joint space width in comparison to men²¹⁰. It appears that this gender effect is also dependent on age, in that women show a quicker reduction in joint space width and a higher incidence of OA over the age of 50 years compared to men^{210,211}. Investigations have shown the protective effect of the female hormone oestrogen on cartilage explants against degradative molecules, such as TNF- α and reactive oxygen species, as well as its ability to enhance the production of GAGs in rabbit chondrocytes *in vitro*^{212,213}. The levels of estrogen in women plummet as they get older due to menopause, which could in part account for the onset of OA in women after the age of 50 year²¹⁴.

1.6.4.3 Previous trauma

Cross-sectional and longitudinal investigations have shown that previous trauma to the knee joint is a significant risk factor for the occurrence of degenerative knee disease^{215–217}. Joint instability, muscular weakness and tendon malalignment have all been proposed as effects of trauma that progressively lead to OA²¹⁵. High levels of physical activity (>20 miles running per week), but not moderate levels, have also been correlated with the high risk of developing OA²¹⁸.

1.6.4.4 Obesity

A strong association has been made between obesity and the incidence of OA^{219,220}. Obese women are 4 times more likely to develop OA than healthy women, while obese men are 5 times more likely to develop the disease than healthy men²²¹. It was traditionally thought that overloading of joints was the link between obesity and OA, considering that increased loading has been shown to augment expression of pro-inflammatory molecules and catabolic factors in cultured human articular chondrocytes^{222,223}. However, this mechanism does not explain the high prevalence of OA in low or nonloading joints, such as the hand, in obese individuals²²⁴. Moreover, a loss of weight provides symptomatic relief for patients with hand OA, suggesting that mechanical overloading is not the only cause of obesity-related OA²²⁵. Recent evidence now points to the metabolic and inflammatory role of obesity in driving joint destruction in subsets of OA patients^{223,226,227}. Obesity is accompanied by low-grade systemic inflammation, which is the end product of cytokines and adipokines being released into the circulatory system from inflamed fat tissues²²⁸. Factors including (but not limited to) IL-1, IL-6, leptin and insulin-like growth factor 1 have all been associated with obesity related systemic inflammation, of which leptin is the most extensively linked to OA^{229–231}. The concentrations of leptin in the synovial fluid of OA patients have been significantly correlated to body mass index (BMI), formation of osteophytes and cartilage degradation²³¹. The emergence of systemic inflammation and metabolic syndrome as facets of certain OA groups opens new avenues for patient screening and adapting treatments.

1.7 General management of OA

Adequate treatment is vital for the symptomatic relief and improvement in the quality of life of OA patients. Patient education and physical therapy are important treatment modalities,

but are insufficient effective treatments, alone, in advanced joint failure^{232,233}. In this case, pharmacological and surgical treatments need to be considered. Intra-articular injections of corticosteroids (eg. hydrocortisone tebutate or triamcinolone acetonide) and non-steroidal anti-inflammatory drugs suppress joint inflammation and provide short-term pain relief.^{234–236} Conditions such as infections and anticoagulant therapy are however contraindications to corticosteroids injections. Surgical procedures can be used as alternatives to steroids, which may provide relief over the long term. Osteotomy involves the removal of a wedge of bone to realign a movement axis and, or to alter the distribution of load in the joint^{237,238}. This procedure is often indicated for younger patients with moderate joint degradation, and some healthy cartilage remaining on the articular surface. Debridement is a less invasive procedure where the cartilage surface is smoothed and rid of any flaps or loose tissue bodies²³⁹, but is not considered appropriate for the more advanced stages of OA.

To harness the bodies' inherent ability to repair itself, mesenchymal stem cells (MSCs) can be recruited from the subchondral bone marrow (easily accessible in full thickness cartilage defects) by abrasion or microfracture. However, the fibrocartilage produced by such marrow stimulatory methods is not mechanically comparable to hyaline cartilage. Surgeons also have the option of harvesting cylindrical osteochondral grafts from low weight bearing regions in the knee to then re-implant them into a cartilage defect. This technique, known as mosaicplasty, has the advantage of filling large defects with a biologically functional graft, but may cause some donor site morbidity²⁴⁰. Arthrodesis is the fusion of bones, and can be beneficial in joints such as the spine, ankle or carpus to relieve pain^{241–243}. As aforementioned, advanced stages of OA are characterised by significant pain, reduced range of motion and the deterioration of joint elements. Partial or full joint replacement is then the most effective form of treatment and comprises the substitution of the affected articulating elements with artificial metal, ceramic, or plastic prosthetics.

Although this procedure is relatively expensive, it offers the most reliable results in terms of pain relief and improvements to joint function. Notwithstanding the efficacy of surgical management of OA, there are some limitations that include invasiveness, possibility of infection, implant failure and high costs²⁴³. Joint replacement is not recommended for young patients as the finite lifespan of the implant means revision surgery would be required to replace the implant. This has a further significant cost implication and could ultimately lead to the loss of the limb.

1.8 Autologous Chondrocyte Implantation (ACI) for Cartilage Repair

1.8.1 Introduction to cell based therapies

According to Langer and Vacanti, tissue engineering brings together principles of engineering and biology to produce constructs that can replace damaged body tissues²⁴⁴. In this promising multidisciplinary field, biologically compatible materials are employed to either bring structural support to the native tissue or as a means of delivering cells and small molecules (for example growth factors) to a specific site. Biomaterials are selected according to their physicochemical properties and may take the form of metals, ceramics or polymers^{245–247}. Despite the significant promise and hype, few tissue engineered products and cell therapies have been applied routinely in the clinic. Skin replacements Apligraf® and Epicel® were amongst the first products to be approved by the Food and Drug Administration (FDA)^{248,249}. Since then, the tissue engineering and regenerative medicine (TERM) industry has grown significantly being estimated at approximately \$3.6 billion worldwide in 2012²⁵⁰. Orthopaedic products represented the highest market impact with over \$1.7 billion in sales worldwide. The most important challenge for the TERM and cell therapy industry is the translation phase between basic science and preclinical/clinical

application, despite the remarkable number of clinical trials in progress using stem cells (1618 ongoing trials according to www.clinicaltrials.gov). Most of these proposed therapies rarely show superior patient benefits compared to gold standard treatments, thus making governing bodies hesitant in bringing them to market.

1.8.2 History of ACI

Grande *et al.* initially demonstrated the repair of surgically induced cartilage defects in the patellae of rabbits by the transplantation of chondrocytes isolated from cartilage biopsies in 1989²⁵¹. Five years later, the first results for successful cartilage repair using ACI in 23 human subjects were published⁶. Genzyme's Carticel® was the first cell therapy procedure for the repair of cartilage defects to be approved by the United States (US) Food and Drug Administration (FDA) and is the result of a series of investigations by a group in Gothenburg (Sweden). The basic principle of ACI involves the harvesting of small cartilage biopsies from minor load-bearing areas of the joint during arthroscopy (from the upper medial femoral condyle in the original study), from which chondrocytes are isolated by enzymic digestion. Chondrocytes are then grown *in vitro* in Good Manufacturing Practice (GMP)-compliant conditions for 2-3 weeks. During a second surgical procedure, the chondrocytes are injected as a suspension into the defect, which is then covered with a periosteal flap or some form of collagen membrane such as Chondro-Gide® (1st generation ACI). A retrospective observation of the first patients to receive ACI treatment reported an improvement in joint function which was correlated with the formation of hyaline-like cartilage and in some cases, impressive tissue integration^{252,253}.

Advances in material sciences have offered biocompatible scaffolds upon which cells can be seeded before transplantation (2nd generation ACI). These structures provide a 3 dimensional matrix which has the advantage of retaining the cells within the target site, as opposed to having cells “swimming” freely in a suspension, these structures also negate the possibility of donor site hypertrophy caused by the recovery of a periosteal flap²⁵⁴. This procedure is often referred to as matrix assisted chondrocyte implantation or transplantation (MACI or MACT). In spite of the overwhelming amount of published research demonstrating cartilage regeneration with ACI, the procedure is still not recommended for general clinical use. According to the latest Technology Appraisal from the National Institute of Health and Care Excellence (NICE) in 2008, ACI is not recommended for the treatment of cartilage defects in the knee unless it is part of a research study aimed at proving the efficacy of the procedure²⁵⁵. The reviewing committee highlighted the need for more comparative studies of ACI against surgical techniques such as mosaicplasty and non-surgical methods such as intense physiotherapy. Finally, the paucity of data with regards to the cost effectiveness of ACI is also a limiting factor to its widespread, mainstream clinical translation. The cost of the *in vitro* manipulation of cells alone varies between £2000 and £5000 per patient in the UK, which suggests that efforts will have to be focussed on reducing the general cost of ACI to notably improve its accessibility to patients²⁵⁵.

1.8.3 Clinical outcomes of ACI

Evaluating the efficacy of ACI is normally achieved by assessing joint function, biological repair and the quality and integration of the repair cartilage produced (magnetic resonance imaging (MRI) scans, arthroscopic probing and histology), as well as general outcome measures related to factors such as pain and generic quality of life of the patient^{256,257}. In the follow up assessment performed on the first 101 ACI cases in Sweden, 92% of the subjects

with femoral condyle defects showed good to excellent clinical outcome according to the Brittberg scoring system²⁵². Similar results were obtained for 75% of subjects with femoral condylar defects with ligament reconstruction and 89% subjects with osteochondritis dissecans. Subjects with multiple chondral lesions and those with patella lesions had the lowest scores of 67% and 68%, respectively. Importantly, the presence of hyaline-like cartilage was also reported at the repair site.

A number of other groups have reported varying outcomes in ACI clinical trials. In a 12-24 months follow-up study of 169 ACI patients, a statistically significant functional improvement (Cincinnati score) was reported in cohorts with simple and complex defects (4.3 cm² - 6.75 cm²) post-treatment²⁵⁴. Subjects with salvage defects (11.66 cm²) showed marked improvements in quality of life, based on the Short Form-36 quality of life scoring system²⁵⁴. Another study has demonstrated that patients with a history of prior knee surgeries also show general clinical improvement after ACI treatment²⁵⁸. However, the authors failed to describe the nature of the previous treatment modalities, such that improvements noted may have been as a result of the combined effects of multiple treatments. A multicentre study in the US involving 50 patients also reported significant functional joint improvement 36 months following 1st generation ACI²⁵⁹.

In a randomised trial comparing the clinical outcome (4 scoring systems and histology of repair cartilage) of ACI and microfracture 12 and 24 months postoperatively, the investigators reported no significant differences between the two procedures²⁶⁰. Younger and more active patients did however show better improvement in both groups. A 5-year follow-up assessment revealed an increase in failures with time for both procedures, but also highlighted that patients with predominantly hyaline cartilage at 24 months had no reported subsequent failures²⁶¹.

From a histological perspective, both hyaline and fibrocartilage have been reported following ACI. Haematoxylin and eosin (H&E) and immunohistochemical staining for collagens have been employed to identify areas within the repair site that contain hyaline cartilage, fibrocartilage and a mixture of both²⁶². Less GAG production in the repair sites of ACI subjects than in matched cadaver controls has been previously observed, with chondroitin sulphate chains being significantly shorter in ACI samples²⁶³. Evidence also suggests that some matrix remodelling occurs through enzyme degradation and *de novo* synthesis of structural components such as collagen type II²⁶⁴.

Notwithstanding the relative success of ACI in the majority of reported studies, some complications related to the procedure have been identified. In a systematic review, ACI failure was summarized according to a number of parameters including: insufficient production of regenerative cartilage, symptomatic (pain including joint locking) and/or arthroscopic hypertrophy, poor fusion of new cartilage with native tissue (delamination), chondromalacia and other events requiring reoperation²⁶⁵. Other studies have indicated that male subjects respond significantly better to ACI treatment than women and that age appears to be a key factor in the overall clinical outcome^{266,267}. Obesity and smoking are also recognised as patient-specific markers that negatively influence clinical results²⁶⁸.

The quality of the cells that are transplanted into the patients after *in vitro* expansion has been suggested as a significant factor influencing the efficacy of ACI. One study assessed the viability, CD44 expression and the chondrogenic phenotype of freshly isolated chondrocytes from the knees of 80 patients who received ACI²⁶⁹. These cell characteristics were then correlated against postoperative functional scores. Results showed that cell viability, CD44 and collagen type II expression all significantly influenced the improvement of knee function in this study. Interestingly, aggrecan did not seem to influence clinical outcome. The same research group had previously shown that chondrocytes from young ACI

patients (age 20 or less) showed stronger chondrogenic phenotypes after *in vitro* expansion than those chondrocytes isolated from older patients, an observation that could account for the superior clinical results in younger subjects²⁷⁰.

1.9 Optimisation of ACI

1.9.1 Cell-Matrix combinations

As mentioned previously, a number of biomaterials have been developed to improve the quality of grafts used for ACI. These materials are generally comprised of hyaluronan or collagen. Chondro-Gide® is a porous bilayer membrane comprised of porcine type I and III collagen developed by Geistlich Biomaterials²⁷¹. Hyalofast™ (Anika Therapeutics) is a non-woven pad made of hyaluronan and can operate as a cell scaffold or as a matrix to retain reparative elements from marrow stimulation within a specific site²⁷². BioTissue have created BioSeed®-C and Chondrotissue®, both comprised of a two compartment structure made of a synthetic polymer fleece and either hyaluronan (Chondrotissue®) or a biological glue (BioSeed®-C)²⁷³. These materials have been used in clinical trials worldwide, there is, however, a lack of studies investigating the behaviour of cells within the matrix of these materials.

1.9.2 Alternative cell based strategies for cartilage repair and osteoarthritis

Another strategy for improving the outcome of cell therapies for cartilage repair is by using alternative sources of cells, or a combination of cell types. Stem cells have generated tremendous hope for treating numerous diseases that are otherwise incurable. Stem cells are generally described as having the ability to maintain an undifferentiated state until an appropriate external stimulus (chemical or physical) initiates commitment to other cell lineages. Although their classification and nomenclature remains a contentious debate, stem

cells are commonly categorised according to the origin of the source tissue (embryonic or adult) or their differentiation potential (pluripotent or multipotent).

1.9.2.1 BM-MSCs

Since the discovery of bone marrow derived mesenchymal stem cells (BM-MSCs) in a series of work by Friedenstein *et al.* ²⁷⁴⁻²⁷⁶, a tremendous amount of research has revealed the therapeutic value of these cells ²⁷⁷⁻²⁷⁹. The International Society for Cell Therapy (ISCT) established 3 minimal criteria for the characterisation of BM-MSCs: 1) adherence to tissue culture plastic, 2) expression of specific surface antigens, 3) multipotent differentiation (Figure 1.8)²⁸⁰. When exposed to specific biochemical stimuli, such as TGF- β and dexamethasone, BM-MSCs undergo chondrogenesis *in vitro* making them a candidate cell type for cartilage repair²⁸¹.

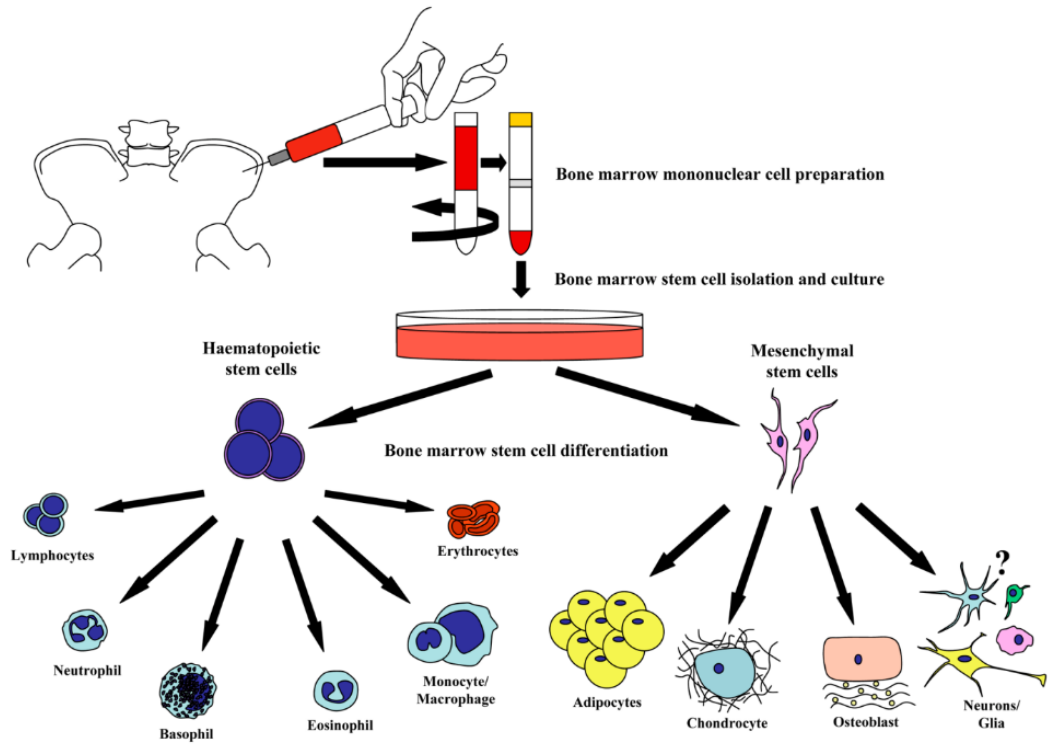


Figure 1.8: Illustration of the isolation and multiple cell lineages into which MSCs have been shown to differentiate. Image taken from Wright *et al*²⁸².

Another key attribute of BM-MSCs that later entered the discussions of MSC characterisation by the ISCT²⁸³, is their ability to modulate the activity of immune cells, notably lymphocytes and macrophages. This has been demonstrated by their capability to diminish the proliferation of peripheral blood lymphocytes both *in vitro* and *in vivo* in a dose dependent manner²⁸⁴. This observation is confirmed in both autologous and allogeneic scenarios and is thought to be mediated by the secretion of molecules by BM-MSCs (paracrine effect)^{284–286}. Similarly, BM-MSCs have the ability to switch the phenotype of macrophages from a pro-inflammatory M1 state to anti-inflammatory M2 state through a paracrine effect involving molecules such as IL-10 and IL-1RA^{287–289}.

The clinical relevance of this immunomodulatory property was revealed when BMSCs were used to successfully treat graft versus host disease in 55 patients who had received haematopoietic stem cell transplantations²⁹⁰. The use of BMSCs for treating OA is thus an attractive option as they may contribute to suppressing the joint inflammation often associated with OA^{35,291}. Contradictory results have been published regarding the capacity of BM-MSCs (and other stem cells) to retain their immunomodulatory properties after differentiation. Some studies showed no difference in the immunomodulatory properties of undifferentiated and chondrogenically differentiated BM-MSCs²⁹², whereas other studies show that BM-MSCs do not simultaneously portray enhanced chondrogenic ability and immunomodulatory properties, but rather display either one or the other²⁹³. In fact, one study has shown that chondrogenically differentiated allogeneic BM-MSCs have lost their ability to inhibit lymphocyte proliferation, but have increased positivity of immunogenic markers such as CD80 and CD86²⁹⁴. This concern needs clarification, but also raises the question of whether BM-MSCs should be used for the regeneration of cartilage (differentiation) or to dampen joint inflammation (paracrine effect). Achieving both functions simultaneously may not be possible²⁹⁵.

Wakitani *et al.*, were among the first to demonstrate the possible use of BM-MSCs for treating full thickness cartilage defects in an animal model²⁹⁶. Numerous human studies have assessed the use of MSCs as either culture expanded cells or as a bone marrow concentrate to treat OA of the knee²⁹⁷⁻²⁹⁹. Histological observations in 2 year follow-ups of cartilage defects that were treated with BM-MSCs showed the formation of normal cartilage (or almost normal according to the ICRS histological score) for only 24% of treated patients³⁰⁰. However, in one comparative study, cultured MSCs were found to be just as effective as chondrocytes (1st generation ACI) in terms of overall knee function and the quality of life of patients. Donor age has been shown to significantly affect the quality, phenotype and differentiation potential of BMSCs and could prove to be a limiting factor in autologous therapies for older patients³⁰¹⁻³⁰³. In addition, retrieving bone marrow aspirate samples can be an invasive procedure resulting in some significant patient discomfort.

1.9.2.2 Adipose stem cells

Adipose tissue derived MSCs (ASCs) have also emerged as an interesting alternative cell source, probably because of the relative abundance and ease of access of fat tissue (usually lipoaspirate or subcutaneous fat biopsies) in the body³⁰⁴. Adipose tissue yields higher cell numbers than bone marrow, with cells having a higher proliferation rate and a comparable differentiation potential *in vitro*^{305,306}. ASCs do not display the same surface marker expression profile compared to BM-MSCs, however the two cell populations share similar immunomodulatory properties³⁰⁷⁻³⁰⁹. The FP is easily accessible during arthroscopy and has been investigated as a source of ASCs (FP-MSCs) for autologous OA therapies³¹⁰⁻³¹². FP-MSCs have been shown to have a higher chondrogenic potential than BM-MSCs, however their immunomodulatory properties have not yet been explored. A recent clinical trial demonstrated the safety (after 6 months) of ASCs from lipoaspirate when injected intra-

articularly to treat OA³¹³. According to the investigators, patients administered with a low dose of ASCs (2×10^6) showed an improvement in joint function and less pain compared to baseline assessments.

1.9.2.3 Synovium and synovial fluid derived stem cells

In addition to its established function in maintaining the composition of the synovial fluid, the knee synovium also harbours a niche of MSCs (SM-MSCs) originally characterised as highly proliferative and multipotent³¹⁴. Three years later, another source of MSCs (SF-MSCs) were discovered in the synovial fluid of patients with OA, RA and other arthropathies³¹⁵. SF-MSCs are believed to originate from the synovium, but this has not yet been proven³¹⁶. There is evidence to support the theory that SM- and SF-MSCs have the role of repairing damaged tissues in the joint notably cartilage, ligament and tendon³¹⁷⁻³¹⁹. A subpopulation of SM-MSCs have been identified and isolated using the markers CD73 and CD39³²⁰. The immunomodulatory properties of SM- and SF-MSCs have not been fully explored. To date, SM- and SF-MSCs have not yet been applied in clinically for the treatment of OA.

1.9.2.4 Embryonic and induced pluripotent stem cells

Embryonic stem cells (ESCs) possess the ability to differentiate into any cell type of the three primary germ layers: ectoderm, mesoderm and endoderm (pluripotent)^{321,322}. The isolation of ESCs from the blastocysts of surplus human embryos intended for *in vitro* fertilisation have initiated some ethical concerns. Furthermore, the ability of ESCs to form teratomas after transplantation in animal models has raised safety issues for cell based therapies³²². However, cell culture and differentiation protocols have been developed to

efficiently generate chondrocytes from ESCs either through direct differentiation, or by multi-step protocols usually involving an intermediate stage of differentiation (such as embryoid bodies or MSCs)^{323–325}.

In a ground breaking investigation, it was demonstrated that pluripotent stem cells could be derived from skin fibroblasts by retroviral transduction of four genes: octamer-binding transcription factor 4 (*Oct4*), (sex determining region Y)-box 2 (*Sox2*), Myc (*c-Myc*) and Kruppel-like factor 4 (*Klf4*)³²⁶. These induced pluripotent stem cells (iPSCs) which have provided the ideal platform for the development of patient specific cells without the concern of immunological rejection. However, like ESCs, safety concerns soon emerged for iPSCs, including the use of viral means of transferring genes into cells, as well as the use of potential oncogenes such as c-Myc to induce pluripotency. Chondrocytes can also be derived from iPSCs using the same protocols mentioned above for ESCs, with the added benefit of the cells being donor-matched to avoid immune rejection^{325,327}. Although chondrocytes obtained from pluripotent stem cells have not yet been tested in humans, these cells provide new possibilities for drug screening and discovery in the field of cartilage regeneration and OA.

1.9.3 Combination of chondrocytes and stem cells

Recent studies have revealed that chondrocyte-MSC co-cultures help to maintain the chondrogenic phenotype of culture expanded chondrocytes *in vitro*; an effect believed to be mediated by the secreted molecules from both cell types^{328–331}. Maumus *et al.* were able to demonstrate this paracrine effect after observing an increase in the expression of hepatocyte growth factor (HGF) in FP-MSCs that were co-cultured with articular chondrocytes³³². When anti-HGF antibodies were added to the culture, the authors observed an increased fibrotic phenotype in the chondrocytes. In another study, the reciprocal effect was also

observed as chondrocytes secreted parathyroid hormone-related protein (PTHrP) to presumably inhibit the hypertrophic differentiation of BM-MSCs³²⁹. ASCs and SM-MSCs were also found to enhance the re-differentiation of chondrocytes^{333,334}.

Results from one of the first human trials involving the co-transplantation of allogeneic BM-MSCs together with freshly isolated autologous chondrons, showed a complete fill of the cartilage defect with hyalin-like cartilage at 12 months follow-up³³⁵. Short tandem repeat analysis revealed the absence of BM-MSCs in the repair tissue after 12 months, which was attributed to their possible clearance by immune cells. This one-step procedure would indeed be less demanding for the patient and would reduce the overall cost of the therapy. Using stem cells and chondrocytes in combination can be advantageous to treat both cartilage defects and joint inflammation.

1.9.4 Hypoxic conditions for cell expansion

Cells in culture are usually incubated at 20% O₂ and 5% CO₂. However, it is important to highlight that these conditions do not recapitulate those found in the native biological tissue of cartilage. A number of studies have estimated the oxygen tension at the articular surface to be approximately 6% which is reduced to as low as 0.5% at the cartilage-bone interface^{336–338}. Consequently, hypoxic (or physiological normoxic) incubation platforms have been developed as a means of maintaining the original cell phenotype *in vitro*. Several studies have shown that BM-MSCs proliferated quicker, produced higher cell yields (30-fold) and upregulate HIF-2 α after 6 weeks culture in 2% O₂ as compared to 20% O₂³³⁹. More recent studies have also showed that hypoxic conditions do not affect the differentiation potential of BM-MSCs³⁴⁰. Oxygen tensions of 2% not only suppress the hypertrophic differentiation of articular chondrocytes, but also induce the re-differentiation of osteoarthritic chondrocytes

by the upregulation of key chondrogenic genes (collagen type II and aggrecan) and the downregulation of collagen type I and genes for MMP1, MMP2, MMP3 and MMP13^{341,342}. Chondrocytes and BMSCs co-cultured on electrospun poly(ϵ -caprolactone) scaffolds at 5% and 20% O₂ produced more GAG and collagen type II at 5% O₂³⁴³.

1.10 Aims of PhD Project

The purpose of this thesis was to explore MSCs derived from the articular joint as alternatives to chondrocytes for the treatment of cartilage defects and OA. This would be accomplished by *in vitro* experiments to characterise the chondrogenic and immunomodulatory of these MSCs, as follows:

- To characterise donor-matched FP- and SF-MSCs a battery of tests was used to compare the growth kinetics, multipotency and immunoprofile of surface markers in the two cell populations. Investigations were also conducted to determine the immunogenic and immunomodulatory properties of FP- and SF-MSCs in response to an inflammatory stimulus (Chapter 3).
- To determine the chondrogenic ability of MSCs and chondrocytes that were culture expanded in normoxia, in hypoxia (Chapter 4).
- To establish a hierarchy of chondrogenic potency among donor-matched BM-MSCs, FP-MSCs subcutaneous fat (SCF-MSCs) and chondrocytes. To identify surface and genetic markers that predict chondrogenesis in matched MSCs and chondrocytes (Chapter 4).

- To characterise the polarisation status of macrophage subsets from the synovium and FP of patients with various arthropathies, and to determine if they can be modulated *in vitro* (Chapter 5).
- To determine whether adipocyte hypertrophy occurs in the FP of obese patients as it does in subcutaneous fat. (Chapter 5).

Chapter 2

Material and Methods

2.1 Cell isolation, culture and maintenance techniques.

2.1.1 Isolation of BM-MSCs

Bone marrow aspirates and bone chips were obtained from the tibial plateau of patients undergoing total knee replacement (TKR). Bone marrow was first diluted with an equal volume of phosphate buffered saline (PBS, Life Technologies Paisley, UK) then layered onto 20 ml of Lymphoprep™ (Alerre Technologies AS, Oslo, Norway) split between two 50 ml tubes (Sarstedt, Nümbrecht, Germany) and centrifuged at 900g for 20 minutes (Figure 2.1). The buffy coat, containing mononuclear cells was aspirated and added to complete culture medium and centrifuged at 750g for 10 minutes. The resulting cell pellet was re-suspended in complete culture medium comprised of Dulbecco's Modified Eagle's Medium/F-12 (DMEM/F-12, Life Technologies) with 1% (v/v) penicillin/streptomycin (P/S, Life Technologies) and 10% (v/v) foetal calf serum (FCS, Life Technologies) and cells were seeded at 20 million cells per 75 cm² tissue culture flask (Sarstedt). After 24 hours incubation, the medium was changed and the non-adherent cells washed off.

Bone chips (5-10cm²) were perfused with complete medium and the wash out was seeded into a 75 cm² tissue culture flask. The bone chips were then placed in a 175 cm² culture flask with 30 ml of complete medium for 7 days to allow the plastic adherent cells to migrate out of the bone chips. All cultures were maintained in a humidified incubator set at 37°C and 5% CO₂.

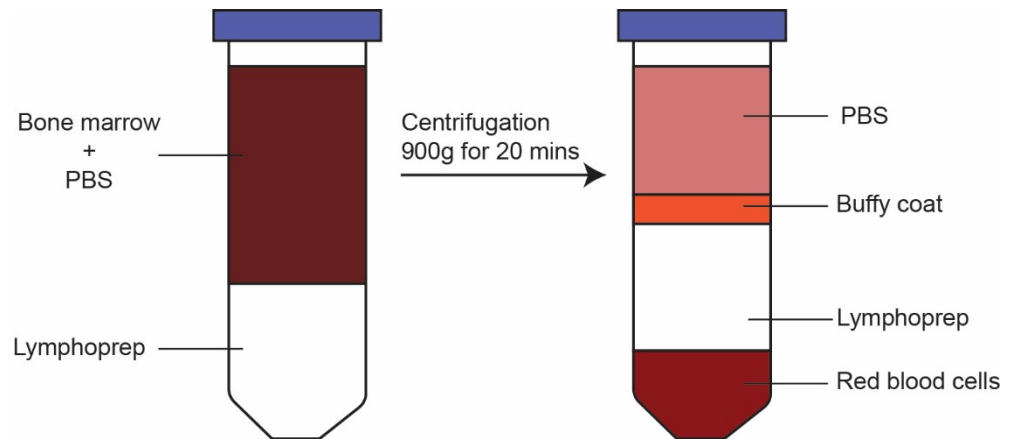


Figure 2.1: Isolation of mononuclear cells from bone marrow. Lymphoprep allows the separation of the bone marrow by density gradient after centrifugation. The BM-MSCs of interests are found in the layer labelled as buffy coat.

2.1.2 Isolation of MSCs from adipose tissues

Human FP and subcutaneous fat (SCF) samples were obtained from patients undergoing either ACI or TKR. FP was assessed macroscopically under sterile conditions using a Nikon SMZ800 dissecting microscope (Nikon, Surrey, UK) and any remaining synovium was removed with a sterile scalpel. The synovium, which is often inflamed in end stage OA, appears red in contrast to the yellow adipose tissue in the deeper layers (Figure 2.2). After dissection, the remaining fat tissue was weighed and transferred to a 25 ml tube (Sarstedt) and washed with PBS to remove blood cells. The FP or SCF samples were then transferred to a dissection dish, minced thoroughly using a sterile scalpel, and placed in a 15 ml tube containing a solution of 1 mg/ml collagenase type I (>125 digesting units/mg, Sigma, Poole, UK) in DMEM/F12 with P/S. This suspension was incubated at 37°C, 5% CO₂ for 1 hour and given a gentle shake every 20 minutes. The resulting digest was strained through a 40 µm nylon cell strainer and centrifuged (350g for 10 minutes), and the supernatant was discarded. The resulting cell pellet was resuspended in complete culture medium and seeded at 5000 cells per cm² in a 25 cm² tissue culture flask (Sarstedt). After 24 hours incubation, the medium was changed and non-adherent cells were washed off.

2.1.3 Isolation of SF-MSCs

A surgeon obtained SF from the knees of patients undergoing ACI by injecting 20 ml of 0.9% saline solution into the joint, followed by flexing of the knee to mix with the SF, after which a needle was used to aspirate the fluid³⁴⁴. SF was also obtained from patients undergoing TKR by inserting a needle into the joint cavity and aspirating the fluid.

SF was centrifuged at 800g for 15 minutes, the resulting pellet was resuspended in complete medium and seeded into a 25 cm² tissue culture flask. Non-adherent cells were washed off after 24 hours and cultures maintained as stated before.

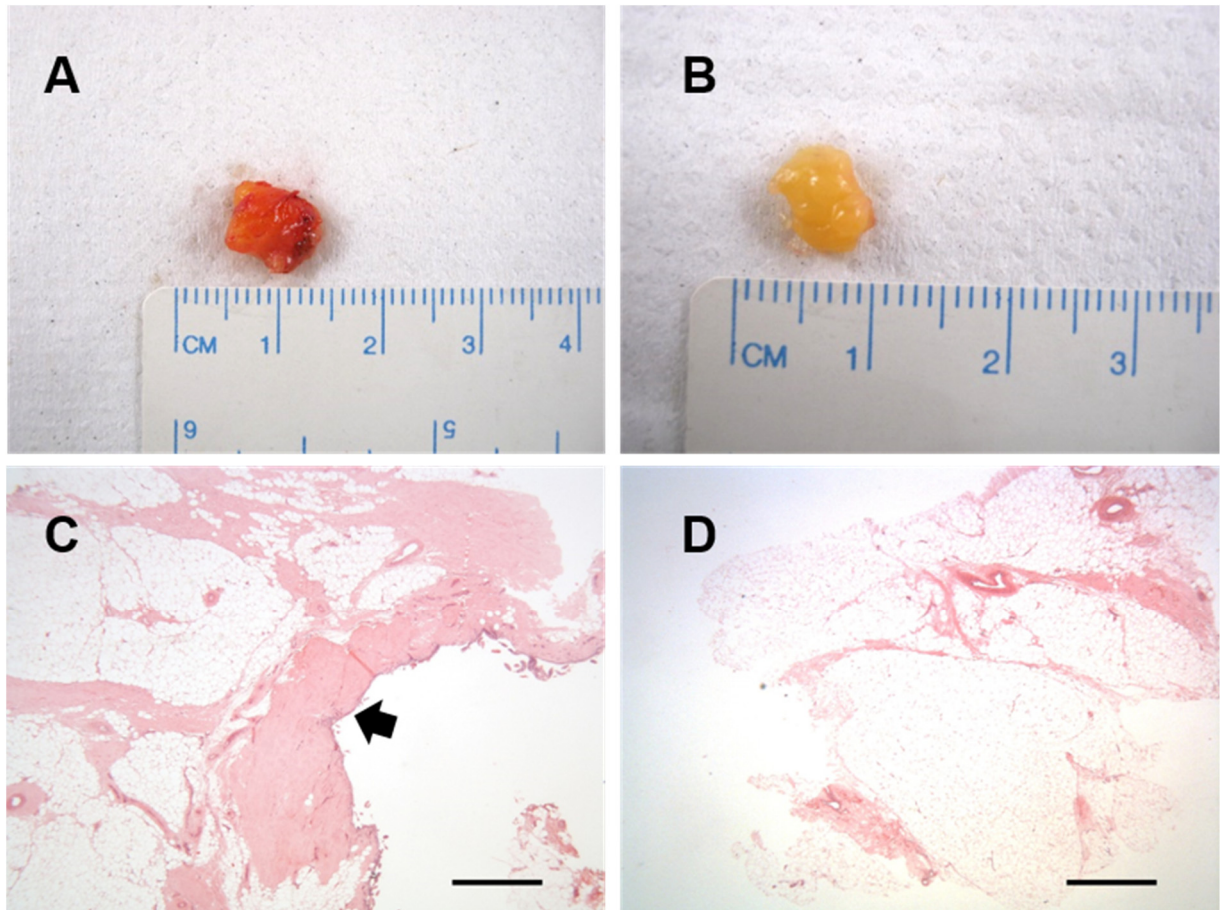


Figure 2.2: Representative images of synovium and FP tissues from an end-stage OA donor. A) The inflamed synovium attached the FP appears red. B) The deep regions of the FP containing predominantly adipose tissue appears yellow. C) Histological representation of synovium (black arrow) attached to FP. D) Histological representation of adipose tissue from deep regions of the FP.

2.1.4 Isolation of chondrocytes

Articular cartilage was excised from the femoral condyles of patients undergoing TKR. Cartilage tissue was weighed, minced into small pieces with a sterile scalpel and digested in collagenase type 2 (≥ 125 units/mg, Worthington, New Jersey, USA) for 16 hours at 37°C. The suspension was passed through a 40 μm strainer and centrifuged (350g for 10 minutes) to produce a cell pellet that was resuspended in complete medium and seeded at a density of 5×10^3 cells/cm³.

2.1.5 Passaging of cells in monolayer culture

After reaching 70-80% confluence, cells were harvested by removal of the spent culture medium, washing once with PBS and incubating with pre-warmed 0.05% trypsin/0.53 mM EDTA (Gibco) at 37°C for 5 minutes. Cells were observed using an inverted light microscope (Nikon) and gentle tapping was applied to help cell detachment from the culture plastic. The activity of the trypsin was neutralised using an equal volume of complete medium and the cell suspension was centrifuged for 10 minutes at 350g. The supernatant was discarded and the resulting cell pellet resuspended in 1 ml of complete medium. 10 μl of the cell suspension was diluted in an equal volume of trypan blue (Sigma) in a microcentrifuge tube; 10 μl of this solution was pipetted under a coverslip on a haemocytometer. Trypan blue was used to assess the viability of the harvested cells; dead cells appeared blue, while live cells excluded the dye and appeared bright. Using an inverted light microscope, at least 200 cells were counted within a certain number of grids on the haemocytometer, to give an estimate of the cell number in the suspension using the following calculation:

$$\text{Number of cells harvested} = N \times 2 (\text{trypan blue dilution factor}) \times 10000 \times V$$

where N is the total number of cells harvested and V is the volume (in millilitres) in which the cells were resuspended. Cells were reseeded at a density of $5 \times 10^3/\text{cm}^2$ in tissue culture flasks, which corresponds to a split ratio of 1:3. The process of trypsinising, counting and reseeding cells will be referred to as a passage throughout this thesis.

2.1.6 Mycoplasma testing of cells

Mycoplasma are a common source of bacterial infection in cell culture that can alter the *in vitro* phenotype of cells including morphology gene expression and viability.³⁴⁵ Routine tests to probe for specific gene sequences using polymerase chain reaction (PCR) were routinely conducted to detect the presence/absence of mycoplasma in cultures.

Firstly, 1 ml of cell culture medium was collected in a sterile microcentrifuge tube and centrifuged at 500g for 5 minutes to pellet any cellular debris. The supernatant was collected and placed in a sterile microcentrifuge tube and centrifuged at 14,000g for 15 minutes to pellet any mycoplasma present. After discarding the supernatant, the pellet was resuspended in 100 μl DNAase /RNAase free water (Sigma). A reaction mix was then prepared according to manufacturer's instructions (Promokine, Heidelberg, Germany).

For each sample, including positive and negative controls, a reaction mix containing 22 μl of rehydration buffer and 1 μl of TAQ polymerase was prepared in a sterile microcentrifuge tube. The contents of each PCR tube provided in the kit were resuspended in 23 μl reaction mix, to which 2 μl of test sample was added (2 μl DNAase /RNAase free water was added for negative controls). Tubes containing positive control templates were prepared with 23 μl reaction mix and 2 μl DNAase/RNAase free water. The contents of each tube was mixed well by agitation, and a thermocycler (Thermo Hybaid, Middlesex, UK) was used to run the following program: 3 minutes at 94°C, followed by 36 cycles of denaturation for 30 seconds

at 94°C, annealing for 2 minutes at 60°C, elongation for 1 minute at 72°C and a final holding step for 5 minutes at 72°C. A 1% (v/v) agarose gel containing SYBR safe DNA stain (1 in 10,000 dilution, Life Technologies) was prepared and loaded into a gel tank with a well comb appropriately positioned. The comb was removed when the gel was set and the tank filled with 89 mM TRIS-borate, 2.5 mM ethylenediaminetetraacetic acid (EDTA) (TBE) buffer. Test samples (7 µl), controls (7 µl) and a DNA ladder (4 µl, Sigma) were loaded into wells within the gel and run at 100V until the PCR products had run at least 2-3 cm. A Gel Doc EZ Imager (BIO-RAD, California, USA) was used to visualise bands under ultra violet light (an example of a whole gel is given in Appendix 1).

2.1.7 Cryopreservation and thawing of cells

Cells were banked for future experiments by cryopreservation using a mixture of dimethyl sulfoxide (DMSO) and FCS. Cells were harvested by trypsinisation, counted as explained in 2.1.5 and resuspended in a solution of 10% (v/v) DMSO in FBS to obtain a final suspension of 1×10^6 cells/ml. This suspension was then slowly pipetted into labelled cryovials (1 ml per tube) and placed into a cryofreezing container (Nalgene, New York, USA), filled with 100% isopropanol at room temperature. The container was then placed in a freezer at -80°C for 24 hours, after which, the cryovials were transferred to liquid N₂ at -196°C for long term storage.

To thaw cells, cryovials were defrosted rapidly in a water bath at 30°C, until a small piece of ice remained. The thawed cell suspension was then transferred in a drop-wise manner to a 25 ml tube containing 10 ml of ice cold complete medium and then centrifuged at 350g for 10 minutes. The supernatant was removed and the cell pellet resuspended in complete medium. At this stage, the cells were counted and reseeded at a density of $5 \times 10^3/\text{cm}^2$.

2.2 Phenotyping of cells

2.2.1 Growth Kinetics

The proliferation rate of cells was assessed by calculating the doubling time (DT) at every passage. Cells were seeded in T25 cm² flasks at a density of 5x10³/cm² until 80% confluence prior to trypsinisation, counting and reseeding into a T25 (1:3 split). The following formula was used to calculate DT at a given passage:

$$\text{Doubling Time} = (t_2 - t_1) \times \frac{\ln(2)}{\ln(n_2/n_1)}$$

where, t_2-t_1 represents the number of days in culture (between passages), n_2 is the number of cells harvested and n_1 is the number of cell seeded initially.

To determine the number of population doublings (PDs) produced by cells at each passage, the following formula was used:

$$PDs = 3.32 (\log N_H - \log N_I)$$

Where N_H is the number of cells harvested and N_I is the initial number of cells seeded.

2.2.2 Trilineage Differentiation of MSCs

To assess their multipotency, MSCs at passage 3 were differentiated along osteogenic, adipogenic and chondrogenic lineages. Osteogenic and adipogenic differentiation was conducted on confluent monolayer cells in 24-well plates (Sarstedt), while a 3D pellet culture model was used for chondrogenesis. Cells were fed with their respective differentiation medium every 2-3 days for 21 days as explained below. Chondrogenesis was also conducted for 28 days for specific experiments, which will be discussed later.

2.2.2.1 Osteogenic differentiation

Cultures were differentiated using osteogenic medium composed of DMEM/F12, FCS (10% v/v), β -glycerophosphate (10 mM, Sigma), dexamethasone (10 nM, Sigma) and L-ascorbic-acid (50 μ M, Sigma)³⁴⁶. Control cells were fed with complete medium for the same period of time.

2.2.2.2 Adipogenic differentiation

Cultures were induced with adipogenic medium containing DMEM F12, FCS (10% v/v), Insulin-transferrin-selenium-X (ITS, 1% v/v) (ThermoFisher, Massachusetts, USA), 3-isobutyl-1-methylxanthine (0.5 μ M) (Sigma), dexamethasone (1 μ M) and indomethacin (100 μ M, Sigma)³⁴⁷.

2.2.2.3 Chondrogenic differentiation

A 3D pellet culture system was used to assess the chondrogenic capacity of cultured cells. Cells were trypsinised, counted and 2×10^5 cells were placed into a sterile 1.5 ml microcentrifuge tube containing chondrogenic medium which consisted of DMEM F12, FBS (10% v/v), P/S (1% v/v), ITS (1% v/v), ascorbic-acid (0.1 mM) (Sigma), dexamethasone (10nM) and TGF- β 1 (PeproTech, London, UK) (10ng/ml)²⁸¹. The microcentrifuge tubes were centrifuged at 350g for 8 minutes to obtain cell pellets.

2.2.2.4 Staining for alkaline phosphatase activity

After 21 days of differentiation, osteogenic potential was evaluated by assessing the activity of the enzyme alkaline phosphatase. A staining solution was prepared by adding 25 mg naphthol AS-BI phosphate (Sigma) dissolved in 500 μ l of dimethyl formamide (Sigma) to 50

mg of Fast Red TR (Sigma) dissolved in 50 ml TrisHCl buffer (Sigma) at pH9. The solution was filtered before use.

Culture medium was removed from the wells and cells were washed with PBS and fixed with 500 µl of methanol for 10 minutes. The cells were then washed with PBS and 500 µl of the stain solution was added to each well for 1 hour at room temperature. The wells were then washed 3 times with distilled water and imaged using an inverted light microscope.

2.2.2.5 Oil Red O staining for lipid formation

Adipogenic potential was assessed by the presence of lipid droplets using the Oil red O stain. A stock solution was prepared by dissolving 500mg of Oil Red O (Sigma) in 100 ml of isopropanol (IPA). A working solution was then prepared by adding 6 ml of the stock solution to 4 ml of distilled water and filtered using filter paper (Whatman, Kent, UK).

Cultures were washed with PBS, fixed for 10 minutes with methanol and incubated with 500 µl of the working solution of Oil red O for 1 hour at room temperature. The wells were then washed with distilled water and imaged with an inverted light microscope.

2.2.2.6 Lysine coating of slides

Poly-L-lysine was used to coat glass slides to allow tissues to adhere to the slides after cryosectioning. The slides (CellPath, Newtown, UK) were submerged in 100% IPA, wiped clean with tissue paper and then submerged in a solution of 10% v/v poly-L-lysine (Sigma) in distilled water for 5 minutes. The slides were then drained and dried in an oven at 37°C overnight before use.

2.2.2.7 Snap freezing and cryosectioning of chondrogenic pellets

After 21 days in chondrogenic medium, pellets were carefully removed from culture medium and placed on filter paper before being immersed for 10 seconds in liquid N₂ cooled hexane. Frozen pellets were stored at -80°C until needed. All cryosectioning steps were performed between -20°C and -30°C. TissueTek® (Sakura Finetek, Zoeterwoude, Netherlands) was placed on a cold chuck, the frozen pellets were submerged in the TissueTek® and frozen using cryospray (CellPath). The chuck was then mounted onto a cryostat where pellets were sectioned at 7 µm and collected on poly-L-lysine coated slides and stored at -20°C until further use.

2.2.2.8 Toluidine blue staining and scoring of chondrogenic pellets for GAGs

Toluidine blue is a metachromatic stain generally used to reveal the presence of GAGs samples³⁴⁸. Frozen slides containing cryosectioned chondrogenic pellets were thawed at room temperature and allowed to air dry. Slides were then flooded with a 1% (w/v) toluidine blue (pH 2.5) (BDH Lab Supplies, Poole, UK) for 30 seconds and briefly immersed in a staining trough filled with tap water to remove excess toluidine blue. The stained slides were air dried and mounted with Pertex (HistoLab, Gothenburg, Sweden) and a coverslip before imaging.

A modified version of the Bern Score³⁴⁹ was used to assess three histological features of chondrogenically differentiated cells in pellet culture: 1) Uniformity and intensity of toluidine blue staining, 2) Distance between cells (amount of matrix produced), 3) morphology of cells (Table 2.1). Each of the three features is given a score between 0-3 and the total sum of the scores is calculated to give one overall histological score (0-9). This

scoring method was modified in that it was performed on pellet sections stained with toluidine blue, as opposed to Safranin O–fast green³⁴⁹.

Table 2.1: Modified Bern Score used to assess chondrogenic pellets stained with toluidine blue³⁴⁹.

Scoring categories	Score
Uniformity and intensity of toluidine blue stain	
No stain	0
Weak staining of poorly formed matrix	1
Moderately even staining	2
Even dark stain	3
Distance between cells/amount of matrix accumulated	
High cell densities with no matrix in between (no spacing between cells)	0
High cell densities with little matrix in between (cells <1 cell-size apart)	1
Moderate cell density with matrix (cells approx. 1 cell-size apart)	2
Low cell density with moderate distance between cells (>1 cell) and an extensive matrix	3
Cell morphologies represented	
Condensed/necrotic bodies	0
Spindle/fibrous cells	1
Mixed spindle/fibrous with rounded chondrogenic morphology	2
Majority rounded/chondrogenic	3

2.2.2.9 Papain digestion of chondrogenic pellets

Chondrogenic pellets were digested with the enzyme papain to release GAGs and DNA. A digestion buffer consisting of 50 mM sodium phosphate (BDH), 2mM EDTA (Sigma) and 20mM N-acetyl cysteine (BDH) was prepared and the pH adjusted to 6. Papain (Sigma) was added to the digestion buffer to reach a final concentration of 125 µg/ml. The solution was then aliquoted and stored at -20°C. Each chondrogenic pellet was placed in a microcentrifuge tube with 200 µl of papain digest and placed in an oven at 60°C for 3 hours. The digest suspension was mixed vigorously every 30 minutes by tapping the tubes. Samples were centrifuged at 1000g for 5 minutes, aliquoted and stored at -20°C until analysed.

2.2.2.10 Dimethylmethylene Blue Assay (DMMB)

The DMMB assay is commonly used to measure the quantity of GAGs in tissues or fluids^{350,351}. The staining solution was prepared by adding 0.59 g NaCl (Sigma), 0.76 g of glycine (Sigma) and 0.4 g of 1, 9-dimethylmethylene-blue (Serva Electrophoresis, Heidelberg, Germany) in 225 ml of distilled water. The pH was adjusted to pH 3.0 using 2M HCl and the volume made up to 250 ml with distilled water. The solution was then filtered using filter paper and protected from light in aluminium foil and stored at room temperature for later use.

Standards were prepared by dissolving chondroitin sulphate (Sigma, C9819) from bovine trachea in PBS to create solutions of 0, 0.05, 0.1, 0.15, 0.2 µg/µL in microcentrifuge tubes. 50 µl of samples or standards were added to the wells of a 96-well plate in triplicate and 200 µl of the DMMB staining solution was added to each well. The absorbance was immediately read at A_{530nm} and A_{590nm}. Each sample and standard were processed as follows:

$$(A_{530\text{nm}}/A_{590\text{nm}})-(A_{530\text{nmblank}}/A_{590\text{nmblank}})$$

where $A_{530\text{nm}}$ =absorbance of samples (or standards) at 530 nm, $A_{590\text{nm}}$ = absorbance at 590 nm, $A_{530\text{nmblank}}$ = absorbance of 0 $\mu\text{g}/\mu\text{l}$ standard at 530 nm and $A_{590\text{nmblank}}$ = absorbance of 0 $\mu\text{g}/\mu\text{l}$ standard at 590 nm. A standard curve was plotted from which the total GAG content in each sample was calculated using the equation of the curve.

2.2.2.11 DNA Assay

Results obtained from the quantification of GAGs using the DMMB assay requires normalisation to DNA content due to the variability observed in the cellularity of the pellets. The PicoGreen® fluorescence assay (Invitrogen, Paisley, UK) allows for the quantitation of double stranded DNA in solution and was conducted according to the manufacturer's instructions. A 1:200 dilution of the PicoGreen reagent was made in 10 mM Tris-HCl, 1 mM EDTA, pH 7.5 buffer (TE buffer) and kept in the dark at room temperature. A 1:50 dilution of the lambda DNA standard provided in the PicoGreen® kit was prepared and further diluted to 1:40 in TE buffer for a final DNA concentration of 2 $\mu\text{g}/\text{mL}$. This stock solution was then used to create standard concentrations of 1 $\mu\text{g}/\text{mL}$, 100 ng/mL , 10 ng/mL , 1 ng/mL in TE buffer and TE buffer alone was used as a blank. Experimental samples were diluted 1:20 in TE buffer. Both the standards and the experimental samples (100 μL) were dispensed in triplicate into the wells of a flat-bottomed 96-well plate, and 100 μL of the diluted PicoGreen reagent was added to each well. The plate was incubated at room temperature for 2-5 minutes in the dark after which the fluorescence was read on a plate reader (BMG Labtech, Ortenberg, Germany) configured to excitation=480nm and emission=520nm. The fluorescence value of the blank was subtracted from each sample/standard and the concentration of DNA was determined using the standard curve. The normalisation of GAG content in chondrogenic pellets was achieved by dividing the total GAG content of a given pellet by the DNA content of that same pellet.

2.2.3 Cell surface marker detection by flow cytometry

2.2.3.1 Introduction

Flow cytometry is a technology that utilises a combination of fluidics, optics and electronics to measure the physical attributes of cells (and other particles). A fluidics system is used to channel a stream of cells in single file through lasers resulting in the deviation (or scatter) of light depending on the physical properties of a cell (such as size and granularity), and the emission of light (fluorescence). Detectors capture these scattered and emitted lights, which are converted into electronic signals by a computer for analysis. Single colour flow cytometry involves the use of fluorochrome conjugate monoclonal antibodies to detect the presence of a specific antigen from emitted fluorescence at a single wavelength. On the other hand, multicolour flow cytometry allows the simultaneous detection of multiple antigens produced by a cell using antibodies against these different antigens that are conjugated to different fluorochromes.

2.2.3.2 Preparation of cells for flow cytometry

A panel of cell surface markers were selected based on the ISCT minimum criteria for characterising cells as MSCs^{280,352} (Table 2.2) , in addition to profiling their chondrogenic potency^{269,320,353–358} and immunomodulatory phenotype³⁵⁹, via multi-colour flow cytometry (Table 2.2). Experiments were conducted on monolayer cells at P3. For the ISCT MSC criteria, 100 000 cells were resuspended in a universal tube containing 1 ml 2% (w/v) bovine serum albumin (BSA, Sigma) in PBS and 10% (v/v) of human IgG (Grifols, Barcelona, Spain) and incubated at 4°C for 1 hour as a blocking step. The tube was centrifuged at 500g for 5 minutes and the pellet was resuspended in 500 µL 2% (w/v) BSA and distributed evenly between 5 flow cytometry tubes (100 µl per tube). Fluorochrome conjugated antibodies against CD73, CD90, CD105, CD11b, CD14, CD19, CD34, CD45, and Human Leukocyte

Antigen-D Related (HLA-DR) (BD Biosciences, Oxford, UK) were added to the tubes according to the dilutions and layout given in Table 2.3 and Figure 2.3, respectively.

The positivity of the following putative chondrogenic potency markers was examined using single/multicolour flow cytometry using conjugated antibodies (Table 2.3 and Figure 2.3 B): CD44, CD166, CD49c, CD151, CD39, CD271, FGFR3 and α ROR2. The presence of the immunomodulatory marker CD106 was also determined. Cells were incubated with antibodies for 30 minutes at 4°C in the dark and then washed with 1 mL of 2% (w/v) BSA per tube, centrifuged at 500g for 5 minutes. The supernatant was carefully aspirated from each tube and the remaining cell pellet resuspended in 300 μ L of 2% (w/v) BSA. Samples were then acquired on the FACS CantoII cytometer. A FACSCanto II flow cytometer (BD Biosciences) was used to acquire data and the FACS Diva version 7.0 or Flowjo version 10 (Ashland, Oregon, USA) software were used to analyse data.

Table 2.2: Description of markers used to characterise MSC and chondrogenic potency.

Marker (ref)	Cell selection	Marker Name
CD73 ⁽²⁸⁰⁾	MSC (+)	5'-nucleotidase
CD90 ⁽²⁸⁰⁾	MSC (+)	Thy-1
CD105 ⁽²⁸⁰⁾	MSC (+)	Endoglin
CD14 ⁽²⁸⁰⁾	MSC (-)	Monocyte differentiation antigen
CD11b ⁽²⁸⁰⁾	MSC (-)	Integrin alpha M
CD19 ⁽²⁸⁰⁾	MSC (-)	B-lymphocyte antigen
CD34 ^(280,352)	MSC (-/+)	Hematopoietic progenitor cell antigen
CD45 ⁽²⁸⁰⁾	MSC (-)	Protein tyrosine phosphatase receptor type C
HLA-DR ⁽²⁸⁰⁾	MSC (-)	Human leukocyte antigens-DR
CD40 ²⁸³	Immunogenic	TNF Receptor Superfamily Member 5
CD80 ²⁸³	Immunogenic	B7-1, costimulatory molecule
CD86 ²⁸³	Immunogenic	CTLA-4 Counter-Receptor B7.2
HLA-G ^{360,361}	Immunomodulatory	Human leukocyte antigens-G
CD44 ^(269,353)	Chondropotency	Hyaluronate Receptor
CD166 ^(354,355)	Chondropotency	Activated leukocyte cell adhesion molecule
CD49c ⁽³⁵³⁾	Chondropotency	Integrin alpha 3
CD106 ⁽³⁵⁹⁾	Immunomodulatory	Vascular cell adhesion protein 1
CD151 ⁽³⁵³⁾	Chondropotency	Raph blood group
CD39 ⁽³²⁰⁾	Chondropotency	Ectonucleoside triphosphate diphosphohydrolase-1
CD271 ^(357,358)	Chondropotency	Low-affinity nerve growth factor receptor
FGFR3 ⁽³⁵⁶⁾	Chondropotency	Fibroblast growth factor receptor 3
α ROR2 ⁽³⁵⁶⁾	Chondropotency	Receptor tyrosine kinase-like orphan receptor 2

Table 2.3: Fluorochrome-conjugated antibodies used to identify MSC and chondrogenic potency surface markers.

Marker (ref)	Clone(s)	Isotype control	Fluorochrome	Dilution
Negative cocktail	ICRF44, HIB19, 581, HI30, TU36	IgG1 IgG2a	PE*	1:5
CD73	AD2	IgG1	BV421*	1:100
CD90	5E10	IgG1	PE	1:200
CD105	266	IgG1	APC*	1:100
CD14	MφP9	IgG2b	PercP-Cy5.5*	1:100
CD11b	ICRF44	IgG1	PE	1:100
CD19	HIB19	IgG1	BV421	1:200
CD34	581	IgG1	APC	1:20
CD45	HI30	IgG1	PE	1:20
HLA-DR	TU36	IgG2b	APC/PE	1:5
CD40	5C3	IgG1	PE	1:20
CD80	L307	IgG1	PE	1:50
CD86	2331	IgG1	PE	1:50
HLA-G	MEM-G/9	IgG1	FITC	1:20
CD44	G44-26	IgG2b	PercP-Cy5.5	1:100
CD166	3A6	IgG1	BV421	1:20
CD49c	C3 II.1	IgG1	PE	1:20
CD106	51-10C9	IgG1	APC	1:2.5
CD151	14A2.H1	IgG1	PE	1:5
CD39	TU66	IgG2b	APC	1:1.25
CD271	C40-1457	IgG1	BV421	1:20
FGFR3	136334	IgG1	APC	1:100
αROR2	231509	IgG2a	APC	1:50

*PE: Phycoerythrin, BV421: Brilliant Violet 421, APC: Allophycocyanin, PercP-Cy5.5: Peridinin-chlorophyll-protein-Cyanine5.5.

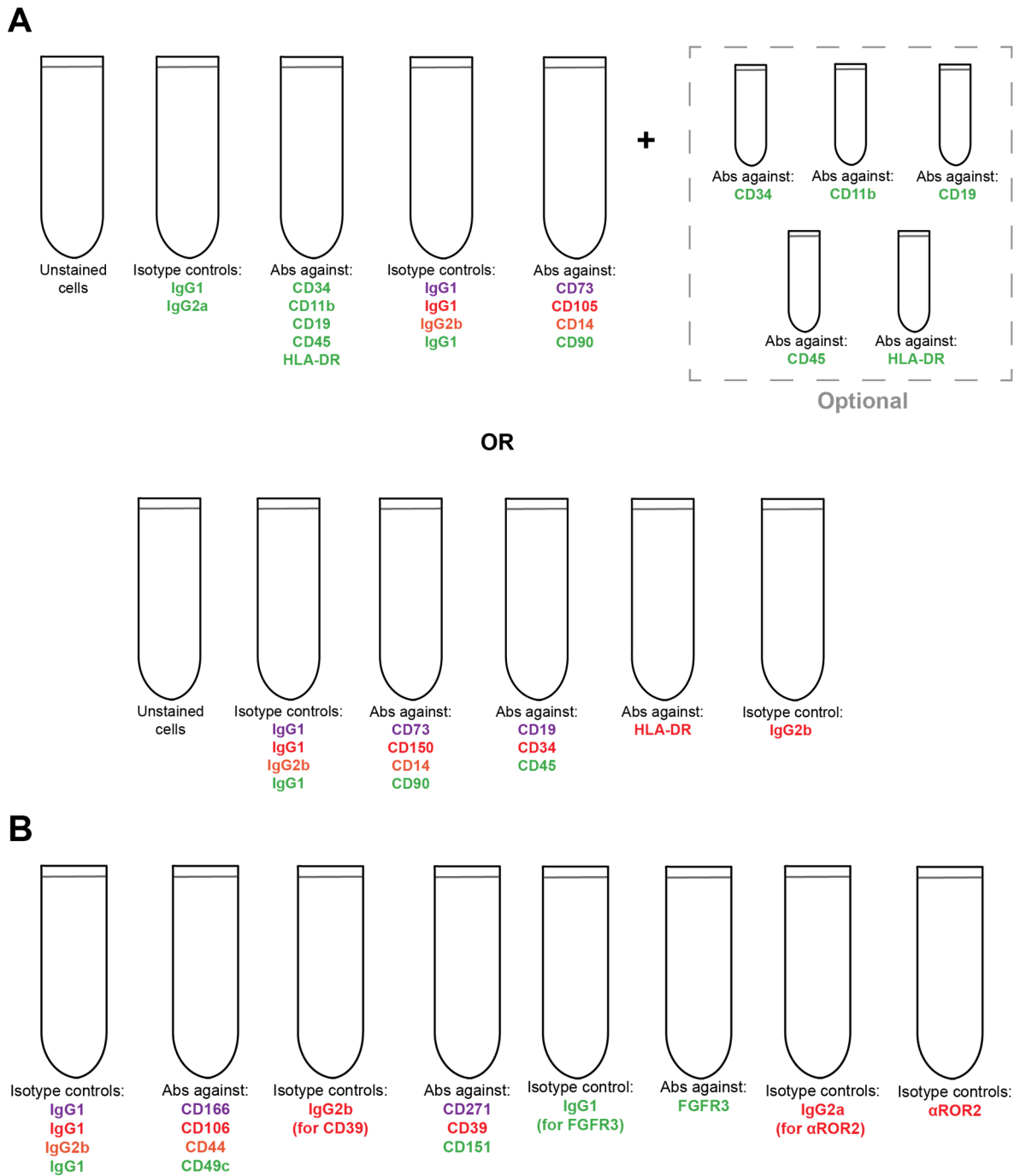


Figure 2.3: Distribution of fluorochrome conjugated antibodies (Abs) in tubes for flow cytometry. A) Abs used to characterise cells for MSC surface markers. B) Abs used to identify putative chondrogenic surface markers. Fluorochromes are indicated as purple (BV421), red (APC), orange (PercP-Cy5.5), green (PE).

2.2.3.3 Analysis of flow cytometry results

The analysis of flow cytometry data was conducted as illustrated in Figure 2.4. Debris and cell doublets (two or more cells attached to each other) were gated from the scatter plots and a positivity gate (i.e. 99% of the cells are negative) is established on the singlet population of cells stained with the isotype controls. This gate is then applied to test sample containing the marker of interest to obtain the percentage of cells that are positive for that marker in the population.

2.2.4 Stimulation of MSCs with IFN- γ

The ISCT have proposed that the assessment of the immunogenic and immunomodulatory properties of MSCs be conducted as part of the characterisation process²⁸³. It was recommended that MSCs be exposed to pro-inflammatory conditions (IFN- γ and or TNF α) and tests be performed to evaluate their response by monitoring the levels of specific molecules as detailed below.

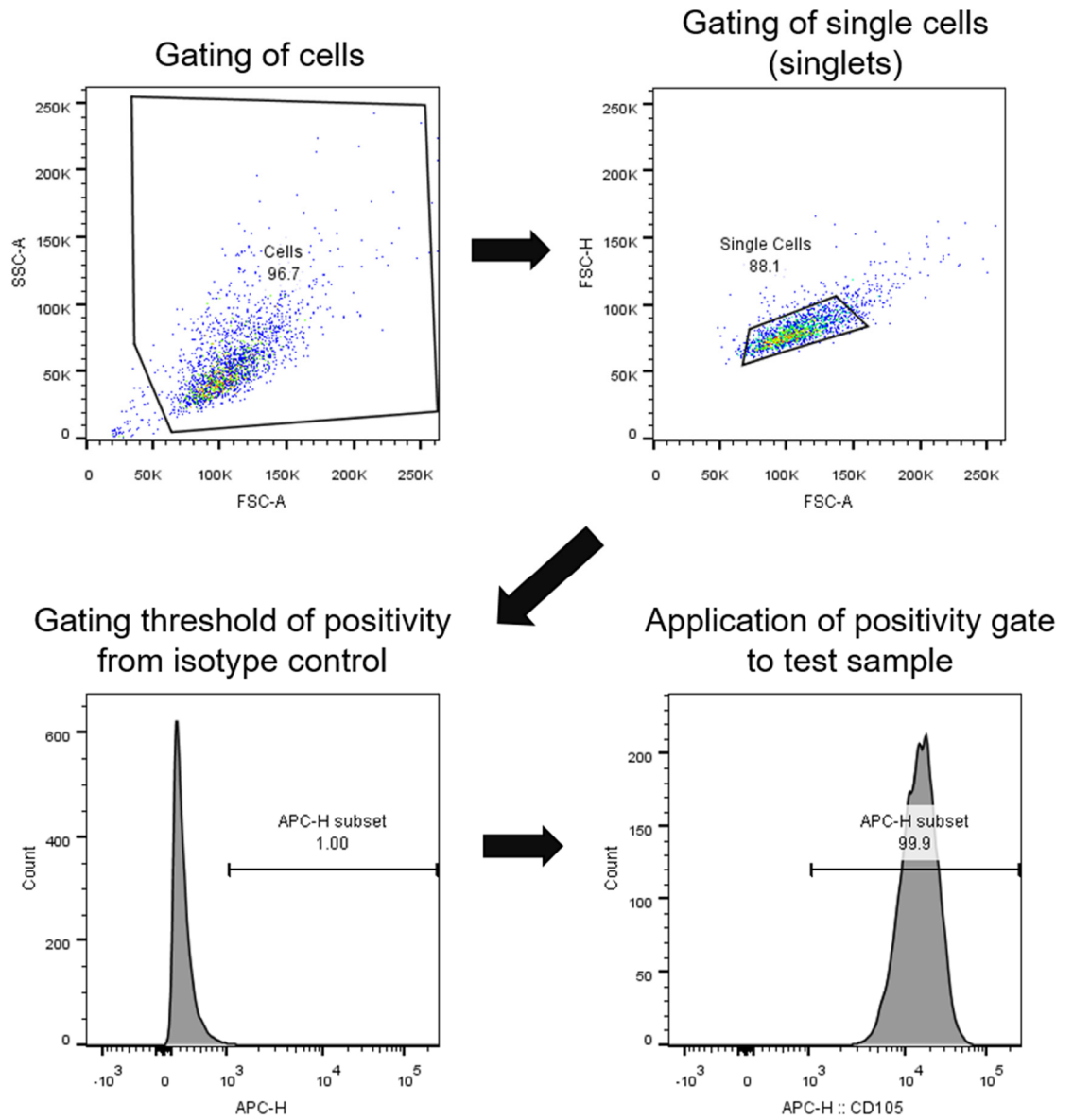


Figure 2.4: Example of flow cytometry analysis to determine the positivity of a surface marker.

2.2.4.1 Characterisation of co-stimulatory and Major Histocompatibility Complex class II markers after stimulation with IFN- γ .

The immunogenic nature of FP-MSCs and SF-MSCs was investigated by assessing the presence of the costimulatory markers CD40, CD80, CD86, and the Major Histocompatibility Complex (MHC) class II marker, HLA-DR, after stimulation with IFN- γ ($\geq 2 \times 10^7$ units/mg, PeproTech). Cells at P3 were exposed to complete culture medium containing either 25 ng/ml (low concentration, ≥ 500 units/ml) or 500 ng/ml (high concentration, 1×10^5 units/ml) of IFN- γ for 48 hours. Untreated cells grown in complete medium were used as controls for comparison. After stimulation, cells were prepared for single colour flow cytometry as described previously with PE-conjugated antibodies against CD40, CD80, CD86 (BD Biosciences) and HLA-DR (Immunotools, Friesoythe, Germany) (Table 2.3).

2.2.4.2 Detection of immunomodulatory markers

Human Leukocyte Antigen- G (HLA-G) was assessed via flow cytometry using antibodies against surface and intracellular antigens (Santa-cruz, Texas, USA). Cells at P3 were incubated for 20 minutes in a Cytofix/CytopermTM solution (BD Biosciences) for fixation and permeabilisation. The cells were then washed and resuspended in 100 μ l of 2% (w/v) BSA, stained with unconjugated antibodies against HLA-G for 30 minutes at 4°C (Table 2.3 for dilution), followed by a wash and resuspension in 100 μ l with 2% (w/v) BSA. A 1:20 dilution of Fluorescein isothiocyanate (FITC) conjugated antibodies against the HLA-G were used to label the cells for 30 minutes at 4°C. After a final wash in 2% (w/v) BSA, flow cytometry data was acquired and analysed as described previously.

The production of indoleamine 2,3-dioxygenase (IDO) by cells at P3 was evaluated after stimulation with IFN- γ by Western blot. Cells were trypsinised as described previously, lysed with cold radioimmunoprecipitation assay buffer (RIPA buffer, 100 μ l buffer per 1×10^6 cells) containing 25 mM Tris-HCl pH 7.6, 150 mM NaCl, 1% NP-40, 1% sodium deoxycholate, 0.1% SDS and protease inhibitors (ThermoFisher) at 4°C, and stored at -20°C until further use.

The bicinchoninic acid (BCA) assay (Life Technologies) was used for the quantification of total protein in each sample. Standards were prepared using BSA according to the manufacturer's guidelines for a working range of 20-2000 μ g/mL. 25 μ L of the standards and samples was dispensed into duplicate wells of a round bottomed 96-well microplate (Sarstedt) prior to the addition of 200 μ L of BCA working reagent to each well and incubation at 37°C for 30 minutes. The plate was allowed to cool for 10 minutes and the absorbance was read at 562 nm. After quantification of total protein, 20 μ g of each sample was loaded into pre-cast NuPAGE® 4-12% Bis-Tris gels (Life Technologies). An iBlot and transfer stack system (Life Technologies) was used to transfer proteins onto a nitrocellulose membrane. Primary and secondary antibodies were added to detect IDO at dilutions of 1:250 and 1:125, respectively, in antibody diluent (Life Technologies). The primary antibody (Abcam, Cambridge, UK), against IDO, was used to probe the membrane for 7 minutes using the iBlot system. The secondary antibody (1:125, Life Technologies, conjugated to horseradish peroxidase) was applied for 7 minutes. Membranes were washed three times with a wash solution (Life Technologies), then twice with autoclaved water on a rocker. A chromogenic substrate solution, Novex^R Alkaline Phosphatase (Life Technologies), was added to the membranes, after which colour development was allowed for no longer than an hour protected from light. Membranes were washed again in autoclaved water before being

allowed to dry in the dark prior to imaging with a Canon Powershot A490 camera (Canon, Tokyo, Japan).

2.2.5 Differentiation of cells in hypoxic conditions

A SCI-tive Hypoxia workstation (Baker Ruskinn, Bridgend, UK) was used to assess the effect of a low oxygen environment on the phenotype and differentiation of chondrocytes and MSCs (Figure 2.5 A). In the experiments presented here, 2% O₂ in 5% CO₂ and 93% air was considered as hypoxia whereas standard culture conditions (21% O₂ in 5% CO₂ and 74% air) was considered normoxia. All experiments in hypoxic conditions were performed using culture medium that was pre-conditioned at 2% oxygen in the HypoxyCOOL™ system (Baker Ruskinn, Figure 2.5 B). To accomplish this, bottles of medium with filtered caps were incubated in the HypoxyCOOL™ configured to run for 3 hours at 4°C with agitation (usage of the HypoxyCOOL™ was kindly provided by Professor Nick Forsyth). Using a low temperature of 4°C with agitation increases the rate of gas exchange and allows the stable conditioning of the culture medium.

A**B**

Figure 2.5: HypoxyCOOL™ and Sci-tive. A) Chondrogenic pellets were incubated and fed in the closed system of Sci-tive at 2%. B) Culture media was conditioned to 2% O₂ in the HypoxyCOOL™.

2.2.5.1 Measuring oxygen levels in culture medium

Two dissolved oxygen meters, the Seven2Go Pro (Mettler Toledo, Columbus, USA) and the Hanna HI2040 (Hanna Instruments, Rhode Island, USA) (Appendix 2), were used to confirm the oxygen levels in the medium that was used to culture cells in hypoxic and normoxic conditions. Oxygen levels were measured in the following conditions:

- Normal medium and pre-conditioned medium measured in ambient conditions (21% O₂).
- Normal medium and pre-conditioned medium incubated in the SCI-tive for 24 hours.
- Medium from cells incubated in a standard incubator (21% O₂) or in the SCI-tive (2% O₂) for 24 hours.
- Pre-conditioned medium (2% O₂) left open in ambient air for 3 hours. Oxygen levels were measured every hour.

For each oxygen meter, measurements were obtained with and without stirring the probe in the fluid to ensure that the measurements were representative of the entire fluid and not just the areas immediately around the probes.

2.2.5.2 Differentiation of cells in hypoxia

Chondrocytes and either BM-MSCs, FP-MSCs or SCF-MSCs isolated and grown in standard normoxic conditions up to P3. Cells were then trypsinised, counted and centrifuged to form 12 chondrogenic pellets for each cell type. Six of the pellets, 3 for GAG/DNA analysis and 3 for histology, were then transferred into the SCI-tive hypoxia work station and fed with pre-conditioned hypoxic complete medium with supplements to induce chondrogenesis (as described previously in section 2.2.2.3). The six other pellets were differentiated in normoxic conditions. Chondrogenic differentiation was conducted for 28

days after which the pellets were harvested and processed as described previously for further analysis.

2.3 Histology of the infrapatellar fat pad and synovium

2.3.1 Tissue fixation and wax embedding

FP tissue samples were obtained from TKR or ACI patients in operating theatres and observed under a dissecting microscope to localise the attached synovium as described in section 2.1.2. Fat and synovium were prepared for embedding as follows. A solution of 4% neutral buffered formalin (NBF) was prepared by mixing formaldehyde (1:10 dilution, BDH) in distilled water containing 0.03 M sodium dihydrogen orthophosphate (BDH) and 0.05 M of disodium hydrogen orthophosphate (BDH) at pH 7.4. After dissection, the tissues were fixed in NBF for at least 48 hours at room temperature. These samples were then processed by the pathology laboratory at the RJAH Orthopaedic Hospital as follows. Following fixation, tissues were mounted onto labelled cassettes, and samples were then placed in the following industrial methylated spirit (IMS, Gent Medical, York, UK) solutions for 1 hour each; 70%, 90%, 95%, 100%, 100% and 100%. The samples were successively immersed in two xylene solutions for 1 hour each prior to immersing twice in Fibrowax™ (VWR, Pennsylvania, USA) at 62°C for 1 hour. The cassettes were mounted onto a mould into which hot Fibrowax was dispensed and allowed to cool for 30 minutes or until wax was solidified. The mould was then detached from the wax blocks and the tissues sectioned.

2.3.2 Sectioning of tissues

Wax embedded tissues blocks were sectioned at 5 µm thickness on a microtome (Leica, Wetzlar, Germany). Serial sections were gently placed in a container of warm water and caught onto slides, followed by drying at 37°C for at least 24 hours.

2.3.3 Haematoxylin and Eosin staining

The H&E stain is commonly used in histology to reveal the general morphology of tissues³⁴⁸. Haematoxylin is a basic dye that stains acidic structures (such as the cell nuclei) purple-blue, whereas eosin is an acidic dye that stains basic structures such as connective tissues and various components of the cytoplasm³⁴⁸. For cryosections, slides were brought to room temperature before staining. Wax embedded samples were deparaffinised by successive immersions in the following solutions for 5 minutes each: xylene x2, 100 % ethanol x2, 96% ethanol and 70% ethanol. Slides were then rinsed twice each with distilled water for 3 minutes.

All slides were placed on a slide rack and flooded with either Gill's Haematoxylin (Sigma) or Harris's Haematoxylin (ATOM Scientific, Cheshire, UK) for 5 mins, then rinsed with tap water for 5 minutes. Slides were then flooded with 1% eosin (v/v in distilled water) for 30 seconds, dipped quickly in distilled water, then placed in 70% (v/v) IPA for 2 minutes. In order to dehydrate the samples, slides were successively submerged in the following ethanol solutions in distilled water (v/v) for 1 minute each: 96% ethanol, 100 % ethanol, xylene x2. The slides were mounted with Depex (Sigma) while still wet with xylene and allowed to dry in a fume hood for at least 1 hour.

2.4 RNA extraction and quantitative real-time polymerase chain reaction (RT-qPCR)

The PCR assay is used to amplify DNA in order to assess the gene expression fold change. PCR involves repeated changes in temperature (cycles) that exponentially produces targeted DNA sequences using the DNA polymerase enzyme. In the experiments below, messenger RNA (mRNA) was first extracted from cells to produce complementary DNA (cDNA), followed by qRT-PCR to evaluate the expression of specific genes. The qRT-PCR method allows for the monitoring, recording and quantitative analysis of PCR as it occurs, as opposed to an end stage analysis of the PCR product.

2.4.1 Extraction of mRNA from cells

An RNeasy extraction Kit (Qiagen, Hilden, Germany) was used to obtain mRNA from cells according to the manufacturer's recommendations. After trypsinisation, 200 000 cells were counted, centrifuged in a 1.5 mL microcentrifuge tubes, snap frozen in liquid N₂ and stored at -80°C until further use. Cells were thawed, and resuspended in 350 µL lysis buffer (provided with kit) containing a 1:100 dilution of 2-mercaptoethanol (Sigma), ensuring the suspension was properly mixed. 350 µL of 70% (v/v) molecular biology grade ethanol in RNase free water (Sigma) was added to the tube and the total volume was then pipetted onto a spin column placed in a 2 mL collection tube and centrifuged at 8000g for 1.5 minutes. The resulting mRNA which was attached to the column was then washed twice by adding 500 µl of RPE buffer (wash solution provided in kit) and centrifugation at 8000g for 1.5 minutes. The mRNA was then eluted from the column using 50 µl of RNase-free water, collected in a sterile microcentrifuge tubes and stored at -80°C until further use.

2.4.2 Generation of cDNA from mRNA

The QuantiTect Reverse Transcription Kit (Qiagen) was used to generate cDNA according to the guidelines provided. This process converts the mRNA previously extracted into complementary strands of DNA to be used in the RT-qPCR. All steps of cDNA production were performed on ice.

The mRNA (25 μ L) was pipetted into a sterile microcentrifuge tube together with a reaction mix containing: 5 μ L of reverse transcriptase buffer, 2 μ L of dNTP mix, 5 μ l random primers, 2.5 μ L of multiscribe reverse transcriptase enzyme and 10.5 μ L of RNase-free water. The tubes were then placed in a thermal cycler (Techne, Cambridge, UK) programmed to incubate at 25°C for 10 minutes, then at 37°C for 2 hours, followed by a final holding step at 4°C. Samples were stored at -20°C until further use.

2.4.3 Assessing gene expression via RT-qPCR

The SYBR Green® chemistry, a dye that specifically binds to double stranded DNA as it is produced, was used to monitor gene amplification. A reaction mix consisting of: 10 μ l of SYBR Green Master Mix (Taq DNA polymerase, dNTP and SYBR Green dye), 2 μ l of primers for the target gene and 6.4 μ l RNase free water was prepared for each gene of interest and kept on ice. Table 2. 4 gives a description of the target genes that were used. 1.6 μ L of the previously generated cDNA were pipetted into triplicate wells of a 96-well PCR reaction plate together with 18.4 μ L of the reaction mix.

Table 2. 4: Primers used for qRT-PCR

Primer name	Description
Reference genes	
<i>PPIA</i>	Peptidylprolyl isomerase A. An enzyme that catalyses the isomerisation of certain peptide bonds.
<i>TBP</i>	TATA-binding protein. A protein that binds to DNA and forms part of a transcription factor involved in the transcription of a wide range of genes.
Chondrogenic Genes	
<i>SOX9</i> ^{78,362}	Sex determining region Y-box 9. Master regulator of chondrogenesis and chondrogenic differentiation.
<i>COL2A1</i> ^{362,363}	Collagen type II. Key component of the extracellular matrix of articular cartilage.
<i>ACAN</i> ^{46,362}	Aggrecan. Key component of the extracellular matrix of articular cartilage.
<i>FRZB</i> ^{362,364}	Frizzled-related protein. Intervenes in the developmental formation of cartilage.
Hypertrophic Genes	
<i>ALK-1</i> ^{362,365}	Activin A receptor type II-like 1. Involved in the hypertrophic differentiation of chondrocytes and is associated with the increased expression of MMP-13.
<i>COL10</i> ³⁶⁶	Collagen type X. This is produced by terminally differentiated chondrocytes

All primers were obtained from Qaigen (Hilden, Germany).

The plate was then sealed with an optical adhesive film (Applied Biosystems, Foster City, USA) and placed in a Quant Studio3 Real-Time PCR System (Applied Biosystems) configured to run the following temperature programme: activation (10 minutes at 95°C); 40 repeated cycles of denaturation (10 seconds at 90°C); annealing (30 seconds at 55°C) and extension (34 seconds at 72°C); followed by a final dissociation step (10 seconds at 94°C, then 30 seconds at 55°C and 10 seconds at 90°C).

Preliminary tests were conducted on commonly used reference genes³⁶⁷ Peptidylprolyl isomerase A (*PPIA*), Beta-2 microglobulin (*B2M*), TATA-binding protein (*TBP*), Glyceraldehyde 3-phosphate dehydrogenase (*GAPDH*) and hypoxanthine phosphoribosyltransferase 1 (*HPTRI*), to determine which two were the most stable across the cells populations tested. *PPIA* and *TBP* showed the most favourable results (Appendix 3) and were used as the reference genes for all RT-qPCR experiments.

The relative expression of each gene was determined using the $2^{-\Delta CT}$ method^{368,369}. The Quant Studio Design and Analysis Software™ (Applied Biosystems) was used to set the baseline (initial cycles with little/no fluorescent signal) and obtain C_T values (the cycle number at which the fluorescence passes the threshold of baseline fluorescence), as illustrated in Figure 2.6.

The following equation was used to determine the relative gene expression, where the PCR signal of the target transcript is compared to the reference gene.

$$2^{-\Delta CT}$$

Where $\Delta C_T = C_T \text{ gene of interest} - C_T \text{ reference genes}$.

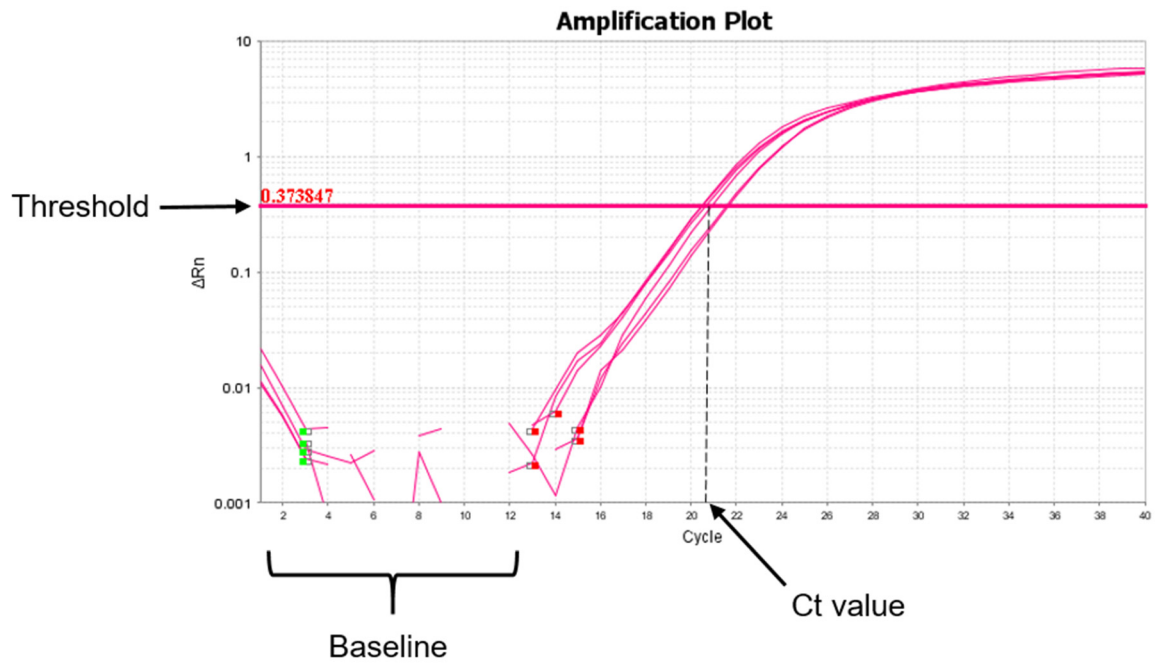


Figure 2.6: Example of a PCR amplification plot. The baseline corresponds to the cycle where no (or little) fluorescence is detected. The threshold, used to determine the Ct value, is placed in the linear phase of all the amplification plots.

2.5 Characterisation of macrophages in synovium and fat pad: *in situ* and freshly isolated

2.5.1 Immunohistochemical characterisation of macrophages in the synovium and infrapatellar fat pad

Immunohistochemistry was used to reveal the presence of cells that were positive for the macrophage markers, CD68³⁷⁰, CD86³⁷¹, CD11c³⁷², CD206³⁷³, and Arginase-1³⁷⁴ (Table 2.5), in donor-matched FP and synovium samples. This technique utilises the specificity of antibodies to bind to target antigens in tissues, which can then be visualised by the reaction of an enzyme conjugated to the antibody with its chromogenic substrate. All steps of immunohistochemistry were performed at room temperature.

Wax embedded FP and synovium samples were deparaffinised as described in section 2.3.3. Heat-induced epitope retrieval was performed by placing the slides in a Coplin jar with a 10 mM sodium citrate (Sigma) buffer at pH 6, pre-heated in a microwave until the solution started to boil, followed by an incubation at 95°C in a water bath for 20 minutes. Samples were allowed to cool at room temperature and washed with PBS for 3 minutes. Slides were mounted into a Sequenza™ rack (ThermoFisher), rinsed twice with PBS, and incubated with a blocking solution consisting of 10% (v/v) normal goat serum (Southern Biotech, Alabama, and USA), 1% (v/v) BSA and 1% (w/v) powdered milk (Campina, Rotterdam, Holland) in PBS for 30 minutes. 180 µL of diluted primary antibodies (Table 2.5) were added to the slides, incubated for 1 hour and washed 3 times with PBS. The biotinylated secondary antibody (BioGenix, California, USA) was applied to the slides at a dilution of 1:50 in a buffer containing 1% (v/v) BSA and 5% (v/v) human serum in PBS and incubated for 30 minutes. Three washes with PBS were performed after which an alkaline phosphatase-

conjugated streptavidin complex was added (1:50 dilution in 1% (v/v) BSA in PBS) for 30 minutes. Streptavidin is a protein with a high affinity for biotin and thus the streptavidin complex would specifically attach to any bound secondary biotinylated antibodies. Slides were washed twice with PBS, placed in a Coplin jar and rinsed once with 0.2 M Tris-HCl solution at pH 8.5. A solution of 1 g in 25 ml 2 M HCl of New Fuchsin (Chroma, Gesellschaft, Kongen, Germany) was mixed with 4% w/v of sodium nitrite (Sigma) in distilled water was prepared, together with a second solution of Naphtol AS-MX phosphate (18 mg in 2 mL Dimethylformamide). Both solutions were then added to a third solution that consisted of 15 mg of levamisole in 60 ml of Tris-HCL and filtered. Slides were immersed in this solution (which is the substrate for alkaline phosphatase), for 20 minutes (protected from light) and washed 3 times with distilled water. A haematoxylin counterstain was performed for 10 seconds followed by a further wash with tap water after which the slides were allowed to air dry overnight and mounted with VectaMount™ (Vector Laboratories, Peterborough, UK). Slides were imaged using an Olympus SC30 camera (Olympus, Zoeterwoude, Netherlands).

Table 2.5: Markers used in immunohistochemistry to identify macrophages in synovium and FP.

Marker	Macrophage polarisation	Antibody clone	Source of antibody (supplier)	Dilution*
CD68	Pan macrophage marker	KP-1	Mouse anti-human Monoclonal (Sigma)	Ready to use
CD11c	M1	EP1347Y	Rabbit anti-human Monoclonal (Genetex, CA, USA)	1:200
CD86	M1	EP1158Y	Rabbit anti-human Monoclonal (Genetex)	1:200
CD206	M2	-	Rabbit anti-human Polyclonal (Abcam)	1:400
Arginase-1	M2	-	Rabbit anti-human Polyclonal (Genetex)	1:1000

2.5.2 Ranking the positivity of macrophage markers in stained tissues

After immunohistochemistry, the positivity of each macrophage marker was ranked separately in the synovium, subsynovial stroma, and FP for a total of 11 donors (Figure 2.7). All microscopic observations were performed using an X20 objective, unless otherwise indicated.

For this study, the synovium was considered to be the layer (or layers) of cells that line the superficial regions of the synovial tissue. Positivity was assessed using three parameters; 1) the presence of cells that are stained red, 2) the intensity of the “redness”, 3) the number of red cells. Samples were then ranked in order of positivity, for example, from 1 (least positive) to 11 (most positive). In the event that two or more samples appeared to have the same level of positivity, they were all attributed a mean rank. For instance, if the first 3 samples were ranked 1-3, and the following 3 samples were equal in positivity, then these 3 equal samples obtain a mean rank of 5 (which is an average of ranks 4+5+6). The next sample would then continue with a rank of 7.

The subsynovial stroma was considered to be the fibrous tissue directly beneath the synovial lining (Figure 2.7). This layer may vary significantly in depth. Positivity was again assessed by the presence of cells that are stained red, the intensity of the stain and the number of red cells. Samples were ranked following the same method as detailed above.

To assess the presence of positive cells in the FP, a high power objective (x200) was needed. The positivity and ranking of the samples was performed as stated above. Samples were ranked by two independent observers using the same ranking method and the mean rank was used for statistical analyses.

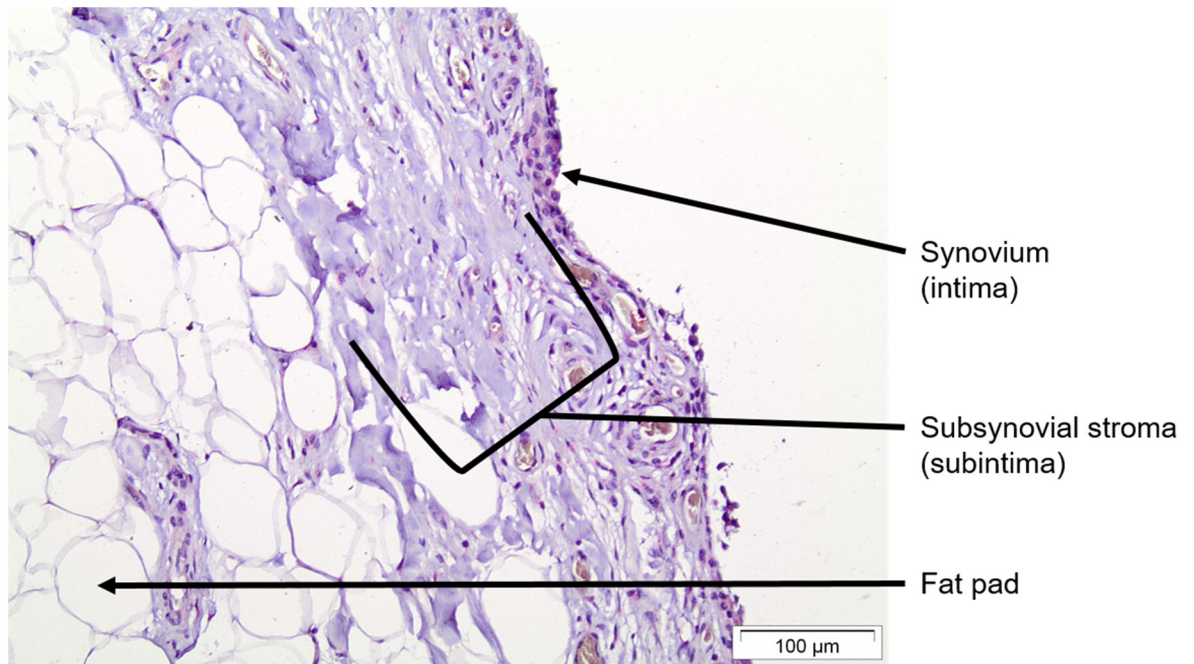


Figure 2.7: Illustration of the different regions that were ranked for each macrophage marker following immunohistochemistry. The synovium is a layer(s) cells in contact with the joint cavity. The subsynovial stroma is the fibrous layer below the synovium, thus separating it from the underlying adipose tissue known as the fat pad.

2.5.3 Synovitis score

The inflammatory status of the synovial tissue was measured based on a previously established synovitis grading system¹⁸⁵. Synovium tissues were wax embedded, sectioned at 5 µm and stained for H&E as previously described in section 2.3.2. The synovitis grading system was based on three parameters: 1) hyperplasia or enlargement of the synovial lining; 2) density of cells in the sub-synovial stroma and 3) infiltration of inflammatory cells. Each of these features was attributed a score ranging between 0-3 according to Table 2.6 and a total grade was determined for each sample by taking the sum of the scores for all three features.

2.5.4 Stimulation of fat pad explants with Triamcinolone acetonide (TA)

Freshly obtained FP samples were dissected to remove any visible synovium as described previously and cut into 2-3 cm² explants that were cultured in an 8-well plate (Sarstedt) with DMEM GlutaMAX (ThermoFisher) supplemented with 1% (v/v) ITS, 5% (v/v) fungizone (ThermoFisher) and 1% (v/v) gentamycin (ThermoFisher). Sufficient medium was added to ensure that the explants were fully submerged (at least 2 mL of medium per well). A 1.4 mg/mL stock solution of Triamcinolone acetonide (TA) (Bristol-Myers Squibb, Woerden, Netherlands) was prepared in DMSO which was added to the explants culture at a 1:100 dilution. Plates were incubated at 37°C and 5% CO₂ for 72 hours.

Table 2.6: Criteria for the grading of synovitis. Adapted from Krenn *et al*¹⁸⁵.

Tissue feature	Score	Description
Hyperplasia or enlargement of the synovial lining	0	The lining cells form one layer
	1	The lining cells form 2–3 layers
	2	The lining cells form 4–5 layers, few multinucleated cells might occur
	3	The lining cells form more than 5 layers, the lining might be ulcerated and multinucleated cells might occur
Density of cells in the sub-synovial stroma	0	The synovial stroma shows normal cellularity
	1	The cellularity is slightly increased
	2	The cellularity is moderately increased, multinucleated cells might occur
	3	The cellularity is greatly increased, multinucleated giant cells, pannus formation and rheumatoid granulomas might occur
Infiltration of inflammatory cells	0	No inflammatory infiltrate
	1	Few mostly perivascular situated lymphocytes or plasma cells
	2	Numerous lymphocytes or plasma cells, sometimes forming follicle-like aggregates
	3	Dense band-like inflammatory infiltrate or numerous large follicle-like aggregates
Overall Synovitis grade		
Sum 0 or 1		No synovitis
Sum 2-4		Low-grade synovitis
Sum 5-9		High-grade synovitis

2.5.5 Extraction of the macrophages from synovium and fat pad tissues or explants

Enzymatic digestion was used to extract cells from synovium and FP tissues to further characterise the phenotype of macrophages via flow cytometry (protocol developed in Professor Gerjo van Osch's lab). After dissection, synovium and FP were weighed and incubated at 37°C with shaking for 3 hours with a digestion solution comprised of 2 mg/ml collagenase IV (ThermoFisher) and 0.2 mg/ml dispase II (Roche, Basel, Switzerland) in Hanks' balanced salt solution (ThermoFisher). After digestion, FBS was added to the suspension (5% v/v) which was then centrifuged at 800g for 8 minutes. The supernatant was gently removed with an automatic pipette set to low suction and the pellet was resuspended in PBS prior to successive straining through 100 µm and 2x40 µm strainers. The suspension was centrifuged again as before and the resulting pellet resuspended in 1 mL of 2% (v/v) BSA in PBS in preparation for flow cytometry. At this stage, the cells were counted with a 1:1 dilution of 3% (v/v) acetic acid with methylene blue (Stem Cell Technologies).

2.5.6 Evaluation of macrophage phenotype by flow cytometry

Cells were prepared for multicolour flow cytometry as described in section 2.2.3.2. A panel of 5 surface markers, CD14³⁷⁵, CD80³⁷⁶, CD86³⁷¹, CD163^{377,378} and CD206³⁷³, was designed to investigate the polarisation status of macrophages (Table 2.7). Cells were equally divided into 3 tubes that were incubated at 4°C for 30 minutes with antibodies as follows; tube 1) no antibody staining; tube 2) fluorochrome-conjugated antibodies of the isotype controls of all 5 markers; tube 3) fluorochrome-conjugated antibodies for all 5 markers. Cells were processed as previously described and data was collected using either a FACSCanto II flow cytometer or a FACSJazz cell sorter (BD Biosciences).

Table 2.7: Panel of surface markers used to investigate macrophage polarisation via multicolour flow cytometry

Marker (antibody clone)	Macrophage polarisation	Conjugated fluorochrome	Dilution of antibody	Isotype Control
CD14 (M5E2)	Pan macrophage Marker	APC	1:100	IgG2a
CD80 (L307.4)	M1	PE	1:20	IgG1
CD86 (2331)	M1	FITC*	1:20	IgG1
CD206 (19.2)	M2	BV421	1:100	IgG1
CD163 (GHI/61)	M2	PerCP-Cy5.5	1:100	IgG1

*FITC: fluorescein isothiocyanate

Results were then analysed using Flowjo (Figure 2. 8). The CD14 positive population was gated, from which the positivity of other markers was determined. Co-positivity of markers was obtained by creating a four-quadrant grid on the isotype controls, where 99% of the cell population is negative for both markers (lower left quadrant) (Figure 2.8). This grid is then applied to the test samples, to reveal cells that are positive for both markers (upper right quadrant).

2.5.7 Measuring the size of adipocytes in adipose tissues

Consent to acquire human tissues was given in accordance with the guidelines of the Federation of Biomedical Scientific Societies (Holland) after approval by the local ethical committee (MEC 2008-181 and MEC 2012-267). SCF and FP were obtained from obese ($\text{BMI} \geq 30 \text{ kg/m}^2$) and non-obese donors ($\text{BMI} \geq 29$) undergoing TKR. Tissue samples were cryosectioned at $7 \mu\text{m}$, stained with H&E and imaged using an Olympus SC30 camera. Multiple images were acquired of each tissue sample using a x100 objective on an Olympus SC30 microscope.

The cross-sectional areas of the imaged adipocytes were calculated using Fiji Is Just ImageJ (Fiji) software with the additional Adiposoft plugin³⁷⁹. Three separate sections, with a minimum of 25 adipocytes in each section were measured per donor tissue. The Adiposoft application was calibrated to identify cells with a diameter between 30-130 μm . A measuring scale of 0.33 $\mu\text{m}/\text{pixel}$ was also used by the application to determine the cross-sectional area (size) of each adipocyte identified in the images. A manual inspection of each output data was performed to confirm the correct identification and measurement of adipocytes by the program (Figure 2.9).

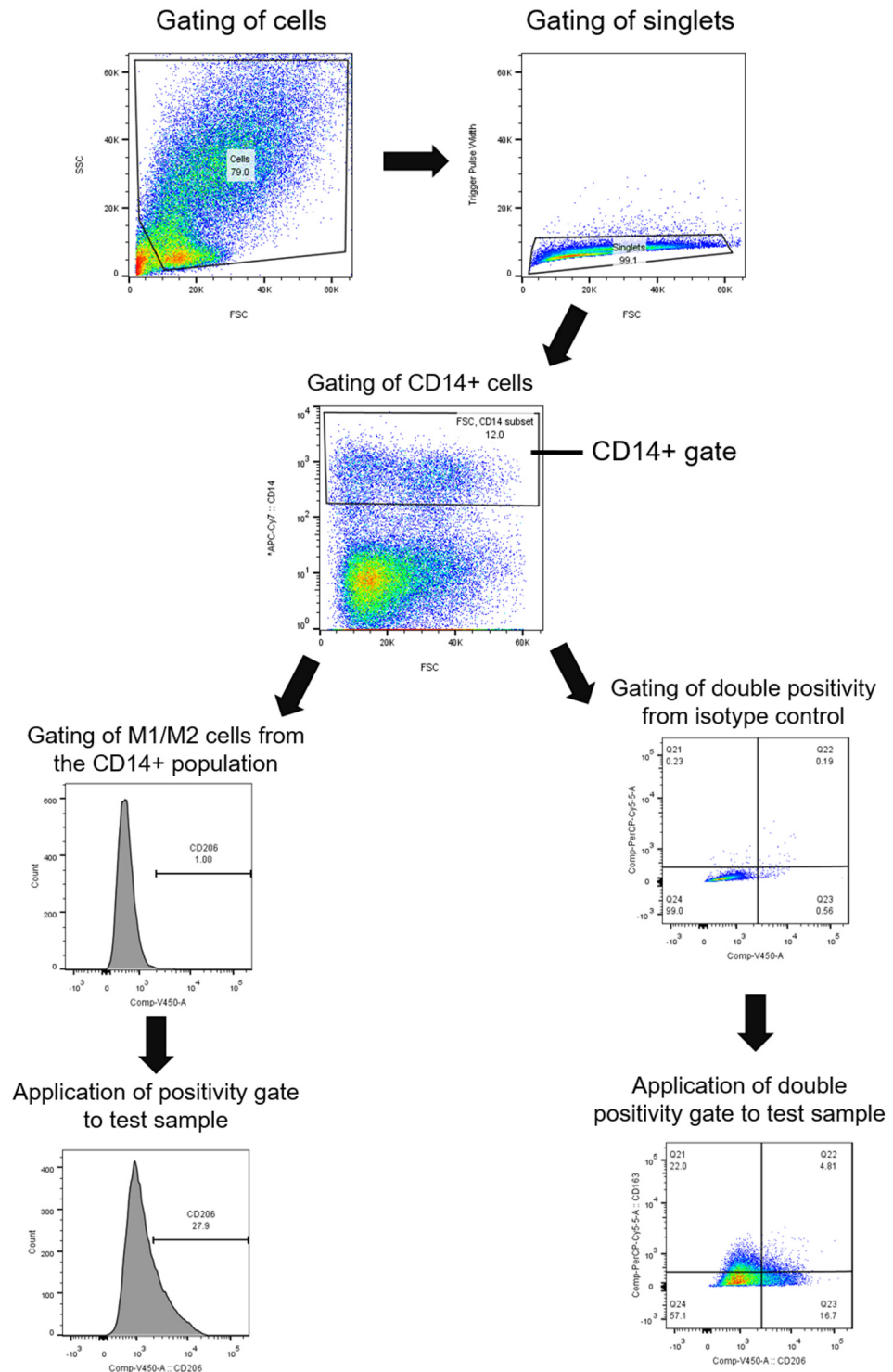


Figure 2. 8: Examples of flow cytometry analyses to determine double positivity of M1 and M2 markers on macrophages.

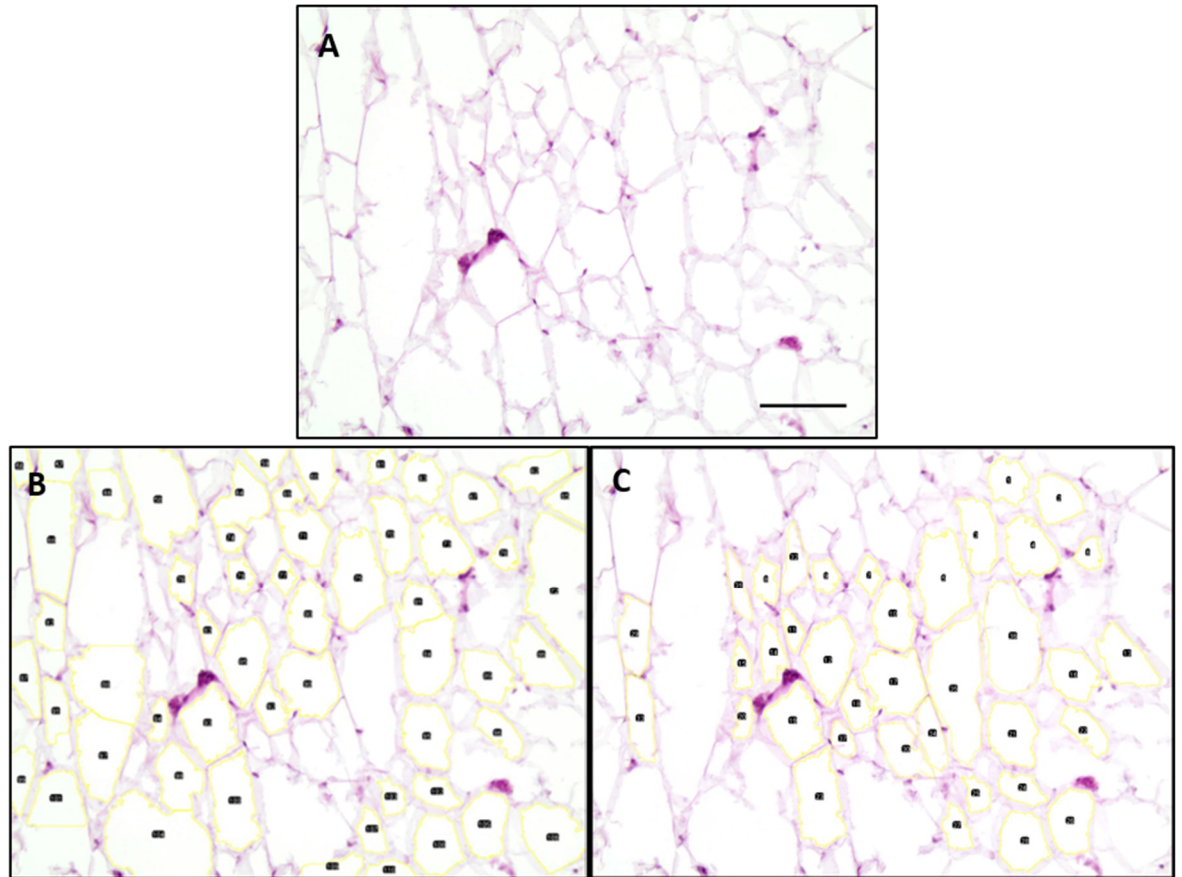


Figure 2.9: Identification of adipocytes using the Adiposoft plugin in Fiji. A) Original image of H&E staining of adipose tissue. B) Output image after being processed in Adiposoft. C) Corrected image after manual inspection of processed imaged. The yellow contours (B and C) represent the cross-sectional area of an adipocyte. Scale bar= 100 μ m.

2.6 Statistical analysis

For all analyses, statistical significance was considered at * $p < 0.05$, ** $p < 0.01$ and *** $p < 0.001$. The distribution of data was determined using the Shapiro-Wilk normality test. Parametric statistical tests were used for normally distributed data, whereas nonparametric tests were applied for data that was not normally distributed. The statistical tests employed for specific experiments are briefly explained in the experimental designs of the results section. All statistical analyses were performed in either GraphPad Prism version 6 (GraphPad Software, California, USA), R version 3.2.1 (The R Foundation, Vienna, Austria) or the statistical package for the social sciences (SPSS) version 21 (IBM, New York, USA).

Chapter 3: Results

Characterisation of donor-matched culture expanded FP-MSCs and SF-MSCs

3.1 Introduction and aim

Although the FP and SF have been shown to be reservoirs of MSCs in the knee with therapeutic benefit, no study has directly compared the phenotype of these cell populations. A number of parameters such as tissue source and donor specificity are often overlooked by researchers, despite the clear evidence indicating that these features influence the phenotype of MSCs. It has been demonstrated that both donor age and gender affect the differentiation of BM-MSCs and ASCs; male and young donors generally produce MSCs with a more enhanced osteogenic and chondrogenic potency than female and older donors³⁸⁰⁻³⁸². Further, older donors are known to produce MSCs that are less proliferative compared to younger donors³⁸². These findings collectively suggest a clear influence of the donor on the phenotype of MSCs and support the need for more robust studies that consider tissue origin and donor demographics as important parameters when developing cell therapies.

In addition to the minimum characterisation criteria of MSCs established by the ISCT²⁸⁰, which assesses cell surface markers and multipotent ability, understanding the immunological properties of MSCs in response to a pro-inflammatory stimulus has also been proposed as an important part of their characterisation²⁸³. BM-MSCs have been shown to increase their production of the immunomodulatory molecule IDO in response to stimulation with the pro-inflammatory cytokine IFN- γ ³⁸³. Like IDO, the human HLA-G is another important immunomodulatory molecule produced by BM-MSC and by the trophoblast cells in the placenta where it plays a role in maternal tolerance to the foetus^{361,384}.

HLA-DR interacts with T cell receptors during an immune response, and whilst it is not constitutively expressed on BM-MSCs, it is known to be upregulated following a pro-inflammatory stimulus³⁸⁵. In contrast, the costimulatory markers CD40, CD80 and CD86, which are also involved in T cell mediated immune reactions³⁸⁶, are not produced on BM-MSCs even after inflammatory stimulation³⁸⁷.

While FP-MSCs and SF-MSCs have been previously characterised in terms of their growth, multipotency and CD marker profile^{310,388}, the immunological and immunomodulatory properties of these cells have not been thoroughly defined. The purpose of this investigation was to assess the influence of tissue sources and donor demographics on the properties of MSCs sourced from donor matched FP and SF isolated from human knees. In addition, the previously unexplored response of FP- and SF-MSCs to a pro-inflammatory stimulus, such as that which may be found in an osteoarthritic joint, was also investigated.

3.2 Experimental design

FP and joint SF were obtained with informed consent from 6 patients undergoing either TKR or ACI surgery (Table 3.1). FP-MSCs and SF-MSCs were isolated from their respective sources and cultured until P10 to assess growth kinetics. Small pieces of the FP were processed for histology. At P3, both cell populations were subject to flow cytometry according to ISCT criteria, and differentiation to assess multipotency. Cells were also stimulated with IFN- γ (0, 25 and 500 ng/mL) before testing for positivity of CD40, CD80, CD86 and HLA-G via flow cytometry, and IDO via Western blotting.

The mean DTs of FP-MSCs and SF-MSCs were compared using a two-way ANOVA with Bonferroni's multiple comparisons tests, while multilevel modelling (or hierarchical regression analysis) with Wald's test was used to determine the effect of donor, cell source and passage number on DT. The multilevel level modelling method takes into account the hierarchical nature of the data, in this case the fact that experiments were performed on two types of cells from individual donors³⁸⁹. The analysis gives simultaneous estimates of significant effects that are constant for all donors (known as "fixed effects" or "constant effects") and significant effects that vary between individual donors (known as "random effects" or "varying effects"). It thus gives a robust framework to disentangle responses that are donor-independent and those that differ between donors. A paired Student's t-test was

used to compare means and a Pearson's test was used to establish correlations where appropriate. Graphs are shown as means \pm standard error of the mean (SEM).

3.3 Results

3.3.1 Macroscopic and histological features of the FP

Donor variability was noted in the apparent level of inflammation of the FP observed by the surgeon as indicated by the size of the FP itself and redness of the attached synovium. The complex and heterogenous features of the FP tissue were clearly visible in our histological preparations showing synovium and adipose regions (Figure 3.1A). Blood vessels appeared scattered throughout the synovium (Figure 3.1B) and deeper adipose tissue (Figure 3.1B). Mast cells, lymphocytes and numerous blood vessels could also be seen in the subsynovial stroma (Figure 3.1C). To avoid contamination of the extracted FP-MSCs with synoviocytes, only the deepest areas of the FP were used for digestion, as highlighted in Figure 3.1D.

Table 3.1: Demographics of donors from which samples were sourced

ID	Gender	Age (years)	Condition	Macroscopic observation the of FP*	Procedure
Donor 1	Male	35	Chondral defect on lateral femoral condyle	Mild inflammation	ACI
Donor 2	Female	42	Chondral defect on patella	Severe inflammation	ACI
Donor 3	Female	49	Osteochondral defect on patella	Hypertrophy	ACI
Donor 4	Female	49	Chondral defect on patella	Hypertrophy	ACI
Donor 5	Male	53	OA degeneration of knee with chondral defect on trochlea	General inflammation	ACI
Donor 6	Male	79	End-stage OA	General inflammation	Total knee replacement

*Macroscopic observations were made by the surgeon at the time of surgery.

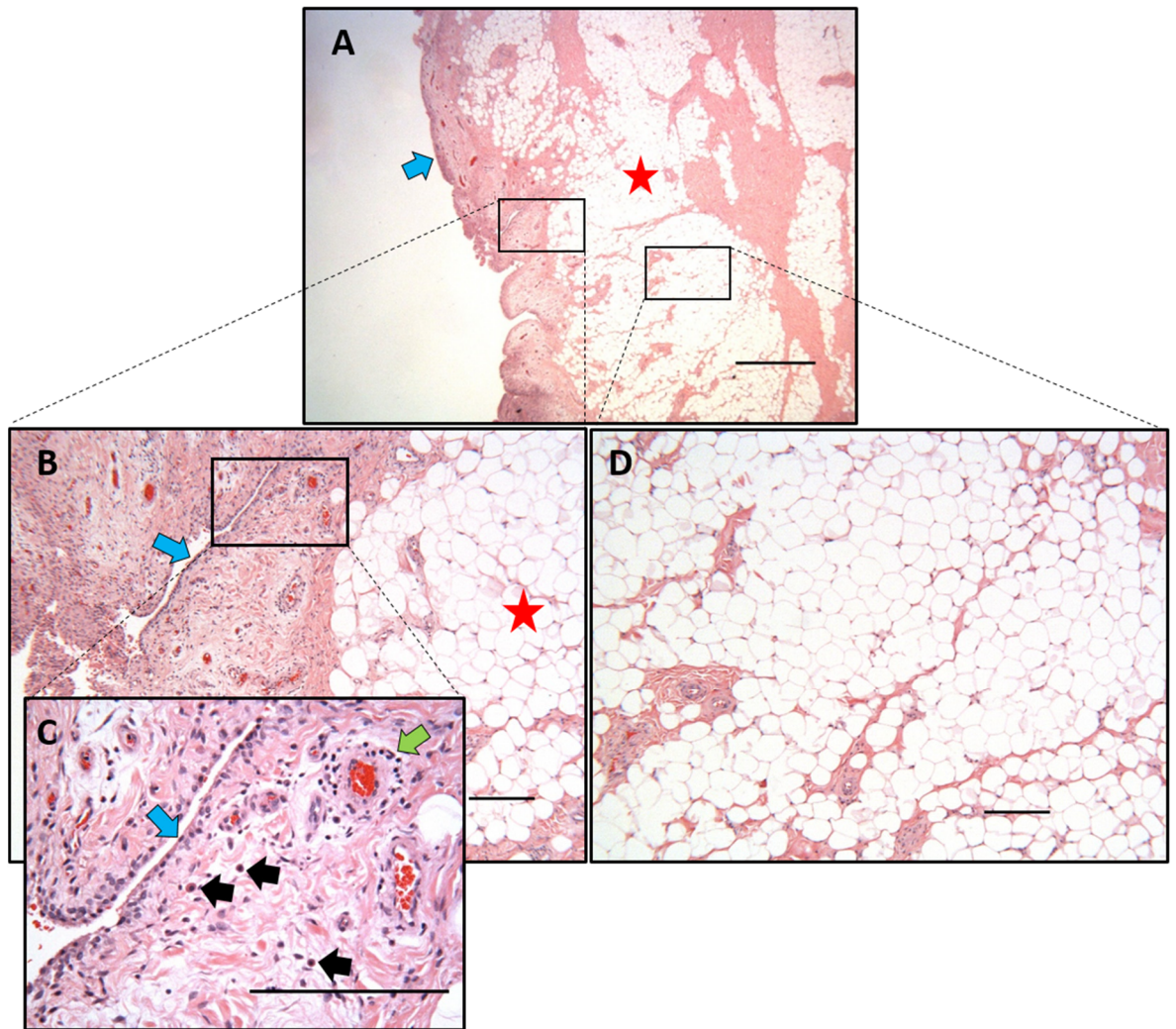


Figure 3.1: Histology of a FP. A) Low power view of the fat pad from a patient having a knee replacement showing synovium (blue arrow) and adipose tissue (red star). B) The deep adipose tissue is indicated by a red star and the adjacent synovium is indicated by a blue arrow. C) High magnification view of the synovium with a layer of synoviocytes (blue arrow), mast cells (black arrows) and a blood vessel surrounded by a cuff of lymphocytes (green arrow). D) Representative region of deep-lying vascularised adipose tissue from which FP-MSCs were isolated. Scale bars represent 1 mm (A) and 200 μ m (B, C and D).

3.3.2 Cell morphology and growth kinetics

MSCs isolated from both FP and SF were plastic adherent and appeared to consistently have a fibroblast-like morphology from early passages (P2) through to the last passage tested (P10) (Figure 3.2 A-D). Although some donor variability was observed, the analysis of growth kinetics showed that FP-MSCs had a significantly shorter mean DT ($p=0.018$) compared to SF-MSCs over the 10 passages tested. The proliferation rate of both FP-MSCs and SF-MSCs appeared to be progressively reduced with increasing passage number. This trend was more noticeable for SF-MSCs than FP-MSCs (Figure 3.3) as they showed a significantly longer DT at P9-10 compared to P1-2 ($p=0.024$) whereas FP-MSCs did not ($p=0.057$). At P1-P2, FP-MSCs and SF-MSCs had a mean DT of 6.3 ± 2.2 days and 10.3 ± 4.0 days, respectively ($p=0.025$), compared to 12.9 ± 10 days and 20.9 ± 6.4 days, respectively at P9-P10 ($p=0.127$).

Multilevel modelling revealed a more complex relationship between cell source, passage number and DT. Not only did cell source and passaging significantly influence the DT of cells in culture (both $p < 0.001$), but the increase in cell DT per passage in SF-MSCs appeared to be significantly dependant on the donor ($p=0.004$, Wald's test, **Error! Reference source not found.**). SF-MSCs had an average increase in DT of 1.4 days at every passage, which was not observed for FP-MSCs. In addition, the average doubling time for SF-MSCs over the 10 passages was 8.3 days longer than for FP-MSCs and this difference was not donor-dependent ($p=0.14$, ANOVA). FP-MSCs produced more population doublings (12.1) over 10 passages than SF-MSCs (8.5), as shown in Figure 3.4. Both cell populations generated similar PDs up to passage 3-4 (4 PDs) when they were for experiments. However, SF-MSCs started generating fewer PDs than FP-MSCs from passage 5.

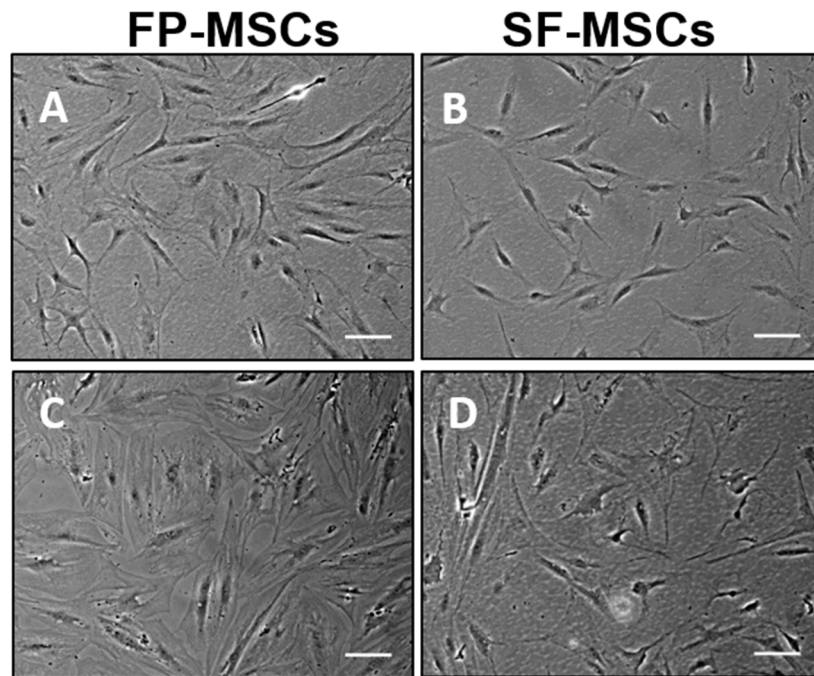


Figure 3.2: Microscopic photographs of FP- and SF-MSCs. Representative images were taken at A-B) passage 2 and C-D) passage 10. Scale bars represent 100 μm.

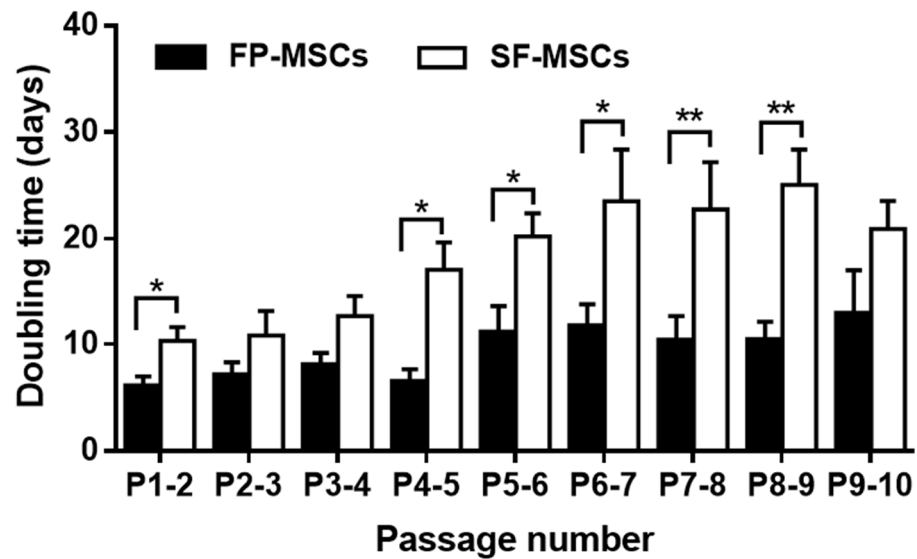


Figure 3.3: Growth kinetics for FP- and SF-MSCs over 10 passages. Data represents the mean doubling time \pm standard error of the mean (SEM) for 6 donor-matched FP and SF samples.

Table 3.2: Results of the Multilevel modelling of the influence of cell source, passage number and donor on doubling time of matched FP- and SF-MSCs.

Factor	Fixed/Random effect	Coefficient or SD (days)	p-value
Cell source (FP vs SF-MSCs)	Fixed	8.3 (6.1 – 10.4)	<0.001
Passage number (SF-MSCs)	Fixed	1.4 (0.8 – 2.0)	<0.001
Passage by donor	Random	0.54 (0.19 – 1.1)	0.004

Note: Coefficients and standard deviation (SD) based on a linear mixed effect model. P-values are from Wald tests (fixed effects) and likelihood ratio tests (random effects).

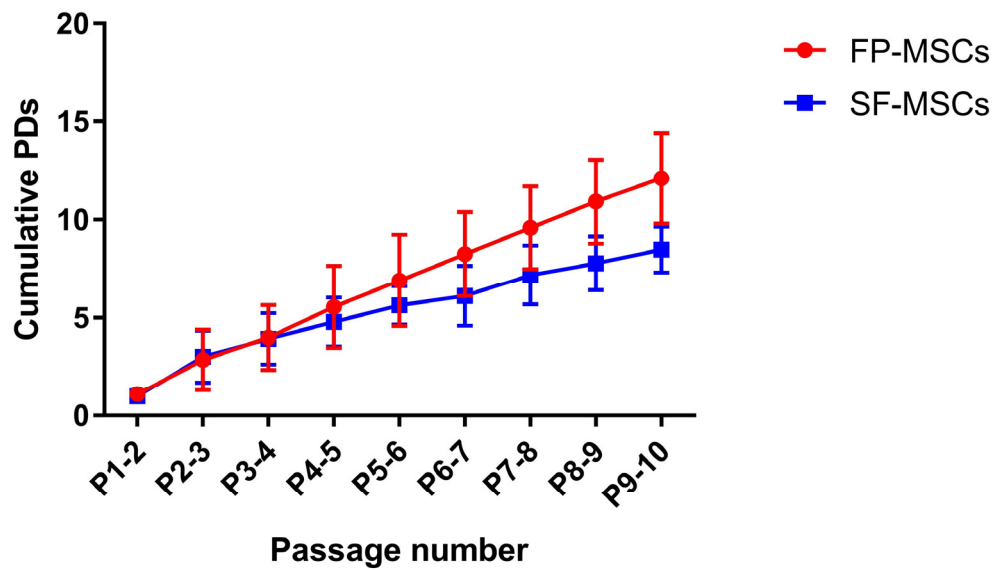


Figure 3.4: Cumulative population doublings (DPs) of for FP- and SF-MSCs. Although both cell populations showed an overall increase in DPs during the over 10 passages, FP-MSCs (12.1) underwent a higher of cumulative number of PDs than SF-MSCs (8.5). Both cell populations displayed similar cumulative PDs profiles between P1-4, but SF-MSCs generated less cells from P5. Error bars show standard deviation.

3.3.3 MSC immunoprofile

Flow cytometry analyses (Figure 3.5 A) revealed that both cell populations were over 95% positive for the MSC markers CD73 and CD105, but CD90 showed only 92.7% \pm 11 positivity in SF-MSCs but 98.3% \pm 3.1 in FP-MSCs. Interestingly, some positivity was recorded for the cocktail of PE conjugated markers expected to be negative on MSC cultures i.e. CD11b, CD19, CD45, CD34 and HLA-DR. FP-MSCs showed significantly ($P=0.046$) greater positivity for the “negative” MSC markers (31.7% \pm 24% of cells) compared to cells sourced from SF (7.8% \pm 6.9% of cells). To explore this further, single PE-conjugated antibodies for CD11b, CD19, CD45, CD34 and HLA-DR were used to analyse FP-MSCs. FP-MSCs were negative for all of these markers, with the exception of CD34 which was 30.1% \pm 18.6% positive (Figure 3.5 B). The macrophage lineage and inflammation marker CD14 was present on both FP-MSCs (30.5% \pm 30.3%) and SF-MSCs cells (7.4% \pm 7.2%, $P=0.14$), with some variability observed between donors (Figure 3.5 C). An increase in CD14 positive was associated with donor age for SF-MSCs ($n=5$, $r=0.94$, $p=0.016$), but not FP-MSCs ($n=5$, $r=0.66$, $P=0.23$).

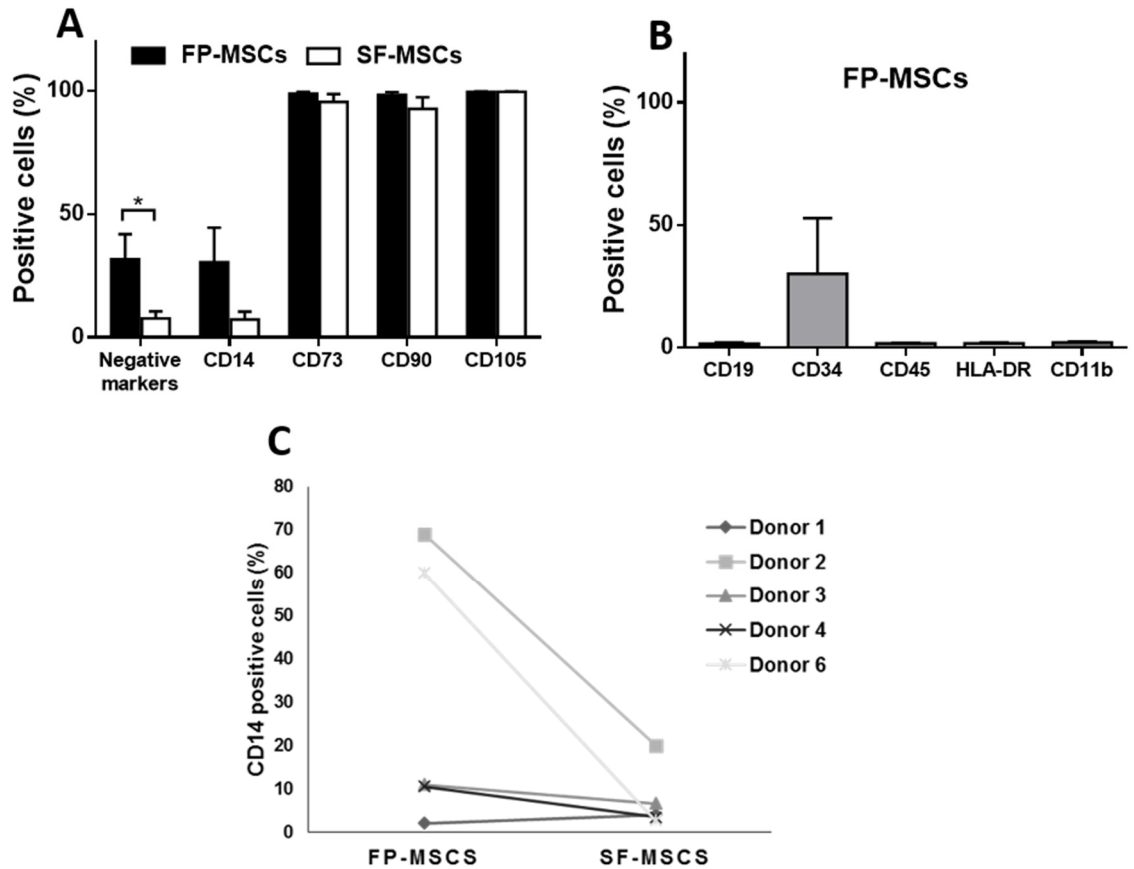


Figure 3.5: MSC immunoprofile of FP and SF-MSCs (flow cytometry) at passage 3. A) Both cells types were immunopositive for CD73, CD90, CD105; FP-MSCs showed significantly higher expression for the cocktail of ISCT defined negative MSC selection markers compared to SF-MSCs ($p=0.046$). B) Single colour cytometric analysis revealed a high positivity for CD34 in FP-MSCs ($n=3$), but no positivity for CD11b, CD19, CD45 and HLA-DR. Error bars indicate SEM. C) Cell positivity for CD14 was variable between donors and matched cell populations ($n=5$).

3.3.4 Multipotency

After 21 days of differentiation, all donor matched samples showed multipotent capability (Figure 3.6). Histological staining for metachromasia, using toluidine blue, of chondrogenic cell pellets after differentiation revealed a similar level of GAG production by both cell populations, with no discernible difference in staining intensity between donors. FP-MSCs and SF-MSCs in adipogenic medium produced lipids which stained positively with oil red O, with those produced by FP-MSCs being more numerous and larger than those produced by SF-MSCs. Furthermore, they also showed stronger staining for alkaline phosphatase compared to SF-MSCs, which suggests greater osteogenic potential for the FP-MSCs.

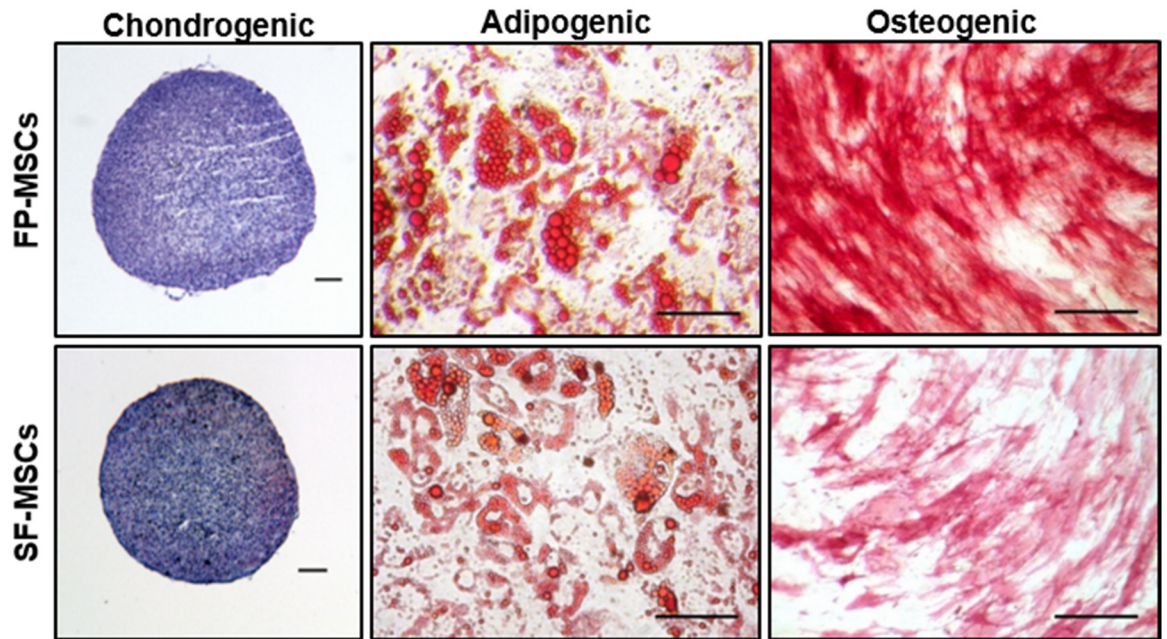


Figure 3.6: Trilineage differentiation of FP and SF-MSCs at passage 3. The two MSC populations demonstrate multilineage differentiation potential when grown in specific differentiation media; Chondrogenesis is shown by sulphated GAG production (purple metachromasia when stained with toluidine blue), adipogenesis is shown by the formation of lipid vesicles (oil red O) and osteogenesis is shown by the activity of alkaline phosphatase (red staining). Images are representative of the differentiation potential of all six donor matched samples. Scale bars represent 100 μm .

3.3.5 Immunogenic and immunomodulatory properties of FP- and SF-MSCs in a pro-inflammatory environment

After 48 hours of treatment with either 25 or 500 ng/ml of the pro-inflammatory cytokine, IFN- γ , analysis via flow cytometry showed that CD40, CD80 and CD86 were not present on either FP-MSCs or SF-MSCs and were similar to the untreated controls (Figure 3.7). In contrast, a low concentration (25 ng/ml) of IFN- γ significantly increased the positivity for HLA-DR in both cell populations compared to their respective controls (FP-MSCs=39.8% \pm 35.1%, SF-MSCs=13.1% \pm 11.7%). FP-MSCs also showed a significantly higher percentage of HLA-DR positive cells (46.9% \pm 36.5) compared to SF-MSCs (10.0% \pm 10.4) with 500 ng/ml IFN- γ (P=0.04). Donor variability was noted with regards to the induction of HLA-DR by IFN- γ , however MSCs derived from both the FP and SF of donor 2 consistently produced more HLA-DR in response to IFN- γ stimulation compared to the other donors, at both doses tested (Figure 3.7 C-D). After stimulation with 25 ng/ml of IFN- γ , FP-MSCs showed enhanced production of HLA-DR, which was positively correlated with an increase in donor age (n=6, r=0.82, P=0.045); SF-MSCs showed no donor age dependant trends (n=6, r=0.72, P=0.105). No correlation between donor age and production of HLA-DR by FP-MSCs (r=0.69, p=0.16) and SF-MSCs (r=0.66, p=0.14) after stimulation with 500 ng/ml.

Both cell populations produced the immunomodulatory marker, HLA-G, regardless of inflammatory stimulus and with no significant difference observed between FP-MSCs and SF-MSCs (n= 3, Figure 3.8A). Western blots showed that the production of IDO in both cell populations was induced by IFN- γ stimulation but was absent in unstimulated controls (Figure 3.8B).

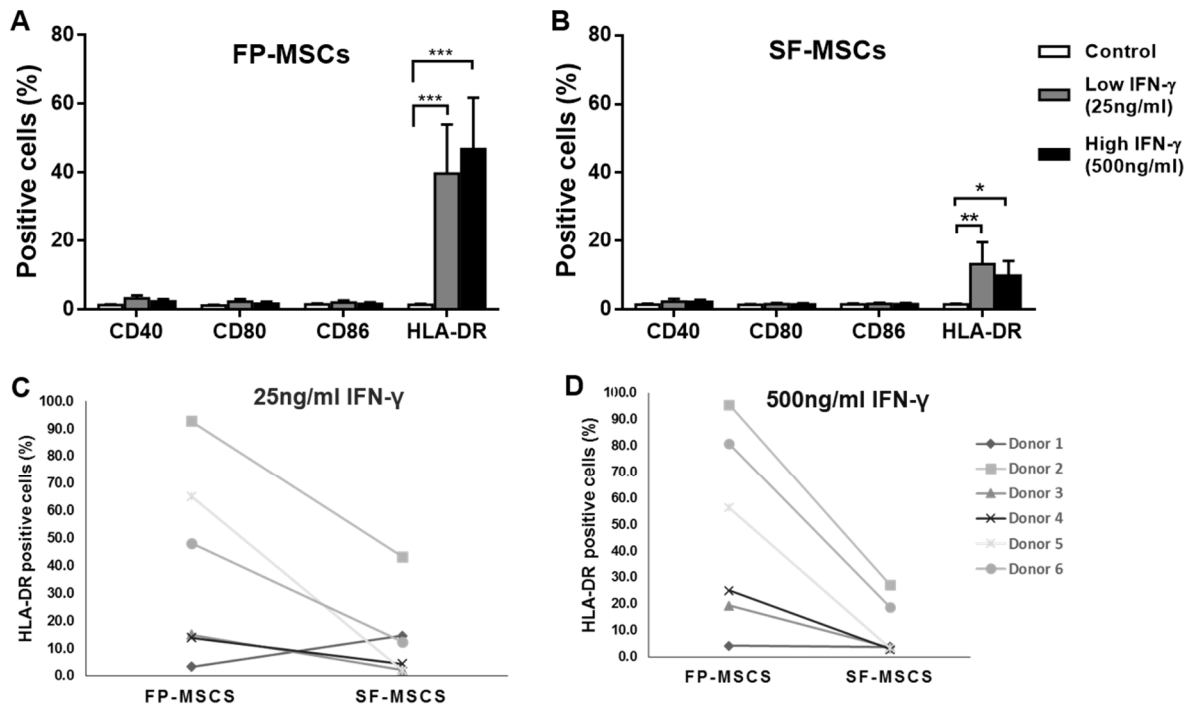


Figure 3.7: Immunogenic properties of FP and SF-MSCs after stimulation with IFN- γ at passage 3. A) The production of co-stimulatory markers (CD40, CD80, and CD86) and the MHC class II receptor, HLA-DR, for FP-MSCs is shown after 48 hours of stimulation with IFN- γ along with unstimulated controls. Unstimulated and stimulated FP-MSCs do not produce co-stimulatory molecules, but show greater HLA-DR positivity at 25 ng/ml ($39.8\% \pm 14.3$, $p < 0.0001$) and at 500 ng/mL ($46.9\% \pm 14.9$, $p < 0.0001$) stimulation with IFN- γ . B) SF-MSCs show no positivity for co-stimulatory markers, even after stimulation, but produce significantly higher levels of HLA-DR at 25 ng/ml ($13.1\% \pm 6.4$, $P = 0.0015$) and 500 ng/mL IFN- γ ($9.8\% \pm 4.3$, $P = 0.025$) compared to unstimulated control. C-D) Donor variability in the levels of induced HLA-DR on FP-MSCs and SF-MSCs was observed at both 25 ng/mL and 500 ng/ml. However, donor 2 (indicated by the square data points) had higher positivity for HLA-DR compared to other donors for both FP-MSCs and SF-MSCs and for both IFN- γ doses tested. Error bars indicate SEM

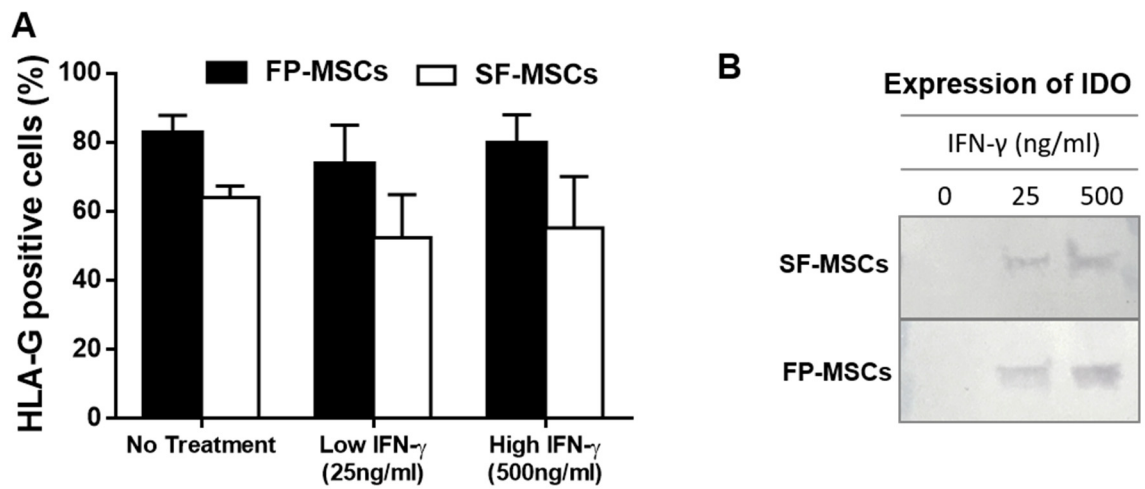


Figure 3.8: Immunomodulatory properties of FP and SF-MSCs after stimulation with IFN- γ (error bars indicate SEM). A) Both FP and SF-MSCs (n=3) constitutively produce HLA-G in control conditions (82.7% \pm 5.1 and 64.0% \pm 3.4 respectively), as well as following treatment with 25 ng/ml (73.8% \pm 11.2 and 52.4% \pm 12.5 respectively) and 500 ng/ml IFN- γ (79.7% \pm 8.3 and 52.2% \pm 14.9 respectively). B) Image of a representative Western blot indicating the production of IDO by FP-MSCs and SF-MSCs after stimulation with IFN- γ , but not in untreated controls.

3.4 Discussion

The results presented in this chapter have characterised the endogenous population of MSCs found in patient matched samples of infrapatellar FP and joint SF and explored the possible influence of a pro-inflammatory stimulus on the immunogenic and immunomodulatory properties of these cells. Histology of the FP and synovium revealed the presence of immune cells, notably mast cells and lymphocytes, in the superficial regions of the tissues. Both of these cell types are known to be present in synovial tissues of arthritic patients and produce molecules that promote joint inflammation^{187,390,391}. Macroscopic inspection of the FP during surgery in the present study revealed some degree of inflammation as indicated by the size of the FP itself and the redness of the attached synovium. Data presented in this thesis chapter shows that both FP- and SF-MSCs are plastic adherent cells with similar fibroblast-like morphologies *in vitro*. A significant increase in the doubling time of SF-MSCs at late passages (compared to FP-MSCs) was noted, which suggests that SF-MSCs lose proliferative capacity earlier than FP-MSCs. Reports have indicated that both human BM-MSC and ASC DTs increase with passage number³⁹²⁻³⁹⁴; a longer culture period may have been required in the current study in order to observe a similar reduction in FP-MSC proliferation. The consistent difference in growth rate observed between FP-MSCs and SF-MSCs, isolated from matched donors, highlights that these cells are biologically different. Interestingly, an investigation observing patient-matched SM-MSCs and SF-MSCs revealed no significant difference in the proliferation rate of the two cell types between P0 and P2³⁹⁵, perhaps providing supportive evidence that these cells share a common origin.

Donor-matched SF-MSCs and FP-MSCs were positive for MSC cell surface markers CD73, CD90, CD105, as well as many of them being positive for the macrophage lineage marker CD14³⁷⁵. The positivity of CD90 displayed by SF-MSCs (<95%), and the presence of CD14 on both cell populations indicates that although joint SF and the stromal fraction of FP

contain cells that in part meet the ISCT criteria for MSCs, they may also harbour a sub-population that do not. CD14 positivity has previously been reported on BM-MSCs³⁹⁶, but not FP-MSCs or SF-MSCs to date. Macrophage-like synoviocytes, which are also positive for CD14, are a likely contaminant sub-population contributing to the heterogeneity in the cultures^{397,398}. SF is known to contain CD14 positive macrophages that secrete pro-inflammatory cytokines, such as IL-1 and TNF- α , that induce enzyme-mediated cartilage degradation^{399,400}. Furthermore, there is increased detectable soluble CD14 in the SF of osteoarthritic patients experiencing increased joint pain⁴⁰¹. Hence, the positive association of CD14 in SF-MSCs and advancing age could be indicative of an increase in pro-inflammatory conditions in the degenerative joints of older subjects^{192,402,403}.

No single surface marker that was investigated in this study allowed for a clear distinction between FP-MSCs and SF-MSCs, which suggests that a broader panel of markers would be required in order to distinguish between these two cell types. Recent guidelines from the ISCT and the International Federation for Adipose Therapeutics and Science now accept CD34 as being positive on adipose stromal cells³⁵². CD34 positive cells in FP-MSCs and other ASCs cultures^{404,405}, are likely to represent subpopulations of either vascular endothelial lineages, pericytes or a mixture of the two, as found in cells isolated from subcutaneous lipoaspirate. Further work would be required to isolate and phenotypically characterise these CD34 positive cells within adipose tissues to assess their function in native and transplanted tissues.

In agreement with previous studies^{315,406}, the results presented here confirm the multipotency of both cell populations. FP-MSCs showed enhanced differentiation towards adipogenic and osteogenic lineages compared to SF-MSCs; this comparison, to date, has not been previously shown. Endothelial cells, that can be found in the enzyme digest of the FP, have been shown to promote the osteogenic differentiation of BM-MSCs^{407,408}. This could account for the

enhanced osteogenic potential of FP-MSCs. Also, as previously described^{388,406}, both FP-MSCs and SF-MSCs populations were shown to possess chondrogenic ability, although no discernible difference in the chondrogenic potential of FP-MSCs or SF-MSCs derived from the same donor was noted.

In addition to surface antigens and differentiation characterisation criteria, the need to understand the immunological properties of MSCs is becoming crucial to the development of cell therapies^{283,409}, particularly in the treatment of conditions which involve inflammatory elements as is the case for OA^{193,410}. Antigen presenting cells, such as macrophages, interact with T cells via MHC class II molecules, such as HLA-DR, to trigger an alloresponse⁴¹¹. This reaction involves the activation, differentiation and proliferation of T cells but is not possible without the expression of costimulatory surface molecules⁴¹². The results presented here are the first to show an increased positivity of HLA-DR and a lack of expression of costimulatory molecules on matched FP-MSCs and SF-MSCs in response to an *in vitro* inflammatory stimulus. BM-MSCs stimulated with IFN- γ have been shown to produce levels of HLA-DR that are comparable to the observations in this study with FP-MSCs³⁸⁷. Conversely, the immunoprofile of IFN- γ induced HLA-DR on SF-MSCs was much lower, perhaps indicating that SF-MSCs are less immunogenic following inflammatory stimulation and hence display a distinct immunological phenotype compared to FP-MSCs and also BM-MSCs. This is the first time that a difference in positivity for HLA-DR on stimulated MSCs derived from the same joint has been reported and requires further investigation. Inflammation of the knee has been reported to increase with age due to elevated levels of pro-inflammatory molecules^{192,413}. The results of this thesis chapter indicate a trend for increased HLA-DR production with age by FP-MSCs after exposure to IFN- γ . It could be hypothesised that the inflammatory nature of the FP is increased with age and in turn pre-conditions the endogenous MSC niche to respond to IFN- γ by augmenting

HLA-DR positivity. The reason why this correlation was not reproduced in the SF-MSCs derived from the same joints remains undetermined, but this observation highlights another biological difference between the two cell populations. *In vivo* investigations evaluating the general effects of natural aging and inflammation on MSC pools within the human knee joint are needed. Such tests could not only elucidate the cellular pathways involved in the pathogenesis of chronic joint diseases, but may also reveal potential therapeutic targets (genetic, molecular or cellular) to counter the degenerative processes. Despite the presence of HLA-DR on FP- and SF-MSCs in the results presented in this chapter, these cells cannot be considered as truly immunogenic without an accompanying increase in the production of costimulatory markers^{412,414}.

It is perhaps also noteworthy that the only donor included in this study observed in surgery to have a 'severely inflamed' infrapatellar FP (donor 2) produced FP-MSCs and SF-MSCs which showed the most pronounced response to an inflammatory stimulus. This might suggest that cells derived from such severely inflamed joints are 'primed' to be more responsive to inflammatory stimuli, however a larger cohort of donors with better defined (macroscopic and histologically quantified) tissues would be required to confirm this hypothesis.

The immunosuppressive properties of SF-MSCs have been demonstrated in mixed lymphocyte reactions⁴¹⁵, but the constitutive production of HLA-G in FP-MSCs and SF-MSCs has not been reported previously. IFN- γ stimulation did not significantly influence the production of HLA-G in either cell population, however, a larger sample size may be required to confirm this result. The levels of HLA-G reported here have also been reported in both BM-MSCs and UC-MSCs^{361,387}. HLA-G positive umbilical cord-MSCs (UC-MSCs) have been shown to inhibit the proliferation of pro-inflammatory T helper 1 cells, which are present in OA joints⁴¹⁶, and to promote the expansion of anti-inflammatory regulatory

T cells. The results presented in this thesis chapter demonstrate that the production of IDO can be induced in both cell populations by an inflammatory stimulus, comparable to BM-MSC and ASC cultures^{417,418}. In a collagen induced arthritis mouse model, IDO deficiency was associated with a high incidence of arthritis and pronounced T cell infiltration⁴¹⁹. The pro-inflammatory conditions within the OA joint could potentially activate the local MSC populations to dampen the influence of certain immune cells such as T cells and macrophages. The present study suggests that FP-MSCs and SF-MSCs may be considered as immunomodulatory cells in inflammatory conditions, due to their ability to produce both of the immunomodulatory molecules tested (HLA-G and IDO). However, a more in depth *in vitro* functional testing alongside BM-MSCs will be required to fully assess their therapeutic value in this respect. Others have shown that conditioned media derived from BM-MSCs, stimulated with IFN- γ and TNF- α , reduced the gene expression of pro-inflammatory and cartilage degrading molecules in synovial and cartilage explants *in vitro*⁴²⁰. This trophic feature remains largely undefined in FP- and SF-MSCs but may provide insight into the possible mechanism of action that these cells might have in an arthritic joint.

The use of donor matched samples in the investigations described here has allowed for the assessment of donor-specific variability. Tissue source appears to be more influential on the proliferative and differentiation properties of joint derived MSCs than the donors themselves or related factors. The reasons for this are still unclear. An increase in donor age, for example, is known to negatively affect the differentiation potential and growth rate of BM-MSCs³⁰² and subcutaneous ASCs³⁸², but this does not seem to apply for the FP- and SF-MSCs observed in our study.

Donors included in this study were predominantly patients with chondral defects and with early signs of OA. However, one donor was described as having end stage OA and was thus undergoing total joint replacement. This heterogeneity in samples may account for some of

the variability observed, but also provides insight into the inherent biological differences in donors that should be considered in the development of new cartilage repair strategies.

3.5 Conclusion

We have characterised the phenotype and have identified biological distinctions between MSCs sourced from the FP and SF within the same articular joint. Table 3. 3 gives a summary of the results presented in this chapter. We have confirmed that there is potential for the use of FP-MSCs or SF-MSCs in the treatment of cartilage defects following *ex-vivo* expansion. However, it may be more advantageous to find a means of recruiting these resident MSCs with chondrogenic potency from their respective niches *in vivo*, as opposed to current methods of transplanting culture expanded cells. The advantage of this approach would be that the significant costs and regulatory hurdles involved with the *in vitro* manufacturing of cells may be circumvented.

Further, the results presented in this chapter have shown that the levels of CD14 on SF-MSCs and the inducibility of HLA-DR on FP-MSCs are potentially related to age-associated inflammation. These results confirm for the first time, an immunomodulatory capacity for FP- and SF-MSCs which confers further therapeutic value to these cells with regards to treating the inflammatory aspect of OA. This also highlights the need to understand the physiological inflammatory conditions to which transplanted cells return and how this could affect the outcome of a cellular treatment. FP-MSCs and SF-MSCs may not realistically be suited for large-scale allogeneic therapies due to limited sample availability and low cell numbers, but certainly represent sources of autologous cells for cartilage regeneration in addition to sourcing chondrocytes from healthy cartilage, as is used currently. Further investigations will seek to understand how these MSCs can be directed to effect repair endogenously, either by means of dampening down inflammatory processes, by producing repair cartilage themselves or even by encouraging recruitment of reparative cells.

Table 3. 3: Summary of the main findings presented in this results chapter comparing the phenotype of donor matched FP- and SF-MSCs.

	FP-MSCs	SF-MSCs
Grow Kinetics	<ul style="list-style-type: none"> • Sustained average DT over 10 passages 	<ul style="list-style-type: none"> • Increase in average DT over 10 passages • Reduced proliferation from P4-5
Surface marker profile	<ul style="list-style-type: none"> • Positive for: CD73, CD90, CD105, 34, CD14 • Negative for: CD19, CD45, HLA-DR, CD11b 	<ul style="list-style-type: none"> • Positive for: CD73, CD90, CD105, CD14 • Negative for: CD19, CD45, HLA-DR, CD11b
Multipotency	<ul style="list-style-type: none"> • Chondrogenic, Osteogenic Adipogenic 	<ul style="list-style-type: none"> • Chondrogenic Osteogenic Adipogenic
Response to inflammatory stimulus	<ul style="list-style-type: none"> • No CD40, CD80, CD86 positivity • Increased HLA-DR • No change in HLA-G • Increased IDO 	<ul style="list-style-type: none"> • No CD40, CD80, CD86 positivity • Increased HLA-DR • No change in HLA-G • Increased IDO

Chapter 4: Results

Assessment of the chondrogenic potential of donor matched MSCs and chondrocytes.

4.1 Introduction and aim

BM-MSCs have been used in several clinical trials as an alternative cell source for use in cell therapies to treat cartilage injuries and OA^{421–423}. The process of acquiring a sample of bone marrow however, results in an additional painful procedure for the patient. The FP and SCF are also accessible alternative sources of MSCs that have been considered for cartilage regeneration, however, few studies have directly compared the chondrogenic potency of BM-MSCs, FP-MSCs and SCF-MSCs to chondrocytes^{311,424–426}.

An important factor to consider when comparing and contrasting the properties of different cell types is the “donor impact” as donor demographics, such as age and gender, are factors which are known to affect cell proliferation and differentiation capacity^{380–382}. The impact of donor is particularly critical for autologous treatment regimes, and in deciding whether such a cell-based therapy represents the appropriate treatment option for an individual patient. Unravelling the impact of tissue and donor source and developing tools to predict the efficacy of cell-based treatments will likely result in the refinement of existing treatments and may provide valuable additional information for consideration during the decision making process of cost benefit versus clinical efficacy.

Furthermore, low oxygen cell culture conditions have been extensively investigated as a means of improving the quality of cells before transplantation for cartilage repair^{342,427}. Chondrocytes used for ACI are grown in standard culture conditions at an elevated oxygen level compared to the articular joint to which they return³³⁸. Since MSCs are currently being investigated as a replacement for chondrocytes, it is important to assess the differentiation potential of both cell types, preferably from the same donors.

In this study, the chondrogenic potential of 4 different cell types (chondrocytes, BM-MSCs, FP-MSCs and SCF-MSCs) was examined. Donor-matched cell types were compared in this

investigation to establish the impact of tissue source and donor on chondrogenic differentiation capacity and to continue the process of establishing a marker panel indicative of chondrogenic potency and likely clinical success. Such markers could be screened for and used in the selection of a particular cell type and/or sub-population of cells with enhanced chondrogenic capability prior to treatment.

Previous studies assessing the chondrogenic potential of SF-MSCs have focused on cells sourced from the SF of end stage OA donors, with only a few studies investigating cells from normal or early OA donors^{388,428}. Also, no study to date has applied a panel of markers as part of the chondrogenic characterisation of SF-MSCs.

4.2 Experimental design-1

Cartilage, BM, FP and SCF were obtained from 5 patients undergoing TKR (Table 4.1 provides information on the demographics of the patients used in this study). Chondrocytes and MSCs were isolated as explained in sections 2.1.4, 2.1.1 and 2.1.2. Cells were maintained in standard tissue culture conditions (5% CO₂, 21% O₂, 37°C) up to P3, after which 6 chondrogenic pellets were created (section 2.2.2.3) for each cell population. A set of 6 sister pellets were differentiated in the SCI-tive™ hypoxic work station set at 5% CO₂, 2% O₂, and 37°C. Measurements were performed to determine the oxygen levels in pre-conditioned culture media in the SCI-tive™ and standard culture media (section 2.2.5.1). Prior to differentiation, cells were prepared for flow cytometry and RNA extraction for PCR (sections 2.2.3 and 2.4). After chondrogenic induction for 28 days, pellets were either frozen and processed for histology (toluidine blue staining and scoring), or quantitation of GAG via the DMMB and PicoGreen® assays (sections 2.2.2.8, 2.2.2.10 and 2.2.2.11).

Table 4.1: Demographics of patients used in experimental design 1

Gender	Age (years)	Pathology
Male	71	OA with extensive joint degeneration
Female	67	OA with loss of joint space
Female	75	Patello-femoral OA and loss of joint space in medial compartment
Female	81	OA
Male	74	OA with joint stiffness

A one-way ANOVA was used to compare means of variables across cell populations where applicable and multilevel modelling (Section 3.2) was used to correlate the expression of genes and the positivity of surface markers to the chondrogenic outcome of the various cell populations (histology/GAG quantitation). In these models, cell source, gene expression, and cell surface marker positivity were considered as fixed effects, while the donor was considered as a random effect. The donor effect was determined using Wald's tests. A correlation matrix was used to determine associations between genes. Figure 4.1 gives an illustration of the experimental workflow.

4.3 Experimental design-2

SF was obtained from 15 patients undergoing cell therapy, and MSCs were isolated as described in section 2.1.3 (Table 4.2 provides information on the demographics of the patients used in this study). Cells were cultured until P3, after which flow cytometry and RT-qPCR analyses were undertaken prior to chondrogenic induction, which was assessed after 28 days via pellet histology and GAG quantification, performed as described in section 4.2 (chondrogenic differentiation was not performed in hypoxic conditions). Pearson's and Spearman's correlation analyses were performed to find associations between gene expression and the positivity of surface markers prior to differentiation, to production of GAG by SF-MSCs after differentiation.

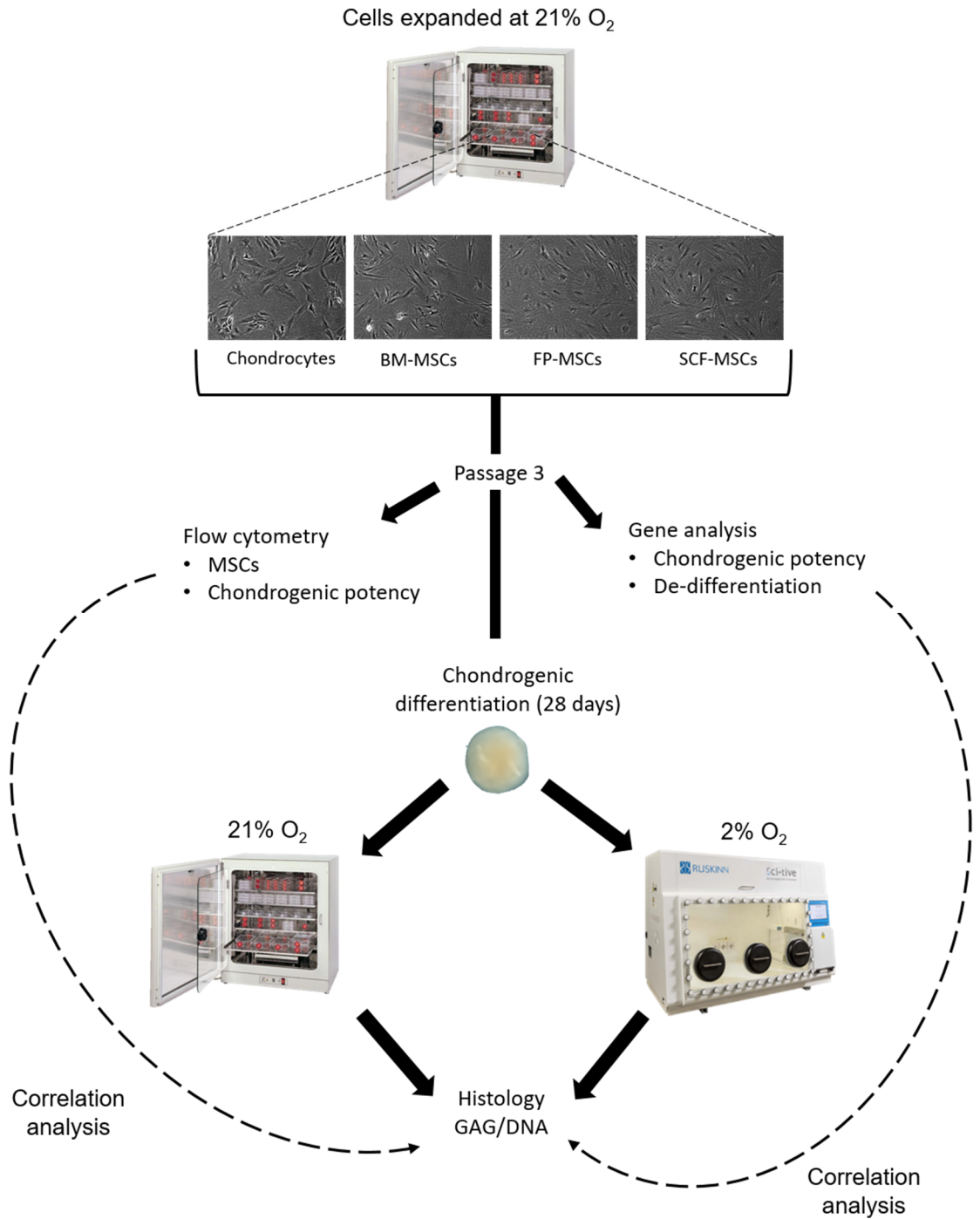


Figure 4.1: Workflow of experiments to compare the chondrogenic potential of donor matched chondrocytes and MSCs. All cell populations were isolated and expanded in normoxia. At passage 3 cells were characterised by flow cytometry and gene analysis and chondrogenically differentiated in normoxia and hypoxia. Correlation analyses were used to relate chondrogenic outcome with baseline flow cytometry and gene data.

Table 4.2: Demographics of patients used in experimental design 2

Donor number	Gender	Age	BMI
1	Male	22	35.0
2	Female	48	29.5
3	Male	21	37.6
4	Female	19	34.1
5	Male	36	23.6
6	Male	28	30.5
7	Male	28	27.0
8	Female	30	27.8
9	Male	47	26.6
10	Female	35	23.8
11	Male	29	19.4
12	Male	30	36.3
13	Female	36	21.1
14	Female	63	23.7
15	Female	42	25.0

BMI: body mass index

4.4 Results: Comparing the chondrogenic induction of donor matched chondrocytes and MSCs

4.4.1 Measurement of oxygen levels in culture media

The levels of dissolved oxygen in culture conditions were measured using two different probes (HI2040 and Seven2Go). The manufacturers of the HI2040 recommended that measurements be made while stirring the probe in the fluid, however, this was not required for the Seven2Go. Measurements were conducted with and without stirring for both probes for comparison. Dissolved oxygen was measured at 17.3-22.2% in the unconditioned media commonly used for tissue culture, whereas media that was preconditioned in the HypoxyCOOL™ displayed levels of dissolved oxygen in the 3.6-5.0% range (Figure 4.2 A-B). These oxygen levels did not vary when monitored in cell cultures growing in hypoxic and normoxic conditions (Figure 4.2 C-D).

4.4.2 Comparison of the formation of chondrogenic pellets in hypoxia and normoxia

Cells that were grown in normoxia were chondrogenically differentiated in hypoxic and normoxic conditions. In general, cells failed to develop into 3D spherical pellets in hypoxic conditions, but instead formed fragile (disintegrating) structures (Figure 4.3), making them difficult to section and analyse. However, in normoxic conditions, as expected, cells successfully formed 3D chondrogenic pellets. For this reason, pellets formed in hypoxia were discarded and further analysis was only performed on pellets formed in normoxia.

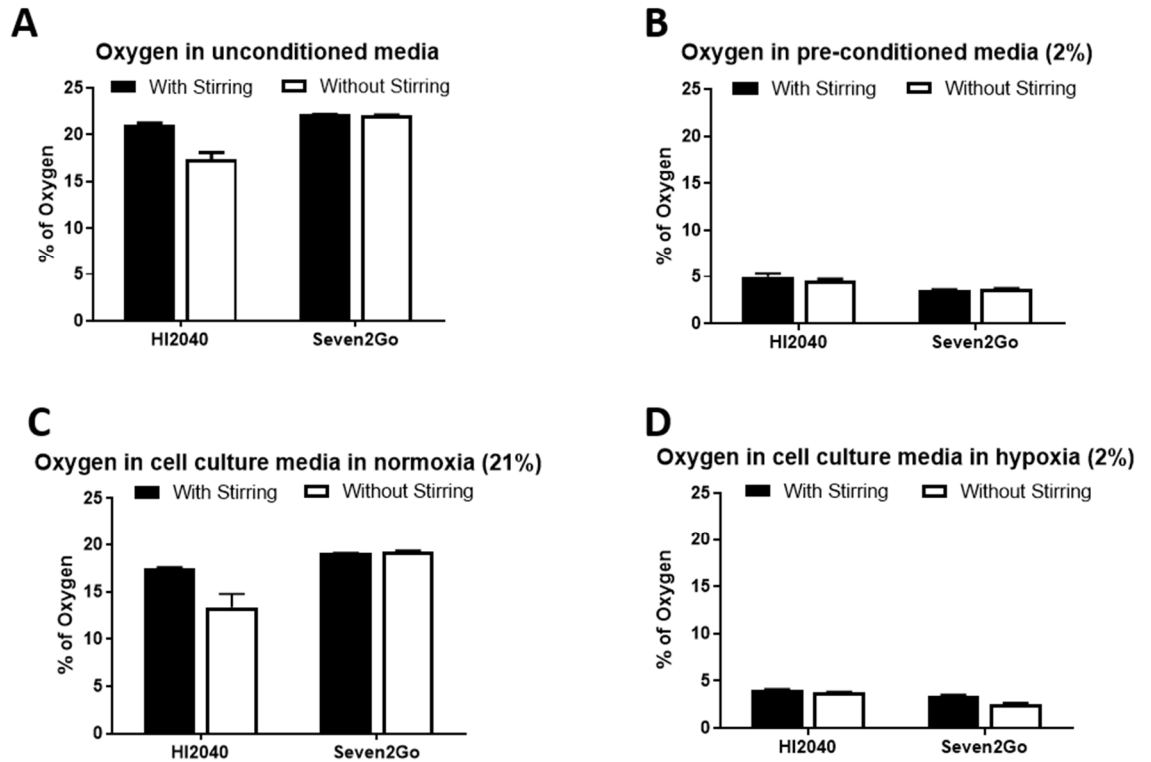


Figure 4.2: Measurement of oxygen levels in culture media in various conditions. A-B) Dissolved oxygen in unconditioned media and media pre-conditioned in the HypoxyCOOL™. C-D) Dissolved oxygen in media from cell cultures in normoxia (21%) and hypoxia (2%). Measurements were obtained using the HI2040 and Seven2Go oxygen probes with and without stirring of the probes. Error bars represent the standard deviation (SD) of triplicate measurements.

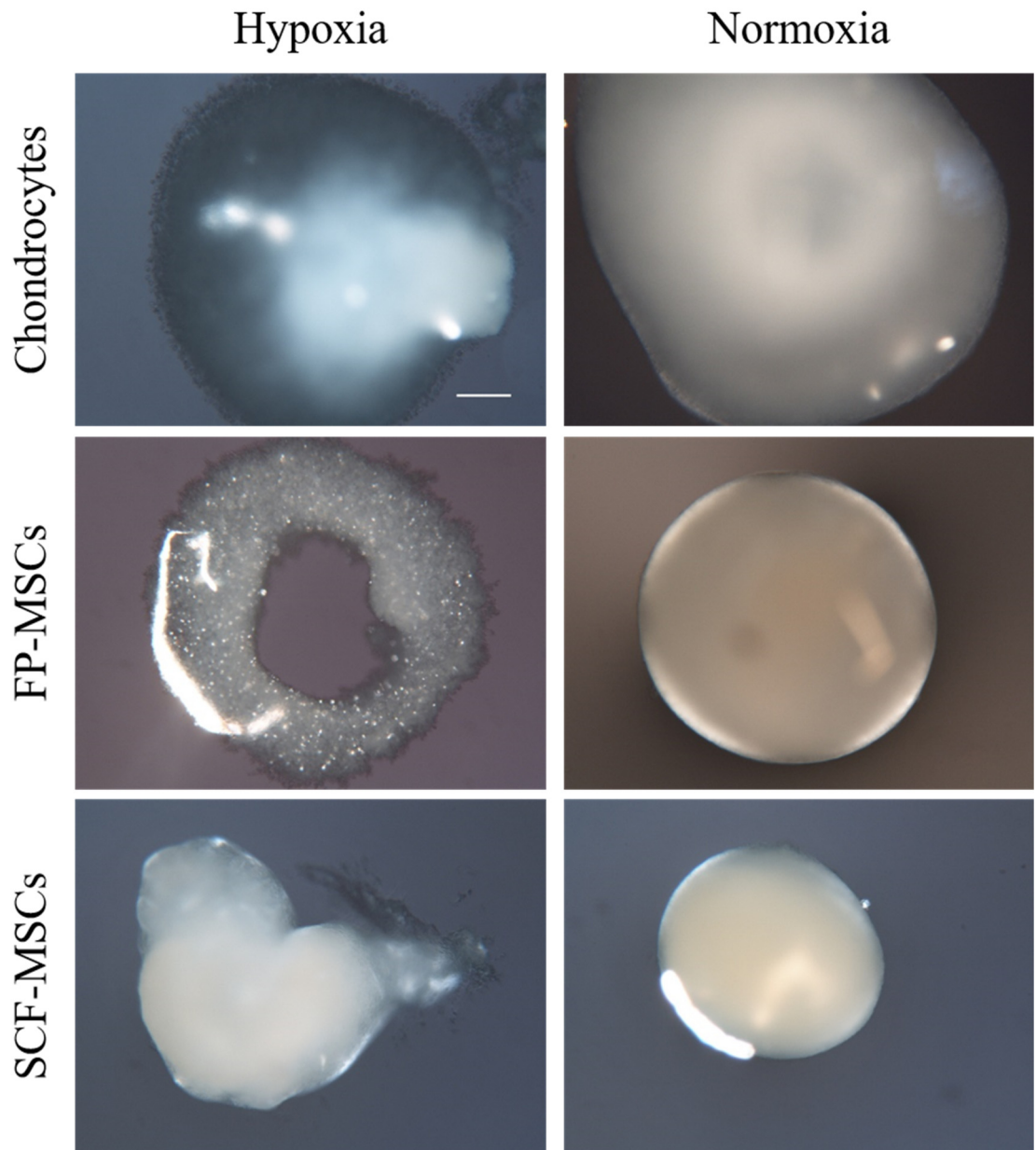


Figure 4.3: Pellets formed in hypoxic and normoxic conditions. Cells were culture expanded in monolayer in normoxic conditions and subsequently differentiated in pellet cultures in hypoxic and normoxic conditions at passage 3. Representative images acquired using polarised light under a light microscope immediately after chondrogenic differentiation are shown. Scale bar represents 200 μm .

4.4.3 Immunoprofiling of cells for MSC and chondrogenic markers

Flow cytometry analyses revealed immunopositivity for the MSC markers CD73, CD90 and CD105 for all of the populations of cells examined, but to varying levels (Table 4.3). FP and SCF derived MSCs adhered to ISCT²⁸⁰ criteria (i.e. were >95% positive), chondrocytes and BM-MSCs also adhered to ISCT criteria for CD90 and CD105 positivity, but were <95% positive for CD73 (Table 4.3). All of the cell populations tested were <2% positive for CD19, CD45 and HLA-DR, in line with ISCT criteria. Some positivity was recorded in all of the cell populations tested for CD34 with the highest levels (62.2-74.4% positivity) seen in the adipose derived MSCs, which also adheres to ISCT criteria³⁵² (Table 4.3). CD14 was present on all the cell populations tested, ranging on average between 14.8-21.4% positivity for each cell type (Figure 4.5). Interestingly, chondrocytes and BM-MSCs displayed significantly higher levels of CD106 than FP and SCF-MSCs ($p < 0.001$).

Differences between cell types for putative chondrogenic potency marker positivity were noted for CD49c, CD166 and CD39 (Figure 4.5). Chondrocytes showed significantly greater positivity for CD49c compared to SCF-MSCs ($p = 0.014$), whereas the adipose derived MSCs showed significantly higher positivity for CD166 compared to chondrocytes or BM-MSCs ($p = 0.0046$ and $p = 0.0002$, respectively for FP-MSCs and $p = 0.021$ and $p = 0.01$, respectively for SCF-MSCs). No differences were noted for CD44, CD151 or CD271, in that all cell types were >95% positive for CD44 and CD151, and <5% positive for CD271. No positivity for α ROR2 as recorded.

Table 4.3: Immunoprofiles for MSC markers on cell culture expanded cells at passage 3 prior to chondrogenic differentiation (n=6).

Surface Markers	Percentage of positive cells (mean% \pm SD)			
	Chondrocytes	BM-MSCs	FP-MSCs	SCF-MSCs
CD73	91.2 (\pm 17.7)	87.1 (\pm 18.0)	99.9 (\pm 0.1)	99.9 (\pm 0.0)
CD90	98.0 (\pm 3.8)	96.4 (\pm 2.5)	99.9 (\pm 0.0)	99.9 (\pm 0.1)
CD105	99.4 (\pm 0.7)	96.7 (\pm 4.1)	98.1 (\pm 4.1)	99.9 (\pm 0.1)
CD34	9.5 (\pm 8.0)	5.1 (\pm 5.4)	74.5 (\pm 15.6)	62.2 (\pm 20.8)
CD45	1.5 (\pm 0.6)	1.3 (\pm 0.4)	2.4 (1.3)	1.6 (\pm 0.6)
CD14	20.4 (\pm 27.1)	14.8 (\pm 12.0)	17.9 (\pm 36.5)	21.4 (\pm 39.3)
CD19	1.3 (\pm 0.8)	2.0 (\pm 1.2)	1.4 (\pm 0.6)	1.6 (\pm 0.5)
HLA-DR	1.4 (\pm 0.6)	1.3 (\pm 0.8)	1.7 (\pm 0.7)	1.3 (\pm 0.6)
CD106	71.9 (\pm 39.8)	67.5 (\pm 30.3)	29.9 (\pm 43.3)	31.1 (\pm 45.6)

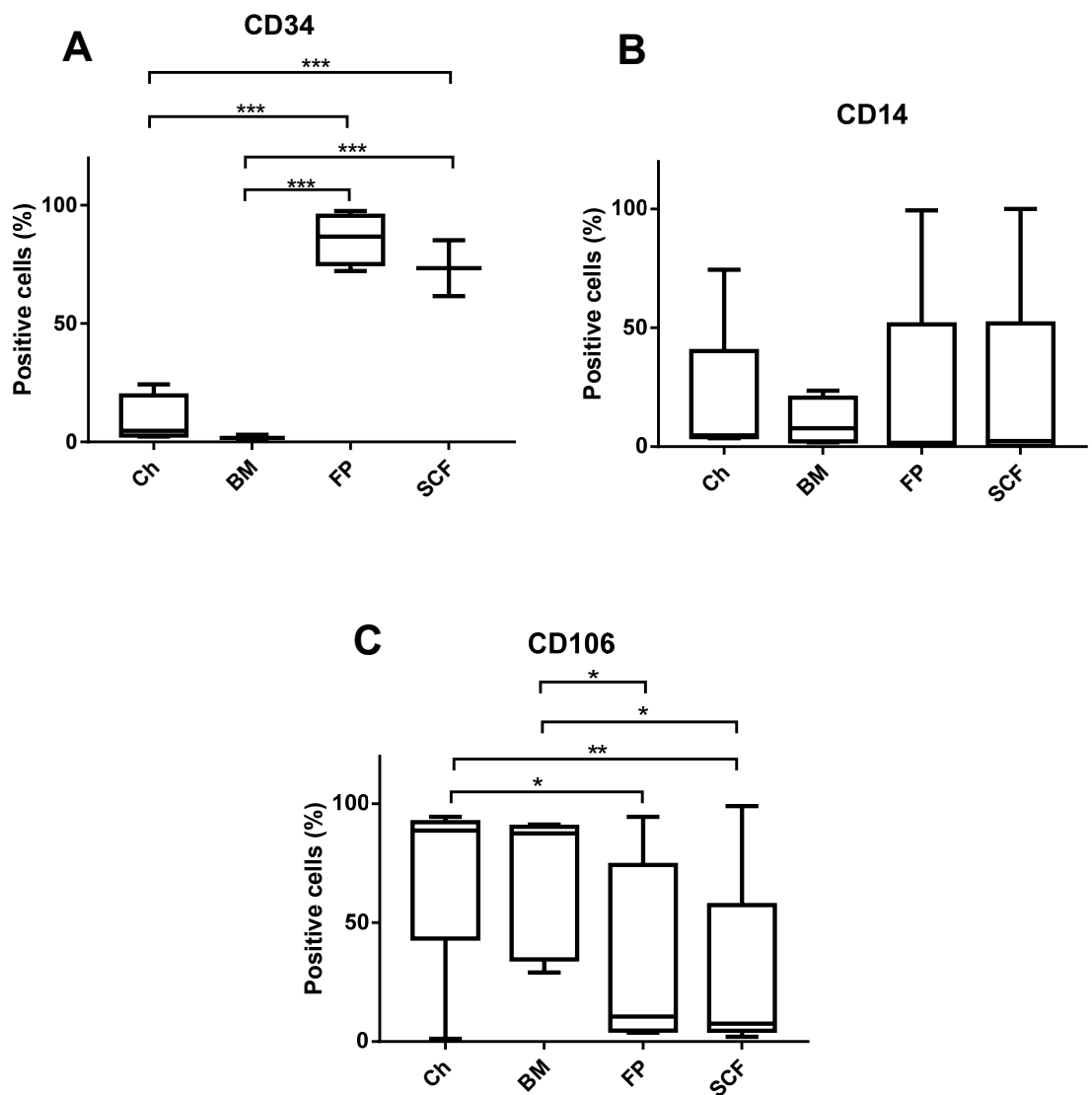


Figure 4.4: Immunoprofile of MSC selection markers that showed significant variability (a 2-way ANOVA was used to compare marker positivity between cell populations). A) CD34 was significantly more positive FP and SCF-MSCs compared to chondrocytes and BM-MSCs ($p < 0.001$). B) No significant difference was noted between the cell populations for CD14 positivity. C) Chondrocytes and BM-MSCs were significantly more positive for CD106 than FP and SCF-MSCs.

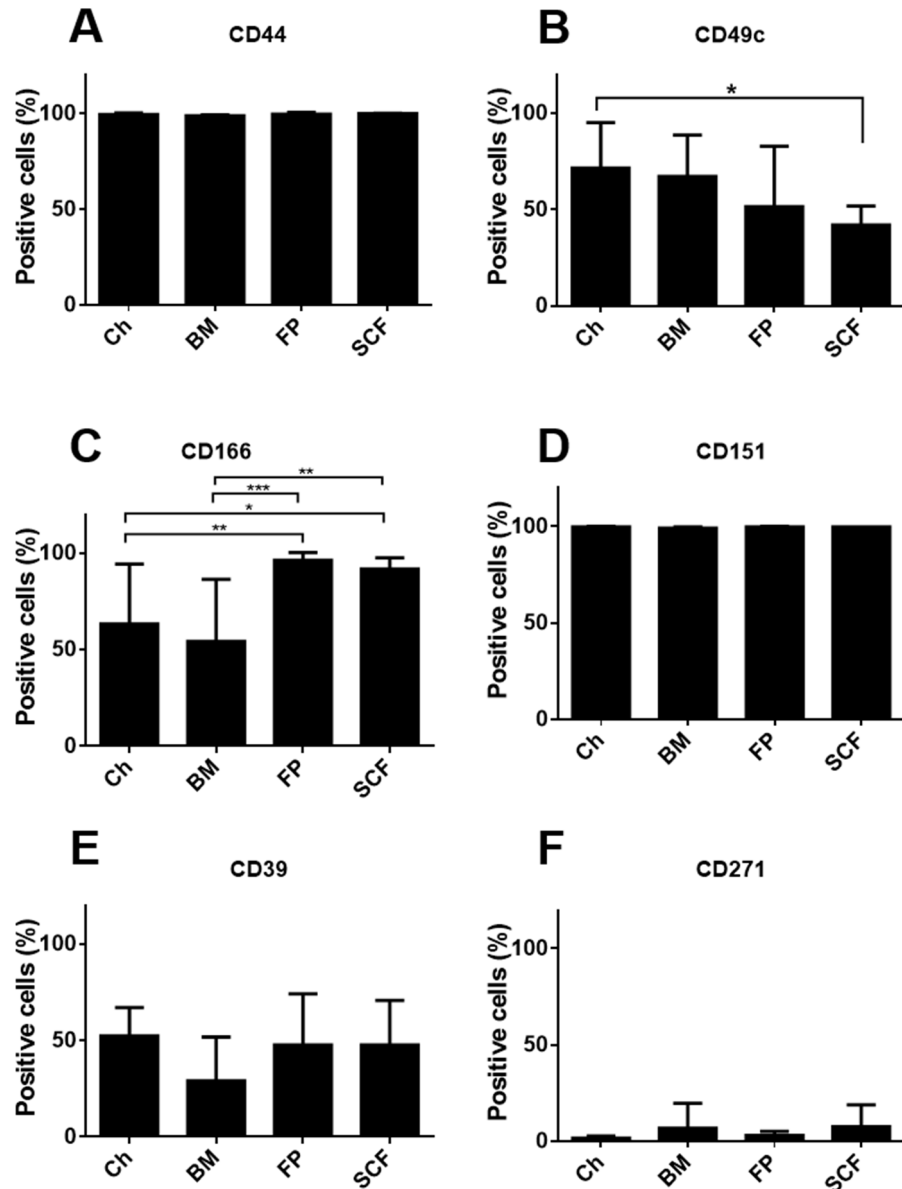


Figure 4.5: Immunoprofiles for putative chondrogenic potency markers on culture expanded cells prior to chondrogenic induction. Flow cytometry was used to detect the percentage of positive cells for each marker on monolayer cell populations of chondrocytes (Ch), bone marrow MSC (BM), fat pad MSC (FP) and sub cutaneous fat MSC (SCF) prior to chondrogenic differentiation in pellet cultures. A) All cell populations showed high positivity for CD44. B) Chondrocytes showed significantly higher levels of CD49c than SCF-MSCs. C) FP- and SCF-MSCs had a significantly higher positivity for CD166 than chondrocytes and BM-MSCs. D) No significant difference was observed for CD151 which was highly expressed in all cell populations. E) The positivity of CD39 was similar for across cell populations. F) Data shown are the means +/- the standard deviation of 5 donors for each cell population. One-way ANOVA and post-hoc Bonferroni tests were used to test for significant differences in the positivity of cell surface markers between cell types.

4.4.4 Gene expression prior to chondrogenic differentiation

Of the cell types tested in this study, the chondrogenic potency genes (*Sox9*, *Coll II*, *aggrecan*, and *FRZB*) were expressed at the highest levels in culture expanded chondrocytes (Figure 4.6 A, B and D). Further, chondrocytes demonstrated the lowest expression profiles for the hypertrophic genes tested (*Alk1* and *Coll X*). Of the MSC cell populations examined, BM-MSCs displayed chondrogenic and hypertrophic profiles that most closely resembled those of culture expanded chondrocytes. In contrast, the adipose sources of MSCs investigated (FP-MSCs and SCF-MSCs) were least like culture expanded chondrocytes and demonstrated the lowest chondrogenic potency and the highest hypertrophic gene expression profiles. SCF-MSCs expressed *Alk1* at significantly higher levels than chondrocytes and BM-MSCs ($p=0.044$ and $p=0.034$, respectively) (Figure 4.6 F).

Gene expression associations for all of the cell types examined in this study were tested using Pearson's correlation coefficient analyses and are presented in a correlation matrix (Table 4.4). Significant interactions noted between the chondrogenic potency genes were as follows; *aggrecan* was positively associated with *Sox9*, *Coll II* and *FRZB*, in addition, *Sox9* was positively associated with *Coll II* ($p=0.026$). There was also a significant negative association observed between *Coll II* and *Alk-1* expression ($p=0.001$).

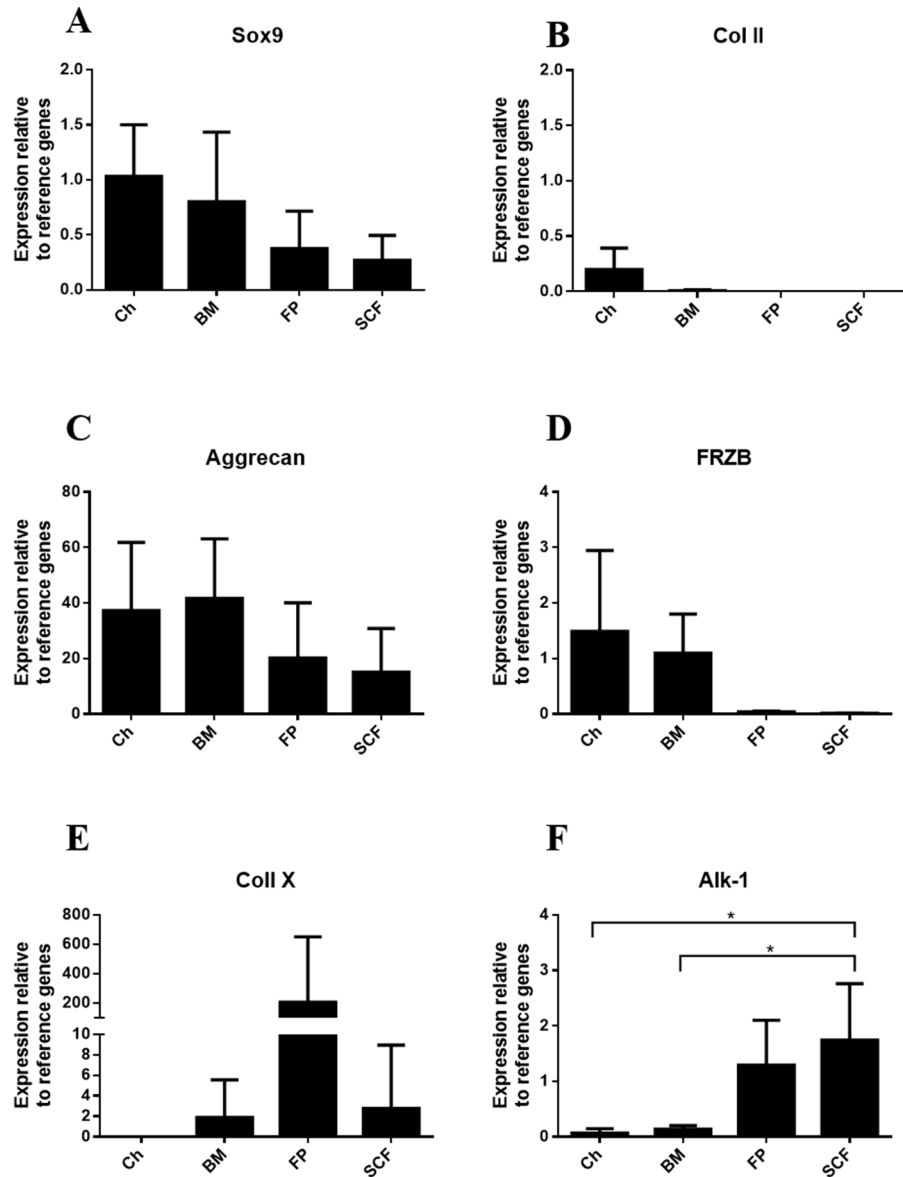


Figure 4.6: The expression of chondrogenic and hypertrophic genes in monolayer cell populations at passage 3, prior to chondrogenic induction. Gene expression is shown relative to the reference genes PPIA and TBP. Data shown are the means \pm the standard deviation of 5 donors for each cell population. One-way ANOVA and post-hoc Bonferroni tests were used to test for significant differences in gene expression levels between cell types.

Table 4.4: Pearson's correlation analysis matrix comparing genes that are predictive of chondrogenic potential. Significant values are highlighted.

	Alk-1	Coll X	FRZB	Aggrecan	Coll II
Sox-9	r=-0.36 p=0.15	r=0.28 p= 0.28	r=0.43 p= 0.09	r=0.70 p= 0.001	r=0.54 p= 0.026
Coll II	r=-0.74 p= 0.001	r=0.30 p=0.23	r=0.45 p= 0.07	r=0.53 p= 0.03	
Aggrecan	r= -0.44 p= 0.076	r= 0.25 p= 0.33	r= 0.65 p= 0.005		
FRZB	r= -0.33 p= 0.19	r= 0.26 p= 0.32			
Coll X	r= -0.33 p= 0.20				

4.4.5 Assessment of GAG production and pellet sizes after chondrogenic differentiation

After 28 days of chondrogenic differentiation, donors demonstrated variability in chondrogenic capacity across the cell types tested. When results from individual donors were examined, chondrocytes consistently produced superior chondrogenic pellets in terms of GAG quantitation (using the DMMB/DNA assays) and histological analyses, but the propensity for MSCs to undergo chondrogenic differentiation was variable between individuals. Although chondrocytes produced the highest average amount of GAGs compared to MSCs, no statistically significant difference was found (Figure 4. 7 A). Similarly, significant variability was observed in the amount of DNA produced in pellets with no significant difference in between cell types (Figure 4. 7), suggesting that some of the cell types continue to proliferate while undergoing chondrogenesis. SF-MSCs produced the most average DNA per pellet, whereas chondrocytes produced the least amount of DNA per pellet.

Normalised GAG/DNA analyses appeared to match the histological findings noted for each patient, i.e. larger pellets with prominent matrix metachromasia had the highest levels of GAG measured (Figure 4.8). Pearson's correlation analyses across donors confirmed that there was a significant association between pellet GAG quantitation and histological score ($p=0.01$). When donors were grouped and chondrogenic analyses were performed comparing differentiation between cell types, chondrocytes consistently demonstrated the most pronounced chondrogenic differentiation in terms of GAG/DNA analyses; they produced significantly more GAG than BM and SCF derived MSCs ($p=0.032$ and $p=0.030$, respectively, Figure 4.9 A). In terms of chondrogenic score SCF-MSC scores were significantly lower than chondrocytes, BM and FP derived MSCs ($p<0.0001$, $p=0.0195$ and $p=0.0082$ respectively) and chondrocytes scored significantly higher than BM-MSCs

($p=0.013$, Figure 4.9 B). Chondrocytes also produced the largest pellets (in terms of diameter) compared to any of the MSCs tested ($p<0.0001$, Figure 4.9 C).

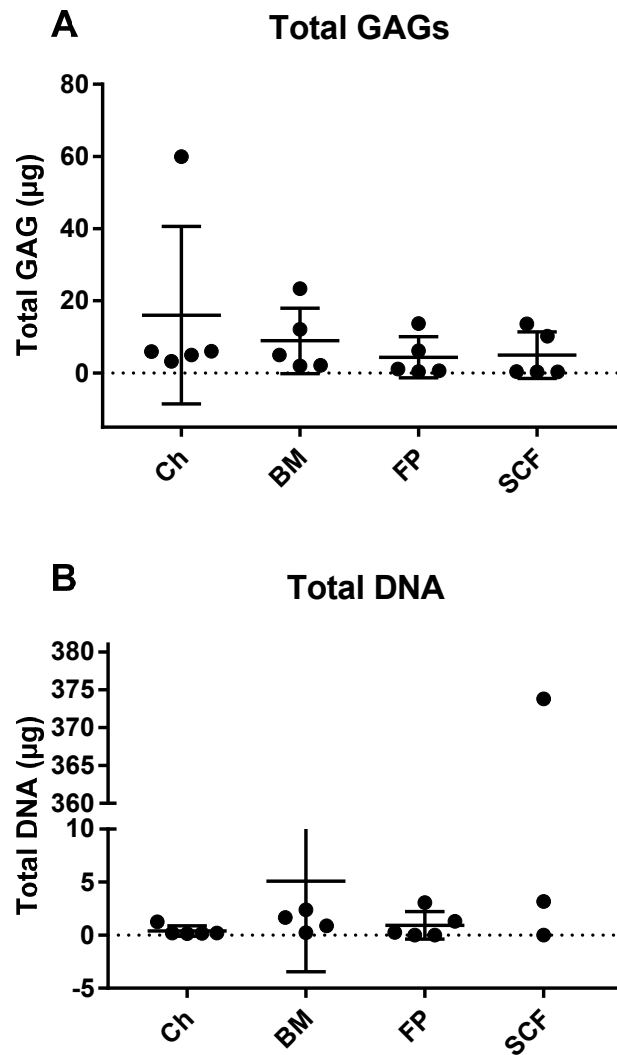


Figure 4. 7: Total GAG and DNA produced per pellet after chondrogenic differentiation. A) GAG content (μg) in pellets cultures from chondrocytes (Ch), bone marrow MSC (BM), fat pad MSC (FP) and subcutaneous fat MSC (SCF) after 28 days of chondrogenic differentiation as determined from the DMMB assay. B) DNA content (μg) in pellets after 28 days of chondrogenic differentiation as determined from the PicoGreen assay. Data is shown as individual points for each donor, with the mean and SD.

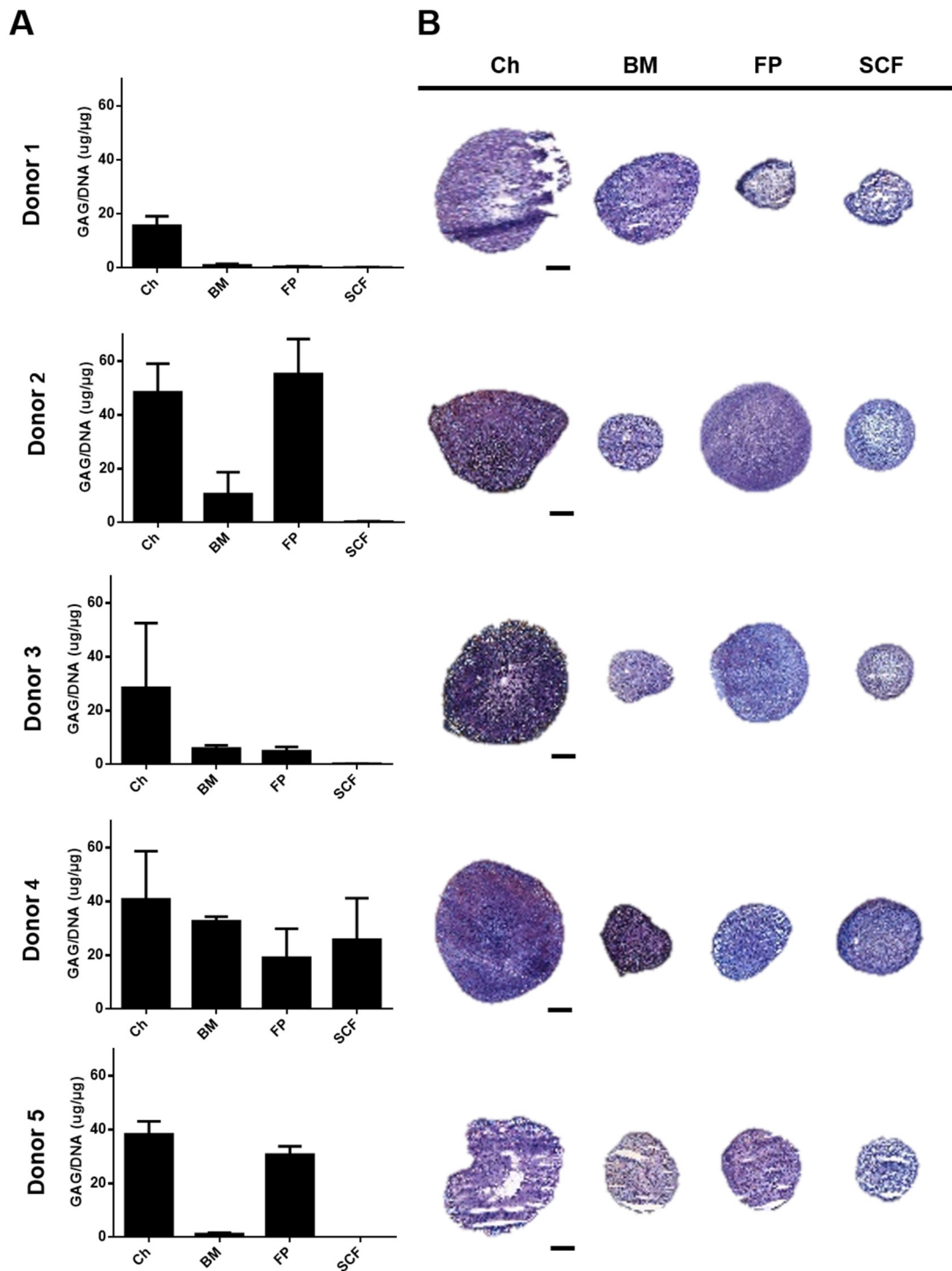


Figure 4.8: Assessments of chondrogenic differentiation in pellet cultures for individual donor. Cells were expanded up to 3 passages before chondrogenic differentiation. A) Production of GAG/DNA in pellet cultures from chondrocytes (Ch), bone marrow MSC (BM), fat pad MSC (FP) and subcutaneous fat MSC (SCF). GAG were measured after chondrogenic differentiation using the DMMB assay and normalised to the DNA content of pellets, each donor is represented in individual graphs. Data shown are the means \pm the standard deviation of triplicate pellets. B) Chondrogenic pellets from Ch, BM, FP and SCF showing representative toluidine blue staining for each donor. Scale bars represent 200 μ M.

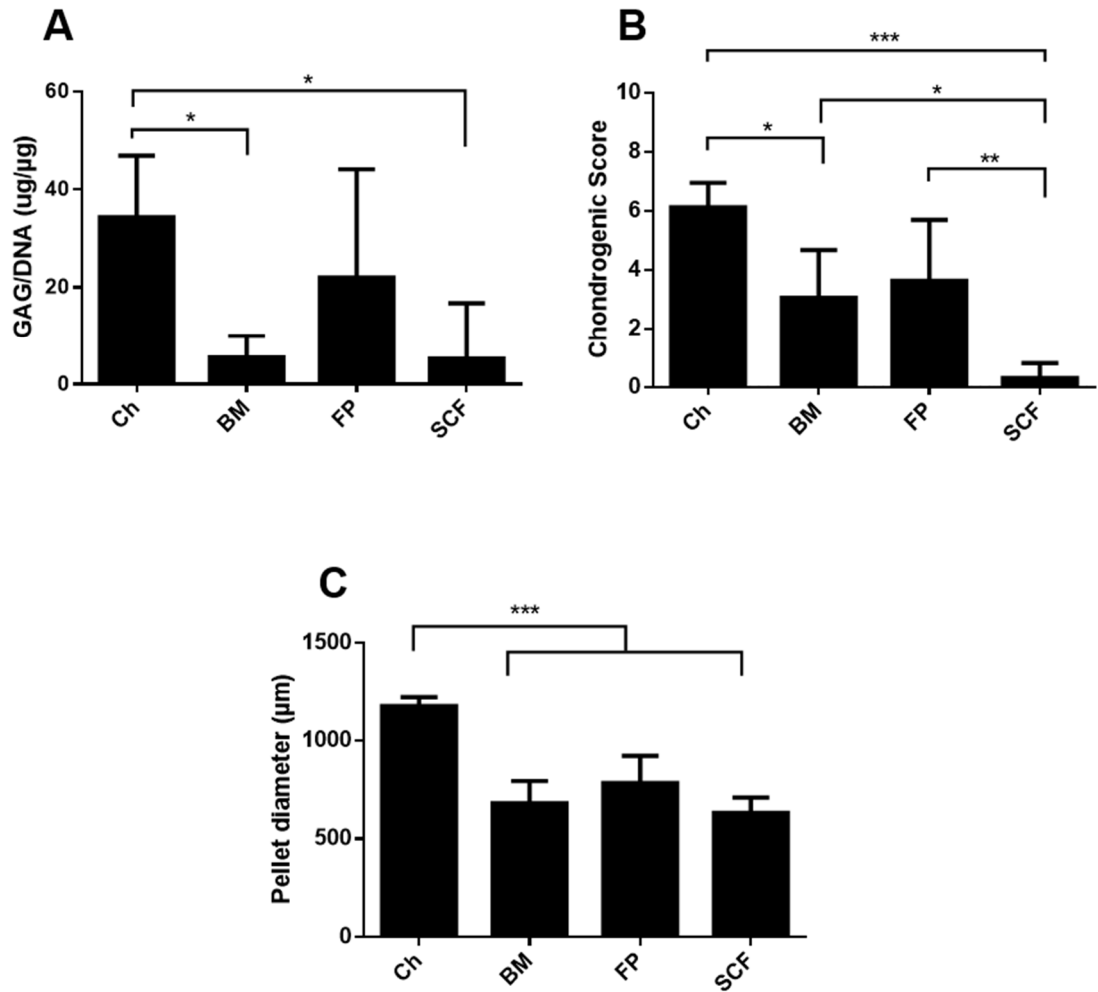


Figure 4.9: Chondrogenic assessments of pellet cultures across cell types for all donors combined. A) Production of GAG/DNA in pellet cultures from chondrocytes (Ch), bone marrow MSC (BM), fat pad MSC (FP) and subcutaneous fat MSC (SCF). (B) Chondrogenic histology scores for Ch, BM, FP and SCF. (C) Mean chondrogenic pellet diameter (μm) for Ch, BM, FP and SCF. Data shown are the means \pm the standard deviation of triplicate pellets and 5 donors for each cell population. One-way ANOVA and post-hoc Bonferroni tests were used to test for significant differences between cell types.

4.4.6 Association between surface markers or gene expression and GAG production

Multilevel modelling analysis was performed in an effort to identify chondrogenic potency predictors prior to chondrogenic differentiation. This analysis demonstrated that *Alkl* expression and CD166 immunopositivity both negatively associated with GAG quantitation in pellet cultures (Table 4.5). However, CD49c and CD39 expression positively associated with GAG quantitation and histological score respectively, post-chondrogenic differentiation (Table 4.5). *Sox9* expression positively associated with chondrogenic histological score, whereas expression of the hypertrophic genes *Coll X* and *Alkl* were shown to negatively associate (Table 4.5).

Further multilevel model analysis showed that cell type (but not donor) had a significant impact on the predictive aspect of gene expression for both of the chondrogenic assessments tested i.e. GAG quantitation ($p < 0.001$) and histological outcome ($p < 0.001$). Similarly, cell type (but not donor source) had a significant impact on the predictive aspect of cell surface marker positivity with regard to both GAG quantitation ($p < 0.001$) and histological outcome ($p < 0.001$). Using an interaction term in a multilevel model consisting only of the cell types and one predictive variable. results showed that the relationship between *Sox9/Alkl* expression and the histological outcome varied significantly across cell source ($p = 0.03$ and $p = 0.034$ respectively), which was not the case for *Coll X* ($p = 0.07$). The relationship between *Alkl* expression and GAG quantitation also did not vary across cell types ($p = 0.43$). In terms of immunopositivity, the relationship between CD39 positive cells and histological outcome varied significantly between cell types ($p < 0.001$) as did the relationship between CD49c or CD166 positive cells and GAG quantitation ($p < 0.001$ for both markers). A Spearman's correlation analysis was also conducted to determine a link between the levels of CD34 and CD106 (due to the variability in the and the chondrogenic outcome of the cell types; however no significant association was found.

Table 4.5: Multilevel modelling of how gene expression and surface markers relate to chondrogenic outcome. Significant associations are highlighted.

	GAG/DNA			Histology score		
	Coefficient	95% CI	p values	Coefficient	95% CI	p values
Sox-9	-5.6	-11.7, 0.5	0.07	1.01	0.18, 1.84	0.02
Coll II	22.3	-7.8, 52.4	0.14	3.96	-0.16, 8.08	0.06
Aggrecan	-0.003	-0.2, 0.2	0.97	-0.019	-0.04, 0.004	0.10
FRZB	33.1	-27.4, 93.6	0.3	0.86	-7.46, 9.18	0.83
Coll X	-0.01	-0.02, 0.003	0.12	-0.002	-0.004, -0.0002	0.03
Alk-1	-9.5	-12.2, 6.7	<0.001	-0.61	-0.99, -0.23	0.003
CD49c	0.2	-0.1, 0.5	0.018	-0.04	-0.02, -0.01	0.63
CD166	-0.3	-0.5, -0.04	0.03	0.01	-0.04, 0.034	0.16
CD39	-0.02	0.01, 0.4	0.78	0.024	0.01, 0.04	0.002

4.5 Results: Predictive analysis of the chondrogenic potential of SF-MSCs

4.5.1 Immunoprofiling SF-MSCs for MSC and chondropotency markers

SF-MSCs were negative for CD19, CD45 and HLA-DR ($\leq 2\%$), but showed positivity for CD34 ($28.4\% \pm 29.0$) and CD14 ($53.8\% \pm 36.0$), which does not fit the recommended ISCT criteria (Table 4.6). Although CD105 ($98.9\% \pm 1.0$) was consistently positive, CD73 ($89.0\% \pm 18.0$) and CD90 (89.8 ± 16.0) positivity varied markedly across donors, again not in accordance with ISCT criteria. SF-MSCs were positive for CD44 ($98.97\% \pm 1.0$), CD151 ($99.51\% \pm 1.0$), CD49c ($26.74\% \pm 18.0$), CD39 (26.77 ± 20.0) and CD271 (5.80 ± 5.0). The immunomodulatory marker CD106 ($87.15\% \pm 12.0$) was also expressed on SF-MSCs.

4.5.2 Expression of chondrogenic and hypertrophic genes in SF-MSCs

SF-MSCs showed significant variability between donors with regards to the expression of chondrogenic and hypertrophic genes (Table 4.7). SF-MSC expression levels of *Sox9* and *aggrecan* relative to reference genes were similar to the levels obtained for SCF-MSCs in the previous results section (section 4.4.4), whereas the expression of *FRZB* and *Alk-1* in SF-MSCs were comparable to FP-MSCs and BM-MSCs, respectively.

Table 4.6: The immunoprofile of SF-MSCs for surface markers at passage 3, prior to chondrogenic differentiation.

Marker	Mean positivity (\pmSD)
CD19	2.1 (\pm 0.30)
CD34	28.4 (\pm 29.0)
CD45	2.1 (\pm 0.40)
HLA-DR	1.3 (\pm 0.7.0)
CD14	53.8 (\pm 36.0)
CD73	89.0 (\pm 18.0)
CD90	89.8 (\pm 16.0)
CD105	98.9 (\pm 1.0)
CD39	26.77 (\pm 20.0)
CD44	98.97 (\pm 1.0)
CD49c	26.74 (\pm 18.0)
CD151	99.51 (\pm 1.0)
CD106	87.15 (\pm 12.0)
CD166	23.42 (\pm 23.0)
CD271	5.80 (\pm 5.0)

Table 4.7: The expression of chondrogenic genes relative to reference genes prior to chondrogenic differentiation by SF-MSCs.

Gene	Mean (\pmSD)
Sox 9	0.28 (\pm 0.26)
Coll II	7.0×10^{-3} (1.3×10^{-2})
Aggrecan	15.27 (\pm 8.6)
FRZB	4.3×10^{-2} ($\pm 3.5 \times 10^{-2}$)
Coll X	1.6×10^{-3} ($\pm 1.5 \times 10^{-3}$)
Alk-1	0.20 (\pm 0.16)

4.5.3 Assessment of GAG production in SF-MSCs after chondrogenic differentiation

SF-MSCs produced relatively low amounts of GAG with a mean of 3.5 μg (± 2.7) of GAG for the 15 donors tested. Histology confirmed this low production of GAG in that only weak patches of positive staining were observed for toluidine blue through the pellets (Figure 4.10 A). Donor 4 however produced on average 12.7 μg of GAG, which was markedly higher than the average produced by other donors. This increased GAG production was confirmed with histological analyses, in that uniform metachromatic staining was observed throughout the pellet (Figure 4.10 B). The average diameter of the SF-MSCs pellets after chondrogenic differentiation was 800 μm (range 659 μm -954 μm).

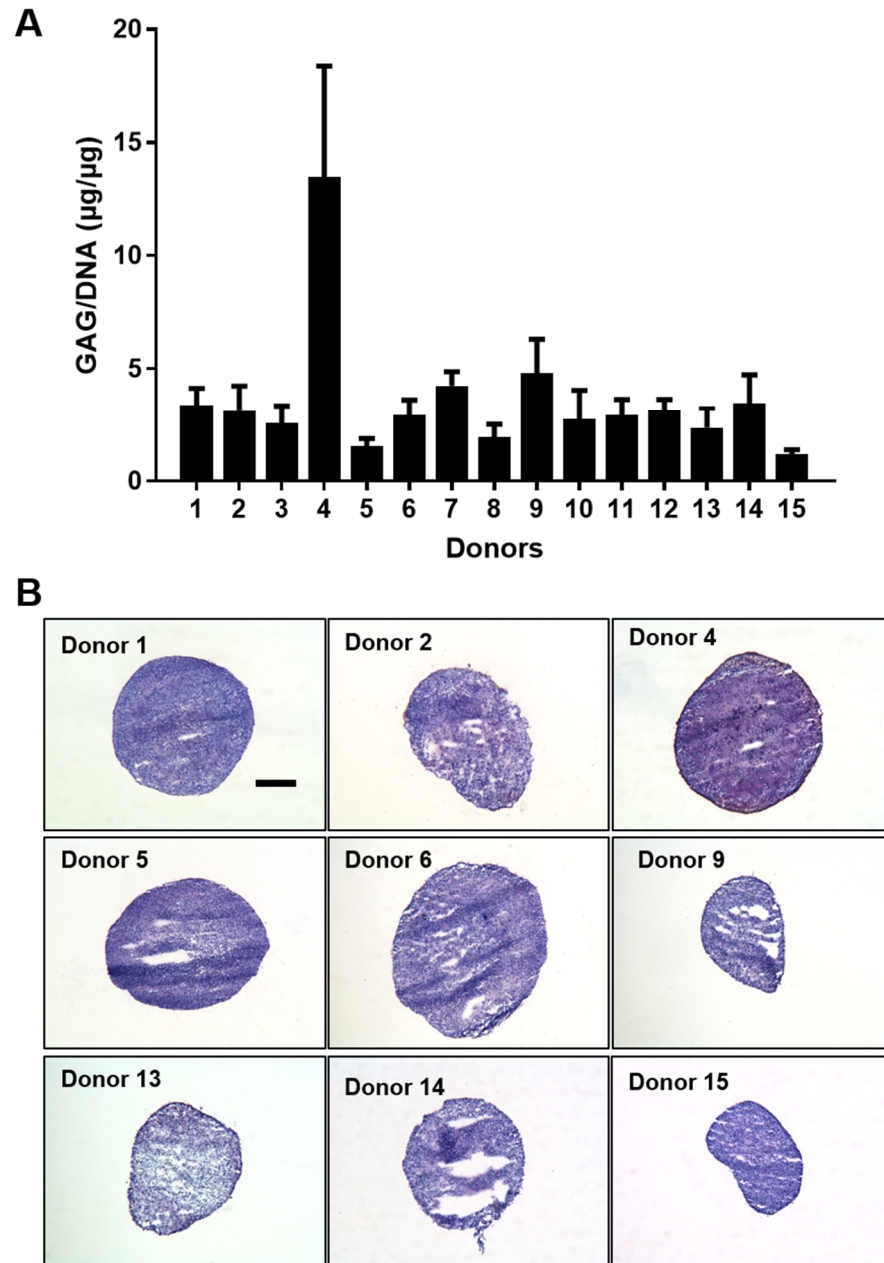


Figure 4.10: The production of GAG by SF-MSCs at passage 3. A) Quantification of GAG from DMMB/DNA assays. Error bars represent the SD of triplicate pellets for the same donor. B) Images are of toluidine blue stained pellets. Scale bar=200 µm.

4.5.4 Correlation between surface markers, gene expression and donor demographics compared to the production of GAG/DNA and histological outcome after chondrogenic differentiation.

The cells from donor 4 produced markedly more GAG/DNA compared to the other donors tested, which caused the occurrence of an outlier that significantly influenced statistical analyses (Figure 4. 11). For instance, the associations between CD49c positivity and GAG/DNA production, showed significantly different trends depending on whether the outlier of donor 4 was included in the analyses. When donor 4 was included in the correlation analyses, no significant association was found between surface markers and GAG/DNA or histological scores. As a result, and for simplicity, data for donor 4 was excluded from all statistical analyses. Of the proposed chondrogenic markers, only CD49c showed a significant (negative) correlation with the production of GAG/DNA (Table 4.8). Due to their unexpected variability for positivity of CD14, CD73 and CD90 across donors, analyses were run to determine whether the positivity of these markers was associated with the production of GAG/DNA by SF-MSCs. The results showed a negative correlation between CD90 positivity and GAG/DNA production. No such pattern was observed for CD14 or CD73. No significant correlations were established between surface markers and histological scores.

Correlation analyses revealed that only the expression of *ColIII* in SF-MSCs prior to chondrogenic induction was positively associated with the production of GAG (Table 4.8); no such trend was observed when correlating gene expression to histological scores. Interestingly, the cells from Donor 4, which produced the highest amount of GAG, also showed the highest expression of *Sox9*.

Neither donor age nor BMI correlated with the chondrogenic potential of SF-MSCs (Table 4.8). However, it is again noteworthy that donor 4, whose cells showed the highest chondrogenic potential, were derived from the youngest donor.

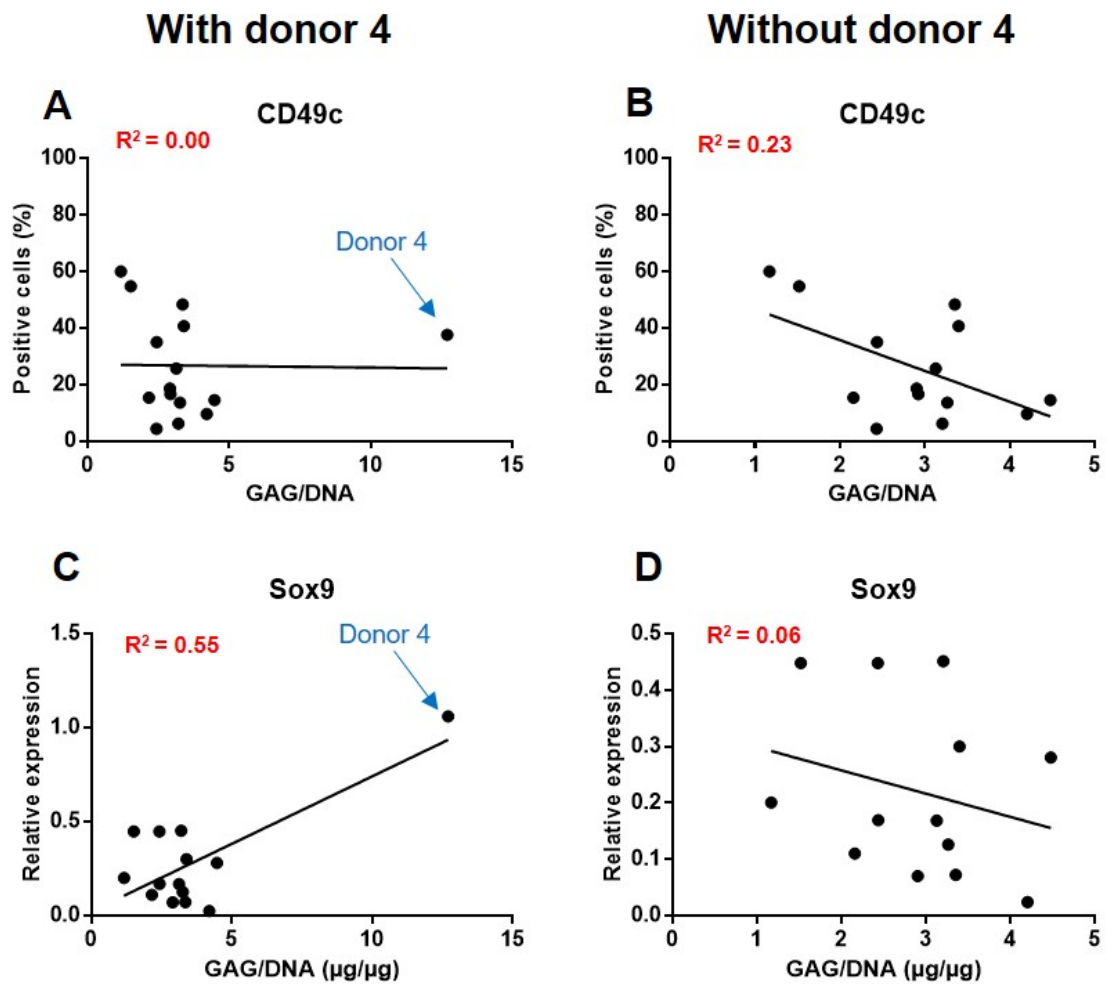


Figure 4. 11: Illustration of the impact of donor 4 as an outlier on correlation analyses. A-B) Scatterplots show that donor 4 significantly influences the trend of the correlation between the positivity of CD49c before differentiation and the production of GAG/DNA after differentiation of SF-MSCs. C-D) Scatterplots show that donor 4 significantly influences the trend of the correlation between the gene expression of *Sox9* before differentiation and the production of GAG/DNA after differentiation of SF-MSCs. In this instance, the correlation is positive when donor 4 is included in the analysis, whereas the association was negative without donor 4.

Table 4.8: Correlation between the positivity of surface markers before chondrogenic induction with the production of GAG and histological score after chondrogenic differentiation of SF-MSCs.

	GAG/DNA		Histology score	
	r	p value	r	p value
Surface markers				
CD49c ^P	-0.54	0.047	-0.04	0.92
CD166 ^P	-0.31	0.28	-0.18	0.64
CD39 ^S	-0.02	0.95	-0.25	0.52
CD271 ^S	0.35	0.21	0.08	0.85
CD73 ^S	-0.16	0.58	-0.14	0.71
CD90 ^S	-0.6	0.03	-0.11	0.78
CD14 ^P	-0.45	0.11	-0.37	0.31
Sox9 ^S	-0.22	0.45	0.59	0.12
Genes				
<i>CollIII</i> ^S	0.73	0.007	-0.56	0.15
<i>Aggrecan</i> ^P	-0.12	0.70	-0.15	0.73
<i>FRZB</i> ^P	0.11	0.71	0.28	0.50
<i>CollX</i> ^S	0.37	0.21	-0.45	0.27
<i>Alkl</i> ^S	0.03	0.93	-0.26	0.54
Demographics				
Age ^P	0.05	0.86	-0.62	0.09
BMI ^P	0.09	0.7	0.32	0.47

^S=Spearman's correlation used for non-normally distributed data; ^P=Pearson's correlation used for normally disturbed data.

4.6 Discussion

Low oxygen conditions have been explored as a method for improving the *in vitro* expansion of cells aimed at cartilage regeneration. However, researchers often fail to measure or report the true levels of oxygen present in hypoxic culture platforms, or ensure that oxygen levels are sustained throughout the whole culture period, including during media changes. The investigations reported here revealed that although culture media was pre-conditioned at 2% and the hypoxic work station was programmed to incubate at 2%, the true levels of oxygen in the culture media were above 2% but less than 5%.

Oxygen concentrations are essential in maintaining the various stem cell niches *in vivo*, but also in preserving the phenotype of stem cells *in vitro*^{429,430}. Hypoxic conditions (1-5% O₂) enhance the isolation, proliferation and differentiation potential of BM-MSCs and adipose derived MSCs^{339,431,432}. The failure of cells grown in hypoxia to form 3D pellets in hypoxia shown in this chapter requires further investigation, to understand their adaptability to low oxygen after being exposed to an oxygen-rich environment during expansion. It is challenging to compare the *in vitro* results obtained in this results chapter to other published studies due to the lack of sufficient information on the detailed culture methods used. For example, many hypoxia studies fail to report whether or not pellets were removed from hypoxic conditions for feeding, or whether preconditioned media was used^{427,433}.

Although results in the literature appear to be contradictory^{432,434}, one study has shown that low oxygen levels (below 5%) were detrimental to the chondrogenic potential of SCF-MSCs that were culture expanded in normoxic conditions⁴³⁵. Normoxia expanded chondrocytes, BM-MSCs and FP-MSCs have been shown to have enhanced chondrogenic propensity in hypoxia^{341,427,436}. When BM-MSCs were expanded in 3% or 21% O₂ and differentiated in both 3% and 21% O₂, it was reported that cells produced more GAG and expressed higher levels of chondrogenic genes (*Sox9* and *Coll II*) when differentiated in 3% compared to 21%

O₂⁴²⁷. Similar results were obtained when chondrocytes expanded in 21% O₂ were differentiated in both 2% and 21% O₂³⁴¹. FP-MSCs also displayed superior chondrogenic potential in 5% compared to 20% O₂ after expansion in 21% O₂⁴³⁶. These results do not corroborate the findings presented in this chapter; possibly due to the different experimental conditions employed such as donor demographics, tissue source (e.g. tibial plateau as opposed to iliac crest for BM-MSCs) and cell density of chondrogenic pellets. Importantly, these contradictory results call for studies with more controlled hypoxic environments. The results presented here were part of a more comprehensive experiment, which included the isolation and culture of chondrocytes in hypoxia. Interestingly, chondrocytes isolated and expanded in low oxygen conditions displayed a superior chondrogenic phenotype (as shown by higher GAG and type II collagen production) compared to the ones isolated and expanded in normoxia (Appendix 4).

While some investigations have compared the *in vitro* chondrogenic potency of donor matched chondrocytes and FP-MSCs (porcine model)⁴³⁷, or matched FP- and SCF-MSCs (human)⁴⁰⁵, no such study has been conducted for matched chondrocytes, BM-, FP- and SCF-MSCs together. As expected, FP and SCF-MSCs showed higher levels of CD34 than BM-MSCs and chondrocytes, due to their origin from adipose tissues³⁵². Chondrocytes appear to exhibit a similar MSC immunoprofile to BM-MSCs, which could be an indication of dedifferentiation as chondrocytes perhaps revert to a phenotype that is more like MSCs after being culture expanded. Previous research directly comparing matched chondrocytes and BM-MSCs has shown that the two cell types displayed multipotency and had similar surface marker profiles. In results section 4.4, known immunoprofiles and gene profiles believed to be indicative of chondrogenic potential were tested in a predictive model comparing chondrocytes, BM, FP and SCF derived MSCs from 5 matched human donors. In terms of immunoprofile, the putative chondrogenic markers CD44, CD151 and CD271

were excluded from predictive analyses due to their uniform expression levels across cell types. CD49c, CD166 and CD39 were also present on all of the cell populations examined but to varying degrees and as such were taken forward into chondrogenic potency analysis.

The expression of the chondrogenic genes, *Sox9*, *CollIII*, *ACAN* and *FRZB*, and the hypertrophy associated genes, *CollX* and *Alkl*, were determined in the various cell populations prior to chondrogenic differentiation. In doing so, it was confirmed that for all the cell populations tested, the master regulator of chondrogenesis, *Sox9*, correlates with the expression of *Coll II* and *ACAN* and that the hypertrophy associated marker *Alkl* is negatively associated with *Coll II* expression. In addition, the data presented in this results section shows that there is a positive association between the expression of *FRZB* and *ACAN*, which has been previously reported in the chondrogenic ATDC5 cell line⁴³⁸.

Following chondrogenic differentiation in cell pellets, quantitative assessment of GAG synthesis demonstrated that chondrocytes generate significantly more GAG compared to BM-MSCs and SCF-MSCs but not FP-MSCs, with some notable variation between donors. These findings are comparable to previous studies which have shown that chondrocytes and FP-MSCs display similar levels of GAG production and that FP-MSCs produce more GAG than BM-MSCs⁴³⁹ and donor matched SCF-MSCs⁴⁰⁵. Further, assessments for chondrogenic differentiation status in terms of GAG quantitation and histological score were significantly correlated. Chondrocyte-generated pellets consistently produced the highest scores, which were significantly greater than those formed by BM- or SCF-MSC populations, whereas SCF-MSCs pellets produced the lowest scores of all the cell populations examined. Measurements of the diameter of pellets showed that chondrocytes produced the largest pellets compared to BM and SCF derived pellets.

Interestingly, stem cells appear to generate pellets with a higher cellularity compared to chondrocytes based on DNA content and histological observations. This could be due to

more cell proliferation in stem cell pellets during differentiation. Taken together, this data suggests that, not too surprisingly, culture expanded chondrocytes have the greatest propensity for chondrogenic differentiation *in vitro*, closely followed by FP-MSCs and then BM-MSCs, whereas SCF-MSCs consistently produced the worst chondrogenic outcome measures, regardless of the assessment used. These findings are corroborated by other studies that have reported paired comparisons between these cell types^{310,405,425,440,441}. However, this is the first time, to date, that all four of these cell populations have been examined in the same study, allowing for a hierarchical chondrogenic potency comparison with the impact of donor taken into account by donor matching the samples tested.

The multilevel modelling analyses performed in this study have allowed the exploration of the relationships between putative chondrogenic potency markers (gene expression and surface marker profiles) and chondrogenic outcome, whilst simultaneously examining the potential influence of donor and cell type. These analyses are derived from a small donor sample size, acknowledged as a limitation of the study, and should be interpreted with caution.

Nonetheless, multilevel analysis indicated that CD49c and CD39 immunopositivity positively predict GAG production and histological score respectively in cell pellets, with no significant difference observed between donors. Other studies have shown that CD49c positivity on chondrocytes and CD39 positivity on synovium derived MSCs is associated with increased *in vitro* chondrogenic potential^{320,353}, however, these relationships across matched chondrocytes, BM-MSCs and adipose derived MSCs presented here have not been demonstrated before. Perhaps surprisingly CD166 positivity did not indicate chondrogenic potential, as has been previously shown³⁵⁴; in fact immunopositivity for this marker was negatively associated with chondrogenic assessments. One potential explanation for this finding might be that CD166 was expressed at significantly greater levels on SCF-MSCs compared to chondrocytes and

BM-MSCs and that the data shown in results section 4.4 indicates that SCF-MSCs consistently demonstrate a poor propensity for chondrogenic differentiation. Interestingly, in this multi-cell type, donor matched study, the source of cells significantly influences both GAG production in pellet culture and also the histological score of the pellet. In contrast, the donor had no demonstrable impact on either of the chondrogenic assessments tested, although these results are based on a small cohort of donors and a larger cohort might be required to demonstrate a “donor effect”.

In addition, multilevel modelling has revealed that the expression of *Alkl* and *Coll X* are negatively associated with chondrogenic potential in terms of histology scores, expression of *Alkl* and the GAG content of chondrogenically induced pellet cultures. In contrast, *Sox9* expression prior to chondrogenic differentiation positively correlated with histological pellet scores. Some of these gene associations match a previous report comparing FP-MSCs and SCF-MSCs⁴⁰⁵. The novelty of this study is that some of these chondrogenic potency gene associations hold true across all of the cell types examined. The poor correlation between the baseline (pre-differentiation) expression of the chondrogenic genes *Coll II* and *ACAN* is noteworthy and comparable to findings in other studies^{442,443}. For example, one study has confirmed that the transplanted chondrocyte expression levels of *ACAN* and *Coll II* in ACI had no bearing on clinical outcome⁴⁴⁴. Further, it has been demonstrated that the genome-wide transcription profile of *Coll II* and *ACAN* (amongst other genes) did not correlate with the production of GAG in a single cell analysis of bovine MSCs and chondrocytes⁴⁴³. The authors attribute this finding to the heterogeneity in single cell transcriptional profiles. It is extremely likely that the gene analysis presented in results section 4.4, derived from heterogenous cell populations and four very different tissue sources will vary to an even greater extent.

The chondrogenic potency of SF-MSCs was also assessed in results section 4.5, but not from donors with end stage OA as in the previous results section (4.4). The immunoprofile of SF-MSCs indicate that they do not meet the recommended ISCT criteria. As stated previously it is possible that a heterogeneous cell population was enriched from the SF of patients receiving ACI. Furthermore, these results corroborate observations by another group where human SF-MSCs, obtained before and after ligament surgery, did not fully meet the ISCT recommended immunoprofile³¹⁸. The positivity of CD14 suggests the presence of macrophages and other immune cells as explained in section 3.8. The levels of CD34 also show the possible presence of perivascular and or endothelial cells⁴⁰⁴. The heterogeneity of these cells is shown by the lower than expected levels of CD73 and CD90, which did not meet the 95% positivity recommended by ISCT. Furthermore the low positivity of proposed chondrogenic markers CD49c, CD39 and CD271 were also previously reported^{315,388,428,445}.

The levels of GAG observed for SF-MSC derived pellets presented in this chapter are comparable with previous reports³¹⁵. The relatively low production of GAG could be explained by the heterogenous phenotypes of these cells, as indicated also by the flow cytometry results obtained. The patchy metachromatic staining of the chondrogenic pellets suggests that there are a subpopulation of SF-MSCs with some chondrogenic potential, although the relative abundance of these cells was perhaps insufficient to produce substantial detectable quantities of GAG in the experiments described. One possible explanation for this observation could be the impact that the degenerative state of the joint could have on the SF-MSC phenotype. It is believed that SF-MSCs may be recruited from other tissues in the joint, such as synovium, bone marrow and ligament³¹⁸ and it has been shown that the OA joint SF contains more SF-MSCs³⁸⁸. It could be hypothesised that the donors in this study did not have sufficient joint degeneration to trigger the recruitment of MSCs into the SF. For instance, it has been suggested that chemoattractant molecules released from a damaged

ligament could be responsible for the increase in SF-MSCs noted after ligament surgery (within weeks)³¹⁸.

The negative correlation established between CD49c and GAG production might suggest that the influence of this marker as an indicator of chondrogenesis in chondrocytes may not be valid for SF-MSCs³⁵³. The available literature that reports the use of surface markers as possible predictors of chondrogenic potential focuses predominantly on chondrocytes, and to a lesser extent, BM-MSCs. CD49c is part of the integrin alpha3 sub-unit, a surface receptor that adheres chondrocytes to components of the cartilage ECM such as laminin and collagens^{353,446}. The data obtained in results section 4.5 indicates that SF-MSCs are composed of a heterogeneous cell population, most of which are likely to originate from different microenvironments *in vivo* which could explain the variability in the expression of CD49c observed across SF-MSC donors. Furthermore, the changes in expression that occur in response to cell culture expansion may vary in the individual cell types that combine to form the SF-MSC cell population. The negative correlation noted between CD90 and GAG production was unexpected. Since CD90 is an MSC characterisation marker, it can be theorised that the presence of fewer MSCs in the mixed population of SF cells resulted in a reduced chondrogenic phenotype.

When correlating gene expression to GAG production by SF-MSCs, only *COLL II* showed a significant association, a finding that has not been previously reported. Donor 4, which showed the highest expression of *Sox9* also showed enhanced production of GAGs and a high chondrogenic histological score, comparable to the results obtained in section 4.4 for other established MSC sources. This might indicate that the MSCs within the SF for this donor were more uniform and could have originated from one of these tissue sources. The “disconnect” between other known chondrogenic genes and the differentiation capacity of

SF-MSCs is akin to the results obtained for donor matched chondrocytes, BM-MSCs, FP-MSCs and SCF-MSCs in results section 4.4.

Donor age and BMI did not correlate with the chondrogenic outcome measures examined for SF-MSCs. Donor 4 was the youngest donor (19 years old) and perhaps unsurprisingly produced SF-MSCs with the best chondrogenic outcome, although cells from a donor only 2 years older (donor 3) did not follow the same trend. Previous investigations have shown that younger donors produce BM-MSCs with superior chondrogenic potential compared to cells derived from older donors³⁸¹.

4.7 Conclusion

The main findings of this chapter are illustrated in Figure 4.12. The results presented here demonstrate the chondrogenic predictive value of high levels of *Sox9* and low levels of *COLL X* or *Alkl* expression as well as immunopositivity for CD49c and CD39 in chondrocytes, BM-MSCs, FP-MSCs and SCF-MSCs. The expression of *COLL II* and immunopositivity for CD49c and CD90 have also been shown to be predictive of chondrogenic potential in SF-MSCs. Using donor-matched samples has shown that, cell type significantly influenced the chondrogenic potency of the MSC sources examined in this study. MSCs sourced from the infrapatellar FP of the knee or bone marrow provide the ‘next best’ alternative to chondrocytes, in terms of *in vitro* chondrogenic differentiation capacity. Further, the results presented in this chapter have consistently shown that SCF-derived MSCs and SF-MSCs have the poorest propensity for chondrogenic differentiation. These findings have important clinical implications, not only for the understanding of MSC chondrogenic differentiation capacity, but also for the development of cell therapy strategies to screen for and select potent cell types prior to application in the treatment of cartilage injuries. Follow-on studies should be geared towards understanding the molecular

mechanisms that account for the differences observed between cell populations and in the development of methods to select cells with enhanced chondrogenic potential.

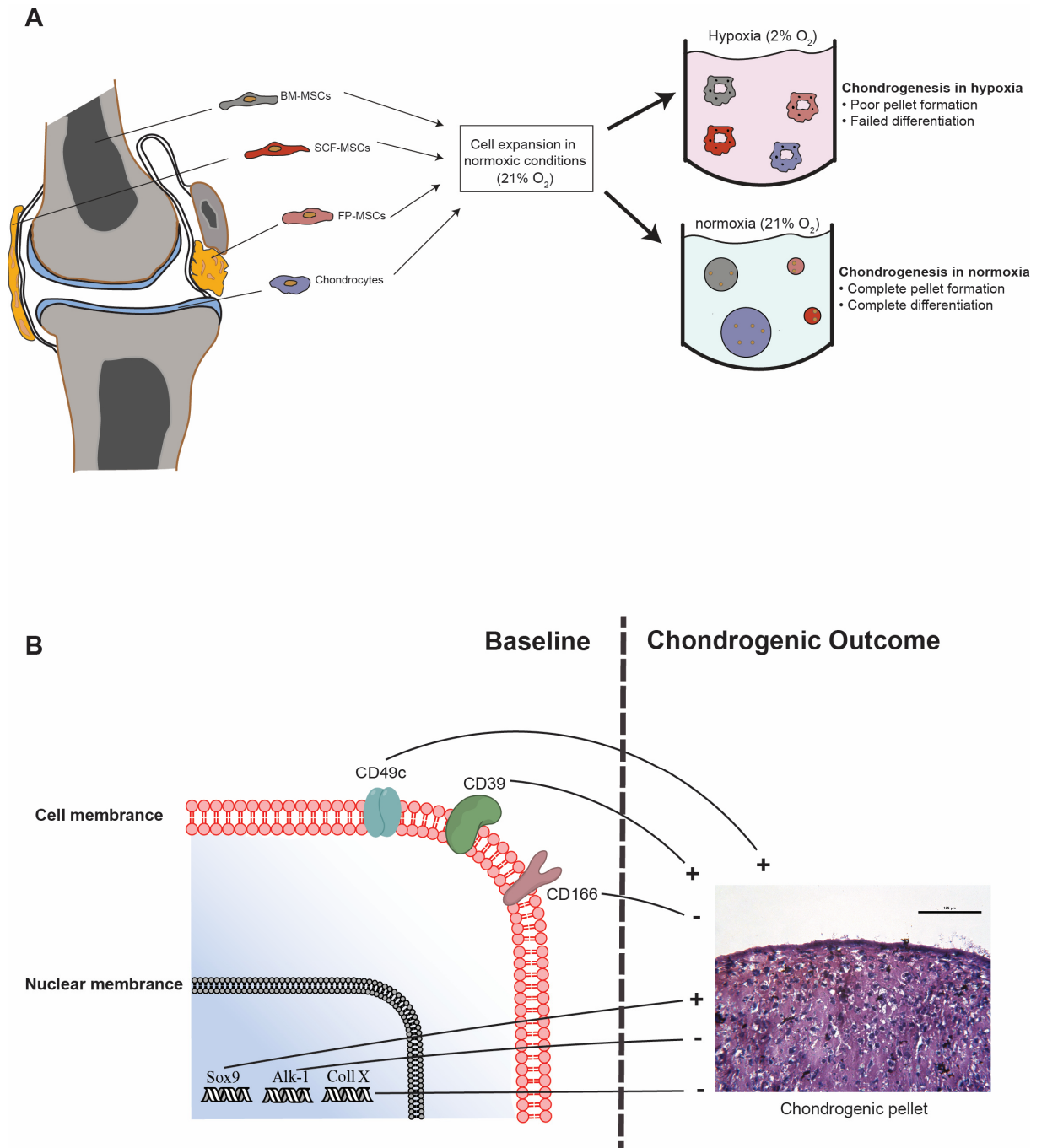


Figure 4.12: Summary of the principle findings presented in Chapter 4. A) Chondrocytes and MSCs isolated from the knee joint and expanded in normoxic conditions (21%) show poor chondrogenic ability in low oxygen (2%), but display enhanced chondrogenesis in normoxia. B) The positivity of surface markers CD49c and CD39 and the expression of Sox9 are positive predictors of the chondrogenic ability of chondrocytes and MSCs. On the contrary, the positivity of CD166 and expression of Alk-1 and Coll X are negative predictors of chondrogenesis these cells.

Chapter 5: Results

Characterisation of joint derived macrophages and adipocytes: implications for inflammation in OA.

5.1 Introduction and aim

In an attempt to understand the parameters involved in the progression of OA, recent studies have revealed the role played by joint inflammation, and more specifically synovial inflammation⁴⁴⁷. Macrophages, which are located in and along the synovial membrane, are one of the cell types responsible for the production of pro-inflammation molecules that contribute to the acceleration of joint degeneration. The ability of these cells to switch from a pro-inflammatory phenotype (M1) to an anti-inflammatory (M2) has not been investigated in the context of OA pathogenesis, and has thus attracted tremendous research interest for the development of novel therapies. Although the contribution of the infrapatellar FP to joint inflammation still remains undefined, studies have indicated the presence of macrophages within this adipose tissue⁴⁴⁸. In addition, certain regions of the FP are in direct contact with the synovium, which has led to the question of whether inflammatory processes occurring in the synovium can influence the FP (and vice versa).

Obesity is considered a risk factor for the development of OA not only with regard to the biomechanical disruptions it engenders in load bearing joints, but also for the systemic inflammatory and metabolic alterations that occur in obesity as suggested by recent studies²²³. The expansion of fat tissues is triggered by an energy imbalance, increased calorie intake coupled with inadequate or low energy expenditure, which in turn engenders metabolic abnormalities and hypertrophy (and or hyperplasia) of adipocytes⁴⁴⁹. The size of adipocytes has been directly correlated with the production of pro-inflammatory molecules (such as IL-6, TNF- α and monocyte chemoattractant protein-1) and is thus considered an indicator of adipose tissue inflammation⁴⁵⁰. However, it is unknown whether these changes occur in the FP in a similar way to other well characterised adipose tissues⁴⁵¹.

5.2 Experimental design-1

Donor-matched FP and synovium tissues were obtained from 11 patients with various arthropathies (Table 5.1). Tissues were wax embedded, sectioned (section 2.3), stained with H&E and a synovitis score was performed to determine the degree of synovial inflammation (section 2.5.3).

Immunohistochemistry was used to reveal the presence of cells that were positive for CD68 (pan macrophage marker), CD86 (M1), CD11c (M1), CD206 (M2) and arginase-1 (Arg-1, M2) (section 2.5.1). The synovium, sub-synovial stroma and FP of the 11 donors were ranked for each marker (section 2.5.2), and Spearman's correlation analysis was performed to determine potential associations in the positivity of markers between tissues.

In addition, donor-matched FP and synovium tissues were obtained from 4 patients undergoing TKR and were digested to obtain the cellular fraction (section 2.5.4). Flow cytometry was used to assess the phenotype of the macrophages, using CD14 (pan macrophage marker), CD163 (M2), CD206 (M2), CD80 (M1) and CD86 (M1) (section 2.5.6). A Friedman's test with Dunn's multiple comparison statistical test was used to compare the abundance of markers in both tissues. FP explants from 2 donors were treated with the corticosteroid, triamcinolone, after which the stromal vascular fraction was extracted and flow cytometry was used to assess the phenotype of the macrophages, as explained above.

5.3 Experimental design-2

FP (n=19) and SCF (n=12) were obtained from obese and non-obese donors undergoing TKR for OA (Table 5.2). Tissue samples were cryosectioned, stained for H&E and image analysis was used to determine the size of adipocytes (Section 2.5.7). Correlation analyses were used to establish associations between donor BMI and adipocyte size.

Table 5.1: Demographics of donors used in the immunohistochemical characterisation of macrophages in synovium and FP.

Donor	Gender	Age	Procedure
1	Female	68	TKR
2	Female	72	TKR
3	Female	46	TKR
4	Female	50	TKR
5	Female	44	Cell therapy
6	Male	57	Amputation, no known joint pathology (normal)
7	Male	51	Debridement
8	Female	44	Cell therapy
9	Female	46	Cell therapy
10	Male	34	Debridement
11	Male	35	Cell therapy

Table 5.2: Demographic information and categorisation for obese and non-obese donors

	Donor	Gender	Age	BMI
FP Obese	1	Male	54	30.4
	2	Male	74	30.0
	4	Female	56	35.4
	5	Female	69	35.8
	6	Female	74	35.8
	7	Male	56	27.3
	8	Female	54	31.8
	9	Female	63	32.8
	10	Female	77	48.5
	11	Female	60	35.9
	FP non-obese	1	Male	58
2		Female	62	24.0
3		Female	75	23.8
4		Female	78	23.9
5		Female	63	22.3
6		Female	60	22.9
7		Male	55	25.9
8		Female	77	25.9
SCF obese	1	Female	58	31.9
	2	Female	66	47.2
	3	Male	69	35.8
	4	Female	54	30.1
	5	Female	53	35.0
	6	Male	63	32.2
	7	Female	77	48.5
	8	Female	65	32.4
SCF non-obese	1	Male	79	26.8
	2	Female	72	25.9
	3	Female	50	26.0
	4	Male	81	24.2

FP: infrapatellar fat pad, SCF: subcutaneous fat

5.4 Results: Characterisation of macrophages from synovium and FP

5.4.1 General histological features of synovium and FP

Histological observations of synovium revealed some variability across donors in terms of morphological features. For instance, the synovium taken from an amputee showed a single layer of synovial cells, whereas all samples from TKR patients displayed hyperplastic synovial linings, indicative of inflammation (Figure 5.1 A-B). Blood vessels also appeared to be more predominant in synovial samples from TKR patients. Fragments of cartilage and bone that were partially or fully embedded in the synovium were common observations in tissues from end-stage OA patients (Figure 5.1 C-D). The morphology of the FP itself did not appear to differ across donors, i.e. it consisted of compact adipocytes with scattered blood vessels and fibrous connective tissues were noted throughout (Figure 5.1 E).

The Krenn scoring system¹⁸⁵, which is an assessment of synovial hyperplasia, cellularity of the subsynovial stroma and the presence of immune cell infiltrate, was used to determine the degree of synovitis in each of the samples. This scoring system then allowed samples to be categorised as no synovitis, low grade synovitis and high grade synovitis (Figure 5.2 A-B compares a sample with no synovitis and another with high grade level of synovitis). A range of different scores was obtained across donors, the lowest being 0 (normal synovium) and the highest being 6 (synovium with severe synovitis) (Figure 5.2 C). Although no statistical significance was established, the mean synovitis score was higher in synovium from TKR donors (5) than donors who received cell therapy (3) (Figure 5.2 D).

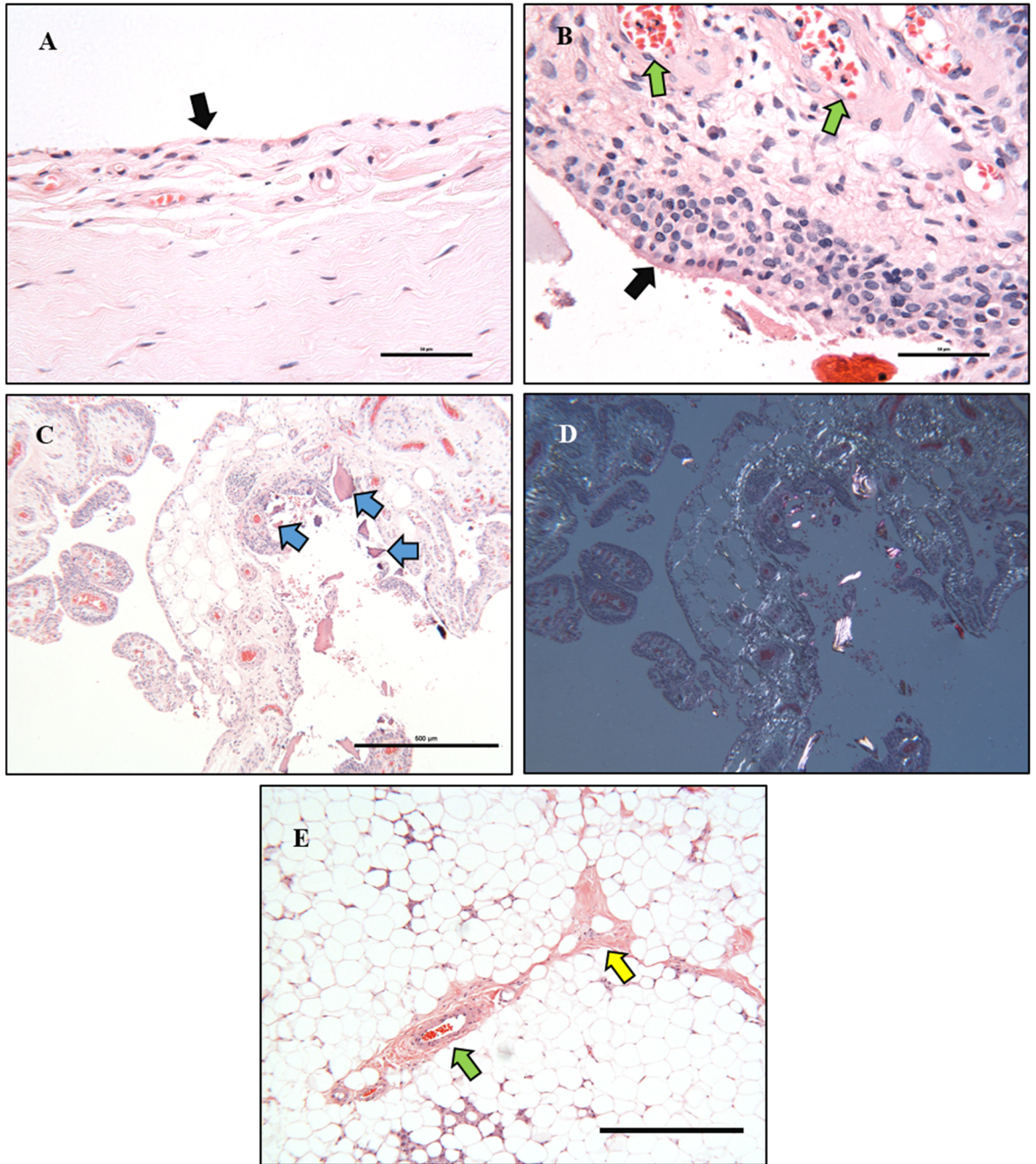


Figure 5.1: General observations of synovium and FP from H&E stain.

A) Synovium from an amputee (donor 6) comprised of a single layer of lining cells (black arrow, scale bar=50 μm). B) Hyperplastic synovium from a TKR patient (Donor 2) with high cellularity in the lining (black arrow). In addition, more numerous and larger blood vessels can be seen in the sub-synovial stroma (green arrows, scale bar=50 μm). C) Bone fragments being embedded in the synovium from donor 2 (blue arrow), confirmed as birefringent bone lamellae striped structures under polarised light (D, scale bar=500 μm). E) Typical FP with blood vessel (green arrow) and fibrous connective tissue (yellow arrow, scale bar=500 μm).

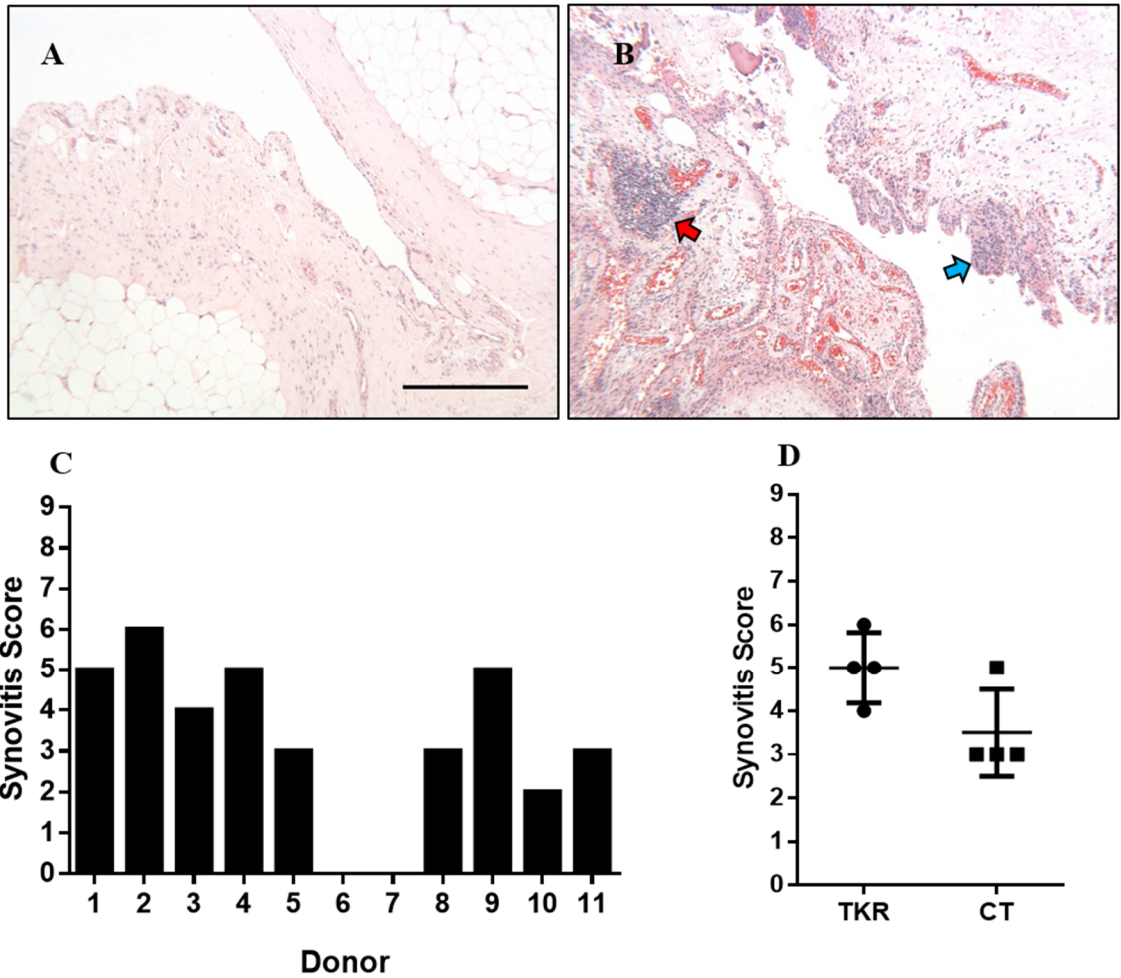


Figure 5.2: Assessment of synovitis. A) Example of synovial tissue showing no synovitis. B) Example of synovial tissue showing high grade synovitis. Follicle-like lymphocyte infiltrate is indicated with the red arrow, hyperplastic synovial lining is shown with the blue arrow. Scale bar = 500 μ m. C) Synovitis score for all donors. D) Comparison of the synovitis score of samples obtained from TKR and cell therapy. An unpaired Mann Whitney test showed no statistical difference between the two groups.

5.4.2 Immunohistochemical characterisation of macrophages in synovium, sub-synovial stroma and FP

The pan macrophage marker CD68 was used to localise macrophages in synovium, sub-synovial stroma and FP. Cells that were CD68⁺ in the synovial lining and the stroma were spherical or elongated (Figure 5.3 C-F), whereas the CD68⁺ cells appeared compact in between neighbouring adipocytes in the FP (Figure 5.3 H) sometimes forming what are known as “crown-like structures”. Physiologically, crown-like structures represent the clearance of dead (or dying) adipocytes from fat tissue by multiple macrophages⁴⁵². Samples from OA donors generally showed a higher staining intensity for CD68 than non-OA donors. Spearman’s correlation analysis showed a strong association between CD68 positivity in the synovial lining and the stroma, but no association was found between CD68 positivity in the synovium and the FP, or in the stroma and the FP (Figure 5.8 A-C).

The markers CD86 and CD11c were used to detect M1 macrophages in the tissues observed. In terms of staining intensity and the number of positive cells, the immunopositivity of CD86 (both intracellular and surface) in the synovial lining appeared relatively low in samples from donors with little or no signs of OA, compared to donors with OA (Figure 5.4 A-D). The sub-synovial stroma and FP of both OA and non-OA donors contained CD86 positive cells (Figure 5.4 E-H). No correlation in CD86 positivity was found between the synovial lining, stroma and FP (Figure 5.8 D-E). Interestingly, a low incidence of CD11c positive cells was observed for synovium, sub-synovial stroma and FP across all donors (with some donor samples showing no positive cells). Tissue samples containing follicle-like lymphocyte infiltrate did however contain some CD11c cells (Figure 5.5 F). Due to the rarity of CD11c positive cells in most of the tissues observed, correlation analyses were not performed for this marker.

Immunohistochemistry was performed to detect the M2 markers, Arg-1 and CD206, on cells in the various tissues. Arg-1 positivity was present in the synovial lining of cells, stroma and FP of healthy and OA donors (Figure 5.6 A-H). Cells that were more intensely stained for Arg-1 were observed inside or in the periphery of blood vessels in the stroma (Figure 5.6 F). A strong positive correlation was found between Arg-1 positivity in the synovial lining and the sub-synovial stroma and also between the synovial lining and the FP, however no significant correlation was found between the stroma and the FP (Figure 5.8 G-I). An abundance of CD206 positive cells was observed in the synovial lining, stroma and FP across all donor samples (Figure 5.7 A-F). Here again, a significant positive correlation was found between the synovial lining and the stroma and between the stroma and the FP, but not between the synovial lining and the FP (Figure 5.8 J-I).

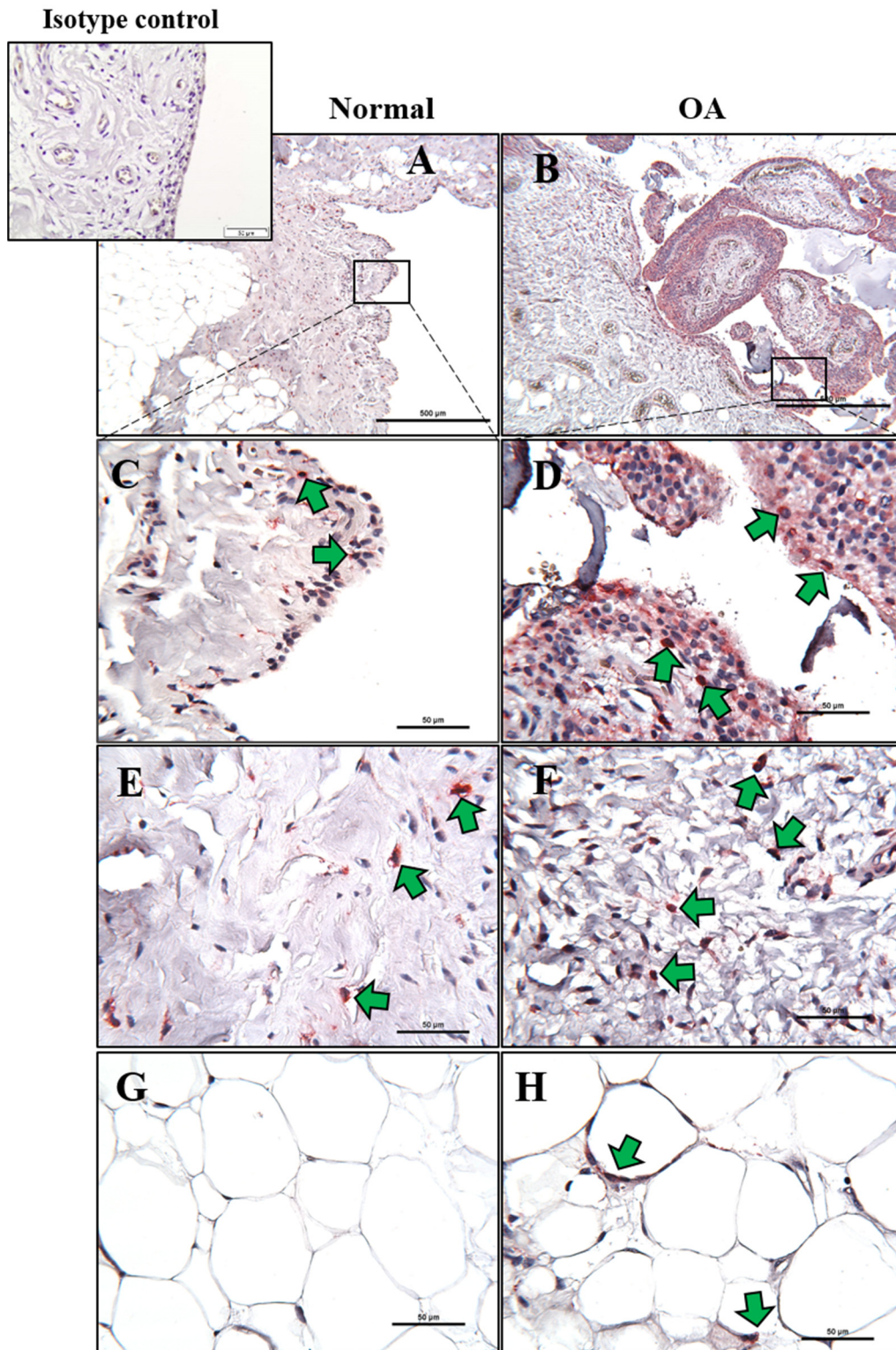


Figure 5.3: Immunohistochemical analysis of CD68 in normal and representative OA synovium and FP. Green arrows indicate cells that are positively stained. A-B) Staining of CD68 in normal and OA synovium (low magnification). C-D) CD68 staining at high magnification. E-F) Comparison of CD68 staining in the sub-synovial stroma of a normal and an OA donor. G-H) CD68 staining in deep regions of the FP derived from a normal and OA donor. Scale bars: A and B= 500 μm , C-H= 50 μm .

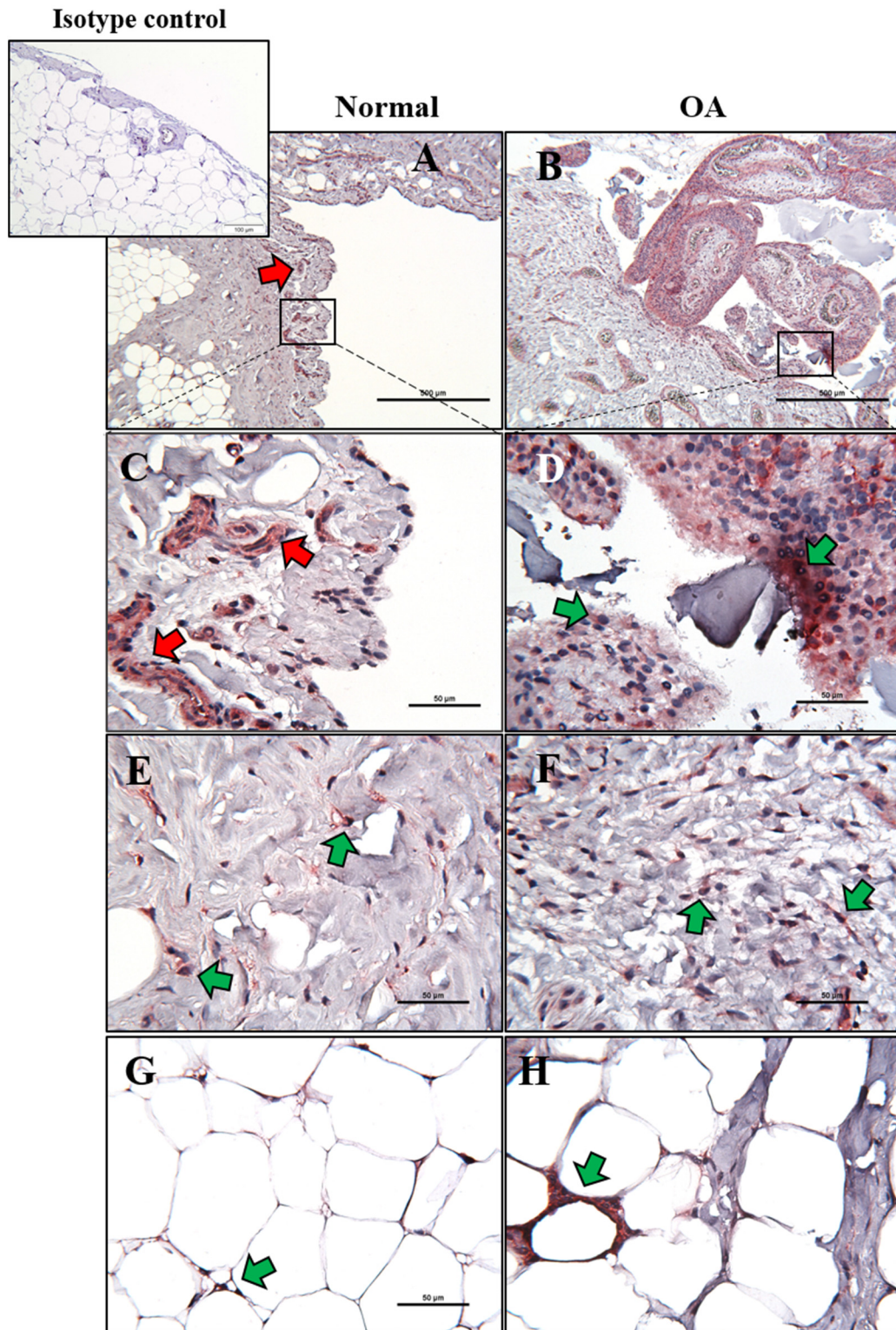


Figure 5.4: Immunohistochemical analysis of CD86 in normal and representative OA synovium and FP. Green arrows indicate examples of synovial cells that are positive, red arrows show positive staining around blood vessels. A-B) Staining of normal and OA synovium for CD86 (low magnification). C-D) CD86 staining at high magnification in normal and OA synovium. E-F) Comparison of CD86 staining in the sub-synovial stroma of a normal and OA donor. G-H) Arrow depicts a crown-like structure in the FP. Scale bars: A and B= 500 μ m, C-H= 50 μ m.

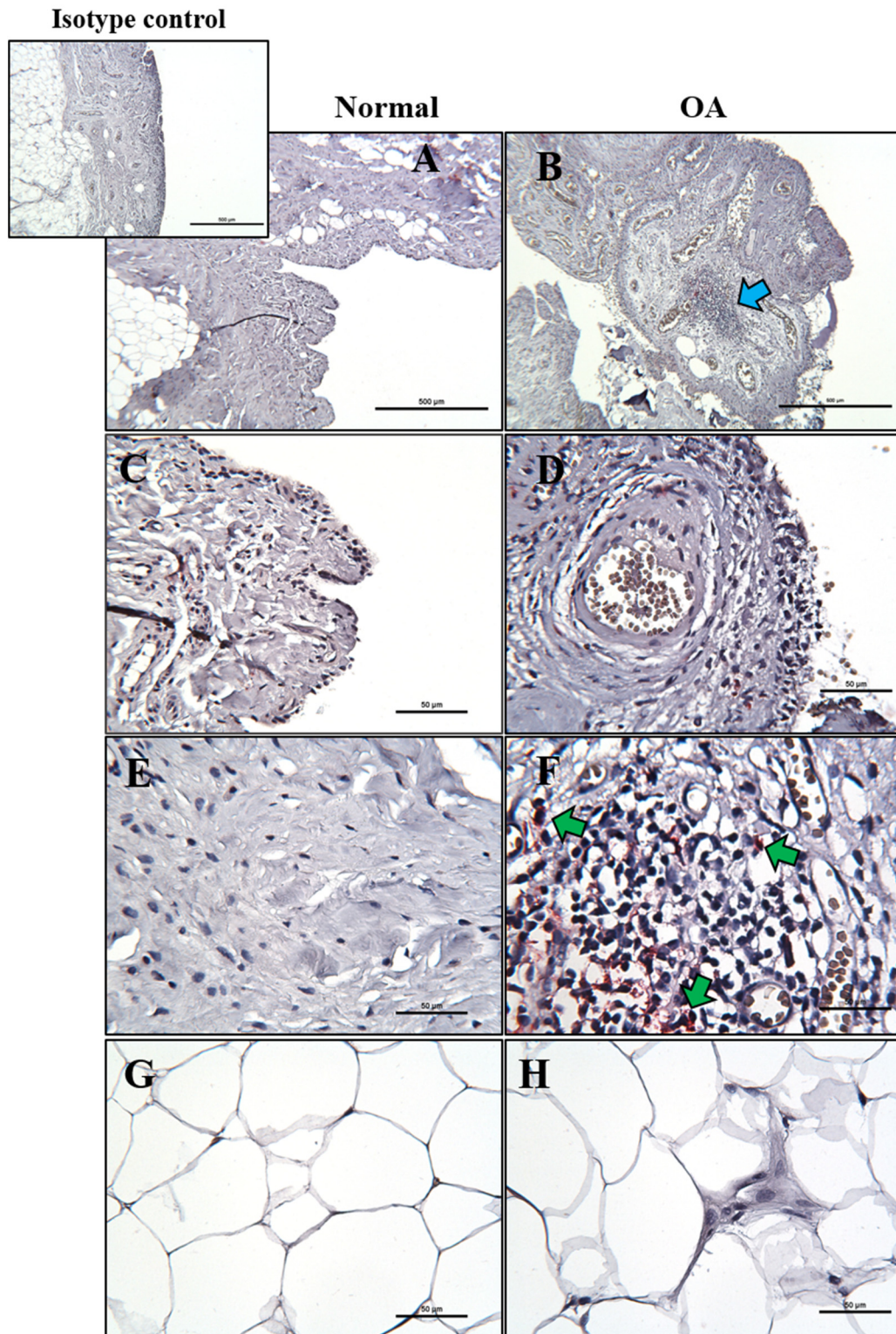


Figure 5.5: Immunohistochemical analysis of CD11c in normal and representative OA synovium and FP. Green arrows indicate examples of cells that are positive, the blue arrow shows indicates a follicle-like lymphocyte infiltrate. A-B) No staining for CD11c in normal and OA synovium was visible (low magnification). C-D) Absence of CD11c positive cells in the synovial lining of both healthy and OA donors. E-F) CD11c positive cells in lymphocyte infiltrate located in the sub-synovial stroma. G-H) Absence of CD11c positivity in the FP. Scale bars: A and B= 500 μm , C-H= 50 μm .

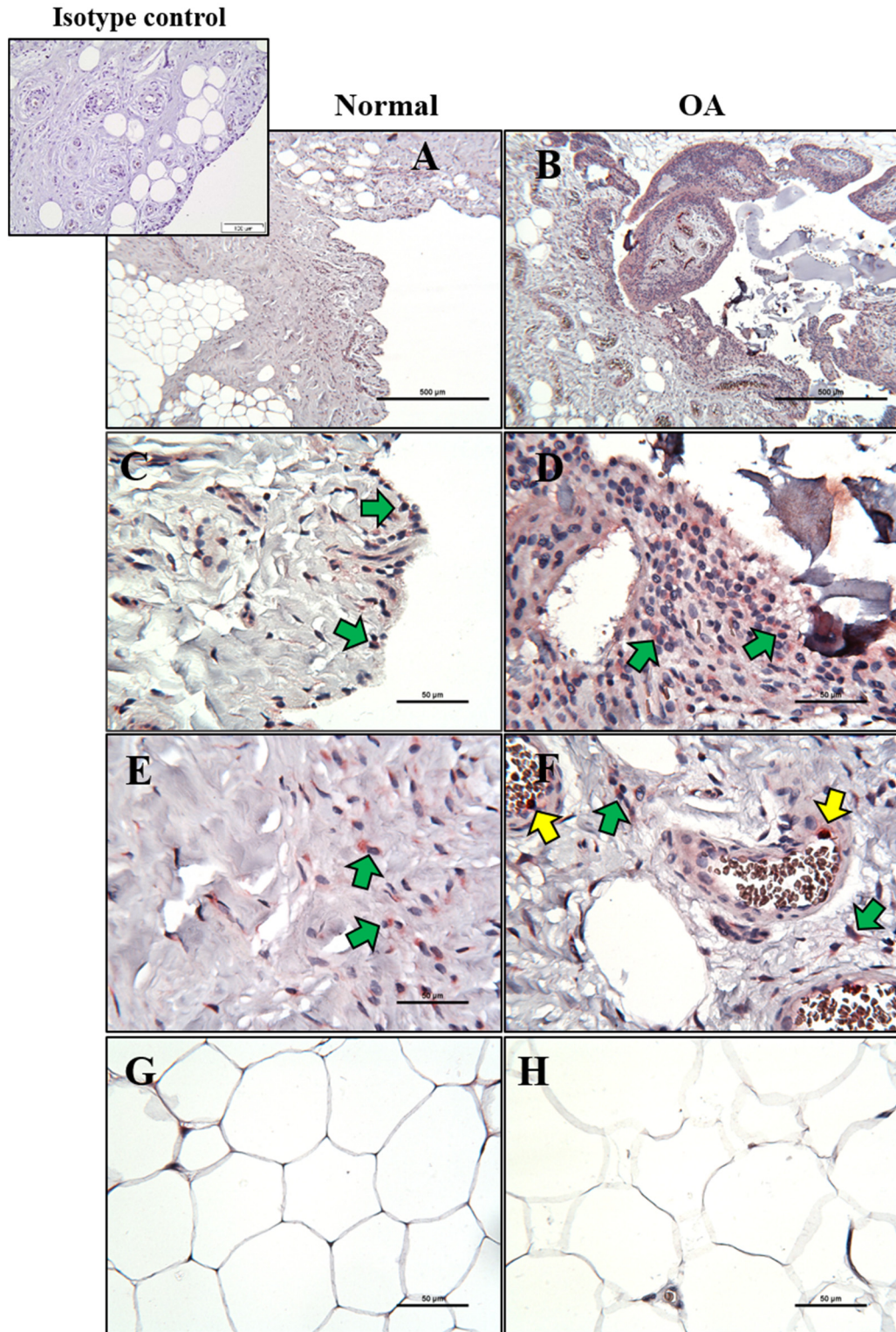


Figure 5.6: Immunohistochemical analysis of Arginase-1 (Arg-1) in normal and representative OA synovium and FP. Green arrows indicate examples of cells that are positive. A-B) Staining of normal and OA synovium for Arg-1 (low magnification). C-D) Comparison of Arg-1 staining at high magnification in normal and OA synovium. E-F) Comparison of Arg-1 staining in the sub-synovial stroma of a normal and OA donor. Yellow arrows show cells lining blood vessels that were more intensely stained. G-H) Weak Arg-1 staining in the deep regions of FP from a normal and OA donor. Scale bars: A and B= 500 μ m, C-H= 50 μ m.

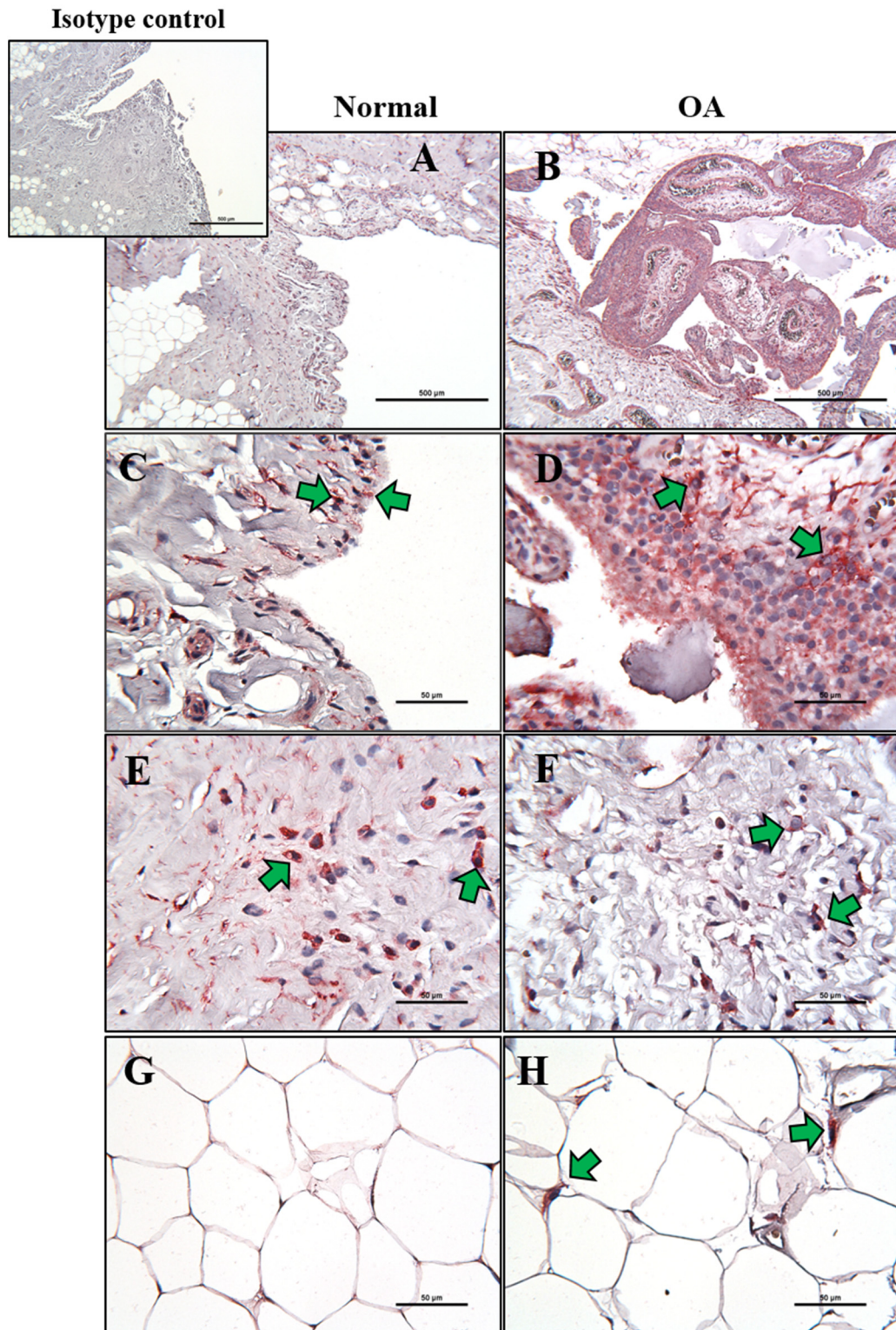


Figure 5.7: Immunohistochemical analysis of CD206 in normal and representative OA synovium and FP. Green arrows indicate cells that are positive. A-B) Staining of normal and OA synovium for CD206 (low magnification). C-D) Comparison of CD206 staining at high magnification in normal and OA synovial lining. E-F) Comparison of CD206 staining in the sub-synovial stroma of a normal and OA donor. G-H) Staining of CD206 in deep regions of FP in a normal and OA donor. Scale bars: A and B= 500 μ m, C-H= 50 μ m.

● End-stage OA ● Cell Therapy ● Debridement ● Normal donors

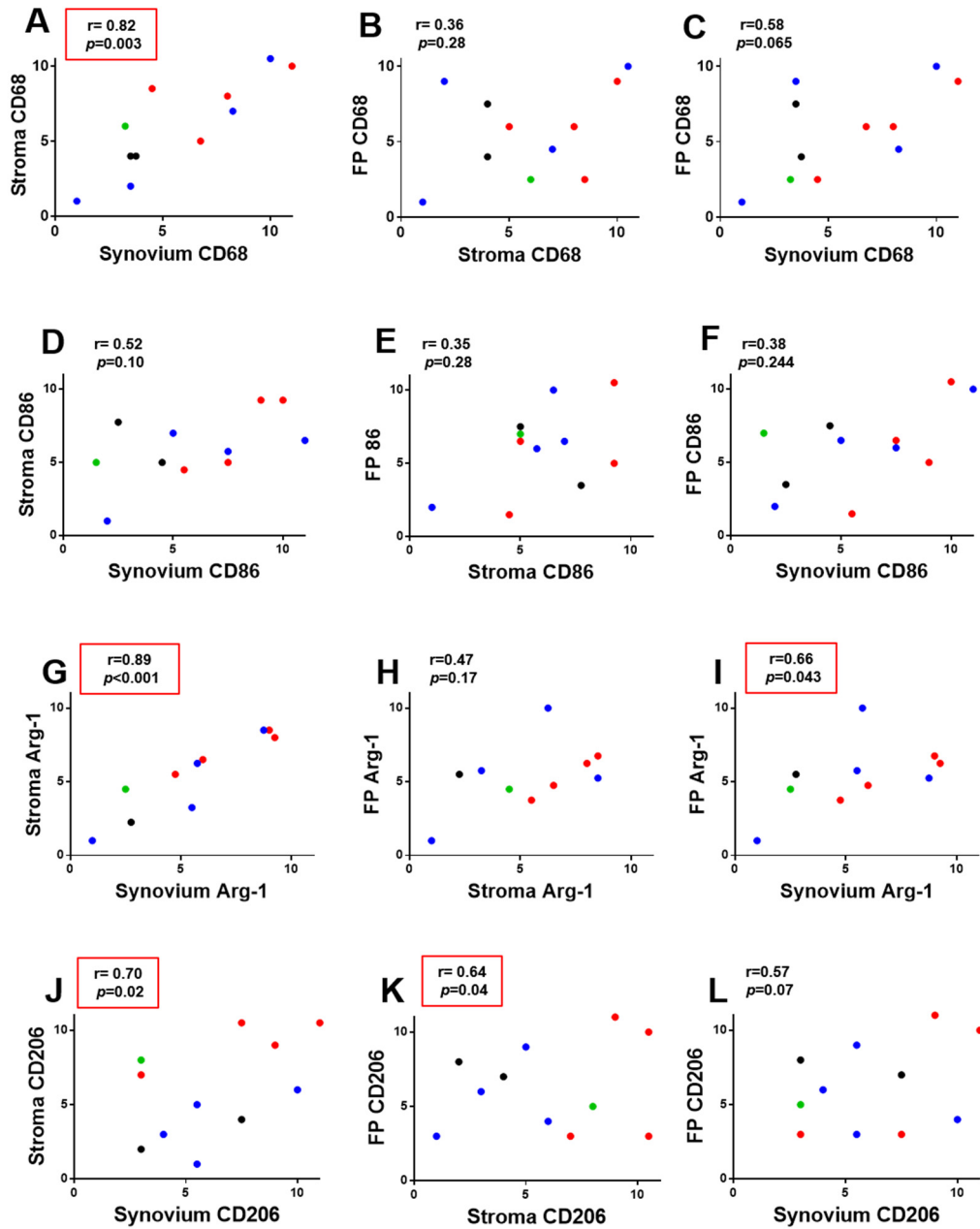


Figure 5.8: Spearman's rank correlation analysis of macrophage staining between tissue layers (red boxes indicate significant correlations). Associations of macrophage positivity between synovium (lining) and stroma (left), stroma and FP (middle), synovium and FP (right) are shown for A-C) CD68, D-F) CD86, G-I) Arginase-1 (Arg-1), J-I) CD206. Red dots= end-stage OA, blue dots= cell therapy, black dots= arthroscopic debridement, green dots=normal donor.

5.4.3 Correlation between synovitis score and macrophage score

Spearman's correlation tests were performed to evaluate associations between the synovitis score and the individual macrophage marker ranks of synovium, stroma and FP of each donor examined. A strong positive correlation was found between the synovitis score and the macrophage rank of the synovium for CD68, CD86, Arg-1 and CD206 (Table 5.3). A similar trend was observed when correlating the synovitis score to the macrophage ranks of the stroma, with the exception of CD86 which showed no significant association (Table 5.3). Synovitis did not significantly correlate with the FP macrophage rank for any of the markers assessed (Table 5.3).

Table 5.3: Spearman’s correlation analysis of the association between the synovitis score and macrophage rank in the synovium, stroma and FP. Values represent correlation coefficients with p values in brackets; significant correlations are highlighted.

Synovitis score vs macrophage rank in:			
	synovium	stroma	FP
CD68	0.73 (p=0.013)	0.70 (p=0.018)	0.42 (p=0.19)
CD86	0.87 (p<0.001)	0.31 (p=0.34)	0.26 (p=0.44)
Arg-1	0.83 (p=0.004)	0.84 (p=0.004)	0.26 (p=0.46)
CD206	0.76 (p=0.009)	0.65 (p=0.034)	0.06 (p=0.86)

5.4.4 Flow cytometric assessment of macrophages from matched synovium and FP

The total cell population of 4 donor matched synovium and FP was extracted by enzymatic digestion and multicolour flow cytometry was used to further investigate the presence of macrophages in donor matched synovium and FP. The pan macrophage marker CD14 was used to gate and analyse only the monocyte/macrophage population in the cell extract of both tissues. The surface marker profile of the subsets of macrophages (M1/M2) was investigated using the markers CD80 (M1), CD86 (M1), CD163 (M2) and CD206 (M2). In the four donors investigated, CD14 positive cells represented 20-35.7% (mean=25%) of the total cells extracted from the synovium, and 14.3-33% (mean=21.5%) of the cells extracted from the FP. Figure 5.9 A illustrates the positivity of CD14 in matched synovium and FP for individual donors. In this population of monocyte/macrophages, synovium and FP showed comparable levels of CD80 (11.8% and 11% respectively), whereas CD86 positivity in macrophages from the synovium was 43.7% compared to 29.5% in the FP derived macrophages (Figure 5.9 B-C). No statistical significance was obtained for the comparison of CD80 and CD86 positivity between synovium and FP. Interestingly, although no statistical difference was obtained, the average positivity of M2 markers CD163 (synovium=51.4%, FP=64.8%) and CD206 (synovium=23%, FP=33.1%) was higher in macrophages from the FP in comparison to those derived from the synovium. However, a bigger sample size would be required to confirm this trend.

Analyses were performed to determine if certain macrophage subsets were more abundant than others in synovium and FP (Figure 5.9). The positivity of CD163 was significantly higher than CD80 in both the synovium ($p=0.03$) and FP ($p=0.003$) (

Table 5. 4). No other significance differences were observed between macrophage markers.

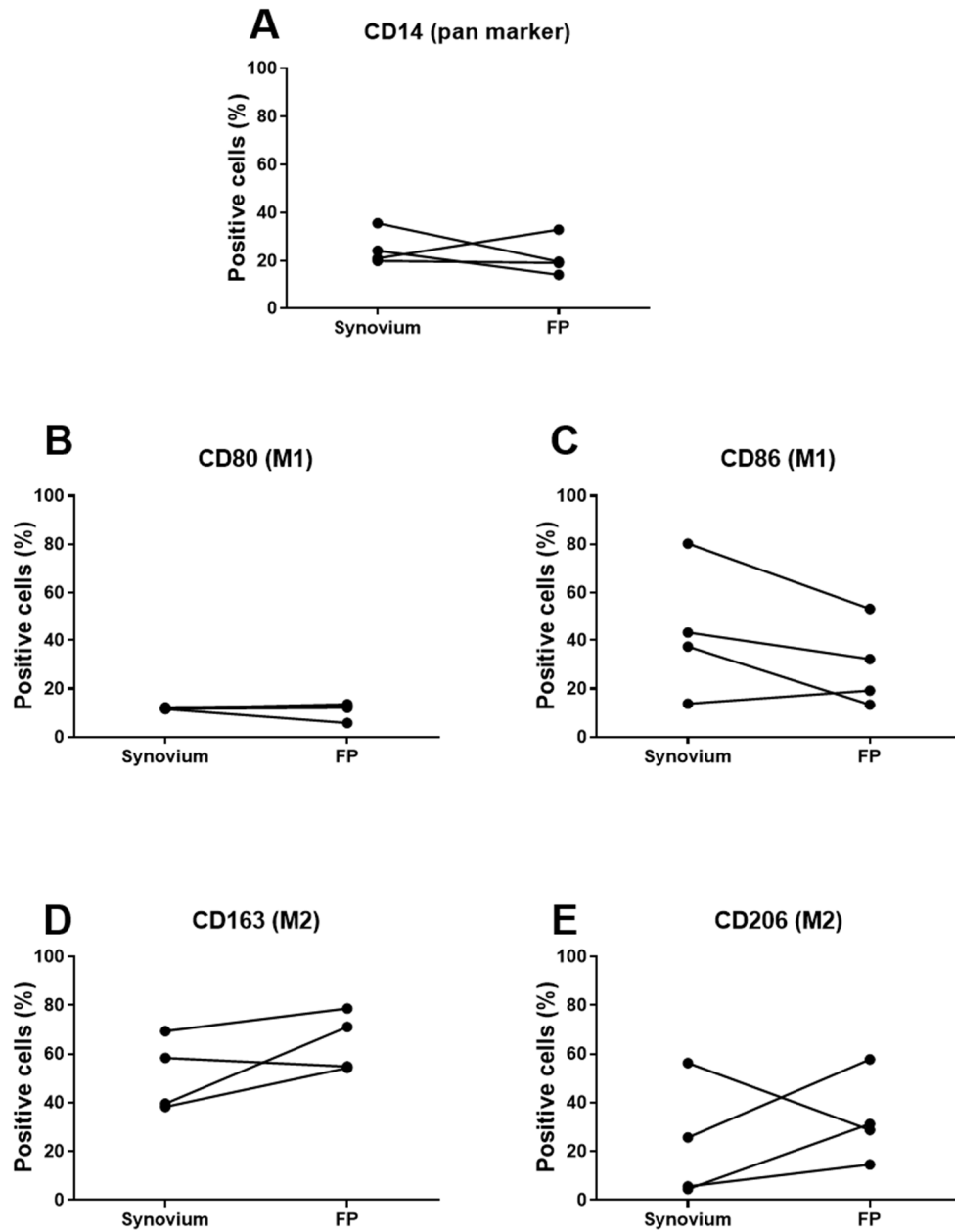


Figure 5.9: Immunopositivity of macrophage markers in cells from donor matched synovium and FP. A) Percentage of CD14 positive cells (monocyte/macrophages) present in the cell extract of synovium and FP. B-C) Percentage of cells within the CD14 populations that were positive for M1 markers CD80 and CD86. D-E) Percentage of cells within the CD14 population that were positive for M2 markers CD163 and CD206

Table 5. 4: Comparison of M1 and M2 markers in CD14 positive macrophages from matched synovium and FP (n=4). P values are from Friedman’s test with Dunn’s multiple comparison. Significant comparisons are highlighted and the marker with the highest levels indicated in brackets.

	Synovium	FP
CD80 vs. CD86	p=0.44	p> 0.57
CD80 vs. CD163	p=0.03	p=0.003
CD80 vs. CD206	p> 0.99	p=0.25
CD86 vs. CD163	p> 0.99	p=0.93
CD86 vs. CD206	p>0.99	p> 0.99
CD163 vs. CD206	p=0.25	p>0.99

To further characterise the subsets of macrophages present in synovium and FP, the co-expression of M1 and M2 markers was investigated. On average, macrophages from the synovium showed co-expressions for, CD86 and CD163 (26.3%), CD86 and 206 (6.3%) and CD163 and CD206 (9.4%) (Figure 5.9). In FP macrophages, only co-expression of CD163 and CD206 (6.9%) was revealed. CD80 showed no co-expression with any of the other macrophage markers investigated.

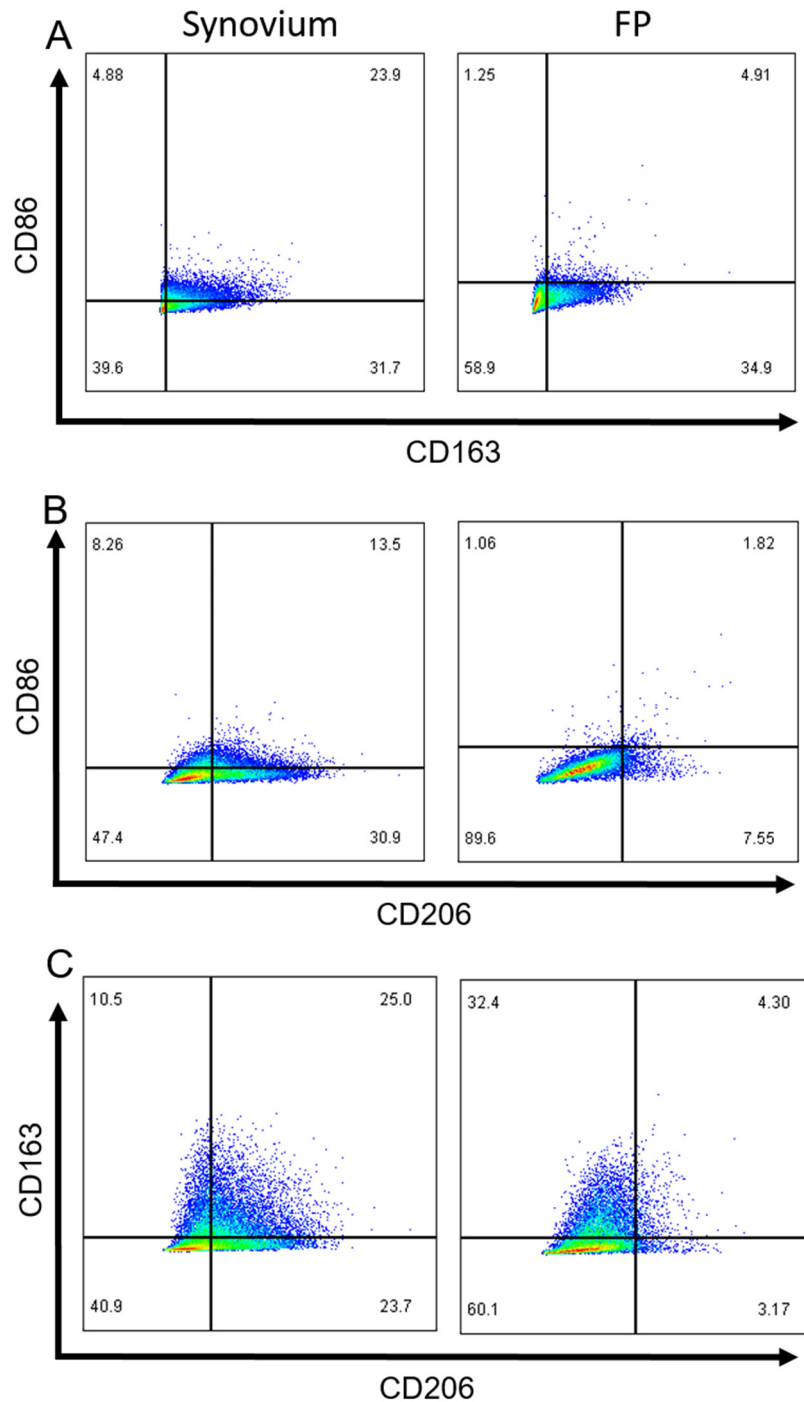


Figure 5.10: Flow cytometry analysis of the co-positivity of M1 and M2 markers. Representative scatter-plots showing the co-positivity of M1 and M2 markers observed in macrophages isolated from donor matched synovium and FP. Comparisons are shown for A) CD163 vs CD86, B) CD206 vs CD86, C) CD206 vs CD163. Values shown in the quadrants represent a percentage of the CD14 positive macrophage population extracted from synovium and FP. The position of the quadrants was determined from isotype controls using a 99% confidence level (not shown).

5.4.5 The influence of anti-inflammatory stimuli on the polarisation of macrophages from FP explant cultures

In order to determine whether the phenotype of the macrophages studied can be modulated, FP explants from two donors were stimulated with the anti-inflammatory drug triamcinolone for 72 hours (compared to an untreated control). Multicolour flow cytometry was used to measure M1 and M2 markers in CD14 positive macrophages extracted from these explants. Results revealed that the M2 markers, CD163 and CD206, were increased in both FP explant macrophages tested after triamcinolone treatment, while the M1 marker CD80 decreased (Figure 5.11). CD86 was unchanged in donor 2 but increased in donor 1 after triamcinolone treatment. Here again, CD86 was co-expressed with CD163; this co-expression was also increased after triamcinolone treatment (Figure 5.12).

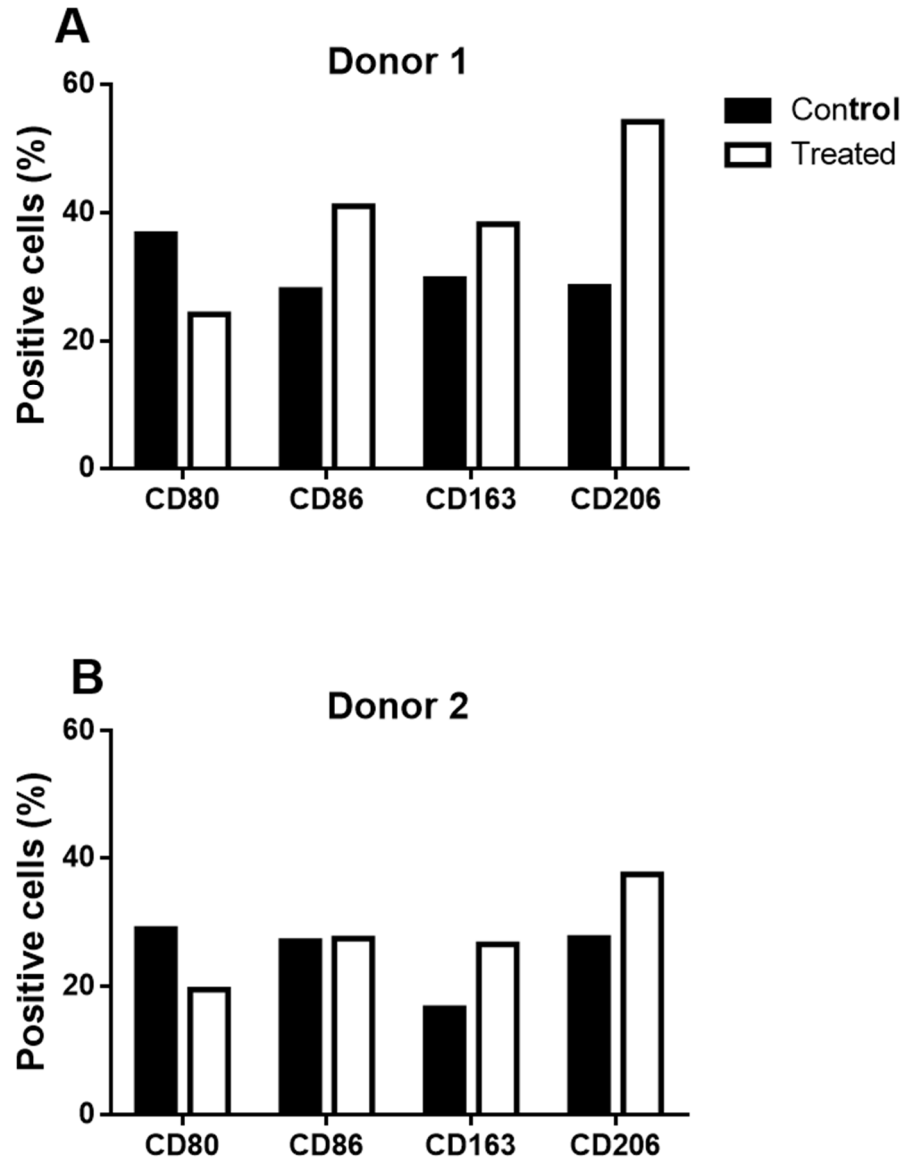


Figure 5.11: The effect of triamcinolone on explant cultured macrophages from the FPs. Multicolour flow cytometry was used to assess the positivity of M1 and M2 markers on CD14 positive macrophages in FP explants after treatment with the anti-inflammatory drug triamcinolone for 72 hours. Results are shown for two donors.

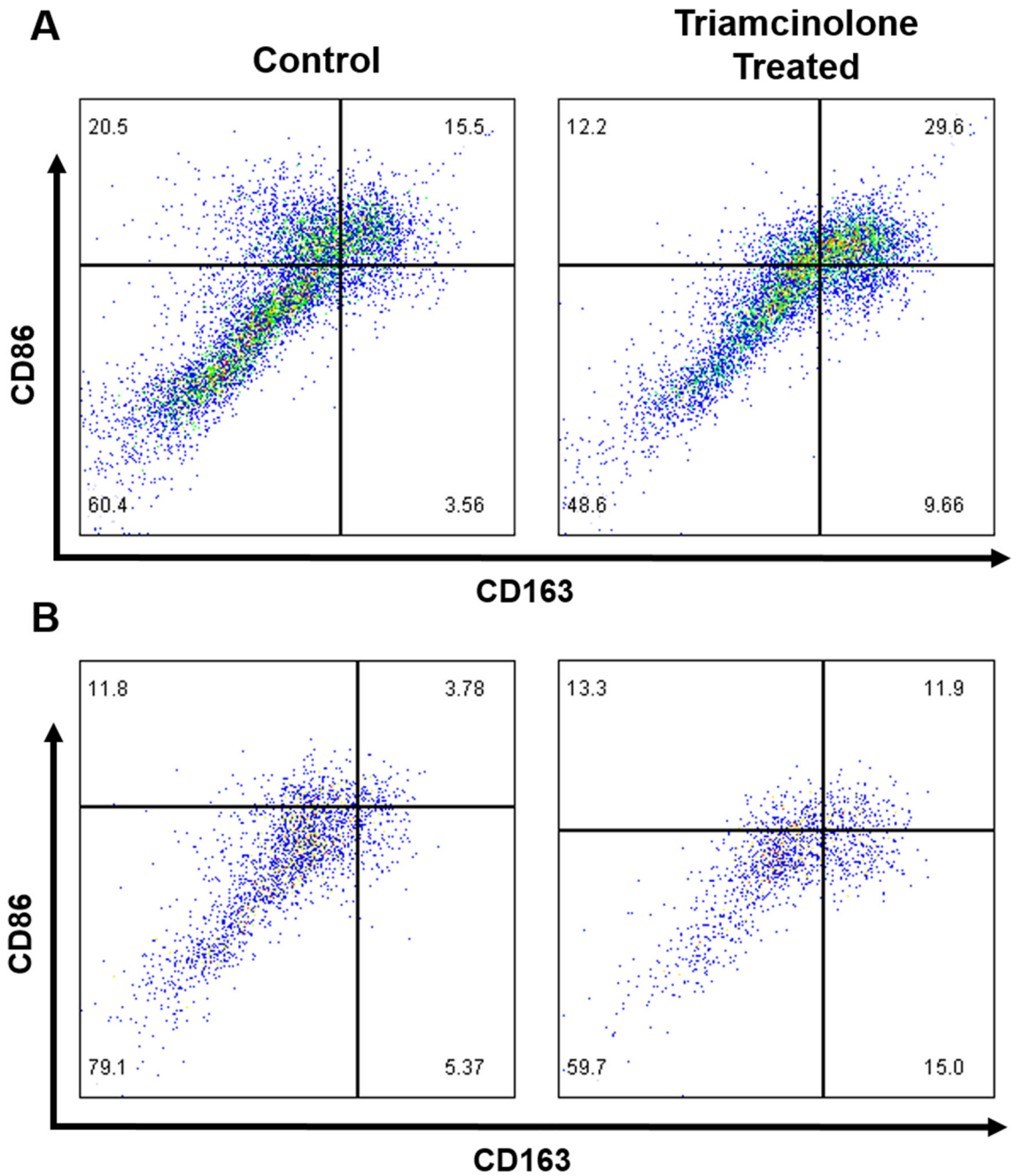


Figure 5.12: Scatter plots illustrating the influence of triamcinolone (72 hours treatment) on the co-expression of CD86 and CD163 markers on macrophages from FP explant cultures. A) Donor 2, B) Donor 2. Triamcinolone induced an increase in the macrophage expression of both CD86 and CD163. The position of the quadrants was determined from isotype controls using a 99% confidence level.

5.4.6 Association between donor BMI and adipocyte size.

Microscopic observation of H&E stained adipose tissues showed no distinct difference between adipocytes in terms of general morphology and distribution when comparing the FP and subcutaneous fat from obese and non-obese donors. However larger adipocytes were noticeable in the subcutaneous fat of obese donors compared to other donor groups (Figure 5.13). The size of adipocytes in subcutaneous adipose tissue was correlated to donor BMI ($r=0.63$, $p=0.028$), which was not the case in the FP ($r= -0.06$, $p=0.82$) (Figure 5.14). For non-obese donors ($BMI < 30$), FP adipocyte size ($1765 \mu\text{m}^2 \pm 163.5$) was not significantly different to subcutaneous adipocyte size ($2157 \mu\text{m}^2 \pm 835.6$, $p > 0.99$). However the size of adipocytes from the FP of obese ($1732 \mu\text{m}^2 \pm 292.4$) and non-obese donors ($1765 \mu\text{m}^2 \pm 163.5$) were significantly smaller than subcutaneous adipocytes from obese donors ($3195 \mu\text{m}^2 \pm 833.9$, $p=0.03$ and $p=0.04$ respectively) (Figure 5.14C).

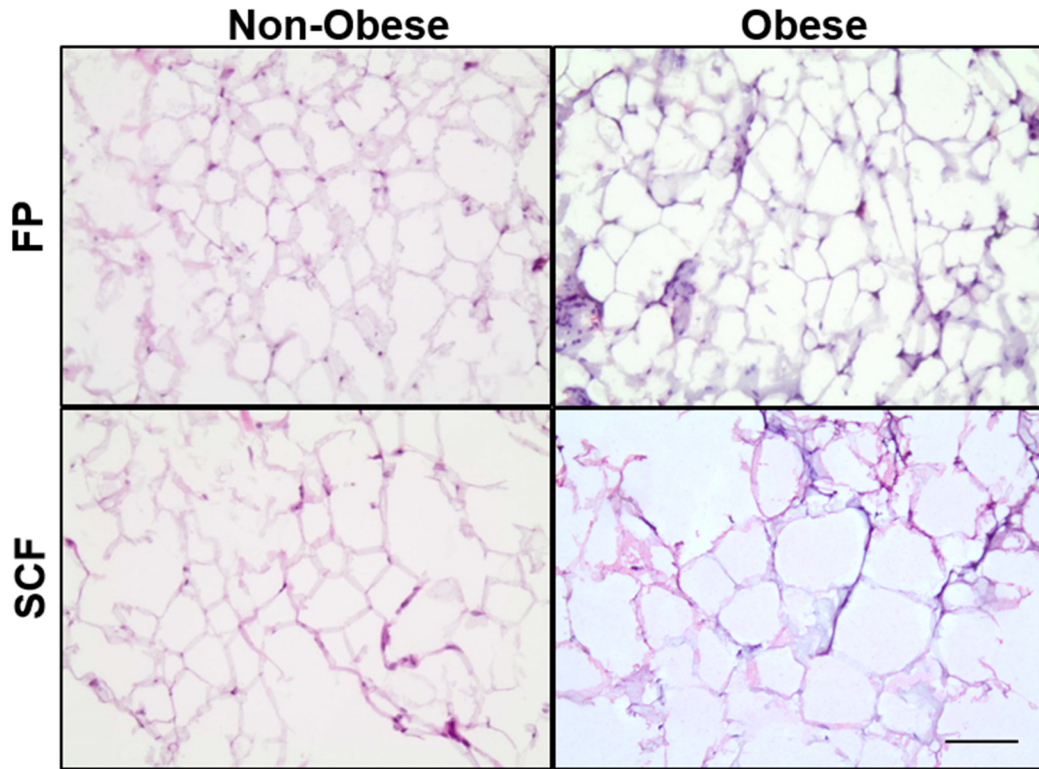


Figure 5.13: Representative images of H&E stained cryosections of adipose tissue derived from the FP and SCF of non-obese and obese donors. Adipocytes in the SCF of obese donor were larger (cross sectional area) than the adipocytes in the FP and of obese donor and the SCF/FP of non-obese donors. Scale bar= 100 μ m.

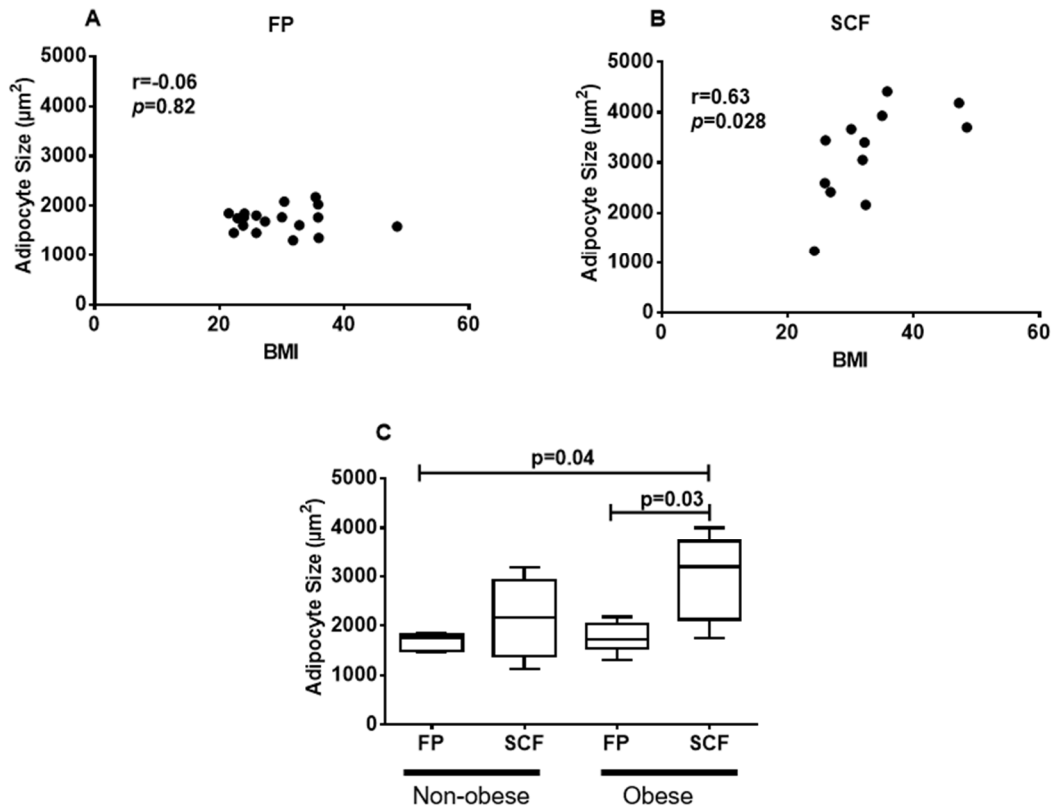


Figure 5.14: Relationship between BMI and adipocyte size. Spearman's test for correlation between donor BMI and adipocyte size in A) the FP and SCF. C) Comparison of the median size of adipocytes in the FP and SCF in obese and non-obese donors.

5.5 Discussion

Joint inflammation, albeit a secondary feature of OA, is considered to be a promotor of joint degeneration¹⁹³. An inflamed synovium (synovitis) is an important player in joint inflammation due to the increased secretion of pro-degradative molecules by synovial cells⁴⁴⁷. The synovial tissues of OA patients examined in this chapter showed typical signs of synovitis, i.e. hyperplasia, immune cell infiltrate and increased cellularity of the stroma. Additionally, an increased number of blood vessels was noted in the synovial tissues of OA donors which corroborates with previous studies showing the histological association between indicators of neovascularisation, such as the proliferation of endothelial cells, and increased synovitis grade in OA patients⁴⁵³. The presence of bone and cartilage fragments in synovial tissues sections is a sign of severe joint degeneration, and is believed to be a trigger for synovitis^{189,454}. Tissue sections from donors receiving cell therapy showed less synovitis, compared to OA donors, which is likely indicative of their lack of severe joint degeneration. However, a larger sample size would be required to confirm the difference in the levels of synovitis when comparing OA and cell therapy donors.

Macrophages are usually resident within both normal and diseased synovium^{183,187}. Although the M1 and M2 subsets of macrophages have been well characterised in other tissues and diseases, their phenotype and role in the articular joint (more specifically the knee), following injury and in disease states has only recently attracted research interest^{201,204}.

The staining intensity for markers tested stronger in OA tissues compared to non-OA tissues, suggesting a higher prevalence of macrophages in OA tissues. CD68 is a lysosomal glycoprotein commonly used as a pan macrophage/monocyte marker in humans³⁷⁰. This predominantly intracellular marker is a member of the family of scavenger molecules which are essential to the function of phagocytic cells such as macrophages^{455,456}. CD68 has also

been employed previously to confirm the presence of macrophages in the FP of OA donors with a similar staining pattern to the immunohistochemical stains shown in this results chapter²⁰⁴.

The M1 marker CD86 is a cell surface transmembrane protein, found on antigen presenting cells, that is central to the activation of T cells during an immune response³⁷¹. The presence of CD86 on macrophages has been confirmed in both the synovium and FP by immunohistochemistry^{201,204}, however the function of this subset of cells in the joint has not yet been revealed. CD11c is a subunit of the integrin alpha X protein specific to leucocytes notably monocytes, macrophages and dendritic cells^{372,457}. Although no CD11c positive cells were found in the FP samples examined, small populations were found near infiltrating lymphocytes in the sub-synovial stroma. This observation, although unexpected, is not entirely surprising as dendritic cells have been reported in lymphocyte-rich regions of lymphoid organs (such as the spleen), where they mediate the pro-inflammatory activity of T-helper and T-killer cells⁴⁵⁷. It remains unclear whether these CD11c dendritic cells are part of the resident population of macrophages in the synovial tissue and, importantly, whether they promote the infiltration of circulating lymphocytes from blood vessels. Recent publications also suggest that T-helper cells contribute to the differentiation of monocytes into dendritic cells by producing high levels of granulocyte macrophage colony-stimulating factor⁴⁵⁸.

Arg-1, an intracellular M2 marker, is an enzyme that catalyses the hydrolysis of arginine into ornithine and urea³⁷⁴. This enzyme directly competes with the nitric oxide synthase (NOS), which converts arginine into NO and in turn facilitates cartilage damage⁴⁵⁹. There is a paucity of literature exploring the activity of Arg-1 in the OA joint and its presence on joint derived macrophages. Immunohistochemical results presented here show that Arg-1 is present in human synovium and to a lesser extent in the FP. The mannose receptor, CD206,

found on the surface of a number of phagocytic cells is involved in the recognition of microbial carbohydrates and the clearance of inflammation-induced enzymes in order to regulate an immune response^{373,460}. Conditioned medium from FP explants was found to have anti-catabolic effect on cartilage *in vitro*; this was attributed to the high prevalence of CD206 positive macrophages in the FP²⁰⁴. The abundance of CD206 cells in the synovium and FP of OA patients reported here confirms recent studies^{201,204}, in which no record of the presence of CD206 cells in normal (or less inflamed) synovium has been reported. In addition, this is the first investigation comparing the presence of cells with M1 and M2 markers in donor matched synovium and FP.

Correlation analyses showed an association in the macrophage ranks when comparing the synovium and sub-synovial stroma for all of the markers investigated, with the exception of CD86. The close proximity between the two tissues could possibly explain this association, that is, a high prevalence of macrophages in the synovium could induce an increase in macrophages within sub-stroma by secreted factors or by the free movement of cells between the two tissues. The lack of a significant association for CD86 remains unclear. When correlating macrophage ranks between the sub-synovial stroma and FP, only CD206 showed a significant association, which has not been demonstrated before. Further, only Arg-1 showed a significant association when correlating macrophage ranks between the synovium and the FP; here again this has not been demonstrated previously. These results present an interesting theory that although the synovium and FP function differently in terms of the general abundance of macrophages (CD68), a link could potentially exist when looking at various subsets of macrophages.

In addition, strong positive correlations were found between the synovitis score and the macrophage rank in the synovium and stroma for all the markers tested (barring CD86 in the stroma). This suggests that the general increase in the number of macrophage as a result of

an inflamed synovium involves⁴⁵³ all the subsets of macrophages. Conversely, synovitis scores did not correlate with any of the macrophage ranks in the FP, which again points to the potential independence of FP and synovium with regards to their inflammatory status.

Ideally, a larger sample size would be more appropriate for more robust results. It is important to note the limitations of immunohistochemical characterisation of macrophages using single markers. The CD markers used in this study, while highly expressed on subpopulations of macrophages, are not always specific to macrophages. For instance, CD68 is known to be present in lymphocytes and fibroblasts, both of which are commonly found in synovial tissue⁴⁶¹. Although this may not be a concern in the FP since macrophages often adopt a specific crown-like structure in adipose tissues, this could introduce bias when observing the synovium and the sub-synovial stroma where macrophages do not have a distinct morphology. Double staining methods which identify two indicative macrophage markers simultaneously in a cell have been developed to characterise macrophage subsets in other human tissues⁴⁶² and the adoption of these techniques here would provide more confidence in the results obtained.

Multicolour flow cytometry is another method that can be used to identify subsets of macrophages by targeting multiple indicative markers on cells following their extraction from tissues. CD14 was used in this chapter to identify the monocyte/macrophage population amongst all the cells extracted from the synovium and FP, from which the positivity of other markers can be determined. A low sample size limits the inferences that can be made from the data obtained in this results chapter, however it is perhaps safe to say that the macrophage content was comparable between the tissues. One other recent study (n=34 donors) which has utilised flow cytometry to compare freshly isolated macrophages in paired synovium and FP samples corroborates this finding⁴⁴⁸. Similarly this report used CD14 to identify

macrophages and found no significant difference between the synovium and FP, however no further experiments were conducted to characterise M1 and M2 subsets.

The evidence gathered in this chapter indicates that M1 and M2 macrophages co-exist within the synovium and FP of OA patients. Interestingly, an observation of the co-expression of surface markers revealed that macrophages from both tissues can simultaneously express M1 and M2 markers. A growing body of literature now confirms that macrophages not only exist in strict polarisation states, but can also be part of a polarisation spectrum that incorporates the cells that are between the M1 and M2 phenotypes^{197,198}. In the synovial joint, the presence of multiple macrophage subsets could perhaps be accounted for by the plethora of different cytokines available. For instance, IFN- γ and TNF- α are known to induce the expression of CD80, while IL-4 and IL-10 induce the expression of CD163 and CD206 in the differentiation process of naive peripheral blood derived monocytes^{463,464}. All of these cytokines are known to be present in the knee joint¹⁶⁴, which would logically lead to the potential differentiation of freshly recruited monocytes along multiple macrophage lineages and could induce the expression of multiple M1 and M2 markers in the same cell.

It is now believed that the M2 subset of macrophages is comprised of M2a, M2b, and M2c categories representing parasite clearance, immunoregulatory and wound healing cells phenotypes, respectively¹⁹⁸. The co-positivity of CD163 and CD206 shown in synovium and FP tissues suggests the presence of M2c cells^{465,466}, while the co-positivity of CD86 and CD163 suggests the presence of M2b cells⁴⁶⁵. The panel of markers chosen here did not allow for the identification of M2a cells due to the absence of markers such as CD209⁴⁶⁶ and Fizz1⁴⁶⁵, amongst others.

To determine whether the phenotype, or polarisation state, of joint derived macrophages could be modulated. The anti-inflammatory drug triamcinolone was applied to FP explant

cultures in an experiment using tissues derived from two donors. The results from these two donors were comparable but should be taken as preliminary data which will be discussed but will need further study (with increased donor size) before conclusions can be drawn. In this preliminary data set an increase in the number of cells that were positive for CD163 and CD206 after treatment with triamcinolone was observed, however, the M1 marker CD80 (which has a similar co-stimulatory function to CD86) was only partially diminished. The increased co-expression of CD86 and CD163 could indicate a possible mechanism of action of triamcinolone within the joint, i.e., to induce a shift in macrophage polarisation towards the M2b immunoregulatory phenotype. One mouse study showed that the administration of triamcinolone prevented the formation of osteophytes which was linked to the induction of CD163 positive macrophages, however, this study did not mention a particular macrophage subset⁴⁶⁷. Techniques that are used to characterise the cellular component of tissues such as immunohistochemistry and flow cytometry capture a snapshot of macrophages at a particular time, which may not reflect the true transient phenotype of the cell if it is indeed between M1 and M2 on the polarisation spectrum.

In addition to surface markers, assessing the secretory profile and gene expression may be a more reliable characterisation method to determine macrophages polarisation states. To delineate M1 cells, secretory factors such as IL-1, IFN- γ , TNF- α and IL-6 should be assessed together with the signal transducer and activator of transcription 1 (STAT1) and surface markers CD80 and CD86¹⁹⁸. For M2 cells, secreted antiinflammatory factors such as IL-10 and IL-1 receptor antagonist (IL-1ra) can be measured together with the transcription factor STAT6 and surface markers CD163 and CD206^{377,468}.

The obesity-related alterations that occur in adipose tissues away from the joint, such as increased adipocyte size⁴⁶⁹, are not well characterised in the FP. The results in this chapter have shown that unlike subcutaneous adipose tissue adipocytes, the size of FP adipocytes was not associated with BMI. These observations in human tissues provide evidence that the FP adipocytes do not undergo the metabolic alterations that often engenders cellular hypertrophy⁴⁴⁹, and confirms a previous investigation that showed the absence of hypertrophic adipocytes in the FP of obese mice⁴⁷⁰. Subcutaneous adipose tissue is considered as both an energy storage and an endocrine organ that is susceptible to inflammatory macrophage infiltration during obesity^{471,472}. The FP is a potential contributor to local joint inflammation via the production of adipokines and cytokines⁴⁷³ that exacerbate joint degeneration. It has been shown that inflammation of the FP is associated with knee pain and disability in obese OA patients.⁴⁷⁴ Since the adipocytes of the FP itself are not altered, at least not in size as a result of obesity, it could be inferred that the FP derived adipocytes do not possess the same obesity induced pro-inflammatory phenotype as subcutaneous adipocytes. Hence, the findings presented here could highlight novel functional differences between the FP and subcutaneous adipose tissue in obesity, indicating perhaps that the inflammatory role of the FP in the pathogenesis of obesity related OA is separate to that of subcutaneous fat. The cellular, genetic or molecular mechanisms that cause this difference in sensitivity to obesity in the FP and other adipose tissues is not fully understood and warrants further investigation.

It is noteworthy however, that recent MRI based studies have associated a large FP with a reduced number of bone marrow lesions, reduced walking pain and higher total cartilage volume in OA patients⁴⁷⁵. Furthermore, conditioned media of FP adipocytes from obese OA patients was found to have no effect on the secretion of TNF- α in lipopolysaccharide stimulated macrophages *in vitro*, but interestingly inhibited the production of IL-12p40 in

these stimulated macrophages.⁴⁷⁶ Other studies have also shown that there were no differences between the quantity of secreted factors in conditioned media derived from the FP from obese and non-obese OA donors²⁰⁵; conditioned media from OA FP explants had a chondroprotective effect on cartilage.²⁰⁴ In a rat model of ageing, the only OA feature which correlated with FP adipocyte size was synovial thickness and this correlation was independent of age. The secretion of the pro-inflammatory cytokine TNF- α from FP was associated with age, but no association between FP adipocyte size and cytokine release was reported⁴⁷⁷. The progressive age-dependant downregulation of genes related to anti-inflammatory macrophages in FP explants from these rats suggests that a shift towards a pro-inflammatory phenotype is likely to be mediated by immune cells rather than adipocytes. Taken together, it is clear that further investigations are required to clarify whether and how obesity influences the FP (particularly in humans), and if so, what the implications are for OA.

The use of unmatched FP and subcutaneous fat is a limitation to the interpretation of the results presented in this chapter. Assessing a larger sample size with matched FP and subcutaneous fat would further confirm the differences in adipocyte size in the two tissues within a particular donor. A recent human study reported considerably larger adipocyte sizes for both FP ($3708 \pm 976 \mu\text{m}^2$) and subcutaneous fat ($6082 \pm 628 \mu\text{m}^2$) in normal donors compared to the average sizes observed in our study⁴⁷⁸. This difference in comparison to our results could be attributed to the difference in methods used to measure cell size.

Analysis of the molecules secreted by individual adipocytes would also provide valuable insight into the inflammatory status of the FP in obese and non-obese patients. One investigation revealed that the secretory profile of FP explants and the presence of macrophages in the FP are not influenced by donor BMI^{205,473}. This provides supporting evidence for our hypothesis that perhaps an increased BMI does not have a significant

influence on the adipocytes in the FP. Furthermore, we did not have samples from non-OA FP donors. Therefore, the possibility that OA could already have influenced the adipocyte size in the donors cannot be excluded. Further, the FP can also become fibrotic which could possibly limit the enlargement of adipocytes.

5.6 Conclusion

Figure 5.15 gives an illustration of the results obtained in this chapter regarding the phenotype and polarisation of macrophages. The characterisation of joint derived macrophages has significant implications in understanding their role in the progression of OA and in developing therapies to target macrophage related joint inflammation. The potential for modulating the phenotype of macrophages as a treatment option to inhibit, or even reverse, the molecular processes that promote cartilage degeneration is of particular interest and requires further study. A difference in the physiological roles of the FP and subcutaneous fat could possibly account for the difference in susceptibility of their adipocytes to hypertrophy. The data presented here adds novel insights into the physiological function of the FP and its role in the development OA.

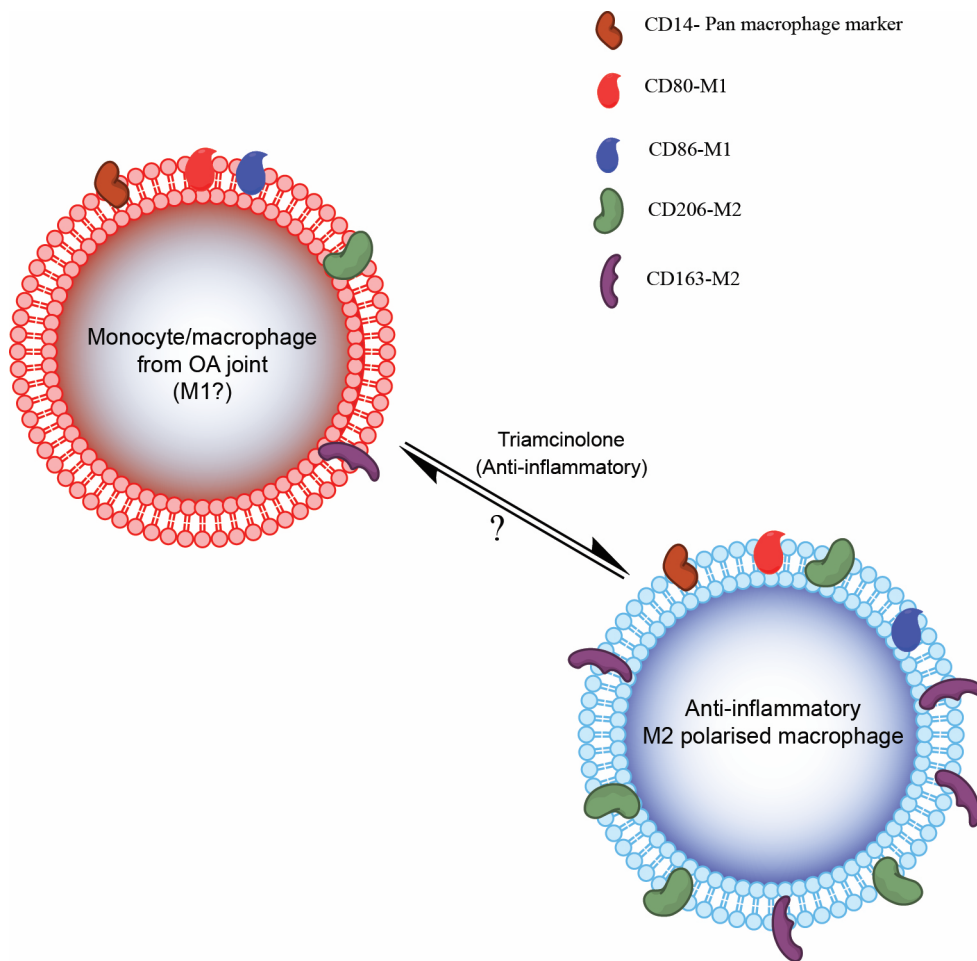


Figure 5.15: Summary of key findings presented in Chapter 5. Monocyte/macrophages from OA joints (synovium and infrapatellar fatpad) express both M1 (CD80 and CD86), pro-inflammatory, and M2 (CD206 and CD163), anti-inflammatory markers. Although the exact functional phenotype of these cells remains unknown, the results shown in this chapter suggest that these cells respond to anti-inflammatory stimuli (i.e. corticosteroids) by producing more M2 marker. The expression of M1 markers however, does not appear to be affected by this stimulus. The plasticity of polarised macrophages from the joint to revert to a previous or different phenotype warrants further studies.

Chapter 6:

General Discussion

6.1 General Discussion

Despite the numerous treatment modalities available, OA remains a major clinical challenge for clinicians, healthcare services and patients. Over the years, a tremendous amount of research has been conducted by scientists worldwide to find new ways of treating cartilage injury and OA and more specifically cartilage degeneration. The cell therapy ACI was developed to address the problem of cartilage damage, which is known to be a risk factor in the progression of OA^{479,480}. Notwithstanding the advances that have been made to improve the procedure, many scientific questions remain unanswered. One of these questions is, which cell type is most appropriate for regenerating damaged cartilage: chondrocytes, stem cells (embryonic or adult), or combinations of more than one cell type? Furthermore, one of the limitations of ACI is the need to harvest healthy cartilage to obtain chondrocytes, which is a process of creating an injury capable of producing pro-inflammatory conditions in the joint^{164,481}.

The aim of this thesis was to evaluate the chondrogenic potency of multiple sources of MSCs in an attempt to determine the most appropriate for treating cartilage defects and OA. Donor matched BM-MSCs, FP-MSCs, SCF-MSCs and SF-MSCs were investigated in this thesis as alternative cells for cartilage regeneration, with BM-MSCs and FP-MSCs displaying the highest propensity for chondrogenic differentiation *in vitro*. Although BM-MSCs are often considered the “gold standard” adult stem cell for regenerative therapies, there is growing evidence (including clinical studies) to support the use of adipose derived stem cells, such as FP-MSCs, in cartilage repair. Fat tissues are more easily accessible than bone marrow and would thus be an ideal source of therapeutic cells. The results illustrating the immunomodulatory properties of FP-MSCs, together with the fact that obesity does not alter the inflammatory status of the FP are additional advantages of this tissue over other adipose tissues⁴⁷⁰.

Another current debate is centred on whether allogeneic therapies are more appropriate than autologous. While both methods are being trialled clinically, a single-step allogeneic therapy has been suggested as perhaps the most cost effective and “patient friendly” approach^{482,483}. More than 40 companies worldwide having already investigated ways of improving cartilage tissue engineering⁴⁸⁴. An allogeneic “off the shelf” source of cells would significantly simplify the clinical translation and commercial viability of cell therapies for cartilage injury and OA. The development of advanced cell culture platforms that allow a well-controlled environment (such as sustained oxygen tension) for optimal cell expansion is key to the translation of these procedures.

Defining what are the key attributes of the ideal cell, as well as deciding upon the appropriate patients to treat and at what stage of the disease are also important factors to consider when developing cell therapies for cartilage repair. A number of markers, both cell surface and genetic, have been identified as indicative of chondrogenic potency, however these markers may not be consistent across chondrocytes and stem cells. As a result, it may be more appropriate to test and establish separate panels for chondrocytes and MSCs. Furthermore, distinct panels may even be required for subsets of MSCs depending on their tissue of origin. The lack of a clear definition of OA, particularly in its early phases, presents a challenge for applying a treatment since clinical symptoms often manifest when the disease is relatively advanced⁴⁸⁵. This poses a challenge for the screening process to identifying suitable patients to recruit in cell therapy trials. The significant progress made in OA and cartilage injury biomarkers studies (including genomics, proteomics and metabolomics) have aided in the understanding of the molecular pathways involved in the pathogenesis of OA^{486,487} and are promising tools for the stratification of patients. In addition predictive, biomarker assessment will allow the identification of patients that are most likely (or least likely) to benefit from the therapy⁴⁸⁸.

A large body of research is now aimed at harnessing the immunomodulatory properties of MSCs to attenuate joint inflammation in OA. This holds great promise for treating some of the symptoms of OA although it has been shown that MSCs with enhanced immunoregulatory properties have a poor propensity to undergo chondrogenesis²⁹³. In this respect, a co-transplantation of MSCs with immunoregulatory properties together with chondrocytes may offer an interesting option. One such clinical study is currently being performed at the Robert Jones and Agnes Hunt Orthopaedic Hospital (Autologous Stem cells Chondrocytes or the Two (ASCOT trial)). Patients are recruited as part of a three-arm trial to receive one of the following autologous therapies to treat focal cartilage defects: 1) chondrocytes, 2) BM-MSCs from the iliac crest, or 3) a combination of chondrocytes and BM-MSCs. This unique study will permit the analysis of the immunomodulatory factors expressed and secreted by the cells as well as their chondrogenic potency, both of which will be related to clinical outcome and histological analysis of repair tissues.

In the design of a cell therapy, the target may dictate the type of delivery system used to apply the cells into the injured joint: intra articular or into the defect itself. This delivery decision may be significantly influenced by the therapeutic target, ie for cartilage repair or the treatment of inflammation. The transplantation of cells into a defect, as is the case for traditional ACI, would be aimed at regenerating the damaged cartilage, whereas an intra-articular injection of cells would treat the entire joint, including dampening joint inflammation. Another option for cartilage injury or OA cell therapy development would be to trigger the endogenous cells into repairing damaged tissues or resolving inflammation⁴⁸⁹⁻⁴⁹¹. For example, MSCs have been identified in the synovium, synovial fluid, cartilage, and fat inside the knee joint^{315,320,406,492}, all of which could potentially serve endogenous as sources of s reparative cells. Finding the molecules that could target and initiate reparative processes in these cells remains an unmet research question worthy of

further study. The homing of reparative cells to an injury site was illustrated when labeled BM-MSCs intra articulary injected into a canine model of chondral defects, were able to migrating to cartilage defect sites to promote repair⁴⁹³. However, the mechanism by which this process occurred was not investigated, neither has the homing capability MSCs been demonstrated endogenously in humans.

Addressing the challenge of joint inflammation has lead researchers to identify the cells that are actively involved in producing pro-inflammatory molecules in the OA joint, such as macrophages. While these are not the only cells that promote joint degeneration, macrophages have attracted research interest due to their plasticity and their ability to induce pro-inflammatory processes in other immune cells such as T cells. A clearer understanding of the phenotype (s) of macrophages and the molecular triggers that induce their activation during the pathogenesis of OA is needed. New treatment options, and perhaps diagnostics tools, could potentially be developed by manipulating how the various subsets of macrophages influence inflammatory state in the different stages of OA. For example, there is scope for the use of MSCs as macrophage immunoregulators in the treatment of OA, as MSCs conditioned media has been shown to induce induce an anti-inflammatory phenotype in macrophages (measured by the increase in positivity for CD206 and CD163 and synthesis of IL-10⁴⁹⁴). Thus, the use of MSC conditioned media, or the therapeutic molecules secreted by these cells, have been proposed as novel additional treatment modalities.

Finally, the influence of low grade systemic inflammation in obesity-related OA is slowly coming to light^{227,495}. While the adipocytes in fat depots in the knee joint may not undergo obesity induced hypertrophy to contribute to joint inflammation, infiltrating pro-inflammatory cytokines produced by fat tissue around the body during obesity can damage the joint, and poses a significant scientific challenge to overcome. It is clear that consideration should also be given to educating individuals on the relatively simple lifestyle

changes that could help reduce the risk of OA, such as a healthy diet and frequent physical activity.

6.2 Conclusions and future work

Tremendous strides have been made in the research race to find new and innovative treatments for OA. The hope and excitement that has accompanied the field of regenerative medicine, should be balanced with less promissory discourses to reduce the often misleading hype and expectation in the general public. The overall findings in this thesis are summarised in Figure 6.1. This work adds to the current literature by shedding light on the chondrogenic and immunomodulatory nature of joint derived MSCs and elucidating the phenotypes of macrophages found in the synovium and FP of the knee. Of the stem cell populations examined, BM-MSCs and FP-MSCs displayed the highest chondrogenic potential; however, joint derived MSCs were inferior to chondrocytes in terms of chondrogenesis. Macrophages exist on a spectrum of different phenotypes and are more prevalent in the synovium of end stage OA patients than non-OA patients. Inevitably, as some questions were answered, other new research questions arose, which themselves warrant further investigation. For instance, it is still unknown whether MSCs be triggered to migrate from their respective niches in the joint to naturally repair an injury site. The difference in differentiation potential of FP and SCF-MSCs, two types of ASCs also remains unclear. Macrophages are important players in joint inflammation that require further study to understand how they can be targeted for intraarticular immunomodulation. Taken as a whole, the results presented here provides new insights into the biology of joint derived stem cells and inflammatory cells, and their potential implications in the development of cellular therapies for OA and cartilage regeneration.

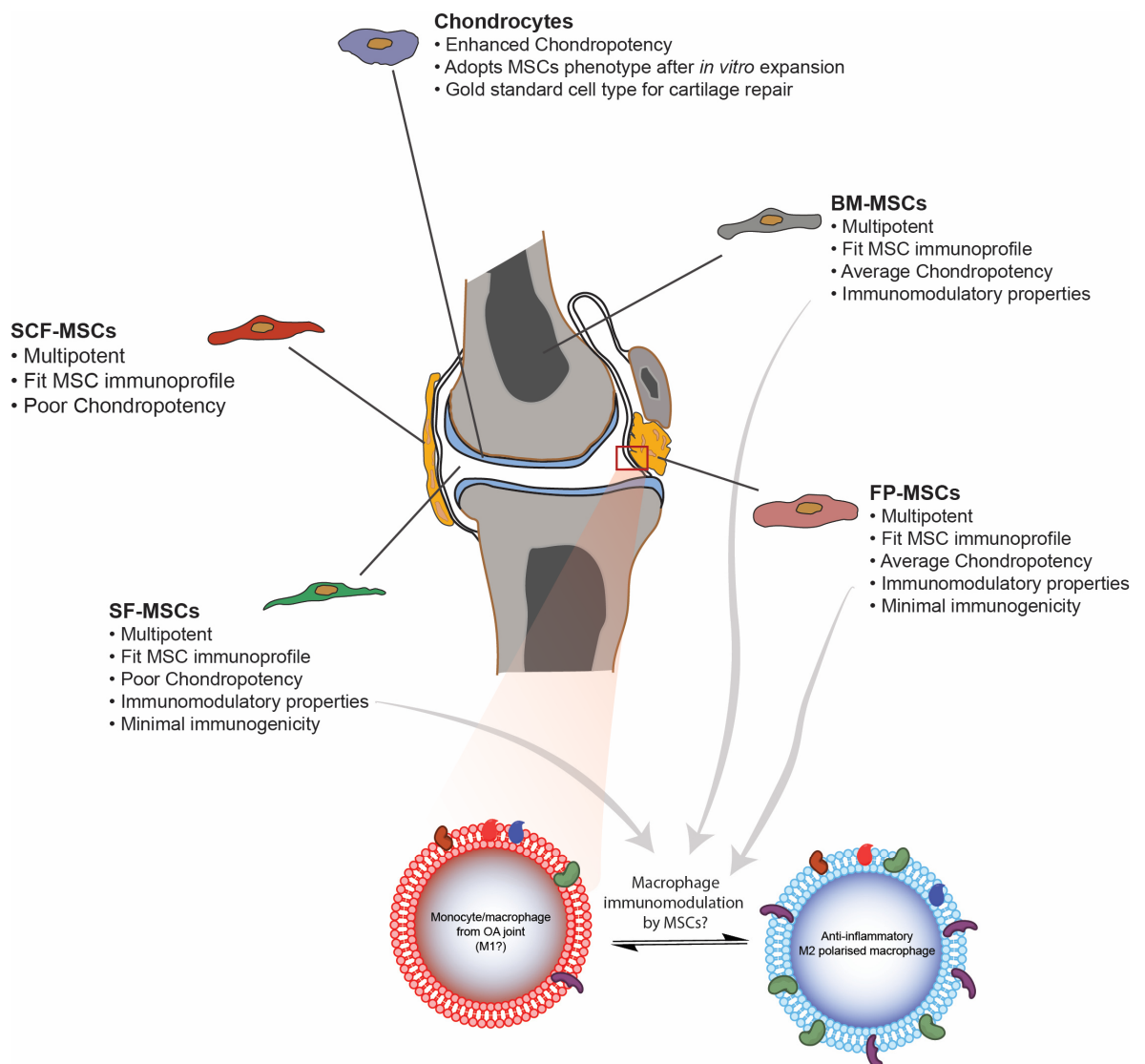


Figure 6.1: Illustration of the overarching findings presented in this thesis. The human knee harbours multiple sources of MSCs. To determine which of these cell populations is most suited for cartilage repair, a series of characterisation experiments were performed. MSCs from the bone marrow (BM-MSCs) and infrapatellar fatpad (FP-MSCs) displayed the highest chondrogenic propensities, compared to synovial fluid (SF-MSCs) and subcutaneous fat (SCF-MSCs) derived cells that showed poor chondrogenic potential. All MSCs were inferior to chondrocytes in terms of chondrogenic ability. Macrophages are immune cells that actively contribute to joint inflammation and joint destruction. It was discovered that although macrophages from the synovium and fatpad express both pro- and anti-inflammatory markers, they can be stimulated to an M2 phenotype. Further investigations are needed to determine how the immunomodulatory properties of MSCs can help attenuate inflammation by “switching” the phenotype of macrophages from M1 to M2, and hence reduce joint degeneration.

References

1. Nilsson, A.-K. & Lohmander, L. S. Age and waiting time as predictors of outcome after total hip replacement for osteoarthritis. *Rheumatology* **41**, 1261–1267 (2002).
2. Easterlin, M. C., Chang, D. G., Talamini, M. & Chang, D. C. Older age increases short-term surgical complications after primary knee arthroplasty. *Clin. Orthop. Relat. Res.* **471**, 2611–20 (2013).
3. Wilson, M., Kelley, K. & Thornhill, T. Infection as a complication of total knee-replacement arthroplasty. Risk factors and treatment in sixty-seven cases. *J. Bone Jt. Surg.* **72**, 878–883 (1990).
4. Singh, J. A., Kwok, C. K., Richardson, D., Chen, W. & Ibrahim, S. A. Sex and surgical outcomes and mortality after primary total knee arthroplasty: a risk-adjusted analysis. *Arthritis Care Res. (Hoboken)*. **65**, 1095–102 (2013).
5. Yeung, E., Jackson, M., Sexton, S., Walter, W. & Zicat, B. The effect of obesity on the outcome of hip and knee arthroplasty. *Int. Orthop.* **35**, 929–34 (2011).
6. Brittberg, M. *et al.* Treatment of deep cartilage defects in the knee with autologous chondrocyte transplantation. *N. Engl. J. Med.* **331**, 889–895 (1994).
7. Jacobi, M., Villa, V., Magnussen, R. a & Neyret, P. MACI - a new era? *Sports Med. Arthrosc. Rehabil. Ther. Technol.* **3**, 10 (2011).
8. Hunter, W. Of the structure and disease of articulating cartilages. *Clin. Orthop. Relat. Res.* 3–6 (1743).
9. Gardner, D. L. & McGillivray, D. C. Surface structure of articular cartilage. Historical review. *Ann. Rheum. Dis.* **30**, 10–4 (1971).
10. Clark, J. M., Norman, A. G., Kaab, M. J. & Notzli, H. P. The surface contour of articular cartilage in an intact, loaded joint. *J. Anat.* **195**, 45–56 (1999).
11. Shepherd, D. E. T. & Seedhom, B. B. Thickness of human articular cartilage in joints of the lower limb. *Ann. Rheum. Dis.* **58**, 27–34 (1999).
12. Lane, L. B. & Bullough, P. G. Age-related changes in the thickness of the calcified zone and the number of tidemarks in adult human articular cartilage. *J. Bone Joint Surg. Br.* **62**, 372–5 (1980).
13. Staines, K. a, Pollard, a S., McGonnell, I. M., Farquharson, C. & Pitsillides, a a. Cartilage to bone transitions in health and disease. *J. Endocrinol.* **219**, R1–R12 (2013).
14. Oegema, T. R., Carpenter, R. J., Hofmeister, F. & Thompson, R. C. The interaction of the zone of calcified cartilage and subchondral bone in osteoarthritis. *Microsc. Res. Tech.* **37**, 324–32 (1997).
15. Wong, M. & Carter, D. . Articular cartilage functional histomorphology and mechanobiology: a research perspective. *Bone* **33**, 1–13 (2003).
16. Huber, M., Trattig, S. & Lintner, F. Anatomy, biochemistry, and physiology of articular cartilage. *Invest. Radiol.* **35**, 573–80 (2000).

17. Hall, A. C., Horwitz, E. R. & Wilkins, R. J. The cellular physiology of articular cartilage. *Exp. Physiol.* **81**, 535–45 (1996).
18. Rajpurohit, R., Koch, C. J., Tao, Z., Teixeira, C. M. & Shapiro, I. M. Adaptation of chondrocytes to low oxygen tension: relationship between hypoxia and cellular metabolism. *J. Cell. Physiol.* **168**, 424–32 (1996).
19. Murphy, C. L., Thoms, B. L., Vaghjiani, R. J. & Lafont, J. E. Hypoxia. HIF-mediated articular chondrocyte function: prospects for cartilage repair. *Arthritis Res. Ther.* **11**, 213 (2009).
20. Schipani, E. *et al.* Hypoxia in cartilage: HIF-1alpha is essential for chondrocyte growth arrest and survival. *Genes Dev.* **15**, 2865–76 (2001).
21. Stockwell, R. A. The interrelationship of cell density and cartilage thickness in mammalian articular cartilage. *J. Anat.* **109**, 411–21 (1971).
22. Stockwell, R. A. The cell density of human articular and costal cartilage. *J. Anat.* **101**, 753–63 (1967).
23. Bush, P. G. & Hall, A. C. The volume and morphology of chondrocytes within non-degenerate and degenerate human articular cartilage. *Osteoarthr. Cartil.* **11**, 242–251 (2003).
24. Gannon, J. M. *et al.* Localization of type X collagen in canine growth plate and adult canine articular cartilage. *J. Orthop. Res.* **9**, 485–94 (1991).
25. Heinegård, D. & Oldberg, A. Structure and biology of cartilage and bone matrix noncollagenous macromolecules. *FASEB J.* **3**, 2042–51 (1989).
26. Stephens, M., Kwan, A. P., Bayliss, M. T. & Archer, C. W. Human articular surface chondrocytes initiate alkaline phosphatase and type X collagen synthesis in suspension culture. *J. Cell Sci.* **103** (Pt 4, 1111–6 (1992).
27. Tallheden, T. *et al.* Phenotypic Plasticity of Human Articular Chondrocytes. *J. Bone Jt. Surg.* **85**, 93–100 (2003).
28. Barbero, A., Ploegert, S., Heberer, M. & Martin, I. Plasticity of clonal populations of dedifferentiated adult human articular chondrocytes. *Arthritis Rheum.* **48**, 1315–1325 (2003).
29. Poole, C. A. *et al.* Chondrons from articular cartilage (II): Analysis of the glycosaminoglycans in the cellular microenvironment of isolated canine chondrons. *Connect. Tissue Res.* **24**, 319–30 (1990).
30. Poole, C. A. Articular cartilage chondrons: form, function and failure. *J. Anat.* **191** (Pt 1, 1–13 (1997).
31. Mason, R. M. Recent advances in the biochemistry of hyaluronic acid in cartilage. *Prog. Clin. Biol. Res.* **54**, 87–112 (1981).
32. Quinn, T., Grodzinsky, A., Buschmann, M., Kim, Y. & Hunziker, E. Mechanical compression alters proteoglycan deposition and matrix deformation around individual cells in cartilage explants. *J. Cell Sci.* **111**, 573–583 (1998).
33. Wong, M., Wuethrich, P., Buschmann, M. D., Egli, P. & Hunziker, E. Chondrocyte biosynthesis correlates with local tissue strain in statically compressed adult

- articular cartilage. *J. Orthop. Res.* **15**, 189–96 (1997).
34. Millward-Sadler, S. J., Wright, M. O., Davies, L. W., Nuki, G. & Salter, D. M. Mechanotransduction via integrins and interleukin-4 results in altered aggrecan and matrix metalloproteinase 3 gene expression in normal, but not osteoarthritic, human articular chondrocytes. *Arthritis Rheum.* **43**, 2091–9 (2000).
 35. Houard, X., Goldring, M. B. & Berenbaum, F. Homeostatic mechanisms in articular cartilage and role of inflammation in osteoarthritis. *Curr. Rheumatol. Rep.* **15**, 375 (2013).
 36. Leong, D. J., Hardin, J. A., Cobelli, N. J. & Sun, H. B. Mechanotransduction and cartilage integrity. *Ann. N. Y. Acad. Sci.* **1240**, 32–7 (2011).
 37. Eyre, D. Collagen of articular cartilage. *Arthritis Res.* **4**, 30–5 (2002).
 38. Shoulders, M. D. & Raines, R. T. Collagen structure and stability. *Annu. Rev. Biochem.* **78**, 929–58 (2009).
 39. Mendler, M., Eich-Bender, S. G., Vaughan, L., Winterhalter, K. H. & Bruckner, P. Cartilage contains mixed fibrils of collagen types II, IX, and XI. *J. Cell Biol.* **108**, 191–7 (1989).
 40. Wu, J. J., Woods, P. E. & Eyre, D. R. Identification of cross-linking sites in bovine cartilage type IX collagen reveals an antiparallel type II-type IX molecular relationship and type IX to type IX bonding. *J. Biol. Chem.* **267**, 23007–14 (1992).
 41. Wu, J. J. & Eyre, D. R. Structural analysis of cross-linking domains in cartilage type XI collagen. Insights on polymeric assembly. *J. Biol. Chem.* **270**, 18865–70 (1995).
 42. Chen, M.-H. & Broom, N. On the ultrastructure of softened cartilage: a possible model for structural transformation. *J. Anat.* **192**, 329–341 (1998).
 43. Minns, R. J. & Steven, F. S. The collagen fibril organization in human articular cartilage. *J. Anat.* **123**, 437–457 (1977).
 44. Campbell, NA, JB Reece, LA Urry, ML Cain, SA Wasserman, PV Minorsky, R. J. *Biology*. (Pearson/Benjamin Cummings, 2006).
 45. *Essentials of Glycobiology*. (Cold Spring Harbor Laboratory Press, 2009).
 46. Watanabe, H., Yamada, Y. & Kimata, K. Roles of aggrecan, a large chondroitin sulfate proteoglycan, in cartilage structure and function. *J. Biochem.* **124**, 687–93 (1998).
 47. Fosang, A. J. & Little, C. B. Drug Insight: aggrecanases as therapeutic targets for osteoarthritis. *Nat. Clin. Pract. Rheumatol.* **4**, 420–427 (2008).
 48. Geng, Y., McQuillan, D. & Roughley, P. J. SLRP interaction can protect collagen fibrils from cleavage by collagenases. *Matrix Biol.* **25**, 484–91 (2006).
 49. Merline, R., Schaefer, R. M. & Schaefer, L. The matricellular functions of small leucine-rich proteoglycans (SLRPs). *J. Cell Commun. Signal.* **3**, 323–35 (2009).
 50. Svensson, L. *et al.* Fibromodulin-null mice have abnormal collagen fibrils, tissue organization, and altered lumican deposition in tendon. *J. Biol. Chem.* **274**, 9636–47 (1999).

51. Wadhwa, S., Embree, M. C., Kilts, T., Young, M. F. & Ameye, L. G. Accelerated osteoarthritis in the temporomandibular joint of biglycan/fibromodulin double-deficient mice. *Osteoarthritis Cartilage* **13**, 817–27 (2005).
52. Ameye, L. *et al.* Abnormal collagen fibrils in tendons of biglycan/fibromodulin-deficient mice lead to gait impairment, ectopic ossification, and osteoarthritis. *FASEB J.* **16**, 673–680 (2002).
53. Rhee, D. K. *et al.* The secreted glycoprotein lubricin protects cartilage surfaces and inhibits synovial cell overgrowth. *J. Clin. Invest.* **115**, 622–31 (2005).
54. Hui, A. Y., McCarty, W. J., Masuda, K., Firestein, G. S. & Sah, R. L. A systems biology approach to synovial joint lubrication in health, injury, and disease. *Wiley Interdiscip. Rev. Syst. Biol. Med.* **4**, 15–37 (2012).
55. Swann, D. A., Silver, F. H., Slayter, H. S., Stafford, W. & Shore, E. The molecular structure and lubricating activity of lubricin isolated from bovine and human synovial fluids. *Biochem. J.* **225**, 195–201 (1985).
56. Hardingham, T. E. & Fosang, A. J. Proteoglycans: many forms and many functions. *FASEB J.* **6**, 861–870 (1992).
57. Erickson, G. R., Alexopoulos, L. G. & Guilak, F. Hyper-osmotic stress induces volume change and calcium transients in chondrocytes by transmembrane, phospholipid, and G-protein pathways. *J. Biomech.* **34**, 1527–35 (2001).
58. Mobasheri, A. *et al.* Potassium channels in articular chondrocytes. *Channels (Austin)*. **6**, 416–25
59. Wilkins, R. J. & Hall, a C. Measurement of intracellular pH in isolated bovine articular chondrocytes. *Exp. Physiol.* **77**, 521–4 (1992).
60. Ingber, D. E. Tensegrity I. Cell structure and hierarchical systems biology. *J. Cell Sci.* **116**, 1157–1173 (2003).
61. Ingber, D. E. Tensegrity-Based Mechanosensing from Macro to Micro. *Pathology* **97**, 163–179 (2009).
62. Fell, H. B. The histogenesis of cartilage and bone in the long bones of the embryonic fowl. *J. Morphol.* **40**, 417–459 (1925).
63. Fell, H. B. & Canti, R. G. Experiments on the Development in vitro of the Avian Knee-Joint. *Proc. R. Soc. B Biol. Sci.* **116**, 316–351 (1934).
64. Thorogood, P. V & Hinchliffe, J. R. An analysis of the condensation process during chondrogenesis in the embryonic chick hind limb. *J. Embryol. Exp. Morphol.* **33**, 581–606 (1975).
65. Oberlender, S. A. & Tuan, R. S. Expression and functional involvement of N-cadherin in embryonic limb chondrogenesis. *Development* **120**, 177–87 (1994).
66. Oberlender, S. A. & Tuan, R. S. Spatiotemporal profile of N-cadherin expression in the developing limb mesenchyme. *Cell Adhes. Commun.* **2**, 521–37 (1994).
67. Tufan, A. C., Daumer, K. M. & Tuan, R. S. Frizzled-7 and limb mesenchymal chondrogenesis: effect of misexpression and involvement of N-cadherin. *Dev. Dyn.* **223**, 241–53 (2002).

68. Tavella, S., Raffo, P., Tacchetti, C., Cancedda, R. & Castagnola, P. N-CAM and N-cadherin expression during in vitro chondrogenesis. *Exp. Cell Res.* **215**, 354–62 (1994).
69. Widelitz, R. B., Jiang, T. X., Murray, B. A. & Chuong, C. M. Adhesion molecules in skeletogenesis: II. Neural cell adhesion molecules mediate precartilaginous mesenchymal condensations and enhance chondrogenesis. *J. Cell. Physiol.* **156**, 399–411 (1993).
70. Kosher, R. A., Kulyk, W. M. & Gay, S. W. Collagen gene expression during limb cartilage differentiation. *J. Cell Biol.* **102**, 1151–6 (1986).
71. Hascall, V. C., Oegema, T. R. & Brown, M. Isolation and characterization of proteoglycans from chick limb bud chondrocytes grown in vitro. *J. Biol. Chem.* **251**, 3511–9 (1976).
72. DeLise, a M., Fischer, L. & Tuan, R. S. Cellular interactions and signaling in cartilage development. *Osteoarthritis Cartilage* **8**, 309–34 (2000).
73. Hall, B. K. & Miyake, T. All for one and one for all: condensations and the initiation of skeletal development. *Bioessays* **22**, 138–47 (2000).
74. Hall, B. K. & Miyake, T. Divide, accumulate, differentiate: cell condensation in skeletal development revisited. *Int. J. Dev. Biol.* **39**, 881–93 (1995).
75. Olsen, B. R., Reginato, A. M. & Wang, W. Bone development. *Annu. Rev. Cell Dev. Biol.* **16**, 191–220 (2000).
76. Mackie, E. J., Ahmed, Y. A., Tatarczuch, L., Chen, K.-S. & Mirams, M. Endochondral ossification: How cartilage is converted into bone in the developing skeleton. *Int. J. Biochem. Cell Biol.* **40**, 46–62 (2008).
77. R, S. *Treatment of Fractures in Children and Adolescents*. (Springer Berlin Heidelberg, 1980). doi:10.1007/978-3-642-67271-2
78. Wright, E. *et al.* The Sry-related gene Sox9 is expressed during chondrogenesis in mouse embryos. *Nat. Genet.* **9**, 15–20 (1995).
79. Lefebvre, R., Huang, W., Harley, V. R., Goodfellow, P. N. & Crombrughe, B. D. E. SOX9 Is a Potent Activator of the Chondrocyte-Specific Enhancer of the Pro α 1(II) Collagen Collagen Gene. *Mol. Cell. Biol.* **17**, 2336–2346 (1997).
80. Wagner, T. *et al.* Autosomal sex reversal and campomelic dysplasia are caused by mutations in and around the SRY-related gene SOX9. *Cell* **79**, 1111–1120 (1994).
81. Yang, X. TGF-beta/Smad3 Signals Repress Chondrocyte Hypertrophic Differentiation and Are Required for Maintaining Articular Cartilage. *J. Cell Biol.* **153**, 35–46 (2001).
82. Kulyk, W. M., Rodgers, B. J., Greer, K. & Kosher, R. A. Promotion of embryonic chick limb cartilage differentiation by transforming growth factor-beta. *Dev. Biol.* **135**, 424–30 (1989).
83. De Luca F *et al.* Regulation of growth plate chondrogenesis by bone morphogenetic protein-2. *Endocrinology* **142**, 430–6 (2001).
84. Yi, S., Daluiski, A., Pederson, R., Rosen, V. & Lyons, K. The type I BMP receptor

- BMPRIB is required for chondrogenesis in the mouse limb. *Development* **127**, 621–630 (2000).
85. Maroudas, A., Bayliss, M. T., Uchitel-Kaushansky, N., Schneiderman, R. & Gilav, E. Aggrecan turnover in human articular cartilage: use of aspartic acid racemization as a marker of molecular age. *Arch. Biochem. Biophys.* **350**, 61–71 (1998).
 86. Verzijl, N. *et al.* Effect of collagen turnover on the accumulation of advanced glycation end products. *J. Biol. Chem.* **275**, 39027–31 (2000).
 87. Pelletier, J. P. *et al.* Collagenase and collagenolytic activity in human osteoarthritic cartilage. *Arthritis Rheum.* **26**, 63–8 (1983).
 88. Mitchell, P. G. *et al.* Cloning, expression, and type II collagenolytic activity of matrix metalloproteinase-13 from human osteoarthritic cartilage. *J. Clin. Invest.* **97**, 761–8 (1996).
 89. Miller, E. J. *et al.* Cleavage of Type II and III collagens with mammalian collagenase: site of cleavage and primary structure at the NH₂-terminal portion of the smaller fragment released from both collagens. *Biochemistry* **15**, 787–92 (1976).
 90. Tortorella, M. D., Malfait, a M., Deccico, C. & Arner, E. The role of ADAM-TS4 (aggrecanase-1) and ADAM-TS5 (aggrecanase-2) in a model of cartilage degradation. *Osteoarthritis Cartilage* **9**, 539–52 (2001).
 91. Arner, E. C. Aggrecanase-mediated cartilage degradation. *Curr. Opin. Pharmacol.* **2**, 322–9 (2002).
 92. Cawston, T. *et al.* The regulation of MMPs and TIMPs in cartilage turnover. *Ann. N. Y. Acad. Sci.* **878**, 120–9 (1999).
 93. Dean, D. D., Martel-pelletier, J., Pelletier, J., Howell, D. S. & Woessner, J. F. Evidence for Metalloproteinase and Metalloproteinase Inhibitor Imbalance in Human Osteoarthritic Cartilage MEDIAL. *J. Clin. Invest.* **84**, 678–685 (1989).
 94. Martel-Pelletier, J. *et al.* Excess of metalloproteases over tissue inhibitor of metalloprotease may contribute to cartilage degradation in osteoarthritis and rheumatoid arthritis. *Lab. Invest.* **70**, 807–15 (1994).
 95. Wang, Y. *et al.* Factors affecting progression of knee cartilage defects in normal subjects over 2 years. *Rheumatology (Oxford)*. **45**, 79–84 (2006).
 96. Davies-Tuck, M. L. *et al.* The natural history of cartilage defects in people with knee osteoarthritis. *Osteoarthr. Cartil.* **16**, 337–342 (2008).
 97. Dell’accio, F. & Vincent, T. L. Joint surface defects: clinical course and cellular response in spontaneous and experimental lesions. *Eur. Cell. Mater.* **20**, 210–217 (2010).
 98. Anderson, D. D. *et al.* Post-traumatic osteoarthritis: Improved understanding and opportunities for early intervention. *J. Orthop. Res.* **29**, 802–809 (2011).
 99. Curl, W. W. *et al.* Cartilage injuries: a review of 31,516 knee arthroscopies. *Arthroscopy* **13**, 456–60 (1997).
 100. Brittberg, M. & Winalski, C. S. Evaluation of cartilage injuries and repair. *J. Bone Joint Surg. Am.* **85–A Suppl**, 58–69 (2003).

101. Grimm, N. L., Weiss, J. M., Kessler, J. I. & Aoki, S. K. Osteochondritis Dissecans of the Knee. *Clin. Sports Med.* (2014). doi:10.1016/j.csm.2013.11.006
102. Kessler, J. I. *et al.* The demographics and epidemiology of osteochondritis dissecans of the knee in children and adolescents. *Am. J. Sports Med.* **42**, 320–6 (2014).
103. Pappas, A. M. Osteochondrosis dissecans. *Clin. Orthop. Relat. Res.* 59–69 (1981).
104. Chen, a, Gupte, C., Akhtar, K., Smith, P. & Cobb, J. The Global Economic Cost of Osteoarthritis: How the UK Compares. *Arthritis* **2012**, 698709 (2012).
105. Arthritis Research UK. *Osteoarthritis in General Practice.* (2013).
106. Mezhev, V. *et al.* Does obesity affect knee cartilage? A systematic review of magnetic resonance imaging data. *Obes. Rev.* **15**, 143–57 (2014).
107. Felson, D. T. *et al.* Risk factors for incident radiographic knee osteoarthritis in the elderly: the Framingham Study. *Arthritis Rheum.* **40**, 728–33 (1997).
108. Karlson, E. W. *et al.* Total hip replacement due to osteoarthritis: the importance of age, obesity, and other modifiable risk factors. *Am. J. Med.* **114**, 93–8 (2003).
109. Ghosh, P. & Smith, M. Osteoarthritis, genetic and molecular mechanisms. *Biogerontology* **3**, 85–8 (2002).
110. Reynard, L. N. & Loughlin, J. Genetics and epigenetics of osteoarthritis. *Maturitas* **71**, 200–4 (2012).
111. Hodler, J. & Resnick, D. Current status of imaging of articular cartilage. *Skeletal Radiol.* **25**, 703–9 (1996).
112. Aigner, T. *et al.* SOX9 expression does not correlate with type II collagen expression in adult articular chondrocytes. *Matrix Biol.* **22**, 363–372 (2003).
113. Orfanidou, T., Iliopoulos, D., Malizos, K. N. & Tsezou, A. Involvement of SOX-9 and FGF-23 in RUNX-2 regulation in osteoarthritic chondrocytes. *J. Cell. Mol. Med.* **13**, 3186–94 (2009).
114. Pitsillides, A. a & Beier, F. Cartilage biology in osteoarthritis--lessons from developmental biology. *Nat. Rev. Rheumatol.* **7**, 654–63 (2011).
115. van der Kraan, P. M. & van den Berg, W. B. Chondrocyte hypertrophy and osteoarthritis: role in initiation and progression of cartilage degeneration? *Osteoarthritis Cartilage* **20**, 223–32 (2012).
116. Sandell, L. J. & Aigner, T. Articular cartilage and changes in arthritis. An introduction: cell biology of osteoarthritis. *Arthritis Res.* **3**, 107–13 (2001).
117. Pritzker, K. P. H. *et al.* Osteoarthritis cartilage histopathology: grading and staging. *Osteoarthritis Cartilage* **14**, 13–29 (2006).
118. Hulth, A., Lindberg, L. & Telhag, H. Mitosis in human osteoarthritic cartilage. *Clin. Orthop. Relat. Res.* **84**, 197–9 (1972).
119. Rothwell, A. G. & Bentley, G. Chondrocyte multiplication in osteoarthritic articular cartilage. *J. Bone Joint Surg. Br.* **55**, 588–94 (1973).
120. Hermansson, M. *et al.* Proteomic analysis of articular cartilage shows increased type

- II collagen synthesis in osteoarthritis and expression of inhibin betaA (activin A), a regulatory molecule for chondrocytes. *J. Biol. Chem.* **279**, 43514–21 (2004).
121. Tchetina, E. V, Squires, G. & Poole, A. R. Increased type II collagen degradation and very early focal cartilage degeneration is associated with upregulation of chondrocyte differentiation related genes in early human articular cartilage lesions. *J. Rheumatol.* **32**, 876–86 (2005).
 122. Li, Y., Wei, X., Zhou, J. & Wei, L. The age-related changes in cartilage and osteoarthritis. *Biomed Res. Int.* **2013**, 916530 (2013).
 123. Von Der Mark, K. *et al.* Type x collagen synthesis in human osteoarthritic cartilage. indication of chondrocyte hypertrophy. *Arthritis Rheum.* **35**, 806–811 (1992).
 124. Walker, G. D., Fischer, M., Gannon, J., Thompson, R. C. & Oegema, T. R. Expression of type-X collagen in osteoarthritis. *J. Orthop. Res.* **13**, 4–12 (1995).
 125. von der Mark, K. *et al.* Upregulation of type X collagen expression in osteoarthritic cartilage. *Acta Orthop. Scand. Suppl.* **266**, 125–9 (1995).
 126. Murphy, G. & Nagase, H. Reappraising metalloproteinases in rheumatoid arthritis and osteoarthritis: destruction or repair? *Nat. Clin. Pract. Rheumatol.* **4**, 128–35 (2008).
 127. Nagase, H. & Kashiwagi, M. Aggrecanases and cartilage matrix degradation. *Arthritis Res. Ther.* **5**, 94–103 (2003).
 128. Kevorkian, L. *et al.* Expression profiling of metalloproteinases and their inhibitors in cartilage. *Arthritis Rheum.* **50**, 131–41 (2004).
 129. Su, S. *et al.* Expression of the tissue inhibitor of metalloproteinases (TIMP) gene family in normal and osteoarthritic joints. *Rheumatol. Int.* **18**, 183–91 (1999).
 130. Goyal, N., Gupta, M., Joshi, K. & Nagi, O. N. Immunohistochemical analysis of ageing and osteoarthritic articular cartilage. *J. Mol. Histol.* **41**, 193–7 (2010).
 131. Nakamura, S. *et al.* Enhancement of SPARC (osteonectin) synthesis in arthritic cartilage. Increased levels in synovial fluids from patients with rheumatoid arthritis and regulation by growth factors and cytokines in chondrocyte cultures. *Arthritis Rheum.* **39**, 539–51 (1996).
 132. Pfander, D., Swoboda, B. & Kirsch, T. Expression of early and late differentiation markers (proliferating cell nuclear antigen, syndecan-3, annexin VI, and alkaline phosphatase) by human osteoarthritic chondrocytes. *Am. J. Pathol.* **159**, 1777–83 (2001).
 133. Pullig, O., Weseloh, G., Gauer, S. & Swoboda, B. Osteopontin is expressed by adult human osteoarthritic chondrocytes: protein and mRNA analysis of normal and osteoarthritic cartilage. *Matrix Biol.* **19**, 245–255 (2000).
 134. Rees, J. A. & Ali, S. Y. Ultrastructural localisation of alkaline phosphatase activity in osteoarthritic human articular cartilage. *Ann. Rheum. Dis.* **47**, 747–753 (1988).
 135. Wang, X. *et al.* Regulation of MMP-13 expression by RUNX2 and FGF2 in osteoarthritic cartilage. *Osteoarthritis Cartilage* **12**, 963–73 (2004).
 136. Solomon, L. A., Bérubé, N. G. & Beier, F. Transcriptional regulators of chondrocyte

- hypertrophy. *Birth Defects Res. C. Embryo Today* **84**, 123–30 (2008).
137. Blanco, F. J., Guitian, R., Vázquez-Martul, E., de Toro, F. J. & Galdo, F. Osteoarthritis chondrocytes die by apoptosis. A possible pathway for osteoarthritis pathology. *Arthritis Rheum.* **41**, 284–9 (1998).
 138. Kim, H. A., Lee, Y. J., Seong, S. C., Choe, K. W. & Song, Y. W. Apoptotic chondrocyte death in human osteoarthritis. *J. Rheumatol.* **27**, 455–62 (2000).
 139. Reboul, P., Pelletier, J. P., Tardif, G., Cloutier, J. M. & Martel-Pelletier, J. The new collagenase, collagenase-3, is expressed and synthesized by human chondrocytes but not by synoviocytes. A role in osteoarthritis. *J. Clin. Invest.* **97**, 2011–9 (1996).
 140. Hollander, a P. *et al.* Increased damage to type II collagen in osteoarthritic articular cartilage detected by a new immunoassay. *J. Clin. Invest.* **93**, 1722–32 (1994).
 141. Hollander, a P. *et al.* Damage to type II collagen in aging and osteoarthritis starts at the articular surface, originates around chondrocytes, and extends into the cartilage with progressive degeneration. *J. Clin. Invest.* **96**, 2859–69 (1995).
 142. Takahashi, M. *et al.* Quantitative analysis of crosslinks pyridinoline and pentosidine in articular cartilage of patients with bone and joint disorders. *Arthritis Rheum.* **37**, 724–8 (1994).
 143. Verzijl, N. *et al.* Age-related accumulation of Maillard reaction products in human articular cartilage collagen. *Biochem. J.* **350 Pt 2**, 381–7 (2000).
 144. Verzijl, N. *et al.* Crosslinking by Advanced Glycation End Products Increases the Stiffness of the Collagen Network in Human Articular Cartilage A Possible Mechanism Through Which Age Is a Risk Factor for Osteoarthritis. *Arthritis Rheum.* **46**, 114–123 (2002).
 145. Hashimoto, S., Ochs, R. L., Komiya, S. & Lotz, M. Linkage of chondrocyte apoptosis and cartilage degradation in human osteoarthritis. *Arthritis Rheum.* **41**, 1632–8 (1998).
 146. Tanamas, S. K. *et al.* The association between subchondral bone cysts and tibial cartilage volume and risk of joint replacement in people with knee osteoarthritis: a longitudinal study. *Arthritis Res. Ther.* **12**, R58 (2010).
 147. Landells, J. W. The Bone Cyst of Osteoarthritis. *J. Bone Joint Surg. Br.* **35 B**, 643–649 (1953).
 148. Burr, D. B. Anatomy and physiology of the mineralized tissues: role in the pathogenesis of osteoarthrosis. *Osteoarthritis Cartilage* **12 Suppl A**, S20-30 (2004).
 149. Day, J. S. *et al.* A decreased subchondral trabecular bone tissue elastic modulus is associated with pre-arthritic cartilage damage. *J. Orthop. Res.* **19**, 914–8 (2001).
 150. Goldring, M. B. & Goldring, S. R. Articular cartilage and subchondral bone in the pathogenesis of osteoarthritis. *Ann. N. Y. Acad. Sci.* **1192**, 230–7 (2010).
 151. van der Kraan, P. M. & van den Berg, W. B. Osteophytes: relevance and biology. *Osteoarthritis Cartilage* **15**, 237–44 (2007).
 152. Kerkhof, H. J. M. *et al.* A genome-wide association study identifies an osteoarthritis susceptibility locus on chromosome 7q22. *Arthritis Rheum.* **62**, 499–510 (2010).

153. Zeggini, E. *et al.* Identification of new susceptibility loci for osteoarthritis (arcOGEN): a genome-wide association study. *Lancet* **380**, 815–23 (2012).
154. Ala-Kokko, L., Baldwin, C. T., Moskowitz, R. W. & Prockop, D. J. Single base mutation in the type II procollagen gene (COL2A1) as a cause of primary osteoarthritis associated with a mild chondrodysplasia. *Proc. Natl. Acad. Sci. U. S. A.* **87**, 6565–8 (1990).
155. Uitterlinden, A. G. *et al.* Vitamin D receptor genotype is associated with radiographic osteoarthritis at the knee. *J. Clin. Invest.* **100**, 259–63 (1997).
156. Loughlin, J. *et al.* Association analysis of the vitamin D receptor gene, the type I collagen gene COL1A1, and the estrogen receptor gene in idiopathic osteoarthritis. *J. Rheumatol.* **27**, 779–84 (2000).
157. Kizawa, H. *et al.* An aspartic acid repeat polymorphism in asporin inhibits chondrogenesis and increases susceptibility to osteoarthritis. *Nat. Genet.* **37**, 138–44 (2005).
158. Southam, L. *et al.* An SNP in the 5'-UTR of GDF5 is associated with osteoarthritis susceptibility in Europeans and with in vivo differences in allelic expression in articular cartilage. *Hum. Mol. Genet.* **16**, 2226–32 (2007).
159. Loughlin, J. *et al.* Functional variants within the secreted frizzled-related protein 3 gene are associated with hip osteoarthritis in females. *Proc. Natl. Acad. Sci. U. S. A.* **101**, 9757–62 (2004).
160. Min, J. L. *et al.* Association of the Frizzled-related protein gene with symptomatic osteoarthritis at multiple sites. *Arthritis Rheum.* **52**, 1077–80 (2005).
161. Scott, A., Khan, K. M., Cook, J. L. & Duronio, V. What is 'inflammation'? Are we ready to move beyond Celsus? *Br. J. Sports Med.* **38**, 248–249 (2004).
162. Farahat, M. N., Yanni, G., Poston, R. & Panayi, G. S. Cytokine expression in synovial membranes of patients with rheumatoid arthritis and osteoarthritis. *Ann. Rheum. Dis.* **52**, 870–875 (1993).
163. Choy, E. H. & Panayi, G. S. Cytokine pathways and joint inflammation in rheumatoid arthritis. *N. Engl. J. Med.* **344**, 907–16 (2001).
164. Kapoor, M., Martel-Pelletier, J., Lajeunesse, D., Pelletier, J.-P. & Fahmi, H. Role of proinflammatory cytokines in the pathophysiology of osteoarthritis. *Nat. Rev. Rheumatol.* **7**, 33–42 (2011).
165. Sims, J. E. *et al.* Interleukin 1 signaling occurs exclusively via the type I receptor. *Proc. Natl. Acad. Sci.* **90**, 6155–6159 (1993).
166. Nietfeld, J. J., Wilbrink, B., Den Otter, W., Huber, J. & Huber-Bruning, O. The effect of human interleukin 1 on proteoglycan metabolism in human and porcine cartilage explants. *J. Rheumatol.* **17**, 818–26 (1990).
167. Goldring, M. B., Fukuo, K., Birkhead, J. R., Dudek, E. & Sandell, L. J. Transcriptional suppression by interleukin-1 and interferon-gamma of type II collagen gene expression in human chondrocytes. *J. Cell. Biochem.* **54**, 85–99 (1994).

168. Saklatvala, J. Tumour necrosis factor alpha stimulates resorption and inhibits synthesis of proteoglycan in cartilage. *Nature* **322**, 547–549 (1986).
169. Séguin, C. A. & Bernier, S. M. TNF-alpha suppresses link protein and type II collagen expression in chondrocytes: Role of MEK1/2 and NF-kappaB signaling pathways. *J. Cell. Physiol.* **197**, 356–69 (2003).
170. Lefebvre, V., Peeters-Joris, C. & Vaes, G. Modulation by interleukin 1 and tumor necrosis factor alpha of production of collagenase, tissue inhibitor of metalloproteinases and collagen types in differentiated and dedifferentiated articular chondrocytes. *Biochim. Biophys. Acta* **1052**, 366–78 (1990).
171. Mengshol, J. A., Vincenti, M. P., Coon, C. I., Barchowsky, A. & Brinckerhoff, C. E. Interleukin-1 induction of collagenase 3 (matrix metalloproteinase 13) gene expression in chondrocytes requires p38, c-Jun N-terminal kinase, and nuclear factor kappa-B: Differential regulation of collagenase 1 and collagenase 3. *Arthritis Rheum.* **43**, 801–811 (2000).
172. Lotz, M., Terkeltaub, R. & Villiger, P. M. Cartilage and joint inflammation. Regulation of IL-8 expression by human articular chondrocytes. *J. Immunol.* **148**, 466–73 (1992).
173. Villiger, P. M., Terkeltaub, R. & Lotz, M. Monocyte chemoattractant protein-1 (MCP-1) expression in human articular cartilage. Induction by peptide regulatory factors and differential effects of dexamethasone and retinoic acid. *J. Clin. Invest.* **90**, 488–96 (1992).
174. Guerne, P. A., Carson, D. A. & Lotz, M. IL-6 production by human articular chondrocytes. Modulation of its synthesis by cytokines, growth factors, and hormones in vitro. *J. Immunol.* **144**, 499–505 (1990).
175. Alaaeddine, N. *et al.* Osteoarthritic synovial fibroblasts possess an increased level of tumor necrosis factor-receptor 55 (TNF-R55) that mediates biological activation by TNF-alpha. *J. Rheumatol.* **24**, 1985–94 (1997).
176. Sadouk, M. B. *et al.* Human synovial fibroblasts coexpress IL-1 receptor type I and type II mRNA. The increased level of the IL-1 receptor in osteoarthritic cells is related to an increased level of the type I receptor. *Lab. Invest.* **73**, 347–55 (1995).
177. Okamura, Y. *et al.* The Extra Domain A of Fibronectin Activates Toll-like Receptor 4. *J. Biol. Chem.* **276**, 10229–10233 (2001).
178. Happonen, K. E. *et al.* Regulation of complement by cartilage oligomeric matrix protein allows for a novel molecular diagnostic principle in rheumatoid arthritis. *Arthritis Rheum.* **62**, 3574–3583 (2010).
179. Taylor, K. R. *et al.* Recognition of hyaluronan released in sterile injury involves a unique receptor complex dependent on toll-like receptor 4, CD44, and MD-2. *J. Biol. Chem.* **282**, 18265–18275 (2007).
180. Orłowski, E. W. & Kraus, V. B. The role of innate immunity in osteoarthritis: When our first line of defense goes on the offensive. *J. Rheumatol.* **42**, 363–371 (2015).
181. Kim, H. A. *et al.* The catabolic pathway mediated by Toll-like receptors in human osteoarthritic chondrocytes. *Arthritis Rheum.* **54**, 2152–2163 (2006).

182. Radstake, T. R. D. J. *et al.* Expression of toll-like receptors 2 and 4 in rheumatoid synovial tissue and regulation by proinflammatory cytokines interleukin-12 and interleukin-18 via interferon-gamma. *Arthritis Rheum.* **50**, 3856–65 (2004).
183. Smith, M. D. The normal synovium. *Open Rheumatol. J.* **5**, 100–6 (2011).
184. Singh, J. A., Arayssi, T., Duray, P. & Schumacher, H. R. Immunohistochemistry of normal human knee synovium: a quantitative study. *Ann. Rheum. Dis.* **63**, 785–90 (2004).
185. Krenn, V. *et al.* Synovitis score: Discrimination between chronic low-grade and high-grade synovitis. *Histopathology* **49**, 358–364 (2006).
186. Roemer, F. W. *et al.* Anatomical distribution of synovitis in knee osteoarthritis and its association with joint effusion assessed on non-enhanced and contrast-enhanced MRI. *Osteoarthr. Cartil.* **18**, 1269–1274 (2010).
187. de Lange-Brokaar, B. J. E. *et al.* Synovial inflammation, immune cells and their cytokines in osteoarthritis: A review. *Osteoarthr. Cartil.* **20**, 1484–1499 (2012).
188. de Lange-Brokaar, B. J. E. *et al.* Evolution of synovitis in osteoarthritic knees and its association with clinical features. *Osteoarthritis Cartilage* 1–8 (2016). doi:10.1016/j.joca.2016.05.021
189. O’Connell, J. X. Pathology of the synovium. *Am. J. Clin. Pathol.* **114**, 773–784 (2000).
190. Milgram, J. W. The classification of loose bodies in human joints. *Clin. Orthop. Relat. Res.* 282–91 (1977).
191. Di Giovine, F. S., Malawista, S. E., Nuki, G. & Duff, G. W. Interleukin 1 (IL 1) as a mediator of crystal arthritis. Stimulation of T cell and synovial fibroblast mitogenesis by urate crystal-induced IL 1. *J. Immunol.* **138**, 3213–8 (1987).
192. Greene, M. A. & Loeser, R. F. Aging-related inflammation in osteoarthritis. *Osteoarthr. Cartil.* **23**, 1966–1971 (2015).
193. Goldring, M. B. & Otero, M. Inflammation in osteoarthritis. *Curr. Opin. Rheumatol.* **23**, 471–478 (2011).
194. Wynn, T. A., Chawla, A. & Pollard, J. W. Macrophage biology in development, homeostasis and disease. *Nature* **496**, 445–55 (2013).
195. Okabe, Y. & Medzhitov, R. Tissue biology perspective on macrophages. *Nat. Immunol.* **17**, 9–17 (2015).
196. Verreck, F. A. W. *et al.* Human IL-23-producing type 1 macrophages promote but IL-10-producing type 2 macrophages subvert immunity to (myco)bacteria. *Proc. Natl. Acad. Sci. U. S. A.* **101**, 4560–5 (2004).
197. Mosser, D. M. & Edwards, J. P. Exploring the full spectrum of macrophage activation. *Nat. Rev. Immunol.* **8**, 958–969 (2008).
198. Martinez, F. O. & Gordon, S. The M1 and M2 paradigm of macrophage activation: time for reassessment. *F1000Prime Rep.* **6**, 13 (2014).
199. Novak, M. L. & Koh, T. J. Macrophage phenotypes during tissue repair. *J Leukoc*

- Biol* **93**, 875–881 (2013).
200. Bosch, M. H. Van Den *et al.* Alarmin S100A9 Induces Proinflammatory and Catabolic Effects Predominantly in the M1 Macrophages of Human Osteoarthritic Synovium. *J. Rheumatol.* (2016). doi:10.3899/jrheum.160270
 201. Fahy, N. *et al.* Human osteoarthritic synovium impacts chondrogenic differentiation of mesenchymal stem cells via macrophage polarisation state. *Osteoarthr. Cartil.* **22**, 1167–1175 (2014).
 202. Distel, E. *et al.* The infrapatellar fat pad in knee osteoarthritis: An important source of interleukin-6 and its soluble receptor. *Arthritis Rheum.* **60**, 3374–3377 (2009).
 203. Bastiaansen-jenniskens, Y. M. *et al.* Stimulation of Fibrotic Processes by the Infrapatellar Fat Pad in Cultured Synoviocytes From Patients With Osteoarthritis. *Arthritis Rheum.* **65**, 2070–2080 (2013).
 204. Bastiaansen-Jenniskens, Y. M. *et al.* Infrapatellar fat pad of patients with end-stage osteoarthritis inhibits catabolic mediators in cartilage. *Ann. Rheum. Dis.* **71**, 288–294 (2012).
 205. Clockaerts, S. *et al.* Cytokine production by infrapatellar fat pad can be stimulated by interleukin 1 β and inhibited by peroxisome proliferator activated receptor α agonist. *Ann. Rheum. Dis.* **71**, 1012–8 (2012).
 206. Felson, D. T. *et al.* Osteoarthritis: New Insights. Part 1: The Disease and Its Risk Factors. *Ann. Intern. Med.* **133**, 635 (2000).
 207. Loeser, R. F., Collins, J. A. & Diekman, B. O. Ageing and the pathogenesis of osteoarthritis. *Nat. Rev. Rheumatol.* **12**, 412–20 (2016).
 208. Loeser, R. F. Aging and osteoarthritis : the role of chondrocyte senescence and aging changes in the cartilage matrix. *Osteoarthr. Cartil.* **17**, 971–979 (2009).
 209. Lotz, M. & Loeser, R. F. Effects of aging on articular cartilage homeostasis. *Bone* **51**, 241–8 (2012).
 210. Lanyon, P., Muir, K., Doherty, S. & Doherty, M. Age and sex differences in hip joint space among asymptomatic subjects without structural change: Implications for epidemiologic studies. *Arthritis Rheum.* **48**, 1041–1046 (2003).
 211. Prieto-Alhambra, D. *et al.* Incidence and risk factors for clinically diagnosed knee, hip and hand osteoarthritis: influences of age, gender and osteoarthritis affecting other joints. *Ann. Rheum. Dis.* **73**, 1659–64 (2014).
 212. Claassen, H., Schünke, M. & Kurz, B. Estradiol protects cultured articular chondrocytes from oxygen-radical-induced damage. *Cell Tissue Res.* **319**, 439–445 (2005).
 213. Maneix, L. *et al.* 17Beta-oestradiol up-regulates the expression of a functional UDP-glucose dehydrogenase in articular chondrocytes: comparison with effects of cytokines and growth factors. *Rheumatology (Oxford).* **47**, 281–288 (2008).
 214. Roman-Blas, J. a, Castañeda, S., Largo, R. & Herrero-Beaumont, G. Osteoarthritis associated with estrogen deficiency. *Arthritis Res. Ther.* **11**, 241 (2009).
 215. Hootman, J. M., Macera, C. A., Helmick, C. G. & Blair, S. N. Influence of physical

- activity-related joint stress on the risk of self-reported hip/knee osteoarthritis: A new method to quantify physical activity. *Prev. Med. (Baltim)*. **36**, 636–644 (2003).
216. Cooper, C. *et al.* Risk Factors for the Incidence and Progression of Radiographic Knee Osteoarthritis. *Arthritis Rheum*. **43**, 995–1000 (2000).
 217. Blagojevic, M., Jinks, C., Jeffery, A. & Jordan, K. P. Risk factors for onset of osteoarthritis of the knee in older adults: a systematic review and meta-analysis. *Osteoarthr. Cartil*. **18**, 24–33 (2010).
 218. Cheng, Y. *et al.* Physical activity and self-reported, physician-diagnosed osteoarthritis: Is physical activity a risk factor? *J. Clin. Epidemiol*. **53**, 315–322 (2000).
 219. Reyes, C. *et al.* Association between overweight and obesity and risk of clinically diagnosed knee, hip, and hand osteoarthritis: A population-based cohort study. *Arthritis Rheumatol*. **68**, n/a-n/a (2016).
 220. Niu, J. *et al.* Is obesity a risk factor for progressive radiographic knee osteoarthritis? *Arthritis Care Res*. **61**, 329–335 (2009).
 221. Grotle, M., Hagen, K. B., Natvig, B., Dahl, F. a & Kvien, T. K. Obesity and osteoarthritis in knee, hip and/or hand: an epidemiological study in the general population with 10 years follow-up. *BMC Musculoskelet. Disord*. **9**, 132 (2008).
 222. Fujisawa, T. *et al.* Cyclic mechanical stress induces extracellular matrix degradation in cultured chondrocytes via gene expression of matrix metalloproteinases and interleukin-1. *J Biochem* **125**, 966–975 (1999).
 223. Thijssen, E., van Caam, A. & van der Kraan, P. M. Obesity and osteoarthritis, more than just wear and tear: pivotal roles for inflamed adipose tissue and dyslipidaemia in obesity-induced osteoarthritis. *Rheumatology (Oxford)*. **54**, 588–600 (2015).
 224. Carman, W. J., Sowers, M., Hawthorne, V. M. & Weissfeld, L. A. Obesity as a Risk Factor for Osteoarthritis of the Hand and Wrist: A Prospective Study. *Am. J. Epidemiol*. **139**, 119–129 (1994).
 225. Gudbergsen, H. *et al.* Weight loss is effective for symptomatic relief in obese subjects with knee osteoarthritis independently of joint damage severity assessed by high-field MRI and radiography. *Osteoarthr. Cartil*. **20**, 495–502 (2012).
 226. Ding, C. Metabolic triggered inflammation in osteoarthritis. *Semin. Arthritis Rheum*. **41**, 90–91 (2011).
 227. Zhuo, Q., Yang, W., Chen, J. & Wang, Y. Metabolic syndrome meets osteoarthritis. *Nat. Rev. Rheumatol*. **8**, 729–737 (2012).
 228. Pereira, S. S. & Alvarez-Leite, J. I. Low-Grade Inflammation, Obesity, and Diabetes. *Curr. Obes. Rep*. **3**, 422–431 (2014).
 229. Dumond, H. *et al.* Evidence for a Key Role of Leptin in Osteoarthritis. *Arthritis Rheum*. **48**, 3118–3129 (2003).
 230. Iliopoulos, D., Malizos, K. N. & Tsezou, A. Epigenetic regulation of leptin affects MMP-13 expression in osteoarthritic chondrocytes: possible molecular target for osteoarthritis therapeutic intervention. *Ann. Rheum. Dis*. **66**, 1616–21 (2007).

231. Otero, M., Gomez Reino, J. J. & Gualillo, O. Synergistic induction of nitric oxide synthase type II: In vitro effect of leptin and interferon- γ in human chondrocytes and ATDC5 chondrogenic cells. *Arthritis Rheum.* **48**, 404–409 (2003).
232. Liang, M. H. & Fortin, P. Management of osteoarthritis of the hip and knee. *N. Engl. J. Med.* **325**, 125–7 (1991).
233. Superio-Cabuslay, E., Ward, M. M. & Lorig, K. R. Patient education interventions in osteoarthritis and rheumatoid arthritis: A meta-analytic comparison with nonsteroidal antiinflammatory drug treatment. *Arthritis Care Res. (Hoboken)*. **9**, 292–301 (1996).
234. Bellamy, N. *et al.* Intraarticular corticosteroid for treatment of osteoarthritis of the knee. *Cochrane database Syst. Rev.* CD005328 (2006).
doi:10.1002/14651858.CD005328.pub2
235. Kruse, D. W. Intraarticular cortisone injection for osteoarthritis of the hip. Is it effective? Is it safe? *Curr. Rev. Musculoskelet. Med.* **1**, 227–33 (2008).
236. McAlindon, T. E. *et al.* OARSI Guidelines for the Non-Surgical Management of Knee Osteoarthritis. *Osteoarthritis Cartilage* 1–25 (2014).
doi:10.1016/j.joca.2014.01.003
237. Maquet, P. Valgus osteotomy for osteoarthritis of the knee. *Clin. Orthop. Relat. Res.* 143–8 (1976).
238. Hernigou, P., Medevielle, D., Debeyre, J. & Goutallier, D. Proximal tibial osteotomy for osteoarthritis with varus deformity. Aten to thirteen-year follow-up study. *J. Bone Jt. Surg.* **69**, 332–354 (1987).
239. Gibson, J. N., White, M. D., Chapman, V. M. & Strachan, R. K. Arthroscopic lavage and debridement for osteoarthritis of the knee. *J. Bone Joint Surg. Br.* **74**, 534–7 (1992).
240. Robert, H. Chondral repair of the knee joint using mosaicplasty. *Orthop. Traumatol. Surg. Res.* **97**, 418–29 (2011).
241. Stover, M. D., Beaulé, P. E., Matta, J. M. & Mast, J. W. Hip arthrodesis: a procedure for the new millennium? *Clin. Orthop. Relat. Res.* 126–33 (2004).
242. Takakura, Y., Tanaka, Y., Sugimoto, K., Akiyama, K. & Tamai, S. Long-term results of arthrodesis for osteoarthritis of the ankle. *Clin. Orthop. Relat. Res.* 178–85 (1999).
243. Moskowitz, R. W., Altman, R. D., Hochberg, M. C., Buckwalter, J. A. & GoldberG, V. M. *Osteoarthritis: Diagnosis and Medical/Surgical Management*. (Lippincott Williams & Wilkins, 2007).
244. Langer, R. & Vacanti, J. P. Tissue engineering. *Science* **260**, 920–6 (1993).
245. Kim, B.-S., Baez, C. E. & Atala, A. Biomaterials for tissue engineering. *World J. Urol.* **18**, 2–9 (2000).
246. Hubbell, J. A. Biomaterials in Tissue Engineering. *Bio/Technology* **13**, 565–576 (1995).
247. Shin, H., Jo, S. & Mikos, A. G. Biomimetic materials for tissue engineering.

- Biomaterials* **24**, 4353–4364 (2003).
248. Falanga, V. & Sabolinski, M. A bilayered living skin construct (APLIGRAF®) accelerates complete closure of hard-to-heal venous ulcers. *Wound Repair Regen.* **7**, 201–207 (1999).
 249. Supp, D. M. & Boyce, S. T. Engineered skin substitutes: practices and potentials. *Clin. Dermatol.* **23**, 403–12 (2005).
 250. Sherwin, A., Langer, R. & Sc, D. Progress in the Tissue Engineering and Stem Cell Industry ““ Are we there yet ?”” *Tissue Eng. Part B. Rev.* **18**, (2012).
 251. Grande, D. A., Pitman, M. I., Peterson, L., Menche, D. & Klein, M. The repair of experimentally produced defects in rabbit articular cartilage by autologous chondrocyte transplantation. *J. Orthop. Res.* **7**, 208–18 (1989).
 252. Peterson, L. *et al.* Two-to-9-year outcome after autologous chondrocyte transplantation of the knee. *Clin. Orthop. Relat. Res.* 212–34 (2000).
 253. Wright, K. T. *et al.* Characterization of the cells in repair tissue following autologous chondrocyte implantation in mankind: a novel report of two cases. *Regen. Med.* **8**, 699–709 (2013).
 254. Minas, T. Autologous chondrocyte implantation for focal chondral defects of the knee. *Clin. Orthop. Relat. Res.* S349-61 (2001).
 255. National Institute for Health and Clinical Excellence. *Technology Appraisal 89: The use of autologous chondrocyte implantation for the treatment of cartilage defects in knee joints.* (2008).
 256. Strand, V. & Kelman, A. Outcome measures in osteoarthritis: randomized controlled trials. *Curr. Rheumatol. Rep.* **6**, 20–30 (2004).
 257. Bellamy, N. *et al.* Recommendations for a core set of outcome measures for future phase III clinical trials in knee, hip, and hand osteoarthritis. Consensus development at OMERACT III. *J. Rheumatol.* **24**, 799–802 (1997).
 258. Erggelet, C., Steinwachs, M. R. & Reichelt, A. The operative treatment of full thickness cartilage defects in the knee joint with autologous chondrocyte transplantation. *Saudi Med. J.* **21**, 715–21 (2000).
 259. Micheli, L. J. *et al.* Autologous chondrocyte implantation of the knee: multicenter experience and minimum 3-year follow-up. *Clin. J. Sport Med.* **11**, 223–8 (2001).
 260. Knutsen, G. *et al.* Autologous Chondrocyte Implantation Compared with Microfracture in the Knee: A Randomized Trial. *J. Bone Jt. Surg.* **86**, 455–464 (2004).
 261. Knutsen, G. *et al.* A randomized trial comparing autologous chondrocyte implantation with microfracture. Findings at five years. *J. Bone Joint Surg. Am.* **89**, 2105–12 (2007).
 262. Roberts, S. *et al.* Autologous chondrocyte implantation for cartilage repair : monitoring its success by magnetic resonance imaging and histology. *Arthritis Res. Ther.* **5**, 60–73 (2002).
 263. Sharma, A., Wood, L. D., Richardson, J. B., Roberts, S. & Kuiper, N. J.

- Glycosaminoglycan profiles of repair tissue formed following autologous chondrocyte implantation differ from control cartilage. *Arthritis Res. Ther.* **9**, R79 (2007).
264. Roberts, S., Hollander, A. P., Caterson, B., Menage, J. & Richardson, J. B. Matrix Turnover in Human Cartilage Repair Tissue in Autologous Chondrocyte Implantation. *Arthritis Rheum.* **44**, 2586–2598 (2001).
 265. Harris, J. D. *et al.* Failures, re-operations, and complications after autologous chondrocyte implantation - a systematic review. *Osteoarthritis Cartilage* **19**, 779–91 (2011).
 266. Nejadnik, H., Hui, J. H., Feng Choong, E. P., Tai, B.-C. & Lee, E. H. Autologous bone marrow-derived mesenchymal stem cells versus autologous chondrocyte implantation: an observational cohort study. *Am. J. Sports Med.* **38**, 1110–6 (2010).
 267. Kreuz, P. C. *et al.* Influence of sex on the outcome of autologous chondrocyte implantation in chondral defects of the knee. *Am. J. Sports Med.* **41**, 1541–8 (2013).
 268. Niemeyer, P., Salzmänn, G. M., Hirschmüller, A. & Südkamp, N. P. Factors that influence clinical outcome following autologous chondrocyte implantation for cartilage defects of the knee. *Z. Orthop. Unfall.* **150**, 83–8 (2012).
 269. Niemeyer, P., Pestka, J. M., Salzmänn, G. M., Südkamp, N. P. & Schmal, H. Influence of cell quality on clinical outcome after autologous chondrocyte implantation. *Am. J. Sports Med.* **40**, 556–61 (2012).
 270. Pestka, J. M. *et al.* In vitro cell quality of articular chondrocytes assigned for autologous implantation in dependence of specific patient characteristics. *Arch. Orthop. Trauma Surg.* **131**, 779–89 (2011).
 271. <http://www.geistlich-surgery.com/chondro-gide.html>.
 272. <http://hyalofast.anikatherapeutics.com/en/>.
 273. <http://www.biotissue.de/en-ProductsPatients.html>.
 274. Friedenstein, A. J. *et al.* Precursors for fibroblasts in different populations of hematopoietic cells as detected by the in vitro colony assay method. *Exp. Hematol.* **2**, 83–92 (1974).
 275. Friedenstein, A. J., Chailakhyan, R. K. & Gerasimov, U. V. Bone marrow osteogenic stem cells: in vitro cultivation and transplantation in diffusion chambers. *Cell Tissue Kinet.* **20**, 263–72 (1987).
 276. Friedenstein, A. J., Petrakova, K. V., Kurolesova, A. I. & Frolova, G. P. Heterotopic of bone marrow. Analysis of precursor cells for osteogenic and hematopoietic tissues. *Transplantation* **6**, 230–47 (1968).
 277. Chen, S. *et al.* Effect on left ventricular function of intracoronary transplantation of autologous bone marrow mesenchymal stem cell in patients with acute myocardial infarction. *Am. J. Cardiol.* **94**, 92–5 (2004).
 278. Bang, O. Y., Lee, J. S., Lee, P. H. & Lee, G. Autologous mesenchymal stem cell transplantation in stroke patients. *Ann. Neurol.* **57**, 874–82 (2005).
 279. Le Blanc, K. *et al.* Treatment of severe acute graft-versus-host disease with third

- party haploidentical mesenchymal stem cells. *Lancet* **363**, 1439–41 (2004).
280. Dominici, M. *et al.* Minimal criteria for defining multipotent mesenchymal stromal cells. The International Society for Cellular Therapy position statement. *Cytotherapy* **8**, 315–7 (2006).
 281. Johnstone, B., Hering, T. M., Caplan, A. I., Goldberg, V. M. & Yoo, J. U. In vitro chondrogenesis of bone marrow-derived mesenchymal progenitor cells. *Exp. Cell Res.* **238**, 265–72 (1998).
 282. Wright, K. T., El Masri, W., Osman, A., Chowdhury, J. & Johnson, W. E. B. Concise review: Bone marrow for the treatment of spinal cord injury: mechanisms and clinical applications. *Stem Cells* **29**, 169–78 (2011).
 283. Krampera, M., Galipeau, J., Shi, Y., Tarte, K. & Sensebe, L. Immunological characterization of multipotent mesenchymal stromal cells--The International Society for Cellular Therapy (ISCT) working proposal. *Cytotherapy* **15**, 1054–1061 (2013).
 284. Bartholomew, A. *et al.* Mesenchymal stem cells suppress lymphocyte proliferation in vitro and prolong skin graft survival in vivo. *Exp. Hematol.* **30**, 42–8 (2002).
 285. Di Nicola, M. *et al.* Human bone marrow stromal cells suppress T-lymphocyte proliferation induced by cellular or nonspecific mitogenic stimuli. *Blood* **99**, 3838–3843 (2002).
 286. Aggarwal, S. & Pittenger, M. F. Human mesenchymal stem cells modulate allogeneic immune cell responses. *Blood* **105**, 1815–22 (2005).
 287. Maggini, J. *et al.* Mouse Bone Marrow-Derived Mesenchymal Stromal Cells Turn Activated Macrophages into a Regulatory-Like Profile. *PLoS One* **5**, e9252 (2010).
 288. Kim, J. & Hematti, P. Mesenchymal stem cell-educated macrophages: A novel type of alternatively activated macrophages. *Exp. Hematol.* **37**, 1445–1453 (2009).
 289. Luz-Crawford, P. *et al.* Mesenchymal stem cell-derived IL1RA promotes macrophage polarization and inhibits B cell differentiation. *Stem Cells* **34**, 483–492 (2016).
 290. Le Blanc, K. *et al.* Mesenchymal stem cells for treatment of steroid-resistant, severe, acute graft-versus-host disease: a phase II study. *Lancet* **371**, 1579–86 (2008).
 291. Liu-Bryan, R. Synovium and the innate inflammatory network in osteoarthritis progression. *Curr. Rheumatol. Rep.* **15**, 323 (2013).
 292. Niemeyer, P. *et al.* Comparison of Immunological Properties of Bone Marrow Stromal Cells and Adipose Tissue-Derived Stem Cells Before and After Osteogenic Differentiation *In Vitro*. *Tissue Eng.* **13**, 111–121 (2007).
 293. James, S. *et al.* Multiparameter Analysis of Human Bone Marrow Stromal Cells Identifies Distinct Immunomodulatory and Differentiation-Competent Subtypes. *Stem Cell Reports* **4**, 1004–1015 (2015).
 294. Ryan, A. E. *et al.* Chondrogenic Differentiation Increases Antidonor Immune Response to Allogeneic Mesenchymal Stem Cell Transplantation. *Mol. Ther.* **22**, 655–667 (2013).

295. Lohan, P. *et al.* Changes in immunological profile of allogeneic mesenchymal stem cells after differentiation: should we be concerned? *Stem Cell Res. Ther.* **5**, 99 (2014).
296. Wakitani, S. *et al.* Mesenchymal cell-based repair of large, full-thickness defects of articular cartilage. *J. Bone Jt. Surg.* **76**, 579–592 (1994).
297. Gigante, A. *et al.* Use of collagen scaffold and autologous bone marrow concentrate as a one-step cartilage repair in the knee: histological results of second-look biopsies at 1 year follow-up. *Int. J. Immunopathol. Pharmacol.* **24**, 69–72 (2011).
298. Wakitani, S. *et al.* Autologous Bone Marrow Stromal Cell Transplantation for Repair of Full-Thickness Articular Cartilage Defects in Human Patellae: Two Case Reports. *Cell Transplant.* **13**, 595–600 (2004).
299. Haleem, A. M. *et al.* The Clinical Use of Human Culture-Expanded Autologous Bone Marrow Mesenchymal Stem Cells Transplanted on Platelet-Rich Fibrin Glue in the Treatment of Articular Cartilage Defects: A Pilot Study and Preliminary Results. *Cartilage* **1**, 253–261 (2010).
300. Koh, Y. G., Choi, Y. J., Kwon, O. R. & Kim, Y. S. Second-Look Arthroscopic Evaluation of Cartilage Lesions After Mesenchymal Stem Cell Implantation in Osteoarthritic Knees. *Am. J. Sports Med.* **42**, 1628–1637 (2014).
301. Kretlow, J. D. *et al.* Donor age and cell passage affects differentiation potential of murine bone marrow-derived stem cells. *BMC Cell Biol.* **9**, 60 (2008).
302. Mareschi, K. *et al.* Expansion of mesenchymal stem cells isolated from pediatric and adult donor bone marrow. *J. Cell. Biochem.* **97**, 744–754 (2006).
303. Stenderup, K., Justesen, J., Clausen, C. & Kassem, M. Aging is associated with decreased maximal life span and accelerated senescence of bone marrow stromal cells. *Bone* **33**, 919–26 (2003).
304. Zuk, P. A. *et al.* Human adipose tissue is a source of multipotent stem cells. *Mol. Biol. Cell* **13**, 4279–95 (2002).
305. De Francesco, F., Ricci, G., D’Andrea, F., Nicoletti, G. F. & Ferraro, G. A. Human Adipose Stem Cells: From Bench to Bedside. *Tissue Eng. Part B. Rev.* **21**, 572–84 (2015).
306. Ruetze, M. & Richter, W. Adipose-derived stromal cells for osteoarticular repair: trophic function versus stem cell activity. *Expert Rev Mol Med* **16**, e9 (2014).
307. Lee, R. H. *et al.* Characterization and expression analysis of mesenchymal stem cells from human bone marrow and adipose tissue. *Cell. Physiol. Biochem.* **14**, 311–24 (2004).
308. Izadpanah, R. *et al.* Biologic properties of mesenchymal stem cells derived from bone marrow and adipose tissue. *J. Cell. Biochem.* **99**, 1285–97 (2006).
309. Puissant, B. *et al.* Immunomodulatory effect of human adipose tissue-derived adult stem cells: comparison with bone marrow mesenchymal stem cells. *Br. J. Haematol.* **129**, 118–29 (2005).
310. English, A. *et al.* A comparative assessment of cartilage and joint fat pad as a

- potential source of cells for autologous therapy development in knee osteoarthritis. *Rheumatology (Oxford)*. **46**, 1676–1683 (2007).
311. Dragoo, J. L. *et al.* Tissue-engineered cartilage and bone using stem cells from human infrapatellar fat pads. *J Bone Jt. Surg Br* **85–B**, 740–747 (2003).
 312. Jurgens, W. J. F. M. *et al.* Freshly isolated stromal cells from the infrapatellar fat pad are suitable for a one-step surgical procedure to regenerate cartilage tissue. *Cytotherapy* **11**, 1052–64 (2009).
 313. Pers, Y.-M. *et al.* Adipose Mesenchymal Stromal Cell-Based Therapy for Severe Osteoarthritis of the Knee: A Phase I Dose-Escalation Trial. *Stem Cells Transl. Med.* **5**, 847–56 (2016).
 314. De Bari, C., Dell’Accio, F., Tylzanowski, P. & Luyten, F. P. Multipotent mesenchymal stem cells from adult human synovial membrane. *Arthritis Rheum.* **44**, 1928–42 (2001).
 315. Jones, E. A. *et al.* Enumeration and phenotypic characterization of synovial fluid multipotential mesenchymal progenitor cells in inflammatory and degenerative arthritis. *Arthritis Rheum.* **50**, 817–827 (2004).
 316. Sun, Y., Zheng, Y., Liu, W., Zheng, Y. & Zhang, Z. Synovium fragment-derived cells exhibit characteristics similar to those of dissociated multipotent cells in synovial fluid of the temporomandibular joint. *PLoS One* **9**, e101896 (2014).
 317. Ju, Y.-J., Muneta, T., Yoshimura, H., Koga, H. & Sekiya, I. Synovial mesenchymal stem cells accelerate early remodeling of tendon-bone healing. *Cell Tissue Res.* **332**, 469–78 (2008).
 318. Morito, T. *et al.* Synovial fluid-derived mesenchymal stem cells increase after intra-articular ligament injury in humans. *Rheumatology (Oxford)*. **47**, 1137–43 (2008).
 319. Baboolal, T. G. *et al.* Synovial fluid hyaluronan mediates MSC attachment to cartilage, a potential novel mechanism contributing to cartilage repair in osteoarthritis using knee joint distraction. *Ann Rheum Dis* **75**, 908–915 (2016).
 320. Gullo, F. & Bari, C. De. Prospective purification of a subpopulation of human synovial mesenchymal stem cel014 ls with enhanced chondro-osteogenic potency. *Rheumatology* **53**, 1758–1768 (2013).
 321. Thomson, J. a. Embryonic Stem Cell Lines Derived from Human Blastocysts. *Science (80-.)*. **282**, 1145–1147 (1998).
 322. Martin, G. R. Isolation of a pluripotent cell line from early mouse embryos cultured in medium conditioned by teratocarcinoma stem cells Developmental Biology. *Proc. Natl. Acad. Sci.* **78**, 7634–7638 (1981).
 323. Cheng, A. *et al.* Cartilage repair using human embryonic stem cell-derived chondroprogenitors. *Stem Cells Transl. Med.* **3**, 1287–94 (2014).
 324. Oldershaw, R. A. *et al.* Directed differentiation of human embryonic stem cells toward chondrocytes. *Nat. Biotechnol.* **28**, 1187–94 (2010).
 325. Cheng, A., Hardingham, T. E. & Kimber, S. J. Generating Cartilage Repair from Pluripotent Stem Cells. *Tissue Eng. Part B* **0**, 1–28 (2013).

326. Takahashi, K. & Yamanaka, S. Induction of pluripotent stem cells from mouse embryonic and adult fibroblast cultures by defined factors. *Cell* **126**, 663–676 (2006).
327. Kim, M.-J. *et al.* Generation of human induced pluripotent stem cells from osteoarthritis patient-derived synovial cells. *Arthritis Rheum. Rheum.* **63**, 3010–21 (2011).
328. Tsuchiya, K., Chen, G., Ushida, T., Matsuno, T. & Tateishi, T. The effect of coculture of chondrocytes with mesenchymal stem cells on their cartilaginous phenotype in vitro. *Mater. Sci. Eng. C* **24**, 391–396 (2004).
329. Fischer, J., Dickhut, a, Rickert, M. & Richter, W. Human articular chondrocytes secrete parathyroid hormone-related protein and inhibit hypertrophy of mesenchymal stem cells in coculture during chondrogenesis. *Arthritis Rheum.* **62**, 2696–706 (2010).
330. Zuo, Q. *et al.* Co-cultivated mesenchymal stem cells support chondrocytic differentiation of articular chondrocytes. *Int. Orthop.* **37**, 747–52 (2013).
331. Yang, Y.-H., Lee, A. J. & Barabino, G. A. Coculture-driven mesenchymal stem cell-differentiated articular chondrocyte-like cells support neocartilage development. *Stem Cells Transl. Med.* **1**, 843–54 (2012).
332. Maumus, M. *et al.* Adipose mesenchymal stem cells protect chondrocytes from degeneration associated with osteoarthritis. *Stem Cell Res.* **11**, 834–844 (2013).
333. Hildner, F. *et al.* Human Adipose-Derived Stem Cells Contribute to Chondrogenesis in Coculture with Human Articular Chondrocytes. *Tissue Eng. Part A* **15**, 3961–3969 (2009).
334. Wu, L., Prins, H.-J., Helder, M. N., van Blitterswijk, C. A. & Karperien, M. Trophic Effects of Mesenchymal Stem Cells in Chondrocyte Co-Cultures are Independent of Culture Conditions and Cell Sources. *Tissue Eng. Part A* **18**, 1542–1551 (2012).
335. TS, de W. *et al.* Allogeneic Mesenchymal Stem Cells Stimulate Cartilage Regeneration and Are Safe for Single-Stage Cartilage Repair in Humans upon Mixture with Recycled Autologous Chondrons. *Stem Cells* (2016).
336. Zhou, S., Cui, Z. & Urban, J. P. G. Factors influencing the oxygen concentration gradient from the synovial surface of articular cartilage to the cartilage-bone interface: a modeling study. *Arthritis Rheum.* **50**, 3915–24 (2004).
337. Gibson, J. S., Milner, P. I., White, R., Fairfax, T. P. a & Wilkins, R. J. Oxygen and reactive oxygen species in articular cartilage: modulators of ionic homeostasis. *Pflugers Arch.* **455**, 563–73 (2008).
338. Brighton, C. T. & Heppenstall, R. B. Oxygen tension in zones of the epiphyseal plate, the metaphysis and diaphysis. An in vitro and in vivo study in rats and rabbits. *J. Bone Joint Surg. Am.* **53**, 719–28 (1971).
339. Grayson, W. L., Zhao, F., Bunnell, B. & Ma, T. Hypoxia enhances proliferation and tissue formation of human mesenchymal stem cells. *Biochem. Biophys. Res. Commun.* **358**, 948–53 (2007).
340. Basciano, L. *et al.* Long term culture of mesenchymal stem cells in hypoxia

- promotes a genetic program maintaining their undifferentiated and multipotent status. *BMC Cell Biol.* **12**, 12 (2011).
341. Markway, B. D., Cho, H. & Johnstone, B. Hypoxia promotes redifferentiation and suppresses markers of hypertrophy and degeneration in both healthy and osteoarthritic chondrocytes. *Arthritis Res. Ther.* **15**, R92 (2013).
 342. Schrobback, K. *et al.* Effects of oxygen and culture system on in vitro propagation and redifferentiation of osteoarthritic human articular chondrocytes. *Cell Tissue Res.* **347**, 649–63 (2012).
 343. Meretoja, V. V., Dahlin, R. L., Kasper, F. K. & Mikos, A. G. Enhanced chondrogenesis in co-cultures with articular chondrocytes and mesenchymal stem cells. *Biomaterials* **33**, 6362–6369 (2012).
 344. Roberts, S. *et al.* ADAMTS-4 activity in synovial fluid as a biomarker of inflammation and effusion. *Osteoarthr. Cartil.* **23**, 1622–1626 (2015).
 345. Drexler, H. G. & Uphoff, C. C. Mycoplasma contamination of cell cultures: Incidence, sources, effects, detection, elimination, prevention. *Cytotechnology* **39**, 75–90 (2002).
 346. Jaiswal, N., Haynesworth, S. E., Caplan, A. I. & Bruder, S. P. Osteogenic differentiation of purified, culture-expanded human mesenchymal stem cells in vitro. *J. Cell. Biochem.* **64**, 295–312 (1997).
 347. Pittenger, M. F. *et al.* Multilineage potential of adult human mesenchymal stem cells. *Science* **284**, 143–7 (1999).
 348. Roberts, S. & Menage, J. in *Biopolymer Methods in Tissue Engineering* (eds. Hollander, A. P. & Hatton, P.) 185 (Humana Press, 2004).
 349. Grogan, S. P. *et al.* Visual histological grading system for the evaluation of in vitro-generated neocartilage. *Tissue Eng.* **12**, 2141–9 (2006).
 350. Farndale, R. W., Sayers, C. A. & Barrett, A. J. A direct spectrophotometric microassay for sulfated glycosaminoglycans in cartilage cultures. *Connect. Tissue Res.* **9**, 247–8 (1982).
 351. Farndale, R. W., Buttle, D. J. & Barrett, A. J. Improved quantitation and discrimination of sulphated glycosaminoglycans by use of dimethylmethylene blue. *Biochim. Biophys. Acta* **883**, 173–7 (1986).
 352. Bourin, P. *et al.* Stromal cells from the adipose tissue-derived stromal vascular fraction and culture expanded adipose tissue-derived stromal/stem cells: A joint statement of the International Federation for Adipose Therapeutics and Science (IFATS) and the International So. *Cytotherapy* **15**, 641–648 (2013).
 353. Grogan, S. P. *et al.* Identification of markers to characterize and sort human articular chondrocytes with enhanced in vitro chondrogenic capacity. *Arthritis Rheum.* **56**, 586–95 (2007).
 354. Pretzel, D. *et al.* Relative percentage and zonal distribution of mesenchymal progenitor cells in human osteoarthritic and normal cartilage. *Arthritis Res. Ther.* **13**, R64 (2011).

355. Chang, C. B. *et al.* Chondrogenic potentials of human synovium-derived cells sorted by specific surface markers. *Osteoarthritis Cartilage* **21**, 190–9 (2013).
356. DeChiara, T. M. *et al.* Ror2, encoding a receptor-like tyrosine kinase, is required for cartilage and growth plate development. *Nat. Genet.* **24**, 271–274 (2000).
357. Arufe, M. C., De la Fuente, a, Fuentes, I., de Toro, F. J. & Blanco, F. J. Chondrogenic potential of subpopulations of cells expressing mesenchymal stem cell markers derived from human synovial membranes. *J. Cell. Biochem.* **111**, 834–45 (2010).
358. Battula, V. L. *et al.* Isolation of functionally distinct mesenchymal stem cell subsets using antibodies against CD56, CD271, and mesenchymal stem cell antigen-1. *Haematologica* **94**, 173–184 (2009).
359. Yang, Z. X. *et al.* CD106 Identifies a Subpopulation of Mesenchymal Stem Cells with Unique Immunomodulatory Properties. *PLoS One* **8**, 1–12 (2013).
360. Le Gal, F. a *et al.* HLA-G-mediated inhibition of antigen-specific cytotoxic T lymphocytes. *Int Immunol* **11**, 1351–1356 (1999).
361. Nasef, A. *et al.* Immunosuppressive effects of mesenchymal stem cells: involvement of HLA-G. *Transplantation* **84**, 231–237 (2007).
362. Luyten, F., De Bari, C. & Dell’Accio, F. Marker genes for use in the identification of chondrocyte phenotypic stability and in the screening of factors influencing cartilage production. (2008).
363. Schnabel, M. *et al.* Dedifferentiation-associated changes in morphology and gene expression in primary human articular chondrocytes in cell culture. *Osteoarthr. Cartil.* **10**, 62–70 (2002).
364. Enomoto-Iwamoto, M. *et al.* The Wnt antagonist Frzb-1 regulates chondrocyte maturation and long bone development during limb skeletogenesis. *Dev. Biol.* **251**, 142–156 (2002).
365. Dell’Accio, F., De Bari, C. & Luyten, F. P. Molecular markers predictive of the capacity of expanded human articular chondrocytes to form stable cartilage in vivo. *Arthritis Rheum.* **44**, 1608–1619 (2001).
366. Zheng, Q. *et al.* Type X collagen gene regulation by Runx2 contributes directly to its hypertrophic chondrocyte-specific expression in vivo. *J. Cell Biol.* **162**, 833–842 (2003).
367. Li, X., Yang, Q., Bai, J., Xuan, Y. & Wang, Y. Identification of appropriate reference genes for human mesenchymal stem cell analysis by quantitative real-time PCR. *Biotechnol. Lett.* 67–73 (2014). doi:10.1007/s10529-014-1652-9
368. Livak, K. J. & Schmittgen, T. D. Analysis of relative gene expression data using real-time quantitative PCR and the $2^{-(\Delta\Delta CT)}$ method. *Methods* **25**, 402–408 (2001).
369. Schmittgen, T. D. & Livak, K. J. Analyzing real-time PCR data by the comparative CT method. *Nat. Protoc.* **3**, 1101–1108 (2008).
370. Holness, C. L. & Simmons, D. L. Molecular cloning of CD68, a human macrophage

- marker related to lysosomal glycoproteins. *Blood* **81**, 1607–13 (1993).
371. Engel, B. P. *et al.* The B7-2 (B70) Costimulatory Molecule Expressed by Monocytes and Activated B Lymphocytes Is the CD86 Differentiation Antigen. *Blood* **84**, 1402–1407 (1994).
 372. Corbi, A. L., Miller, L. J., O'Connor, K., Larson, R. S. & Springer, T. A. cDNA cloning and complete primary structure of the α subunit of a leukocyte adhesion glycoprotein, p150,95. *EMBO J.* **6**, 4023–4028 (1987).
 373. East, L. & Isacke, C. M. The mannose receptor family. *Biochim. Biophys. Acta - Gen. Subj.* **1572**, 364–386 (2002).
 374. Chang, C. I., Liao, J. C. & Kuo, L. Arginase modulates nitric oxide production in activated macrophages. *Am. J. Physiol.* **274**, H342–H348 (1998).
 375. Simmons, D. L., Tan, S., Tenen, D. G., Nicholson-Weller, A. & Seed, B. Monocyte antigen CD14 is a phospholipid anchored membrane protein. *Blood* **73**, 284–289 (1989).
 376. Rugtveit, J., Bakka, A. & Brandtzaeg, P. Differential distribution of B7.1 (CD80) and B7.2 (CD86) costimulatory molecules on mucosal macrophage subsets in human inflammatory bowel disease (IBD). *Clin. Exp. Immunol.* **110**, 104–113 (1997).
 377. Sulahian, T. H. *et al.* Human monocytes express CD163, which is upregulated by IL-10 and identical to p155. *Cytokine* **12**, 1312–1321 (2000).
 378. Fabriek, B. O., Dijkstra, C. D. & van den Berg, T. K. The macrophage scavenger receptor CD163. *Immunobiology* **210**, 153–160 (2005).
 379. Galarraga, M. *et al.* Adiposoft: automated software for the analysis of white adipose tissue cellularity in histological sections. *J. Lipid Res.* **53**, 2791–6 (2012).
 380. Aksu, A. E., Rubin, J. P., Dudas, J. R. & Marra, K. G. Role of gender and anatomical region on induction of osteogenic differentiation of human adipose-derived stem cells. *Ann. Plast. Surg.* **60**, 306–322 (2008).
 381. Payne, K. A., Didiano, D. M. & Chu, C. R. Donor sex and age influence the chondrogenic potential of human femoral bone marrow stem cells. *Osteoarthritis Cartilage* **18**, 705–713 (2010).
 382. Choudhery, M. S., Badowski, M., Muise, A., Pierce, J. & Harris, D. T. Donor age negatively impacts adipose tissue-derived mesenchymal stem cell expansion and differentiation. *J. Transl. Med.* **12**, 8 (2014).
 383. Krampera, M. *et al.* Role for interferon-gamma in the immunomodulatory activity of human bone marrow mesenchymal stem cells. *Stem Cells* **24**, 386–398 (2006).
 384. Hunt, J. S., Petroff, M. G., McIntire, R. H. & Ober, C. HLA-G and immune tolerance in pregnancy. *FASEB J.* **19**, 681–93 (2005).
 385. Le Blanc, K., Tammik, C., Rosendahl, K., Zetterberg, E. & Ringdén, O. HLA expression and immunologic properties of differentiated and undifferentiated mesenchymal stem cells. *Exp. Hematol.* **31**, 890–896 (2003).
 386. Li, X. C., Rothstein, D. M. & Sayegh, M. H. Costimulatory pathways in transplantation: challenges and new developments. *Immunol. Rev.* **229**, 271–293

- (2009).
387. Deuse, T. *et al.* Immunogenicity and immunomodulatory properties of umbilical cord lining mesenchymal stem cells. *Cell Transplant.* **20**, 655–667 (2011).
 388. Jones, E. A. *et al.* Synovial fluid mesenchymal stem cells in health and early osteoarthritis: detection and functional evaluation at the single-cell level. *Arthritis Rheum.* **58**, 1731–1740 (2008).
 389. Twisk, J. W. R. *Applied multilevel analysis :A Practical Guide for Medical Researchers.* (Cambridge University Press, 2006).
 390. Nigrovic, P. A. & Lee, D. M. Mast cells in inflammatory arthritis. *Arthritis Res. Ther.* **7**, 1–11 (2005).
 391. Nakamura, H., Yoshino, S., Kato, T., Tsuruha, J. & Nishioka, K. T-cell mediated inflammatory pathway in osteoarthritis. *Osteoarthr. Cartil.* **7**, 401–402 (1999).
 392. Banfi, A. *et al.* Proliferation kinetics and differentiation potential of ex vivo expanded human bone marrow stromal cells: Implications for their use in cell therapy. *Exp. Hematol.* **28**, 707–715 (2000).
 393. Wall, M. E., Bernacki, S. H. & Lobo, E. G. Effects of serial passaging on the adipogenic and osteogenic differentiation potential of adipose-derived human mesenchymal stem cells. *Tissue Eng.* **13**, 1291–1298 (2007).
 394. Muraglia, A., Cancedda, R. & Quarto, R. Clonal mesenchymal progenitors from human bone marrow differentiate in vitro according to a hierarchical model. *J. Cell Sci.* **113**, 1161–1166 (2000).
 395. Lee, D. H. *et al.* Synovial fluid CD34 - CD44 + CD90 + mesenchymal stem cell levels are associated with the severity of primary knee osteoarthritis. *Osteoarthr. Cartil.* **20**, 106–109 (2012).
 396. Pilz, G. *et al.* Human mesenchymal stromal cells express CD14 cross-reactive epitopes. *Cytometry. A* **79**, 635–645 (2011).
 397. Klein-Wieringa, I. R. *et al.* The infrapatellar fat pad of patients with osteoarthritis has an inflammatory phenotype. *Ann. Rheum. Dis.* **70**, 851–857 (2011).
 398. Van Landuyt, K. B., Jones, E. a, McGonagle, D., Luyten, F. P. & Lories, R. J. Flow cytometric characterization of freshly isolated and culture expanded human synovial cell populations in patients with chronic arthritis. *Arthritis Res. Ther.* **12**, R15 (2010).
 399. Bas, S., Gauthier, B. R., Spenato, U., Stingelin, S. & Gabay, C. CD14 is an acute-phase protein. *J. Immunol.* **172**, 4470–4479 (2004).
 400. Bondeson, J., Wainwright, S. D., Lauder, S., Amos, N. & Hughes, C. E. The role of synovial macrophages and macrophage-produced cytokines in driving aggrecanases, matrix metalloproteinases, and other destructive and inflammatory responses in osteoarthritis. *Arthritis Res. Ther.* **8**, R187 (2006).
 401. Daghestani, H. N., Pieper, C. F. & Kraus, V. B. Soluble macrophage biomarkers indicate inflammatory phenotypes in patients with knee osteoarthritis. *Arthritis Rheumatol. (Hoboken, N.J.)* **67**, 956–65 (2015).

402. Loeser, R. F. Age-Related Changes in the Musculoskeletal System and the Development of Osteoarthritis. *Clin. Geriatr. Med.* **26**, 371–386 (2010).
403. Berenbaum, F. Osteoarthritis as an inflammatory disease (osteoarthritis is not osteoarthrosis!). *Osteoarthritis Cartilage* **21**, 16–21 (2013).
404. Traktuev, D. O. *et al.* A population of multipotent CD34-positive adipose stromal cells share pericyte and mesenchymal surface markers, reside in a periendothelial location, and stabilize endothelial networks. *Circ. Res.* **102**, 77–85 (2008).
405. Lopa, S. *et al.* Donor-matched mesenchymal stem cells from knee infrapatellar and subcutaneous adipose tissue of osteoarthritic donors display differential chondrogenic and osteogenic commitment. *Eur. Cell. Mater.* **27**, 298–311 (2014).
406. Wickham, M. Q., Erickson, G. R., Gimble, J. M., Vail, T. P. & Guilak, F. Multipotent stromal cells derived from the infrapatellar fat pad of the knee. *Clin. Orthop. Relat. Res.* **412**, 196–212 (2003).
407. Bidarra, S. J. *et al.* Phenotypic and proliferative modulation of human mesenchymal stem cells via crosstalk with endothelial cells. *Stem Cell Res.* **7**, 186–197 (2011).
408. Saleh, F. A., Whyte, M. & Genever, P. G. Effects of endothelial cells on human mesenchymal stem cell activity in a three-dimensional in vitro model. *Eur. Cell. Mater.* **22**, 242–57 (2011).
409. Sivanathan, K. N., Gronthos, S., Rojas-Canales, D., Thierry, B. & Coates, P. T. Interferon-gamma modification of mesenchymal stem cells: implications of autologous and allogeneic mesenchymal stem cell therapy in allotransplantation. *Stem Cell Rev.* **10**, 351–375 (2014).
410. Hedbom, E. & Häuselmann, H. J. Molecular aspects of pathogenesis in osteoarthritis: the role of inflammation. *Cell. Mol. Life Sci.* **59**, 45–53 (2002).
411. Epstein, F. H. *et al.* T-Lymphocyte-Antigen Interactions in Transplant Rejection. *N. Engl. J. Med.* **322**, 510–517 (1990).
412. Sayegh, M. H. & Turka, L. A. The role of T-cell costimulatory activation pathways in transplant rejection. *N. Engl. J. Med.* **338**, 1813–1821 (1998).
413. Rübenhagen, R., Schüttrumpf, J. P., Stürmer, K. M. & Frosch, K.-H. Interleukin-7 levels in synovial fluid increase with age and MMP-1 levels decrease with progression of osteoarthritis. *Acta Orthop.* **83**, 59–64 (2012).
414. Hancock, W. W. *et al.* Costimulatory function and expression of CD40 ligand, CD80, and CD86 in vascularized murine cardiac allograft rejection. *Proc. Natl. Acad. Sci. U. S. A.* **93**, 13967–13972 (1996).
415. Maillard, N. *et al.* The immunomodulatory properties of mesenchymal stromal cells isolated from the synovial fluid of human osteoarthritic joints. *Osteoarthr. Cartil.* **22**, S23 (2014).
416. Yamada, H. *et al.* Preferential accumulation of activated Th1 cells not only in rheumatoid arthritis but also in osteoarthritis joints. *J. Rheumatol.* **38**, 1569–75 (2011).
417. Ryan, J. M., Barry, F., Murphy, J. M. & Mahon, B. P. Interferon- γ does not break,

- but promotes the immunosuppressive capacity of adult human mesenchymal stem cells. *Clin. Exp. Immunol.* **149**, 353–363 (2007).
418. DelaRosa, O. *et al.* Requirement of IFN-gamma-mediated indoleamine 2,3-dioxygenase expression in the modulation of lymphocyte proliferation by human adipose-derived stem cells. *Tissue Eng. Part A* **15**, 2795–806 (2009).
 419. Criado, G., Šimelyte, E., Inglis, J. J., Essex, D. & Williams, R. O. Indoleamine 2,3 dioxygenase-mediated tryptophan catabolism regulates accumulation of Th1/Th17 cells in the joint in collagen-induced arthritis. *Arthritis Rheum.* **60**, 1342–1351 (2009).
 420. van Buul, G. M. *et al.* Mesenchymal stem cells secrete factors that inhibit inflammatory processes in short-term osteoarthritic synovium and cartilage explant culture. *Osteoarthr. Cartil.* **20**, 1186–1196 (2012).
 421. Wakitani, S. *et al.* Safety of autologous bone marrow-derived mesenchymal stem cell transplantation for cartilage repair in 41 patients with 45 joints followed for up to 11 years and 5 months. *J. Tissue Eng. Regen. Med.* **5**, 146–150 (2011).
 422. Akgun, I. *et al.* Matrix-induced autologous mesenchymal stem cell implantation versus matrix-induced autologous chondrocyte implantation in the treatment of chondral defects of the knee: a 2-year randomized study. *Arch. Orthop. Trauma Surg.* **135**, 251–263 (2015).
 423. Vega, A. *et al.* Treatment of Knee Osteoarthritis With Allogeneic Bone Marrow Mesenchymal Stem Cells: A Randomized Controlled Trial. *Transplantation* **99**, 1681–90 (2015).
 424. Garcia, J. *et al.* Characterisation of synovial fluid and infrapatellar fat pad derived mesenchymal stromal cells: The influence of tissue source and inflammatory stimulus. *Sci. Rep.* **6**, 24295 (2016).
 425. Busser, H. *et al.* Isolation and characterization of human mesenchymal stromal cells subpopulations: comparison of bone marrow and adipose tissue. *Stem Cells Dev.* **24**, 2142–2157 (2015).
 426. Freitag, J. *et al.* Adipose derived mesenchymal stem cell therapy in the treatment of isolated knee chondral lesions: design of a randomised controlled pilot study comparing arthroscopic microfracture versus arthroscopic microfracture combined with postoperative mesenchymal . *BMJ Open* **5**, e009332 (2015).
 427. Adesida, A. B., Mulet-Sierra, A. & Jomha, N. M. Hypoxia mediated isolation and expansion enhances the chondrogenic capacity of bone marrow mesenchymal stromal cells. *Stem Cell Res. Ther.* **3**, 9 (2012).
 428. Sekiya, I. *et al.* Human mesenchymal stem cells in synovial fluid increase in the knee with degenerated cartilage and osteoarthritis. *J. Orthop. Res.* **30**, 943–949 (2012).
 429. Mohyeldin, A., Garzón-Muvdi, T. & Quiñones-Hinojosa, A. Oxygen in stem cell biology: A critical component of the stem cell niche. *Cell Stem Cell* **7**, 150–161 (2010).
 430. Fehrer, C. *et al.* Reduced oxygen tension attenuates differentiation capacity of human mesenchymal stem cells and prolongs their lifespan. *Aging Cell* **6**, 745–757

(2007).

431. Rosová, I., Dao, M., Capoccia, B., Link, D. & Nolte, J. a. Hypoxic preconditioning results in increased motility and improved therapeutic potential of human mesenchymal stem cells. *Stem Cells* **26**, 2173–2182 (2008).
432. Munir, S. *et al.* Hypoxia enhances chondrogenic differentiation of human adipose tissue-derived stromal cells in scaffold-free and scaffold systems. *Cell Tissue Res.* **355**, 89–102 (2014).
433. Leijten, J. *et al.* Metabolic programming of mesenchymal stromal cells by oxygen tension directs chondrogenic cell fate. *Proc. Natl. Acad. Sci. U. S. A.* **111**, (2014).
434. Boyette, L. B., Creasey, O. A., Guzik, L., Lozito, T. & Tuan, R. S. Human bone marrow-derived mesenchymal stem cells display enhanced clonogenicity but impaired differentiation with hypoxic preconditioning. *Stem Cells Transl. Med.* **3**, 241–54 (2014).
435. Pilgaard, L. *et al.* Effect of oxygen concentration, culture format and donor variability on in vitro chondrogenesis of human adipose tissue-derived stem cells. *Regen. Med.* **4**, 539–548 (2009).
436. Khan, W. S., Adesida, A. B. & Hardingham, T. E. Hypoxic conditions increase hypoxia-inducible transcription factor 2 α and enhance chondrogenesis in stem cells from the infrapatellar fat pad of osteoarthritis patients. *Arthritis Res. Ther.* **9**, R55 (2007).
437. Buckley, C. T., Vinardell, T. & Kelly, D. J. Oxygen tension differentially regulates the functional properties of cartilaginous tissues engineered from infrapatellar fat pad derived MSCs and articular chondrocytes. *Osteoarthritis Cartilage* **18**, 1345–54 (2010).
438. Lodewyckx, L., Cailotto, F., Thysen, S., Luyten, F. P. & Lories, R. J. Tight regulation of wntless-type signaling in the articular cartilage - subchondral bone biomechanical unit: transcriptomics in Frzb-knockout mice. *Arthritis Res. Ther.* **14**, R16 (2012).
439. Vinardell, T., Sheehy, E. J., Buckley, C. T. & Kelly, D. J. A comparison of the functionality and in vivo phenotypic stability of cartilaginous tissues engineered from different stem cell sources. *Tissue Eng. Part A* **18**, 1161–70 (2012).
440. Karlsson, C. *et al.* Differentiation of Human Mesenchymal Stem Cells and Articular Chondrocytes : Analysis of Chondrogenic Potential and Expression Pattern of Differentiation-Related Transcription Factors. *J. Orthop. Res.* **25**, 152–163 (2007).
441. Liu, Y., Buckley, C. T., Downey, R., Mulhall, K. J. & Kelly, D. J. The role of environmental factors in regulating the development of cartilaginous grafts engineered using osteoarthritic human infrapatellar fat pad-derived stem cells. *Tissue Eng. Part A* **18**, 1531–41 (2012).
442. Stenberg, J. *et al.* Clinical Outcome 3 Years After Autologous Chondrocyte Implantation Does Not Correlate With the Expression of a Predefined Gene Marker Set in Chondrocytes Prior to Implantation but Is Associated With Critical Signaling Pathways. *Orthop. J. Sport. Med.* **2**, (2014).
443. Cote, A. J. *et al.* Single-cell differences in matrix gene expression do not predict

- matrix deposition. *Nat. Commun.* **7**, 10865 (2016).
444. Stenberg, J. *et al.* Clinical Outcome 3 Years After Autologous Chondrocyte Implantation Does Not Correlate With the Expression of a Predefined Gene Marker Set in Chondrocytes Prior to Implantation but Is Associated With Critical Signaling Pathways. *Orthop. J. Sport. Med.* **2**, 1–14 (2014).
 445. Zhang, S., Muneta, T., Morito, T., Mochizuki, T. & Sekiya, I. Autologous synovial fluid enhances migration of mesenchymal stem cells from synovium of osteoarthritis patients in tissue culture system. *J. Orthop. Res.* **26**, 1413–1418 (2008).
 446. Takada, Y. *et al.* Molecular cloning and expression of the cDNA for alpha 3 subunit of human alpha 3 beta 1 (VLA-3), an integrin receptor for fibronectin, laminin, and collagen. *J. Cell Biol.* **115**, 257–266 (1991).
 447. Sellam, J. & Berenbaum, F. The role of synovitis in pathophysiology and clinical symptoms of osteoarthritis. *Nat. Rev. Rheumatol.* **6**, 625–635 (2010).
 448. Klein-Wieringa, I. R. *et al.* Inflammatory Cells in Patients with Endstage Knee Osteoarthritis: A Comparison between the Synovium and the Infrapatellar Fat Pad. *J. Rheumatol.* **43**, 771–778 (2016).
 449. De Ferranti, S. & Mozaffarian, D. The perfect storm: Obesity, adipocyte dysfunction, and metabolic consequences. *Clin. Chem.* **54**, 945–955 (2008).
 450. Skurk, T., Alberti-huber, C., Herder, C. & Hauner, H. Relationship between Adipocyte Size and Adipokine Expression and Secretion. *J. Clin. Endocrinol. Metab.* **92**, 1023–1033 (2007).
 451. Rutkowski, J. M., Stern, J. H. & Scherer, P. E. The cell biology of fat expansion. *J. Cell Biol.* **208**, 501–512 (2015).
 452. Cinti, S. *et al.* Adipocyte death defines macrophage localization and function in adipose tissue of obese mice and humans. *J. Lipid Res.* **46**, 2347–2355 (2005).
 453. Haywood, L. *et al.* Inflammation and angiogenesis in osteoarthritis. *Arthritis Rheum.* **48**, 2173–2177 (2003).
 454. Dieppe, P., Doherty, M. & Macfarlane, D. Introduction Crystal-related arthropathies. *Ann. Rheum. Dis.* **42**, 1–3 (1983).
 455. Ramprasad, M. P., Terpstra, V., Kondratenko, N., Quehenberger, O. & Steinberg, D. Cell surface expression of mouse macrosialin and human CD68 and their role as macrophage receptors for oxidized low density lipoprotein. *Proc. Natl. Acad. Sci. U. S. A.* **93**, 14833–8 (1996).
 456. Ramprasad, M. P. *et al.* The 94- to 97-kDa mouse macrophage membrane protein that recognizes oxidized low density lipoprotein and phosphatidylserine-rich liposomes is identical to macrosialin, the mouse homologue of human CD68. *Proc. Natl. Acad. Sci. U. S. A.* **92**, 9580–4 (1995).
 457. Steinman, R. M., Pack, M. & Inaba, K. Dendritic cells in the T-cell areas of lymphoid organs. *Immunol. Rev.* **156**, 25–37 (1997).
 458. Campbell, I. K. *et al.* Differentiation of Inflammatory Dendritic Cells Is Mediated by NF- κ B1 – Dependent GM-CSF Production in CD4 T Cells. *J. Immunol.* **186**,

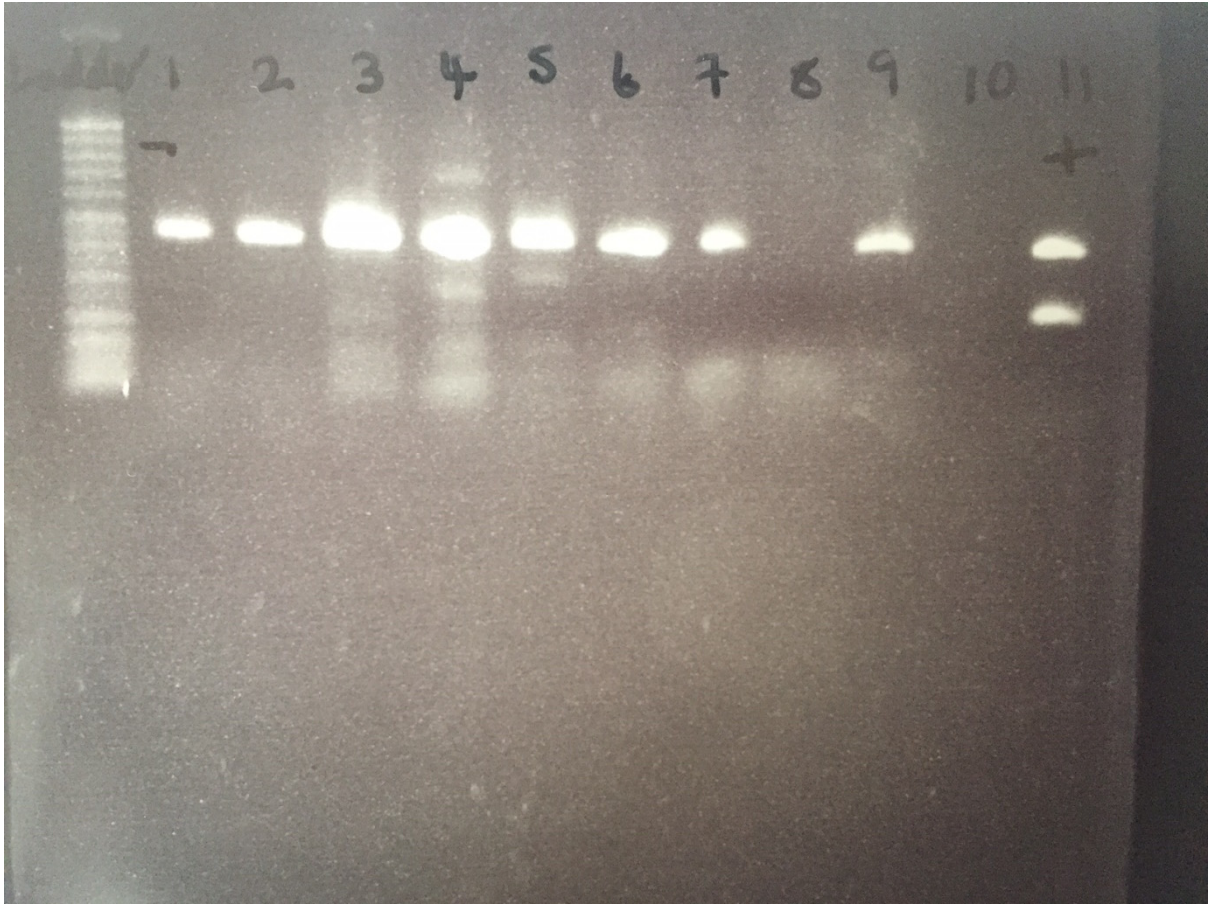
- 5468–5477 (2016).
459. Taskiran, D., Stefanovicracic, M., Georgescu, H. & Evans, C. Nitric-Oxide Mediates Suppression of Cartilage Proteoglycan Synthesis by Interleukin-1. *Biochem. Biophys. Res. Commun.* **200**, 142–148 (1994).
 460. Gazi, U. & Martinez-Pomares, L. Influence of the mannose receptor in host immune responses. *Immunobiology* **214**, 554–561 (2009).
 461. Gottfried, E. *et al.* Expression of CD68 in non-myeloid cell types. *Scand. J. Immunol.* **67**, 453–463 (2008).
 462. Barros, M. H. M., Hauck, F., Dreyer, J. H., Kempkes, B. & Niedobitek, G. Macrophage polarisation: An immunohistochemical approach for identifying M1 and M2 macrophages. *PLoS One* **8**, 1–11 (2013).
 463. Ambarus, C. A. *et al.* Systematic validation of specific phenotypic markers for in vitro polarized human macrophages. *J. Immunol. Methods* **375**, 196–206 (2012).
 464. Mantovani, A. *et al.* The chemokine system in diverse forms of macrophage activation and polarization. *Trends Immunol.* **25**, 677–686 (2004).
 465. Eirin, A. *et al.* Renal vein cytokine release as an index of renal parenchymal inflammation in chronic experimental renal artery stenosis. *Nephrol. Dial. Transplant* **29**, 274–82 (2014).
 466. Zizzo, G. & Cohen, P. L. The PPAR- γ antagonist GW9662 elicits differentiation of M2c-like cells and upregulation of the MerTK/Gas6 axis: a key role for PPAR- γ in human macrophage polarization. *J. Inflamm. (Lond)*. **12**, 36 (2015).
 467. Siebelt, M. *et al.* Triamcinolone acetonide activates an anti-inflammatory and folate receptor-positive macrophage that prevents osteophytosis in vivo. *Arthritis Res. Ther.* **17**, 352 (2015).
 468. Gordon, S. & Martinez, F. O. Alternative activation of macrophages: Mechanism and functions. *Immunity* **32**, 593–604 (2010).
 469. Hirsch, J. & Batchelor, B. Adipose tissue cellularity in human obesity. *Clin. Endocrinol. Metab.* **5**, 299–311 (1976).
 470. Chang, W. *et al.* Infrapatellar fat pad hypertrophy without inflammation in a diet-induced mouse model of obesity and osteoarthritis. *Osteoarthr. Cartil.* **19**, 66 (2011).
 471. Weisberg, S. P. *et al.* Obesity is associated with macrophage accumulation. *J. Clin. Invest.* **112**, 1796–1808 (2003).
 472. Musi, N. & Guardado-Mendoza, R. Adipose Tissue as an Endocrine Organ. *Cell. Endocrinol. Heal. Dis.* **89**, 229–237 (2014).
 473. Clockaerts, S. *et al.* The infrapatellar fat pad should be considered as an active osteoarthritic joint tissue: a narrative review. *Osteoarthritis Cartilage* **18**, 876–882 (2010).
 474. Ballegaard, C. *et al.* Knee pain and inflammation in the infrapatellar fat pad estimated by conventional and dynamic contrast-enhanced magnetic resonance imaging in obese patients with osteoarthritis: A cross-sectional study. *Osteoarthr.*

- Cartil.* **22**, 933–940 (2014).
475. Han, W. *et al.* Infrapatellar fat pad in the knee: is local fat good or bad for knee osteoarthritis? *Arthritis Res. Ther.* **16**, R145 (2014).
 476. Klein-Wieringa, I. R. *et al.* Adipocytes modulate the phenotype of human macrophages through secreted lipids. *J. Immunol.* **191**, 1356–63 (2013).
 477. Fu, Y., Huebner, J. L., Kraus, V. B. & Griffin, T. M. Effect of Aging on Adipose Tissue Inflammation in the Knee Joints of F344BN Rats. *Journals Gerontol. Ser. A Biol. Sci. Med. Sci.* **0**, 1–11 (2015).
 478. Macchi, V. *et al.* The Infrapatellar Adipose Body: A Histotopographic Study. *Cells Tissues Organs* (2016). doi:10.1159/000442876
 479. Ding, C. *et al.* Knee cartilage defects: Association with early radiographic osteoarthritis, decreased cartilage volume, increased joint surface area and type II collagen breakdown. *Osteoarthr. Cartil.* **13**, 198–205 (2005).
 480. Sower, M. F. *et al.* Magnetic resonance-detected subchondral bone marrow and cartilage defect characteristics associated with pain and X-ray-defined knee osteoarthritis. *Osteoarthr. Cartil.* **11**, 387–393 (2003).
 481. Tsuchida, A. I. *et al.* Interleukin-6 is elevated in synovial fluid of patients with focal cartilage defects and stimulates cartilage matrix production in an in vitro regeneration model. *Arthritis Res. Ther.* **14**, (2012).
 482. Vonk, L. a., de Windt, T. S., Slaper-Cortenbach, I. C. M. & Saris, D. B. F. Autologous, allogeneic, induced pluripotent stem cell or a combination stem cell therapy? Where are we headed in cartilage repair and why: a concise review. *Stem Cell Res. Ther.* **6**, 1–11 (2015).
 483. Bekkers, J. E. J. *et al.* Single-stage cell-based cartilage regeneration using a combination of chondrons and mesenchymal stromal cells: comparison with microfracture. *Am. J. Sports Med.* **41**, 2158–66 (2013).
 484. Stuart, B. Y. M. Cartilage Repair : What’s the Right Combination? *Start-Up* **14**, 1–9 (2009).
 485. Ryd, L. *et al.* Pre-Osteoarthritis: Definition and Diagnosis of an Elusive Clinical Entity. *Cartilage* **6**, 156–65 (2015).
 486. Rahmati, M., Mobasheri, A. & Mozafari, M. Inflammatory mediators in osteoarthritis: A critical review of the state-of-the-art, current prospects, and future challenges. *Bone* **85**, 81–90 (2016).
 487. Henrotin, Y., Sanchez, C., Bay-jensen, A. C. & Mobasheri, A. Osteoarthritis biomarkers derived from cartilage extracellular matrix : Current status and future perspectives. *Ann. Phys. Rehabil. Med.* **59**, 145–148 (2016).
 488. Kraus, V. B. *et al.* OARSI Clinical Trials Recommendations: Soluble biomarker assessments in clinical trials in osteoarthritis. *Osteoarthr. Cartil.* **23**, 686–697 (2015).
 489. Desando, G. *et al.* Intra-articular delivery of adipose derived stromal cells attenuates osteoarthritis progression in an experimental rabbit model. *Arthritis Res. Ther.* **15**,

R22 (2013).

490. Evans, C. H., Kraus, V. B. & Setton, L. A. Progress in intra-articular therapy. *Nat. Rev. Rheumatol.* **10**, 11–22 (2013).
491. Jo, C., Lee, Y. & SHIN, W. Intra-Articular Injection of Mesenchymal Stem Cells for the Treatment of Osteoarthritis of the Knee: A Proof-of-Concept Clinical Trial. *Stem Cells* **32**, 1254–1266 (2014).
492. Jiang, Y. & Tuan, R. S. Origin and function of cartilage stem/progenitor cells in osteoarthritis. *Nat. Rev. Rheumatol.* **11**, 206–12 (2015).
493. Mokbel, A. *et al.* Homing and efficacy of intra-articular injection of autologous mesenchymal stem cells in experimental chondral defects in dogs. *Clin. Exp. Rheumatol.* **29**, 275–284 (2011).
494. Melief, S. M. *et al.* Multipotent stromal cells induce human regulatory T cells through a novel pathway involving skewing of monocytes toward anti-inflammatory macrophages. *Stem Cells* **31**, 1980–1991 (2013).
495. Berenbaum, F., Eymard, F. & Houard, X. Osteoarthritis, inflammation and obesity. *Curr. Opin. Rheumatol.* **25**, 1 (2012).

Appendix



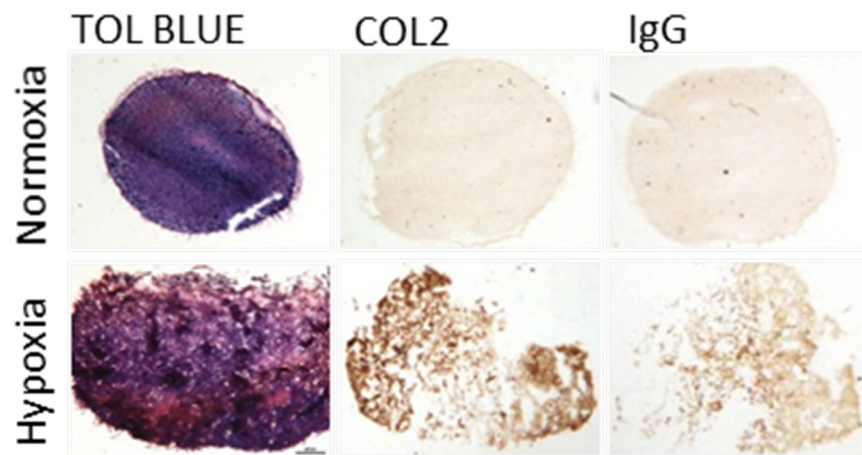
Appendix 1: Image of an electrophoresis gel to detect the presence of mycoplasma in cell culture. Lane 1 is a negative control, lanes 2-9 are test samples and lane 11 is the positive control. In this example, samples 3 and 4 are infected with mycoplasma.



Name	SevenGo SG6-ELK	HI-2040
Type of probe	Optical	Electrode
Range	0-600%	0-300%
Accuracy	$\pm 10.0\%$	$\pm 1.5\%$
Resolution	0.10%	0.10%
Temperature range	0-40°C	0-50°C

	GAPDH	TBP	HPRT1	B2M	PPIA
	15.974	25.046	23.392	17.177	20.133
	16.862	24.958	23.002	17.954	20.393
	15.971	24.852	23.859	16.776	21.357
	15.231	24.048	22.326	15.817	19.461
	15.708	23.953	22.256	15.221	19.479
	14.528	22.713	20.592	15.337	18.649
	14.495	24.187	22.194	14.729	19.886
	15.253	24.518	22.576	15.109	20.032
	15.826	25.564	22.724	15.109	20.881
	15.230	25.299	20.826	15.165	19.315
Ct mean	15.508	24.514	22.375	15.839	19.959
SD	0.67916	0.787045	0.970744	1.026001	0.751196
CV	0.043794	0.032106	0.043385	0.064776	0.037638

Appendix 3: Ct values from preliminary tests conducted to determine the most stable reference genes across cell types. The two genes with the lowest coefficient of variation (CV), TBP and PPIA, were used for PCR experiments.



Appendix 4: Comparison of the chondrogenic differentiation of chondrocytes that were isolated and expanded in normoxia (top panel) or hypoxia (bottom panel). Pellets from cells grown in hypoxia produced more GAGs and type II collagen as shown by toluidine blue staining and immunohistochemistry respectively.

SCIENTIFIC REPORTS



OPEN

Characterisation of synovial fluid and infrapatellar fat pad derived mesenchymal stromal cells: The influence of tissue source and inflammatory stimulus

Received: 23 December 2015

Accepted: 16 March 2016

Published: 13 April 2016

John Garcia^{1,2}, Karina Wright^{1,2}, Sally Roberts^{1,2}, Jan Herman Kuiper^{1,2}, Chas Mangham¹, James Richardson^{1,2} & Claire Mennan^{1,2}

The infrapatellar fat pad (FP) and synovial fluid (SF) in the knee serve as reservoirs of mesenchymal stromal cells (MSCs) with potential therapeutic benefit. We determined the influence of the donor on the phenotype of donor matched FP and SF derived MSCs and examined their immunogenic and immunomodulatory properties before and after stimulation with the pro-inflammatory cytokine interferon-gamma (IFN- γ). Both cell populations were positive for MSC markers CD73, CD90 and CD105, and displayed multipotency. FP-MSCs had a significantly faster proliferation rate than SF-MSCs. CD14 positivity was seen in both FP-MSCs and SF-MSCs, and was positively correlated to donor age but only for SF-MSCs. Neither cell population was positive for the co-stimulatory markers CD40, CD80 and CD86, but both demonstrated increased levels of human leukocyte antigen-DR (HLA-DR) following IFN- γ stimulation. HLA-DR production was positively correlated with donor age for FP-MSCs but not SF-MSCs. The immunomodulatory molecule, HLA-G, was constitutively produced by both cell populations, unlike indoleamine 2, 3-dioxygenase which was only produced following IFN- γ stimulation. FP and SF are accessible cell sources which could be utilised in the treatment of cartilage injuries, either by transplantation following *ex-vivo* expansion or endogenous targeting and mobilisation of cells close to the site of injury.

Regenerating joint tissues that have been damaged by trauma or degenerative diseases, such as osteoarthritis (OA), continues to present a challenge to scientists and clinicians world-wide. Autologous chondrocyte implantation (ACI) is a two-stage procedure that involves harvesting healthy cartilage arthroscopically in the first stage, followed by implantation of culture expanded cells at the damaged site via open surgery in the second stage, in an attempt to induce repair of the damaged tissue¹. Eighty one percent of patients treated at our centre showed improved joint function and pain reduction (assessed via Lysholm scores) over an average follow-up time of 5 years². However, ACI has some disadvantages relating to cost and possible donor site morbidity³⁻⁵, which limits its current use as a standard treatment for cartilage repair. Mesenchymal stromal cells (MSCs) have been isolated from many different tissue sources, including bone marrow (BM-MSCs), adipose tissue (commonly called adipose stem cells, ASCs), synovium (SM-MSCs) and umbilical cord (UC-MSCs) and are promising candidates for use in regenerative cell-based therapies. The infrapatellar fat pad (FP) and synovial fluid (SF) also represent accessible sources of MSCs (FP-MSCs and SF-MSCs, respectively) which are often routinely removed as surgical waste during arthroscopy or open knee surgery. The precise origin of SF-MSCs is not known; reports propose that they come from different tissues within the knee such as cartilage, bone and synovium, with synovium often considered as the most likely⁶⁻⁸. In an *in vitro* model, one study has illustrated that the joint SF of OA patients enhances MSC migration from synovium explants, a process believed to be mediated by transforming growth factor beta-3 (TGF- β 3)⁹.

¹The Robert Jones and Agnes Hunt Orthopaedic Hospital NHS Foundation Trust, Oswestry, Shropshire, SY10 7AG, UK. ²Institute for Science & Technology in Medicine, Keele University, Keele, Staffordshire, ST5 5BG, UK. Correspondence and requests for materials should be addressed to C.M. (email: Claire.Mennan@rjah.nhs.uk)

ID	Gender	Age (years)	Condition	Macroscopic observation of FP	Procedure
Donor 1	Male	35	Chondral defect on lateral femoral condyle	Mild inflammation	ACI
Donor 2	Female	42	Chondral defect on patella	Severe inflammation	ACI
Donor 3	Female	49	Osteochondral defect on patella	Hypertrophy	ACI
Donor 4	Female	49	Chondral defect on patella	Hypertrophy	ACI
Donor 5	Male	53	OA degeneration of knee with chondral defect on trochlea	General inflammation	ACI
Donor 6	Male	79	End-stage OA	General inflammation	Total knee replacement

Table 1. Demographics of donors from which samples were sourced.

Better characterisation of these cells is vital, not only to ensure their safety for *in vivo* use, but also to test their therapeutic efficacy. However, a number of parameters such as tissue source and donor specificity are often overlooked by researchers, despite the clear evidence indicating that these features influence the phenotype of MSCs. It has been demonstrated that both donor age and gender affect the differentiation of BM-MSCs and A-MSCs; male and young donors generally produce MSCs with a more enhanced osteogenic and chondrogenic potency^{10–12}. Further, older donors are known to produce MSCs that are less proliferative compared to younger donors¹². These findings collectively suggest a clear influence of the donor on the phenotype of MSCs, and support the need for more robust studies that consider tissue origin and donor features as important parameters for the development of cell therapies.

In addition to the minimum characterisation criteria of MSCs established by the International Society for Cell Therapy (ISCT)¹³ which assesses cell surface markers and multipotent ability, understanding the immunological properties of MSCs in response to a pro-inflammatory stimulus has also been proposed as an important part of their characterisation¹⁴. BM-MSCs have been shown to increase their production of the immunomodulatory molecule indoleamine 2, 3-dioxygenase (IDO)¹⁵ in response to stimulation with the pro-inflammatory cytokine interferon-gamma (IFN- γ). IDO is an enzyme involved in the depletion of the essential amino acid, tryptophan, resulting in the inhibition of the proliferation of microbes and T cells¹⁶. Like IDO, the human leukocyte antigen-G (HLA-G) is another important immunomodulatory molecule which exerts its immunosuppressive effect on activated T cells¹⁷. It is produced by BM-MSC and by the trophoblast cells in the placenta where it plays a role in maternal tolerance to the foetus. The human leukocyte antigen-DR (HLA-DR), a major histocompatibility complex class II (MHCII) molecule, is found on antigen presenting cells (APCs) of the immune system and interacts with T cell receptors during an immune response. HLA-DR is not inherently expressed on BM-MSCs, but is known to be upregulated following a pro-inflammatory stimulus¹⁸. In contrast, the costimulatory markers CD40, CD80 and CD86, which are also produced by APCs involved in T cell mediated immune reactions¹⁹, are not produced on BM-MSCs even after inflammatory stimulation²⁰. While FP-MSCs and SF-MSCs have been previously characterised in terms of their growth, multipotency and CD profile^{7,21}, the immunological and immunomodulatory properties of these cells have not been thoroughly defined. The purpose of this investigation was to assess the influence of tissue source and donor on the properties of MSCs sourced from donor matched FP and SF isolated from human knees. We also investigated the previously unexplored response of FP- and SF-MSCs to a pro-inflammatory stimulus, such as that which may be found in an osteoarthritic joint.

Results

Macroscopic observations of FP, Histology, Cell culture and Growth kinetics. Donor variability was noted in the apparent level of inflammation observed by the surgeon (Table 1). The complex and heterogeneous features of the intact FP tissue were clearly visible in our histological preparations showing synovium and adipose regions (Fig. 1a). Blood vessels appeared scattered throughout the synovium (Fig. 1c) and deeper adipose tissue (Fig. 1b). For some samples a layer of synovial cells could be found on the superficial regions of the synovium along with mast cells, lymphocytes and numerous blood vessels (Fig. 1c). To avoid contamination of adipose derived cells with synoviocytes, only the deepest areas of the FP were used for digestion, as highlighted in Fig. 1d.

MSCs isolated from both FP and SF were plastic adherent and appeared to consistently have a fibroblastic-like morphology at early passage (P2) through to the last passage tested (P10) (Fig. 2a,b). The results of the hierarchical regression analysis (Table 2) show that the average doubling time (DT) of SF-MSCs was 8.3 days longer than the DT of FP-MSCs ($P < 0.001$) over the 10 passages tested, for all donors. The DT increased with passage number by 1.4 days per passage and this increase was significantly dependant on the donor ($P < 0.001$).

Immunoprofile of FP-MSCs and SF-MSCs. Flow cytometry analyses (Fig. 3a) revealed that both cell populations were over 95% positive for the MSC markers CD73 and CD105, but CD90 showed only $92.7\% \pm 11$ positivity in SF-MSCs but $98.3\% \pm 3.1$ in FP-MSCs. Interestingly, some positivity was recorded for the cocktail of PE conjugated markers expected to be negative on MSC cultures i.e. CD11b, CD19, CD45, CD34 and HLA-DR. FP-MSCs showed significantly ($P = 0.046$) greater positivity for the “negative” MSC markers ($31.7\% \pm 24\%$ of cells) compared to cells sourced from SF ($7.8\% \pm 6.9\%$ of cells). To explore this further, single PE-conjugated antibodies for CD11b, CD19, CD45, CD34 and HLA-DR were used to analyse FP-MSCs. FP-MSCs were negative for all of these markers, with the exception of CD34 which was $30.1\% \pm 18.6\%$

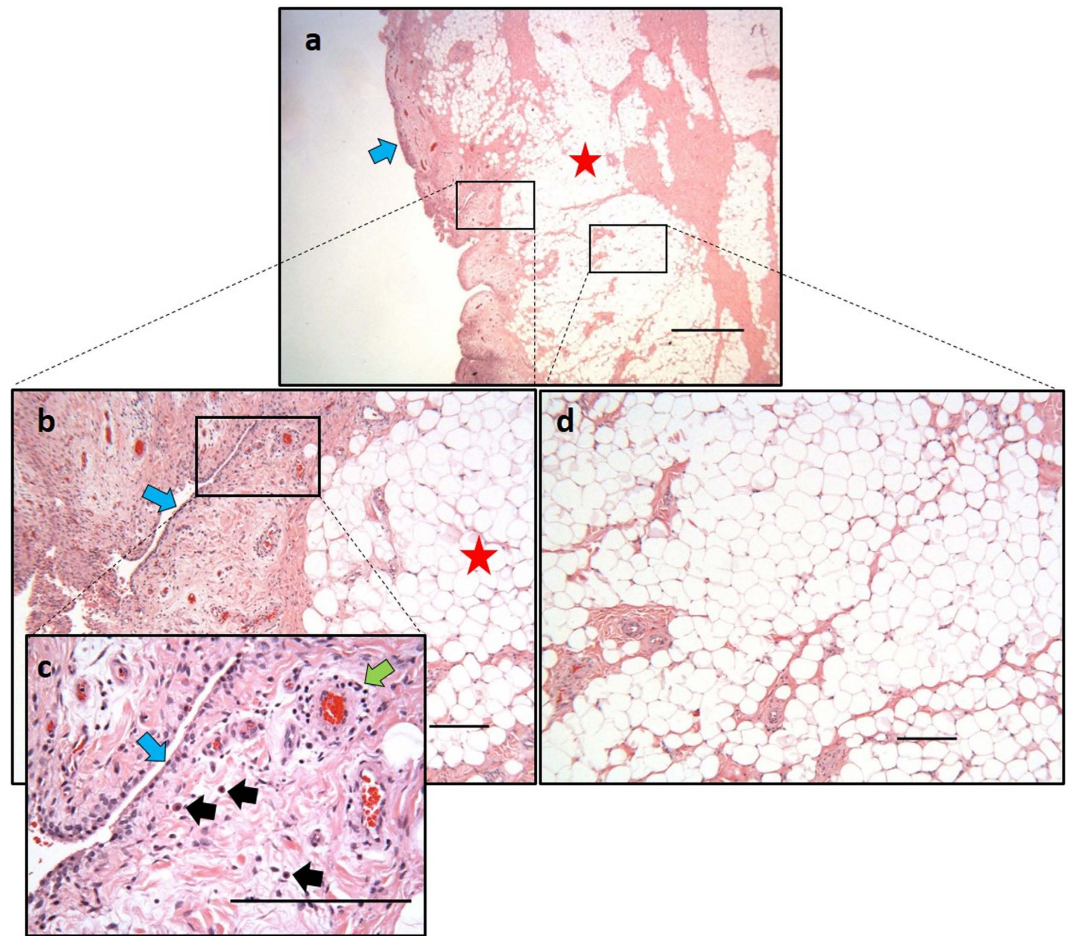


Figure 1. Example histology of a fat pad. Samples were paraffin embedded and stained with H&E. (a) Low power view of the fat pad as received after a knee replacement showing synovium (blue arrow) and adipose tissue (red star). (b) The deep adipose tissue is indicated by a red star and the adjacent synovium is indicated by a blue arrow. (c) High magnification view of the synovium with a layer of synoviocytes (blue arrow), mast cells (black arrows), and a blood vessel surrounded by a cuff of lymphocytes (green arrow). (d) Representative region of deep-lying vascularised adipose tissue from which FP-MSCs are isolated. Scale bars represent 1 mm (a) and 200 μ m (b–d).

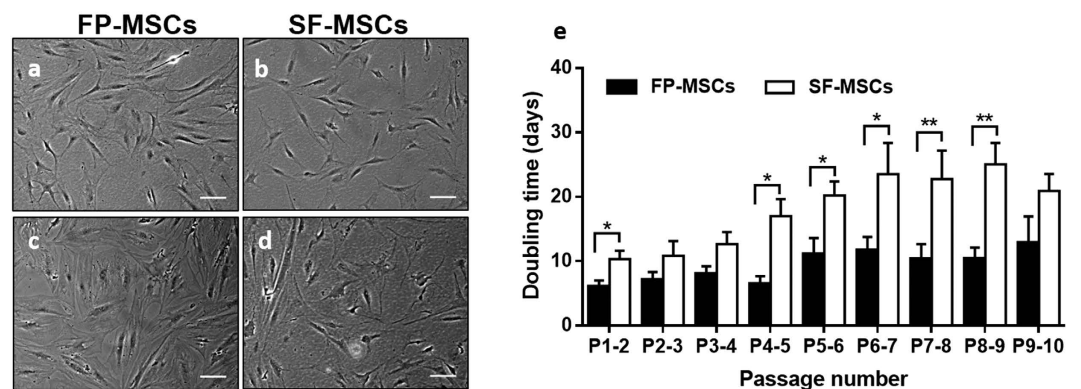


Figure 2. Microscopic photographs and growth kinetics of FP- and SF-MSCs. (a–d) Representative images were taken at passage 2 (a,b) and passage 10 (c,d). Scale bars represent 100 μ m. (e) Growth kinetics data represents the mean doubling time \pm standard error of the mean (SEM) for 6 donor-matched FP and SF samples. Over 10 passages, SF-MSCs show a significantly longer doubling time compared to FP-MSCs ($P = 0.018$). * $P < 0.05$, ** $P < 0.01$.

Factor	Fixed/Random effect	Coefficient or SD (days)	p-value
Cell source (SF)	Fixed	8.3 (6.1–10.4)	<0.001
Passage number	Fixed	1.4 (0.8–2.0)	<0.001
Passage by donor	Random	0.54 (0.19–1.1)	0.004

Table 2. Results of the hierarchical regression analysis for the influence of cell source, passage number and donor on doubling time of matched FP- and SF-MSCs. Note: Coefficients and standard deviation (SD) based on a linear mixed effect model. P-values are from Wald tests (fixed effects) and likelihood ratio tests (random effects).

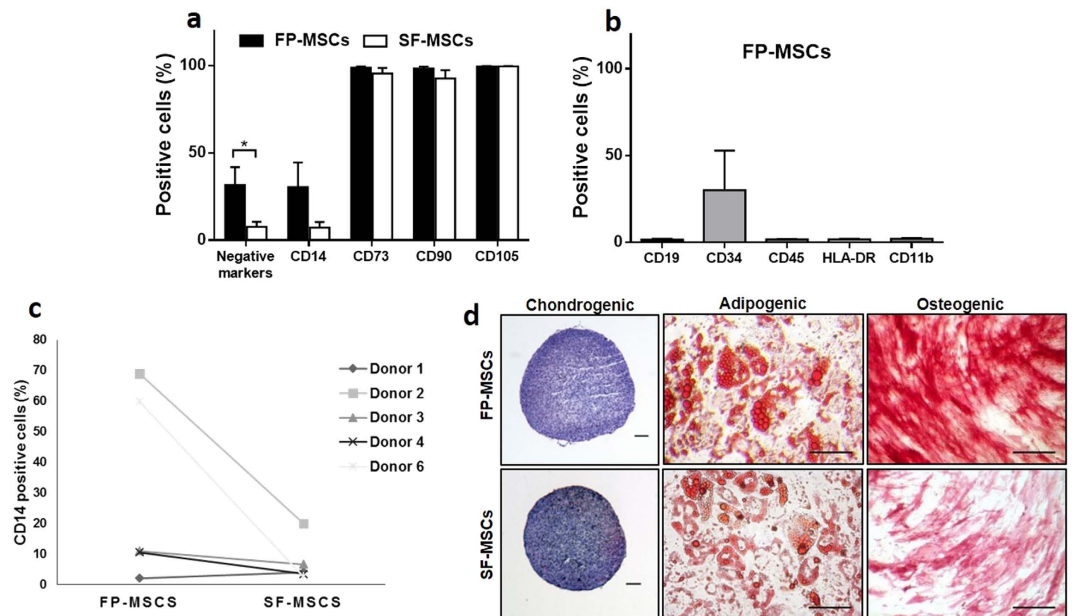


Figure 3. MSC immunoprofile (via flow cytometry) and trilineage differentiation of FP and SF-MSCs. (a) Both FP and SF-MSC populations were immunopositive for CD73 (98.8%), CD90 (98.3%), CD105 (99.6%); FP-MSCs showed significantly more cells which were positive for the cocktail of ISCT defined negative MSC selection markers compared to SF-MSCs ($P = 0.046$). (b) Single antibody cytometric analysis revealed a high positivity for CD34 in FP-MSCs ($n = 3$), but no positivity for CD11b, CD19, CD45 and HLA-DR. Error bars indicate SEM. (c) Cell positivity for CD14 was variable between donors and matched cell populations ($n = 5$). (d) The two MSC populations demonstrate differentiation potential when grown in different media; Chondrogenesis is shown by GAG production (purple metachromasia when stained with toluidine blue), adipogenesis is shown by the formation of lipid vesicles (oil red O) and osteogenesis is shown by the activity of alkaline phosphatase (red staining). Images are representative of the differentiation potential of all six donor matched samples. Scale bars represent 100 μm .

positive (Fig. 3b). The macrophage lineage and inflammation marker CD14 was present on both FP-MSCs ($30.5\% \pm 30.3\%$) and SF-MSCs cells ($7.4\% \pm 7.2\%$, $P = 0.14$), with some variability observed between donors (Fig. 3c). An increase in CD14 positive was associated with donor age for SF-MSCs ($n = 5$, $r = 0.94$, $P = 0.016$), but not FP-MSCs ($n = 5$, $r = 0.66$, $P = 0.23$).

Mesenchymal Trilineage Differential Potential. After 21 days of differentiation, all donor matched samples showed multipotent capability (Fig. 3d). FP-MSCs and SF-MSCs in adipogenic medium produced lipids which stained positively with oil red O, with those produced by FP-MSCs being more numerous and larger than those produced by SF-MSCs. Furthermore, they also showed stronger staining for alkaline phosphatase compared to SF-MSCs, which suggests greater osteogenic potential for the FP-MSCs. Histological staining for metachromasia using toluidine blue of chondrogenic cell pellets after differentiation revealed a similar level of GAG production by both cell populations, with no discernible difference in staining intensity between donors.

Immunogenic and immunomodulatory properties of FP-MSCs and SF-MSCs after IFN- γ stimulation. After 48 h of treatment with the either 25 or 500 ng/ml of the pro-inflammatory cytokine, IFN- γ , analysis via flow cytometry showed that CD40, CD80 and CD86 were not present on FP-MSCs or SF-MSCs and were similar to the untreated controls (Fig. 4a,b). In contrast, a low concentration (25 ng/ml) of IFN- γ significantly increased the positivity for HLA-DR in both cell populations compared to their respective controls

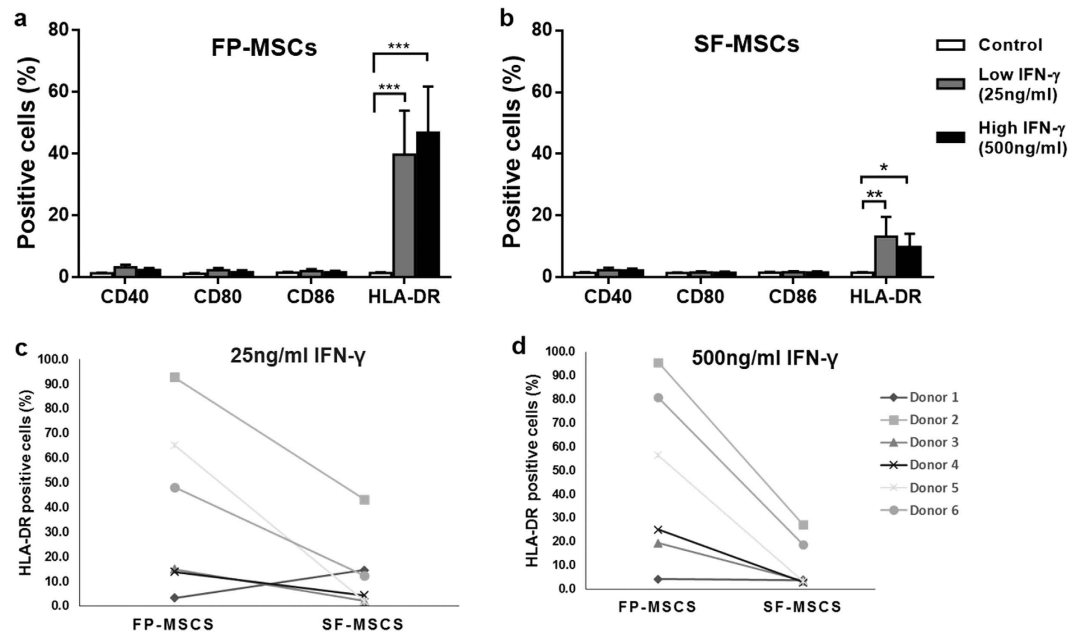


Figure 4. Immunogenic properties of FP and SF-MSCs after stimulation with IFN- γ (error bars indicate SEM). (a) The production of co-stimulatory markers (CD40, CD80, and CD86) and the class II MHC receptor HLA-DR for FP-MSCs is shown after 48 hours of stimulation with IFN- γ along with unstimulated controls. FP-MSCs do not produce co-stimulatory molecules regardless of stimulation, but show greater HLA-DR positivity at 25 ng/ml ($39.8\% \pm 14.3$, $p < 0.0001$) and at 500 ng/ml ($46.9\% \pm 14.9$, $p < 0.0001$) stimulation with IFN- γ . (b) SF-MSCs show no positivity for co-stimulatory marker, even when stimulated, but produce significantly higher levels of HLA-DR at 25 ng/ml ($13.1\% \pm 6.4$, $P = 0.015$) and at 500 ng/ml IFN- γ ($9.8\% \pm 4.3$, $P = 0.025$). (c–d) Donor variability in the levels of induced HLA-DR on FP-MSCs and SF-MSCs was observed at both 25 ng/ml (C) and 500 ng/ml (D). However, donor number 2 (indicated by the square data points) had higher positivity for HLA-DR compared to other donors for both FP-MSCs and SF-MSCs and for both of the IFN- γ doses tested.

(FP-MSCs = $39.8\% \pm 35.1\%$, SF-MSCs = $13.1\% \pm 11.7\%$). FP-MSCs also showed a significantly higher percentage of HLA-DR positive cells ($46.9\% \pm 36.5$) compared to SF-MSCs ($10.0\% \pm 10.4$) at 500 ng/ml IFN- γ ($P = 0.04$). Donor variability was noted with regards to the induction of HLA-DR by IFN- γ , however MSCs derived from both the FP and SF of donor number 2 consistently produced more HLA-DR in response to IFN- γ stimulation compared to the other donors, at both doses tested (Fig. 4c,d). After stimulation with 25 ng/ml of IFN- γ , FP-MSCs showed more production for HLA-DR, which was positively correlated with an increase in donor age ($n = 6$, $r = 0.82$, $P = 0.045$); SF-MSCs showed no such trend ($n = 6$, $r = 0.72$, $P = 0.105$).

Both cell populations produced the immunomodulatory marker, HLA-G, regardless of inflammatory stimulus and with no significant difference observed between FP-MSCs and SF-MSCs (Fig. 5a). Western blots showed that the production of IDO in both cell populations was induced by IFN- γ stimulation but was absent in unstimulated controls (Fig. 5b).

Discussion

In this study, we have characterised the endogenous population of MSCs found in patient matched samples of infrapatellar FP and joint SF, and explored the possible influence of a pro-inflammatory stimulus on the immunogenic and immunomodulatory properties of these cells. Histology of the FP and synovium revealed the presence of immune cells, notably mast cells and lymphocytes, in the superficial regions of the tissues. Both of these cell types are known to be present in synovial tissues of arthritic patients and produce molecules that promote joint inflammation^{22–24}. Macroscopic inspection of the FP during surgery in the present study revealed some degree of inflammation as indicated by the size of the FP itself and redness of the attached synovium. Our results show that both FP- and SF-MSCs are plastic adherent cells with similar fibroblast-like morphologies *in vitro*. We have noted a significant increase in the doubling times of SF-MSCs at late passages (compared to FP-MSCs), which suggests that SF-MSCs lose proliferative capacity earlier than FP-MSCs. Reports have indicated that both human BM-MSC and ASC doubling times increase with passage number^{25–27}; a longer culture period may have been required in the current study in order to observe a similar reduction in FP-MSC proliferation. The consistent difference in growth rate observed between FP-MSCs and SF-MSCs, isolated from matched donors, highlights that these cells are biologically different. Interestingly, an investigation observing patient-matched SM-MSCs and SF-MSCs revealed no significant difference in the proliferation rate of the two cell types between P0 and P2²⁸, perhaps providing supportive evidence that these cells share a common origin.

In agreement with previous studies^{6,29}, we confirm the multipotency of both cell populations, with FP-MSCs showing enhanced differentiation towards adipogenic and osteogenic lineages compared to

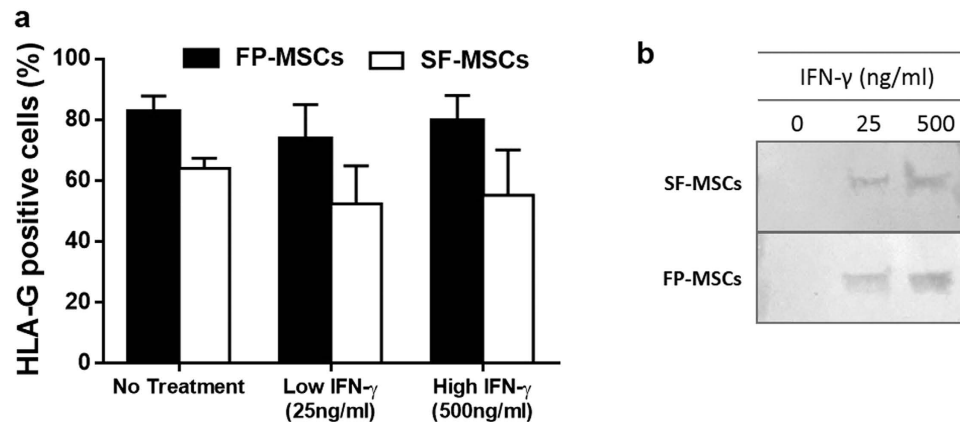


Figure 5. Immunomodulatory properties of FP and SF-MSCs after stimulation with IFN- γ (error bars indicate SEM). (a) Both FP and SF-MSCs ($n = 3$) inherently produce HLA-G in control conditions ($82.7\% \pm 5.1$ and $64.0\% \pm 3.4$ respectively), as well as following treatment with 25 ng/ml ($73.8\% \pm 11.2$ and $52.4\% \pm 12.5$ respectively) and 500 ng/ml IFN- γ ($79.7\% \pm 8.3$ and $52.2\% \pm 14.9$ respectively). (b) Cropped image of a representative western blot indicating the production of IDO by FP-MSCs and SF-MSCs after stimulation with IFN- γ , but not in untreated controls, a full-length blot is presented in Supplementary Figure S1.

SF-MSCs. Also, as previously described^{7,29} we have demonstrated that both FP-MSCs and SF-MSCs populations possess chondrogenic ability, but we have also shown that there was no discernible difference in the chondrogenic potential of FP-MSCs or SF-MSCs derived from the same donor. Our results show that these donor-matched SF-MSCs and FP-MSCs are positive for MSC cell surface markers CD73, CD90, CD105, as well as many of them being positive for the myeloid lineage marker CD14³⁰. This observation indicates that joint SF and the stromal fraction of FP contain cells that in part meet the ISCT criteria for MSCs, but may also harbour a sub-population that do not i.e. those with CD14 positivity. CD14 positivity has previously been reported on BM-MSCs³¹, but not FP-MSCs or SF-MSCs to date. Macrophage-like synoviocytes, which are also positive for CD14, are a likely contaminant sub-population contributing to the heterogeneity of our cultures^{32,33}. SF is known to contain CD14 positive macrophages that secrete pro-inflammatory cytokines, such as IL-1 and TNF- α , that induce enzyme-mediated cartilage degradation^{34,35}. Furthermore, there is increased detectable soluble CD14 in the SF of osteoarthritic patients³⁶. Hence, the positive association of CD14 in SF-MSCs and advancing age could be indicative of an increase in pro-inflammatory conditions in the degenerative joints of older subjects^{37–39}.

No single surface marker that we investigated allowed a clear distinction between FP-MSCs and SF-MSCs, which suggests that a broader panel of markers would be required in order to distinguish between these two cell types. Recent guidelines from the ISCT and the International Federation for Adipose Therapeutics and Science now accept CD34 as being positive on adipose stromal cells⁴⁰. CD34 positive cells in FP-MSCs and other ASCs cultures^{41,42}, are likely to represent subpopulations of either vascular endothelial lineages, pericytes or a mixture of the two, as found in cells isolated from subcutaneous liposarcoma³⁴. Further work would be required to isolate and phenotypically characterise these CD34 positive cells within adipose tissues to assess their function in native and transplanted tissues.

In addition to surface antigens and differentiation characterisation criteria, the need to understand the immunological properties of MSCs is becoming crucial to the development of cell therapies^{14,43}, particularly in the treatment of conditions which involve inflammatory elements as is the case for OA^{44,45}. APCs interact with T cells via MHC class II molecules, such as HLA-DR, to trigger an alloresponse⁴⁶. This reaction involves the activation, differentiation and proliferation of T cells but is not possible without the expression of costimulatory surface molecules⁴⁷. The results we present here are the first to show an increased positivity of MHC class II and a lack of expression of costimulatory molecules on matched FP-MSCs and SF-MSCs in response to an *in vitro* inflammatory stimulus. BM-MSCs stimulated with IFN- γ have been shown to produce levels of HLA-DR that are comparable to our observations with FP-MSCs²⁰. Conversely, the immunoprofile of IFN- γ induced HLA-DR on SF-MSCs was much lower, perhaps indicating that SF-MSCs are less immunogenic following inflammatory stimulation and hence display a distinct immunological phenotype compared to FP-MSCs and also BM-MSCs. This is the first time, to our knowledge, that a difference in positivity for HLA-DR on stimulated MSCs derived from the same joint has been reported and requires further investigation. Inflammation of the knee, due to elevated levels of pro-inflammatory molecules, has been reported to increase with age^{39,48}. Our results indicate an increasing trend with age in the production of HLA-DR by FP-MSCs after exposure to IFN- γ . It could be hypothesised that the inflammatory nature of the FP is increased with age and in turn pre-conditions the endogenous MSC niche to respond to IFN- γ by augmenting HLA-DR positivity. The reason why this correlation was not reproduced in the SF-MSCs derived from the same joints remains undetermined, but this observation highlights another biological difference between the two cell populations. *In vivo* investigations evaluating the general effects of natural aging and inflammation on MSC pools within the human knee joint could not only elucidate the cellular pathways involved in the pathogenesis of chronic joint diseases, but may also reveal potential therapeutic targets

(genetic, molecular or cellular) to counter the degenerative processes. Despite the presence of HLA-DR on FP- and SF-MSCs in this study, these cells cannot be considered as truly immunogenic without an accompanying increase in the production of costimulatory markers^{47,49}.

It is perhaps also noteworthy that the only donor included in this study observed in surgery to have a 'severely inflamed' infrapatellar fat pad (donor 2) produced FP-MSCs and SF-MSCs which showed the most pronounced response to an inflammatory stimulus. We suggest that cells derived from such severely inflamed joints are 'primed' to be more responsive to inflammatory stimuli, but we appreciate that a larger cohort of donors with better defined (macroscopic and histologically quantified) tissues would be required to confirm this hypothesis.

The immunosuppressive properties of SF-MSCs have been demonstrated in mixed lymphocyte reactions⁵⁰, but the constitutive production of HLA-G in FP-MSCs and SF-MSCs has not been reported previously. A similar level of HLA-G production has, however, been observed in both BM-MSCs and UC-MSCs^{17,20}. HLA-G positive UC-MSCs have been shown to inhibit the proliferation of pro-inflammatory T helper 1 cells, which are present in OA joints⁵¹, and promote the expansion of anti-inflammatory regulatory T cells. Further, we have demonstrated that the production of IDO can be induced in both cell populations by an inflammatory stimulus, comparable to BM-MSC and ASC cultures^{52,53}. In a collagen induced arthritis mouse model, IDO deficiency was associated with a high incidence of arthritis and pronounced T cell infiltration⁵⁴. The pro-inflammatory conditions within the OA joint could potentially activate the local MSC populations to dampen the influence of certain immune cells such as T cells and macrophages. The present study suggests that FP-MSCs and SF-MSCs may be considered as immunomodulatory cells but they would require more in depth *in vitro* functional testing alongside BM-MSCs to fully assess their therapeutic value in this respect. Others have shown that conditioned media derived from BM-MSCs that were stimulated with IFN- γ and TNF- α , reduced the gene expression of pro-inflammatory and cartilage degrading molecules in synovial and cartilage explants *in vitro*⁵⁵. This trophic feature remains largely undefined in FP- and SF-MSCs but may provide insight into the possible mechanism of action that these cells might have in an arthritic joint.

The use of donor matched samples in our investigations has allowed us to better identify and analyse donor-specific variability. Tissue source appears to be more influential on the proliferative and differentiation properties of joint derived MSCs than the donors themselves or related factors. The reasons for this are still unclear. An increase in donor age, for example, is known to negatively affect the differentiation potential and growth rate of BM-MSCs⁵⁶ and subcutaneous ASCs¹², but this does not seem to apply for the FP- and SF-MSCs observed in our study.

Donors included in this study were predominantly patients with chondral defects and with early signs of OA. However, one donor was described as having end stage OA and was thus undergoing total joint replacement. This heterogeneity in samples may account for some of the variability observed, but also provides insight into the inherent biological differences in donors that should be considered in the development of new cartilage repair strategies.

Conclusion

We have characterised the phenotype and have identified biological distinctions between MSCs sourced from the FP and SF within the same articular joint. We have confirmed that there is obvious potential for the use of FP-MSCs or SF-MSCs in the treatment of cartilage defects following *ex-vivo* expansion. However, it may be more advantageous to find means of recruiting these resident MSCs with chondrogenic potency from their respective niches *in vivo*, as opposed to current methods of transplanting expanded cells. The advantage of this approach would be that the significant costs and regulatory hurdles involved with the *in vitro* manufacturing of cells may be circumvented.

Further, we have shown that the levels of CD14 on SF-MSCs and the inducibility of HLA-DR on FP-MSCs are possibly due to age-related inflammation. We confirm for the first time, an immunomodulatory capacity for FP- and SF-MSCs which confers further therapeutic value to these cells with regards to treating the inflammatory aspect of OA. This also highlights the need to understand the physiological inflammatory conditions into which transplanted cells are placed and how this could affect the outcome of a cellular treatment. FP-MSCs and SF-MSCs may not realistically be suited for large-scale allogeneic therapies due to limited sample availability and low cell numbers, but certainly represent sources of autologous cells for cartilage regeneration in addition to sourcing chondrocytes from healthy cartilage, as is used currently. Further investigations will seek to understand how these MSCs can be directed to effect repair endogenously either by means of dampening down inflammatory processes or by producing repair cartilage themselves or even by encouraging reparative cellular recruitment.

Methods

Isolation and culture of FP-MSCs and SF-MSCs. All samples were obtained after patients had provided written informed consent; favourable ethical approval was given by the National Research Ethics Service (11/NW/0875) and all experiments were performed in accordance with relevant guidelines and regulations. FP and joint SF were obtained from 6 patients (3 males and 3 females, ages 35–79 years) undergoing either total knee replacement or ACI surgery. At the time of surgery a macroscopic observation of inflammatory state of the FP was made by the operating surgeon and is shown in Table 1, along with all other donor demographics. The FP was dissected from the deepest zone, to avoid contamination with synovium derived cells. To confirm clear dissection of the two tissues, portions of selected samples were fixed and processed for paraffin wax embedding and routine histological study via haematoxylin and eosin staining. FP tissue was washed in phosphate buffered saline (PBS, Life Technologies Paisley, UK), minced into 2–3 mm³ pieces and digested with 1 mg/ml collagenase type I (≥ 125 digesting units/mg, Sigma-Aldrich, Poole, UK) in Dulbecco's Modified Eagle's Medium/F-12 (DMEM/F-12, Life Technologies) with 1% (v/v) penicillin/streptomycin (P/S) (Life Technologies) for 1 h at 37 °C. The resulting cells were strained through a 40 μ m nylon cell strainer and centrifuged (350g for 10 min). Cells were then seeded at a

density of 5000 cells/cm² in the above media supplemented with 10% (v/v) foetal calf serum (Life Technologies). FP was prepared for histology via paraffin embedding and sectioned at 5 µm using a Shandon SME cryotome (Thermo Scientific Loughborough, UK) and tissue sections were collected onto adhesive slides (Leica Biosystems Surgipath, Nussloch, Germany). Haematoxylin and eosin (H and E) staining was conducted as per standard procedure.

SF was centrifuged (800g for 15 minutes) and the resulting pellet seeded into a T25cm² culture flask. All cultures were maintained at 37 °C and 5% CO₂ in a humidified atmosphere. Media was replaced every 2–3 days. At 70% confluence, growth media was removed and the cells washed with PBS to remove residual serum and media. Cells were then detached with 0.05% (v/v) trypsin-EDTA (Life Technologies) and reseeded at 5000 cells/cm².

Growth Kinetics. The proliferation rate of the cells was evaluated by calculating their DT over ten passages (P). Cells were seeded into T25 cm² flasks at a density of 5000 cells/cm² and allowed to proliferate to 70–80% confluence before trypsinisation and reseeded. The cell population DT was calculated using the following equation:

$$\text{Doubling time} = (t_2 - t_1) \times \frac{\ln(2)}{\ln(n_2/n_1)}$$

where t₂-t₁ is the number of days in culture, n₂ is the number of cells recovered after passage and n₁ is the total number of cells seeded.

Microscopy. Histological sections were viewed by light microscopy (Leitz, Wetzlar, Leica Microsystems GmbH, Germany) using ×6.3, ×25 and ×40 objective lenses and a DS-Fi1 camera (Nikon Corporation, Japan), images were analysed using NIS-Elements BR software version 3.2 (Nikon). Cells in monolayer culture were digitally imaged by phase contrast microscopy using a ×10 objective lens (Nikon Eclipse TS100) and a C4742-9S camera (Hamamatsu, Japan), images were analysed using IPLab v3 software (BD Biosciences).

Flow cytometry Immunoprofiling. Flow cytometry was used to assess the immunoprofile of MSCs derived from FP and SF. Cells at P3–4 were harvested, pelleted, and re-suspended in 2% bovine serum albumin (BSA, Sigma-Aldrich, Poole, UK) in PBS. FC receptors were blocked for 1 h at 4 °C using 10% (v/v) human IgG (Grifols, UK) with 2% BSA in PBS. The cells were then washed with 2% (v/v) BSA in PBS and centrifuged (350g for 8 minutes). Cells were stained for (30 minutes at 4 °C) with fluorochrome conjugated antibodies against CD90-phycoerythrin (PE) (clone 5E10), CD105-allophycocyanin (APC) (clone 266), and CD73-brilliant violet 421 (BV421) (clone AD2) (BD Biosciences, Oxford, UK). A commercially available pre-mixed cocktail of PE-conjugated antibodies was initially used for the detection of markers CD11b (clone ICRF44), CD19 (clone HIB19), CD34 (clone 581), CD45 (clone HI30) and HLA-DR (clone TU36) (BD Biosciences) on FP-MSCs and SF-MSCs. Further staining for individual markers was performed for FP-MSCs with fluorochrome conjugated antibodies against CD11b-PE, CD19-BV421, CD34-APC, CD45-PE and HLA-DR-APC (clones stated previously) (BD Biosciences). The expression of CD14 was assessed using a peridinin chlorophyll protein-cyanine5.5 (PercP-Cy5.5) conjugated antibody (clone MφP9) (BD Biosciences). Appropriate isotype-matched IgG controls were used throughout (BD Biosciences). Data from 10,000 stained cells is presented which was collected using a FACSCanto II flow cytometer (BD Biosciences) and analysed using BD FACSDiva v.7.0.

Differentiation assays. The multipotency of FP-MSCs and SF-MSCs at P3 was assessed using osteogenic, adipogenic and chondrogenic differentiation protocols. The osteogenic, and adipogenic differentiation of FP-MSCs and SF-MSCs was investigated using monolayer cultures. Cells were seeded at a density of 5 × 10³/cm² in 24 well plates (Sarstedt, Nümbrecht, Germany), and fed the appropriate differentiation medium, either osteogenic or adipogenic medium for 21 days. Osteogenic differentiation medium contained DMEM F12, FCS (10%), β-glycerophosphate (10 mM), dexamethasone (10 nM) and L-ascorbic-acid (50 µM). Adipogenic differentiation medium contained DMEM F12, FCS (10%), Insulin-transferrin-selenium-X (ITS) (1%) (Gibco UK), isobutylmethylxanthine (0.5 µM) (Sigma, UK), dexamethasone (1 µM) and indomethacin (100 µM). For control cultures, media containing DMEM F12, FCS (10%) and P/S was used. To evaluate the differentiation, cells were fixed with buffered formalin and stained with oil red-O for 1 h to assess lipid formation for adipogenesis or naphthol-AS-BI phosphate and fast red for 1 h to assess alkaline phosphatase activity for osteogenesis.

A pellet culture system (2 × 10⁵ cells/pellet) was used to assess chondrogenic differentiation potential. Cells (2 × 10⁵) were centrifuged in sterile 1.5 ml microcentrifuge tubes with DMEM F12, FBS (10% v/v), P/S (1%) ITS (1%, v/v), ascorbic-acid (0.1 mM) (Sigma-Aldrich), dexamethasone (10nM) and transforming growth factor β-1 (TGF-β1, PeproTech, London, UK) (10 ng/ml)⁵⁷. After 21 days, cell pellets were snap frozen in liquid nitrogen and stored at –80 °C prior to use. Pellets were cryosectioned (7 µM) onto poly-L-lysine coated slides (Cell Path, Newtown, UK) and stained for glycosaminoglycans (GAG) with toluidine blue (BDH) metachromatic stain. Sections were stained with toluidine blue for 30 seconds and then washed briefly in tap water. Slides were left to air dry before mounting in Pertex (Cell Path).

Interferon-γ stimulation. The immunogenic nature of FP-MSCs and SF-MSCs was investigated by assessing the presence of the costimulatory markers CD40, CD80, CD86, and the class II Major Histocompatibility Complex (MHC), HLA-DR, after stimulation with the pro-inflammatory cytokine IFN-γ (20 units/ng, PeproTech). Cells at P3 were treated with culture medium containing either 25 ng/ml (low concentration) or 500 ng/ml (high concentration) of IFN-γ for 48 h. Untreated cells grown in standard culture

medium were used as controls for comparison. After 48 h, cells were prepared for flow cytometry as described previously with PE-conjugated antibodies against CD40, CD80, CD86 (BD Biosciences) and HLA-DR (Immuntools, Friesoythe, Germany). HLA-G was assessed via flow cytometry using antibodies against surface and intracellular antigens (Santa-cruz, Texas, USA), using a Cytofix/Cytoperm™ and Fixation/Permeabilisation Kit (BD Biosciences) to the manufacturer's recommendations.

Western blotting for IDO detection. The production of IDO in cells at P3 was evaluated before and after stimulation with IFN- γ using western blotting. Cells were lysed with cold lysis buffer (100 μ l lysis buffer per 1×10^6 cells) containing 0.005% Tween 20, 0.5% Triton X-100 and protease inhibitors (Sigma-Aldrich, UK) at 4 °C, and kept at -20 °C until further use. After quantification of total protein using the bicinchoninic acid (BCA) assay (Life Technologies), 20 μ g of each sample was loaded into pre-cast NuPAGE® 4–12% Bis-Tris gels (Life Technologies). An iBlot and transfer stacks system (Life Technologies) was used to transfer proteins onto nitrocellulose membranes. Primary and secondary antibodies employed to detect IDO were used at dilutions of 1:250 and 1:125, respectively, in antibody diluent. The primary antibody (Abcam, Cambridge, UK), against IDO, was applied first to the membrane, then the secondary antibody (1:125, Life Technologies) which was conjugated to horseradish peroxidase. Membranes were washed three times with a wash solution (Life Technologies), then twice with autoclaved water. A chromogenic substrate solution, NovexR Alkaline Phosphatase (Life Technologies), was added to the membranes, after which colour development was allowed for no longer than an hour. Membranes were washed again in autoclaved water before being allowed to dry in the dark prior to imaging.

Statistical analyses. Statistical analyses were performed using GraphPad Prism (GraphPad Software, California, USA) and R (The R Foundation, Vienna, Austria). The Shapiro–Wilk test was used to assess the normal distribution of numerical data. The mean doubling times of FP-MSCs and SF-MSCs were compared using a two-way ANOVA with Bonferroni's multiple comparisons tests, while a hierarchical regression analysis was used to determine the effect of donor, cell source and passage number on DT. A paired Student's *t*-test was used to compare means and a Pearson's test was used to establish correlations where appropriate. Graphs are shown as means \pm standard error of the mean (SEM). Statistical significance was considered at **p* < 0.05, ***p* < 0.01 and ****p* < 0.001.

References

1. Brittberg, M. *et al.* Treatment of deep cartilage defects in the knee with autologous chondrocyte transplantation. *N. Engl. J. Med.* **331**, 889–895 (1994).
2. Bhosale, A. M., Kuiper, J. H., Johnson, W. E. B., Harrison, P. E. & Richardson, J. B. Midterm to long-term longitudinal outcome of autologous chondrocyte implantation in the knee joint: a multilevel analysis. *Am. J. Sports Med.* **37**, 131S–138S (2009).
3. LaPrade, R. F. & Botker, J. C. Donor-site morbidity after osteochondral autograft transfer procedures. *Arthroscopy* **20**, e69–73 (2004).
4. Matricali, G. A., Dereymaeker, G. P. E. & Luyten, F. P. Donor site morbidity after articular cartilage repair procedures: a review. *Acta Orthop. Belg.* **76**, 669–674 (2010).
5. Paul, J. *et al.* Donor-site morbidity after osteochondral autologous transplantation for lesions of the talus. *J. Bone Joint Surg. Am.* **91**, 1683–1688 (2009).
6. Jones, E. A. *et al.* Enumeration and phenotypic characterization of synovial fluid multipotential mesenchymal progenitor cells in inflammatory and degenerative arthritis. *Arthritis Rheum.* **50**, 817–827 (2004).
7. Jones, E. A. *et al.* Synovial fluid mesenchymal stem cells in health and early osteoarthritis: detection and functional evaluation at the single-cell level. *Arthritis Rheum.* **58**, 1731–1740 (2008).
8. Sekiya, I. *et al.* Human mesenchymal stem cells in synovial fluid increase in the knee with degenerated cartilage and osteoarthritis. *J. Orthop. Res.* **30**, 943–949 (2012).
9. Zhang, S., Muneta, T., Morito, T., Mochizuki, T. & Sekiya, I. Autologous synovial fluid enhances migration of mesenchymal stem cells from synovium of osteoarthritis patients in tissue culture system. *J. Orthop. Res.* **26**, 1413–1418 (2008).
10. Aksu, A. E., Rubin, J. P., Dudas, J. R. & Marra, K. G. Role of gender and anatomical region on induction of osteogenic differentiation of human adipose-derived stem cells. *Ann. Plast. Surg.* **60**, 306–322 (2008).
11. Payne, K. A., Didiano, D. M. & Chu, C. R. Donor sex and age influence the chondrogenic potential of human femoral bone marrow stem cells. *Osteoarthritis Cartilage* **18**, 705–713 (2010).
12. Choudhery, M. S., Badowski, M., Muise, A., Pierce, J. & Harris, D. T. Donor age negatively impacts adipose tissue-derived mesenchymal stem cell expansion and differentiation. *J. Transl. Med.* **12**, 8 (2014).
13. Dominici, M. *et al.* Minimal criteria for defining multipotent mesenchymal stromal cells. The International Society for Cellular Therapy position statement. *Cytotherapy* **8**, 315–318 (2006).
14. Krampera, M., Galipeau, J., Shi, Y., Tarte, K. & Sensebe, L. Immunological characterization of multipotent mesenchymal stromal cells—The International Society for Cellular Therapy (ISCT) working proposal. *Cytotherapy* **15**, 1054–1061 (2013).
15. Krampera, M. *et al.* Role for interferon-gamma in the immunomodulatory activity of human bone marrow mesenchymal stem cells. *Stem Cells* **24**, 386–398 (2006).
16. Frumento, G. *et al.* Tryptophan-derived catabolites are responsible for inhibition of T and natural killer cell proliferation induced by indoleamine 2,3-dioxygenase. *J. Exp. Med.* **196**, 459–468 (2002).
17. Nasef, A. *et al.* Immunosuppressive effects of mesenchymal stem cells: involvement of HLA-G. *Transplantation* **84**, 231–237 (2007).
18. Le Blanc, K., Tammik, C., Rosendahl, K., Zetterberg, E. & Ringdén, O. HLA expression and immunologic properties of differentiated and undifferentiated mesenchymal stem cells. *Exp. Hematol.* **31**, 890–896 (2003).
19. Li, X. C., Rothstein, D. M. & Sayegh, M. H. Costimulatory pathways in transplantation: challenges and new developments. *Immunol. Rev.* **229**, 271–293 (2009).
20. Deuse, T. *et al.* Immunogenicity and immunomodulatory properties of umbilical cord lining mesenchymal stem cells. *Cell Transplant.* **20**, 655–667 (2011).
21. English, A. *et al.* A comparative assessment of cartilage and joint fat pad as a potential source of cells for autologous therapy development in knee osteoarthritis. *Rheumatology (Oxford)*. **46**, 1676–1683 (2007).
22. Nigrovic, P. A. & Lee, D. M. Mast cells in inflammatory arthritis. *Arthritis Res. Ther.* **7**, 1–11 (2005).
23. Nakamura, H., Yoshino, S., Kato, T., Tsuruha, J. & Nishioka, K. T-cell mediated inflammatory pathway in osteoarthritis. *Osteoarthritis Cartilage*. **7**, 401–402 (1999).

24. de Lange-Brokaar, B. J. E. *et al.* Synovial inflammation, immune cells and their cytokines in osteoarthritis: A review. *Osteoarthr. Cartil.* **20**, 1484–1499 (2012).
25. Banfi, A. *et al.* Proliferation kinetics and differentiation potential of *ex vivo* expanded human bone marrow stromal cells: Implications for their use in cell therapy. *Exp. Hematol.* **28**, 707–715 (2000).
26. Wall, M. E., Bernacki, S. H. & Loboa, E. G. Effects of serial passaging on the adipogenic and osteogenic differentiation potential of adipose-derived human mesenchymal stem cells. *Tissue Eng.* **13**, 1291–1298 (2007).
27. Muraglia, A., Cancedda, R. & Quarto, R. Clonal mesenchymal progenitors from human bone marrow differentiate *in vitro* according to a hierarchical model. *J. Cell Sci.* **113**, 1161–1166 (2000).
28. Lee, D. H. *et al.* Synovial fluid CD34 + CD44 + CD90 + mesenchymal stem cell levels are associated with the severity of primary knee osteoarthritis. *Osteoarthr. Cartil.* **20**, 106–109 (2012).
29. Wickham, M. Q., Erickson, G. R., Gimble, J. M., Vail, T. P. & Guilak, F. Multipotent stromal cells derived from the infrapatellar fat pad of the knee. *Clin. Orthop. Relat. Res.* **412**, 196–212 (2003).
30. Simmons, D. L., Tan, S., Tenen, D. G., Nicholson-Weller, A. & Seed, B. Monocyte antigen CD14 is a phospholipid anchored membrane protein. *Blood* **73**, 284–289 (1989).
31. Pilz, G. *et al.* Human mesenchymal stromal cells express CD14 cross-reactive epitopes. *Cytometry. A* **79**, 635–645 (2011).
32. Klein-Wieringa, I. R. *et al.* The infrapatellar fat pad of patients with osteoarthritis has an inflammatory phenotype. *Ann. Rheum. Dis.* **70**, 851–857 (2011).
33. Van Landuyt, K. B., Jones, E. a, McGonagle, D., Luyten, F. P. & Lories, R. J. Flow cytometric characterization of freshly isolated and culture expanded human synovial cell populations in patients with chronic arthritis. *Arthritis Res. Ther.* **12**, R15 (2010).
34. Bas, S., Gauthier, B. R., Spenato, U., Stingelin, S. & Gabay, C. CD14 is an acute-phase protein. *J. Immunol.* **172**, 4470–4479 (2004).
35. Bondeson, J., Wainwright, S. D., Lauder, S., Amos, N. & Hughes, C. E. The role of synovial macrophages and macrophage-produced cytokines in driving aggrecanases, matrix metalloproteinases, and other destructive and inflammatory responses in osteoarthritis. *Arthritis Res. Ther.* **8**, R187 (2006).
36. Daghestani, H. N., Pieper, C. F. & Kraus, V. B. Soluble macrophage biomarkers indicate inflammatory phenotypes in patients with knee osteoarthritis. *Arthritis Rheumatol. (Hoboken, N.J.)* **67**, 956–65 (2015).
37. Loeser, R. F. Age-Related Changes in the Musculoskeletal System and the Development of Osteoarthritis. *Clin. Geriatr. Med.* **26**, 371–386 (2010).
38. Berenbaum, F. Osteoarthritis as an inflammatory disease (osteoarthritis is not osteoarthrosis!). *Osteoarthritis Cartilage* **21**, 16–21 (2013).
39. Greene, M. A. & Loeser, R. F. Aging-related inflammation in osteoarthritis. *Osteoarthr. Cartil.* **23**, 1966–1971 (2015).
40. Bourin, P. *et al.* Stromal cells from the adipose tissue-derived stromal vascular fraction and culture expanded adipose tissue-derived stromal/stem cells: A joint statement of the International Federation for Adipose Therapeutics and Science (IFATS) and the International So. *Cytotherapy* **15**, 641–648 (2013).
41. Traktuev, D. O. *et al.* A population of multipotent CD34-positive adipose stromal cells share pericyte and mesenchymal surface markers, reside in a periendothelial location, and stabilize endothelial networks. *Circ. Res.* **102**, 77–85 (2008).
42. Lopa, S. *et al.* Donor-matched mesenchymal stem cells from knee infrapatellar and subcutaneous adipose tissue of osteoarthritic donors display differential chondrogenic and osteogenic commitment. *Eur. Cell. Mater.* **27**, 298–311 (2014).
43. Sivanathan, K. N., Gronthos, S., Rojas-Canales, D., Thierry, B. & Coates, P. T. Interferon-gamma modification of mesenchymal stem cells: implications of autologous and allogeneic mesenchymal stem cell therapy in allotransplantation. *Stem Cell Rev.* **10**, 351–375 (2014).
44. Goldring, M. B. & Otero, M. Inflammation in osteoarthritis. *Curr. Opin. Rheumatol.* **23**, 471–478 (2011).
45. Hedbom, E. & Häuselmann, H. J. Molecular aspects of pathogenesis in osteoarthritis: the role of inflammation. *Cell. Mol. Life Sci.* **59**, 45–53 (2002).
46. Epstein, F. H. *et al.* T-Lymphocyte-Antigen Interactions in Transplant Rejection. *N. Engl. J. Med.* **322**, 510–517 (1990).
47. Sayegh, M. H. & Turka, L. A. The role of T-cell costimulatory activation pathways in transplant rejection. *N. Engl. J. Med.* **338**, 1813–1821 (1998).
48. Rübénhagen, R., Schüttrumpf, J. P., Stürmer, K. M. & Frosch, K.-H. Interleukin-7 levels in synovial fluid increase with age and MMP-1 levels decrease with progression of osteoarthritis. *Acta Orthop.* **83**, 59–64 (2012).
49. Hancock, W. W. *et al.* Costimulatory function and expression of CD40 ligand, CD80, and CD86 in vascularized murine cardiac allograft rejection. *Proc. Natl. Acad. Sci. USA.* **93**, 13967–13972 (1996).
50. Maillard, N. *et al.* The immunomodulatory properties of mesenchymal stromal cells isolated from the synovial fluid of human osteoarthritic joints. *Osteoarthr. Cartil.* **22**, S23 (2014).
51. Yamada, H. *et al.* Preferential accumulation of activated Th1 cells not only in rheumatoid arthritis but also in osteoarthritis joints. *J. Rheumatol.* **38**, 1569–75 (2011).
52. Ryan, J. M., Barry, F., Murphy, J. M. & Mahon, B. P. Interferon- γ does not break, but promotes the immunosuppressive capacity of adult human mesenchymal stem cells. *Clin. Exp. Immunol.* **149**, 353–363 (2007).
53. DelaRosa, O. *et al.* Requirement of IFN-gamma-mediated indoleamine 2,3-dioxygenase expression in the modulation of lymphocyte proliferation by human adipose-derived stem cells. *Tissue Eng. Part A* **15**, 2795–806 (2009).
54. Criado, G., Šimelyte, E., Inglis, J. J., Essex, D. & Williams, R. O. Indoleamine 2,3 dioxygenase-mediated tryptophan catabolism regulates accumulation of Th1/Th17 cells in the joint in collagen-induced arthritis. *Arthritis Rheum.* **60**, 1342–1351 (2009).
55. van Buul, G. M. *et al.* Mesenchymal stem cells secrete factors that inhibit inflammatory processes in short-term osteoarthritic synovium and cartilage explant culture. *Osteoarthr. Cartil.* **20**, 1186–1196 (2012).
56. Mareschi, K. *et al.* Expansion of mesenchymal stem cells isolated from pediatric and adult donor bone marrow. *J. Cell. Biochem.* **97**, 744–754 (2006).
57. Mackay, A. M. *et al.* Chondrogenic differentiation of cultured human mesenchymal stem cells from marrow. *Tissue Eng.* **4**, 415–428 (1998).

Acknowledgements

This work was supported by the Engineering and Physical Sciences Research Council and the Arthritis Research UK Tissue Engineering Centre grant 19429 and equipment grant 20253. We also acknowledge Nigel Harness, Martin Pritchard and Pat Evans at the Histopathology Lab at the RJA Orthopaedic Hospital for their assistance with the sectioning of fat samples and Annie Kerr for obtaining patient consent for this study.

Author Contributions

J.G., K.W., S.R. and C.M. designed the study. J.G. and C.M. conducted the experiments. J.R. provided samples for the study. J.G., K.W., S.R., J.H.K., C.h.M. and C.M. contributed to the analysis of the data. All authors contributed to the drafting of manuscript. All of the authors declare that they have no competing financial interests.

Additional Information

Supplementary information accompanies this paper at <http://www.nature.com/srep>

Competing financial interests: The authors declare no competing financial interests.

How to cite this article: Garcia, J. *et al.* Characterisation of synovial fluid and infrapatellar fat pad derived mesenchymal stromal cells: The influence of tissue source and inflammatory stimulus. *Sci. Rep.* **6**, 24295; doi: 10.1038/srep24295 (2016).



This work is licensed under a Creative Commons Attribution 4.0 International License. The images or other third party material in this article are included in the article's Creative Commons license, unless indicated otherwise in the credit line; if the material is not included under the Creative Commons license, users will need to obtain permission from the license holder to reproduce the material. To view a copy of this license, visit <http://creativecommons.org/licenses/by/4.0/>

Research Article

Chondrogenic Potency Analyses of Donor-Matched Chondrocytes and Mesenchymal Stem Cells Derived from Bone Marrow, Infrapatellar Fat Pad, and Subcutaneous Fat

John Garcia, Claire Mennan, Helen S. McCarthy, Sally Roberts, James B. Richardson, and Karina T. Wright

ISTM, Keele University, Robert Jones and Agnes Hunt Orthopaedic Hospital NHS Foundation Trust, Oswestry, Shropshire SY10 7AG, UK

Correspondence should be addressed to Karina T. Wright; karina.wright@rjah.nhs.uk

Received 22 July 2016; Accepted 4 September 2016

Academic Editor: Wesley N. Sivak

Copyright © 2016 John Garcia et al. This is an open access article distributed under the Creative Commons Attribution License, which permits unrestricted use, distribution, and reproduction in any medium, provided the original work is properly cited.

Autologous chondrocyte implantation (ACI) is a cell-based therapy that has been used clinically for over 20 years to treat cartilage injuries more efficiently in order to negate or delay the need for joint replacement surgery. In this time, very little has changed in the ACI procedure, but now many centres are considering or using alternative cell sources for cartilage repair, in particular mesenchymal stem cells (MSCs). In this study, we have tested the chondrogenic potential of donor-matched MSCs derived from bone marrow (BM), infrapatellar fat pad (FP), and subcutaneous fat (SCF), compared to chondrocytes. We have confirmed that there is a chondrogenic potency hierarchy ranging across these cell types, with the most potent being chondrocytes, followed by FP-MSCs, BM-MSCs, and lastly SCF-MSCs. We have also examined gene expression and surface marker profiles in a predictive model to identify cells with enhanced chondrogenic potential. In doing so, we have shown that Sox-9, Alk-1, and Coll X expressions, as well as immunopositivity for CD49c and CD39, have predictive value for all of the cell types tested in indicating chondrogenic potency. The findings from this study have significant clinical implications for the refinement and development of novel cell-based cartilage repair strategies.

1. Introduction

Autologous chondrocyte implantation (ACI) for the treatment of focal chondral and/or osteochondral lesions has changed very little since its inception [1], but there remains scope for improvement. While we and others have reported a significant level of improved joint function and a reduction in pain following treatment with ACI [2–4], disadvantages such as cost, potential donor-site morbidity, and the quality of repair tissue formed remain. Although we have shown donor-site morbidity to be minimal [5], there is also the added risk of chondrocyte dedifferentiation during culture expansion [6, 7], the extent of which is likely to impact on the ability of the chondrocytes to redifferentiate upon implantation into the defect site.

Mesenchymal stem cells (MSCs) isolated from the bone marrow (BM-MSCs) have been used in several clinical trials

as an alternative cell source for use in cell therapies to treat cartilage injuries and osteoarthritis [8–10]. The process of acquiring a sample of bone marrow, however, results in an additional, painful procedure for the patient. The infrapatellar fat pad (FP) is often routinely removed and disposed of as surgical waste during arthroscopy or open knee surgery and may provide an accessible alternative source of MSCs (FP-MSCs) with demonstrable chondrogenic capacity *in vitro* [11, 12]. Another accessible source of MSCs, although studied to a lesser extent for their chondrogenic propensity, is MSCs derived from subcutaneous fat (SCF-MSCs) [13, 14]. The ability to utilise these tissues for the treatment of cartilage injuries has the potential to improve the way we currently treat patients.

An important factor to consider when comparing and contrasting the properties of different cell types is the “donor impact” as donor demographics, such as age and gender, are

TABLE 1: Donor demographics.

ID	Gender	Age (years)	Pathology
Donor 1	Male	71	OA with extensive joint degeneration
Donor 2	Female	67	OA with loss of joint space
Donor 3	Female	75	Patellofemoral OA and loss of joint space in medial compartment
Donor 4	Female	81	OA
Donor 5	Male	74	OA with joint stiffness

factors which are known to affect cell proliferation and differentiation capacity [15–17]. The impact of donor is particularly critical for autologous treatment regimes and in deciding whether such a cell-based therapy represents the appropriate treatment option for an individual patient. Unravelling the impact of tissue and donor source and developing tools to predict the efficacy of cell-based treatments will likely result in the refinement of existing treatments and may provide valuable additional information for consideration during the decision making process of cost benefit versus clinical efficacy.

In this study, we have examined 4 different cell types (chondrocytes, BM-MSCs, FP-MSCs, and SCF-MSCs) and tested the chondrogenic potential of each population of cells. This study compares donor-matched cell types and was designed to establish the impact of tissue source and donor on chondrogenic differentiation capacity and to continue the process of establishing a marker panel indicative of chondrogenic potency and likely clinical success. Such marker(s) could be screened for and used in the selection of a particular cell type and/or subpopulation of cells with enhanced chondrogenic capability prior to treatment. We envisage that taken together this information could significantly improve the success of cell-based therapies for cartilage injuries and perhaps even lead to the development of novel individualised treatments for cartilage repair.

2. Materials and Methods

2.1. Patients. All samples were obtained after patients had provided written informed consent; favourable ethical approval was given by the National Research Ethics Service (11/NW/0875) and all experiments were performed in accordance with relevant guidelines and regulations. Donor-matched samples of cartilage, BM, FP, and SCF were obtained from 5 patients (2 males and 3 females, ages 67–81 years) undergoing total knee replacement (TKR) surgery (Table 1).

2.2. Isolation of Chondrocytes. Macroscopically normal articular cartilage was excised from the femoral condyles of patients undergoing TKR. Cartilage tissue was weighed, minced into small pieces with a sterile scalpel, and digested in collagenase type II (250 IU/mg dry weight, Worthington, New Jersey, USA) for 16 hours at 37°C. The resulting suspension was passed through a 40 µm cell strainer and centrifuged (350 ×g for 10 minutes) to produce a cell pellet that was resuspended in Dulbecco's Modified Eagle's Medium/F-12

(DMEM/F-12) with 1% (v/v) penicillin/streptomycin (P/S) and 10% (v/v) foetal calf serum (FCS, all Life Technologies, Paisley, UK), hereafter referred to as complete culture medium, at a seeding density of $5 \times 10^3/\text{cm}^2$.

2.3. Isolation of MSCs from Bone Marrow. Bone marrow aspirates and bone chips were obtained from the tibial plateau of patients undergoing TKR. Bone marrow was first diluted with an equal volume of phosphate buffered saline (PBS, Life Technologies) then split between two 50 mL tubes, layered onto 10 mL of Lymphoprep™ (Alere Technologies AS, Oslo, Norway), and centrifuged (900 ×g for 20 minutes). The buffy coat, containing mononuclear cells, was aspirated and added to complete culture medium and centrifuged (750 ×g for 10 minutes). The resulting cell pellet was resuspended in complete culture medium and BM-MSCs were seeded at a density of 20 million cells per 75 cm² tissue culture flask. Cells were left to adhere for 24 hours before the media were changed and the nonadherent cells were removed. Bone chips were placed in a 175 cm² culture flask with 30 mL of complete media for 7 days to allow the plastic adherent cells to migrate out of the bone chips.

2.4. Isolation of MSCs from Adipose Tissues. Human FP and SCF tissue samples were obtained from patients and processed within 2 hours of receipt from the operating theatre. The FP was dissected from the innermost zone, to avoid contamination with synovium derived cells as described previously [12]. Dissected FP and SCF tissues were washed in PBS, minced, and digested with 1 mg/mL collagenase type I (≥ 125 digesting units/mg, Sigma-Aldrich, Poole, UK) in serum-free media for 1 h at 37°C. The resulting cells were strained through a 40 µm nylon cell strainer and centrifuged (350 ×g for 10 min). Cells were then seeded at a density of $5 \times 10^3/\text{cm}^2$ in complete culture medium. All cultures were maintained in a humidified incubator at 37°C and 5% CO₂.

2.5. RNA Extraction and Quantitative Real-Time Polymerase Chain Reaction (qRT-PCR). After trypsinisation at passages 3–4, 2×10^5 monolayer cells were centrifuged (500 ×g for 5 minutes), frozen in liquid N₂, and stored at –80°C briefly prior to extraction. Cells were thawed on ice and messenger RNA (mRNA) was extracted using an RNeasy® extraction kit (Qiagen, Hilden, Germany) according to the manufacturer's recommendations. RNA was converted to cDNA using a High-Capacity cDNA Reverse Transcriptase Kit® (Applied Biosystems, Warrington, UK) according to the

manufacturer's instructions. qRT-PCR was used to evaluate the expression of specific genes, indicative of chondrogenic potency or hypertrophy [18]. RT-qPCR analysis was performed on the Quant Studio 3 Real-Time Quantitative PCR System (Applied Biosystems) using SYBR green QuantiTect primer assays for the chondrogenic genes Sox-9, collagen type II (Coll II), aggrecan (ACAN), frizzled-related protein (FRZB), and the following genes indicative of hypertrophy: activin receptor-like kinase 1 (Alk-1) and collagen type X (Coll X). Peptidylprolyl isomerase A (PPIA) and TATA-binding protein (TBP) were used as reference genes (Qiagen). The relative expression of each gene was determined using the comparative C_T method [19].

2.6. Flow Cytometry. Flow cytometry was used to assess the immunoprofile of chondrocytes and MSCs prior to chondrogenic differentiation. Cells at passages 3-4 were harvested, pelleted, and resuspended in 2% bovine serum albumin (BSA, Sigma-Aldrich) in PBS. FC receptors were blocked for 1 h at 4°C using 10% (v/v) human IgG (Grifols, Barcelona, Spain) in 2% (v/v) BSA in PBS (immunobuffer). The cells were then washed with immunobuffer and centrifuged (350 ×g for 8 minutes). Cells were stained for 30 minutes at 4°C with fluorochrome conjugated antibodies against cell surface markers indicative of MSC according to the International Society for Cellular Therapy (ISCT) [20]. Markers probed for were CD90-phycoerythrin (PE) (clone 5E10), CD105-allophycocyanin (APC) (clone 266), and CD73-brilliant violet 421 (BV421) (clone AD2), CD19-BV421 (clone HIB19), CD34-APC (clone 581), CD45-PE (clone HI30), HLA-DR-APC (clone TU36), and CD14-PerCP-Cy5.5 (clone MφP9). CD markers which have been reported as putative chondrogenic potency markers [21–28] were also probed for; these included CD49c-PE (clone C3 II.1), CD166-BV421 (clone 3A6), CD39-APC (clone TU66), CD44-peridinin chlorophyll protein-cyanine 5.5 (PerCp-Cy5.5) (clone G44-26), and CD271-BV421 (clone C40-1457) (BD Biosciences). Appropriate isotype-matched IgG controls were used throughout (BD Biosciences). Data from at least 10,000 stained cells is presented which was analysed using a FACSCanto II flow cytometer (BD Biosciences) and BD FACSDiva v.7.0 software.

2.7. Chondrogenic Differentiation. The chondrogenic potential of all cultured cell populations was assessed at passage 4 using an established 3D pellet culture system [12, 29]. Briefly, 2×10^5 cells were centrifuged to produce a cell pellet which was maintained in DMEM F12, FBS (10% v/v), P/S (1%) ITS (1%, v/v), ascorbic acid (0.1 mM) (Sigma-Aldrich), dexamethasone (10 nM), and transforming growth factor β -1 (TGF- β 1, PeproTech, London, UK) (10 ng/mL). After 28 days, cell pellets were frozen in liquid nitrogen and stored at -80°C prior to use. In total, $n = 6$ pellets per donor were produced, $n = 3$ for glycosaminoglycan (GAG)/DNA analysis and $n = 3$ for histological analysis.

2.8. GAG/DNA Analysis of Chondrogenic Pellets. Pellets were digested using papain to release GAGs and DNA. A digestion buffer consisting of 50 mM sodium phosphate (BDH), 2 mM

EDTA (Sigma-Aldrich), and 20 mM N-acetyl cysteine (BDH) was prepared and the pH adjusted to 6. Papain (Sigma-Aldrich) was added to the digestion buffer to reach a final concentration of 125 $\mu\text{g}/\text{mL}$. Each chondrogenic pellet was digested using 200 μL of papain digest solution and placed in a 60°C oven for 3 hours. The digest suspensions were mixed vigorously every 30 minutes by vortexing the tubes. Samples were then centrifuged at 1000 ×g for 5 mins, aliquoted, and stored at -20°C until further use.

The dimethylmethylene blue (DMMB) assay was used to quantitate GAGs [30, 31]. Standards were prepared by dissolving chondroitin sulphate (Sigma-Aldrich) from bovine trachea in PBS to create appropriate serial dilutions. Fifty microlitres of sample or standard was added in triplicate to a 96-well plate and 200 μL of the DMMB staining solution was added to each well. The absorbance was immediately read at $A_{530\text{ nm}}$ and $A_{590\text{ nm}}$. A standard curve was plotted $(A_{530\text{ nm}}/A_{590\text{ nm}}) - (A_{530\text{ nm blank}}/A_{590\text{ nm blank}})$, from which the total GAG content in each sample was calculated using the equation of the curve.

The PicoGreen® fluorescence assay (Invitrogen) was used to quantitate the amount of double stranded DNA in solution and was conducted according to the manufacturer's instructions. Fluorescence was read on a plate reader configured to excitation = 480 nm and emission = 520 nm. The normalisation of GAG content in chondrogenic pellets was achieved by dividing the total GAG content of a given pellet by the DNA content of that same pellet.

2.9. Histological Analysis of Chondrogenic Pellets. Pellets were cryosectioned (7 μm) onto poly-L-lysine coated slides (Cell Path, Newtown, UK) and stained for GAGs with toluidine blue (BDH) metachromatic stain for 30 seconds and then washed briefly in tap water. Slides were left to air dry before mounting in Pertex (Cell Path). Chondrogenic pellets were assessed following toluidine blue staining using a modified version of the Bern score [32]. In brief, cells pellets were assessed using the following criteria: uniformity and intensity of toluidine blue staining and distance between cells/amount of matrix produced and cell morphology. Each of these three categories was scored from 0 to 3.

2.10. Statistical Analysis. The Shapiro-Wilk normality test was used to assess the distribution of quantitative data. A one-way ANOVA with Bonferroni's multiple comparisons test was used to test for significant differences between cell types with regard to gene expression, immunoprofile, GAG quantitation, and histological scores for chondrogenic pellets. Pearson's correlation coefficients were determined for gene-gene expression analyses and chondrogenic assessments (GAG quantitation and histological analyses). Multilevel modelling was conducted to determine whether gene expression and cell surface marker positivity were predictors of chondrogenic outcome as measured by GAG content of the pellet and histological scoring. In these models, cell source, gene expression, and cell surface marker positivity were considered as fixed effects, while the donor was considered as a random effect. The donor effect was determined using Wald's tests. Graphs

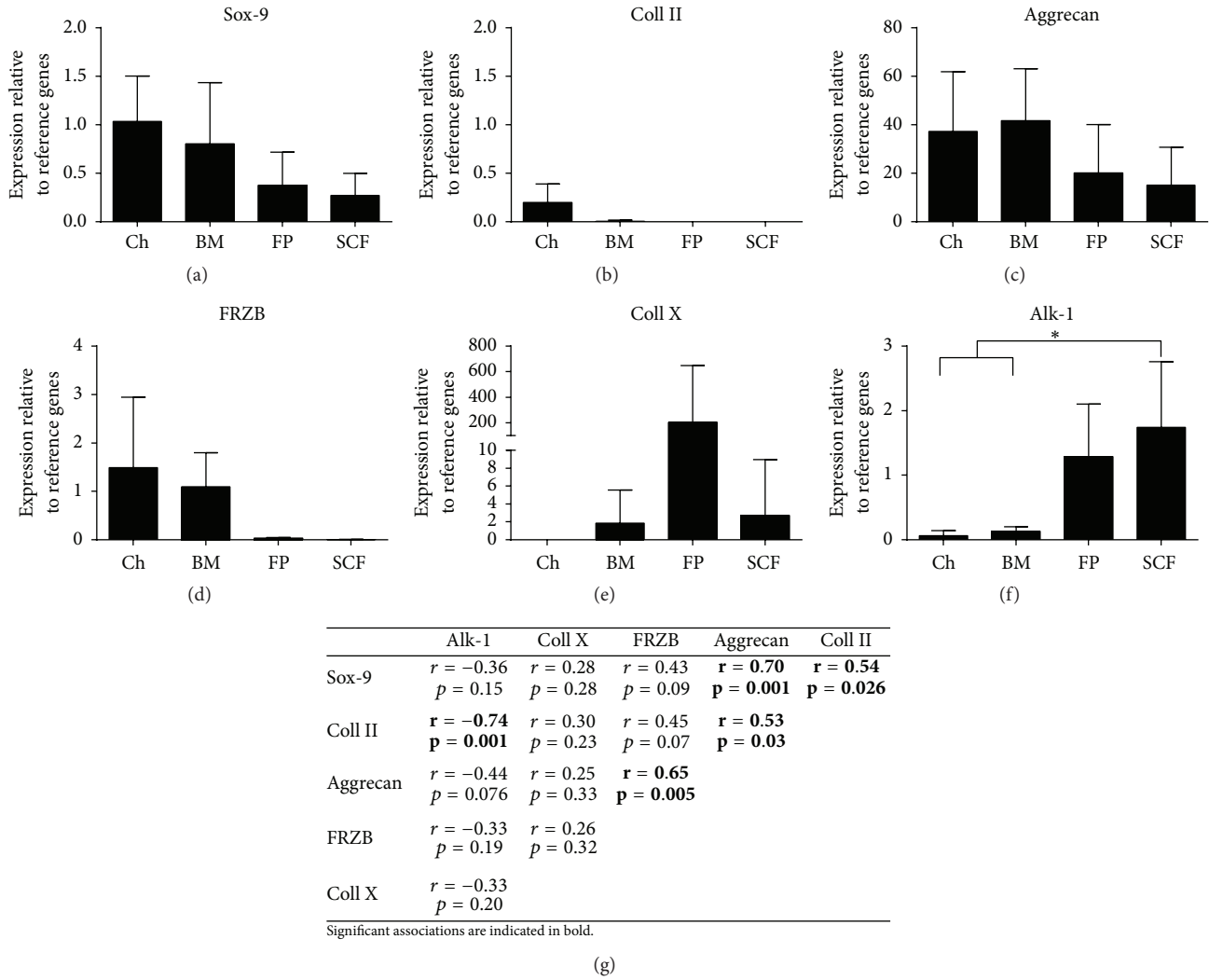


FIGURE 1: The expression of chondrogenic and hypertrophic genes in monolayer cell populations prior to chondrogenesis. ((a)–(f)) Chondrocytes (Ch), bone marrow MSC (BM), fat pad MSC (FP), and subcutaneous fat MSC (SCF). Data shown are the means \pm the standard deviation of triplicate runs and 5 donors for each cell population. One-way ANOVA and *post hoc* Bonferroni tests were used to test for significant differences in gene expression levels between cell types. (g) Pearson's correlation analysis matrix comparing genes which may be predictive of chondrogenic potential; significant correlations are in bold. Gene expression is expressed relative to the reference genes PPIA and TBP.

are shown as means \pm standard deviation, with statistical significance considered at $*p < 0.05$, $**p < 0.01$, and $***p < 0.001$. All statistical analyses were performed in GraphPad Prism version 6 (GraphPad Software, California, USA) and SPSS version 20 (IBM, New York, USA).

3. Results

3.1. Chondrogenic/Hypertrophic Gene Expression prior to Chondrogenic Differentiation. Perhaps not too surprisingly, of the cell types tested in this donor-matched study, the chondrogenic potency genes (Sox-9, Coll II, aggrecan, and FRZB) were consistently expressed at the highest levels in culture expanded chondrocytes. Further, chondrocytes demonstrated the lowest expression profiles for the hypertrophic

genes tested (Alk-1 and Coll X). Of the MSC populations that we have examined, BM-MSCs displayed chondrogenic and hypertrophic profiles that most closely resembled those of culture expanded chondrocytes. In contrast, the adipose sources of MSCs investigated (FP-MSCs and SCF-MSCs) were least like culture expanded chondrocytes and demonstrated the lowest chondrogenic potency and the highest hypertrophic gene expression profiles. SCF-MSCs expressed Alk-1 at significantly higher levels than chondrocytes and BM-MSCs ($p = 0.044$ and $p = 0.034$, resp.) (Figures 1(a)–1(f)).

Gene expression associations for all of the cell types examined in this study were tested using Pearson's correlation coefficient analyses and are presented in a correlation matrix (Figure 1(g)). Significant interactions noted between the chondrogenic potency genes were as follows: aggrecan

Markers	Percentage of positive cells (mean% \pm SD)			
	Chondrocytes	BM-MSCs	FP-MSCs	SCF-MSCs
CD73	91.2 (\pm 17.7)	87.1 (\pm 18.0)	99.9 (\pm 0.1)	99.9 (\pm 0.0)
CD90	98.0 (\pm 3.8)	96.4 (\pm 2.5)	99.9 (\pm 0.0)	99.9 (\pm 0.1)
CD105	99.4 (\pm 0.7)	96.7 (\pm 4.1)	98.1 (\pm 4.1)	99.9 (\pm 0.1)
CD34	9.5 (\pm 8.0)	5.1 (\pm 5.4)	74.5 (\pm 15.6)	62.2 (\pm 20.8)
CD45	1.5 (\pm 0.6)	1.3 (\pm 0.4)	2.4 (1.3)	1.6 (\pm 0.6)
CD14	20.4 (\pm 27.1)	14.8 (\pm 12.0)	17.9 (\pm 36.5)	21.4 (\pm 39.3)
CD19	1.3 (\pm 0.8)	2.0 (\pm 1.2)	1.4 (\pm 0.6)	1.6 (\pm 0.5)
HLA-DR	1.4 (\pm 0.6)	1.3 (\pm 0.8)	1.7 (\pm 0.7)	1.3 (\pm 0.6)

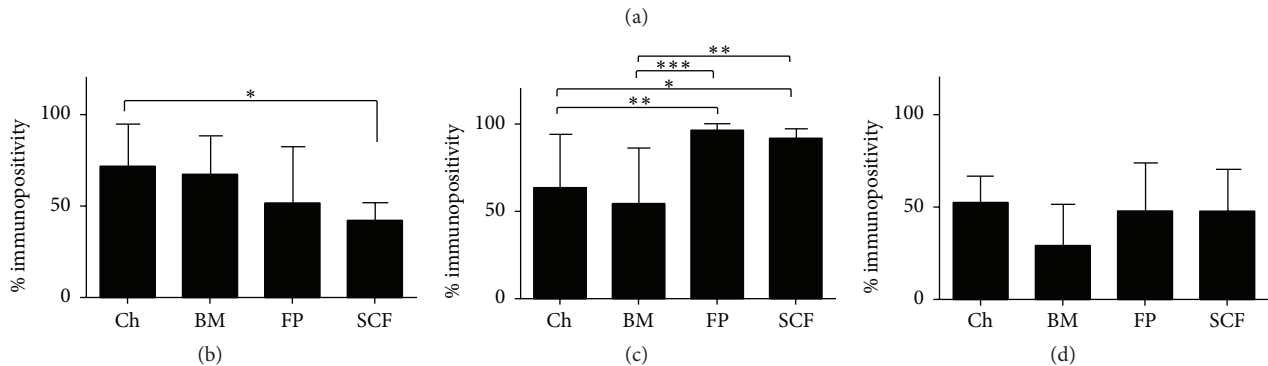


FIGURE 2: Immunoprofiles for MSC markers and putative chondrogenic potency markers of culture expanded cells prior to chondrogenesis. (a) ISCT MSC immunoprofiles. Immunoprofiles for the putative chondrogenic markers CD49c (b), CD166 (c), and CD39 (d). Flow cytometry was used to detect the percentage of positive cells for each marker on monolayer cell populations of chondrocytes (Ch), bone marrow MSC (BM), fat pad MSC (FP), and subcutaneous fat MSC (SCF) prior to chondrogenesis. Data shown are the means \pm the standard deviation of 5 donors for each cell population. One-way ANOVA and *post hoc* Bonferroni tests were used to test for significant differences in the positivity of cell surface markers between cell types.

was positively associated with Sox-9, Coll II, and FRZB; in addition, Sox-9 was positively associated with Coll II. There was also a significant negative association observed between Coll II and Alk-1 expression.

3.2. MSC/Chondrogenic Immunoprofiling. Flow cytometry analyses revealed immunopositivity for the MSC markers CD73, CD90, and CD105 for all of the populations of cells examined, but to varying levels. FP and SCF derived MSCs adhered to ISCT criteria (i.e., >95% positive); chondrocytes and BM-MSCs also adhered to ISCT criteria for CD90 and CD105 positivity but were <95% positive for CD73. All of the cell populations tested were <2% positive for CD19, CD45, and HLA-DR, in line with ISCT criteria. Some positivity was recorded in all of the cell populations tested for CD34 with high levels (62.2–74.4% positivity) seen in the adipose derived MSCs, which also adheres to ISCT [33]; in addition, >2% of BM-MSCs were also CD34 positive, which does not conform to recommendations by the ISCT [20]. CD14 was present on all cell populations, ranging on average between 14.8 and 21.4% positivity for each cell type (Figure 2(a)). Differences between cell types for putative chondrogenic potency marker positivity were noted for CD49c, CD166, and CD39 (Figures 2(b)–2(d)). Chondrocytes showed significantly greater positivity for CD49c compared to SCF-MSCs ($p = 0.014$), whereas the adipose derived MSCs

showed significantly higher positivity for CD166 compared to chondrocytes or BM-MSCs ($p = 0.0046$ and $p = 0.0002$, resp., for FP-MSCs and $p = 0.021$ and $p = 0.01$, resp., for SCF-MSCs). No differences were noted for CD44 or CD271, in that all cell types were >95% positive for CD44 and <5% positive for CD271 (data not shown).

3.3. Chondrogenic Differentiation. After 28 days of differentiation, donors demonstrated variability in chondrogenic capacity across the cell types tested. When results from individual donors were examined, chondrocytes consistently produced chondrogenic pellets in terms of GAG quantitation and histological analyses, but the propensity for MSCs to undergo chondrogenic differentiation was variable between individuals. GAG/DNA analyses appeared to match the histological findings noted for each patient: that is, larger pellets with prominent matrix metachromasia had the highest levels of GAGs measured (Figure 3). Pearson's correlation analyses across donors confirmed that there was a significant association between pellet GAG quantitation and histological score ($p = 0.01$). When donors were grouped and chondrogenic analyses were performed comparing differentiation between cell types, chondrocytes consistently demonstrated the most pronounced chondrogenic differentiation in terms of GAG/DNA analyses; they produced significantly more GAG than BM and SCF derived MSCs

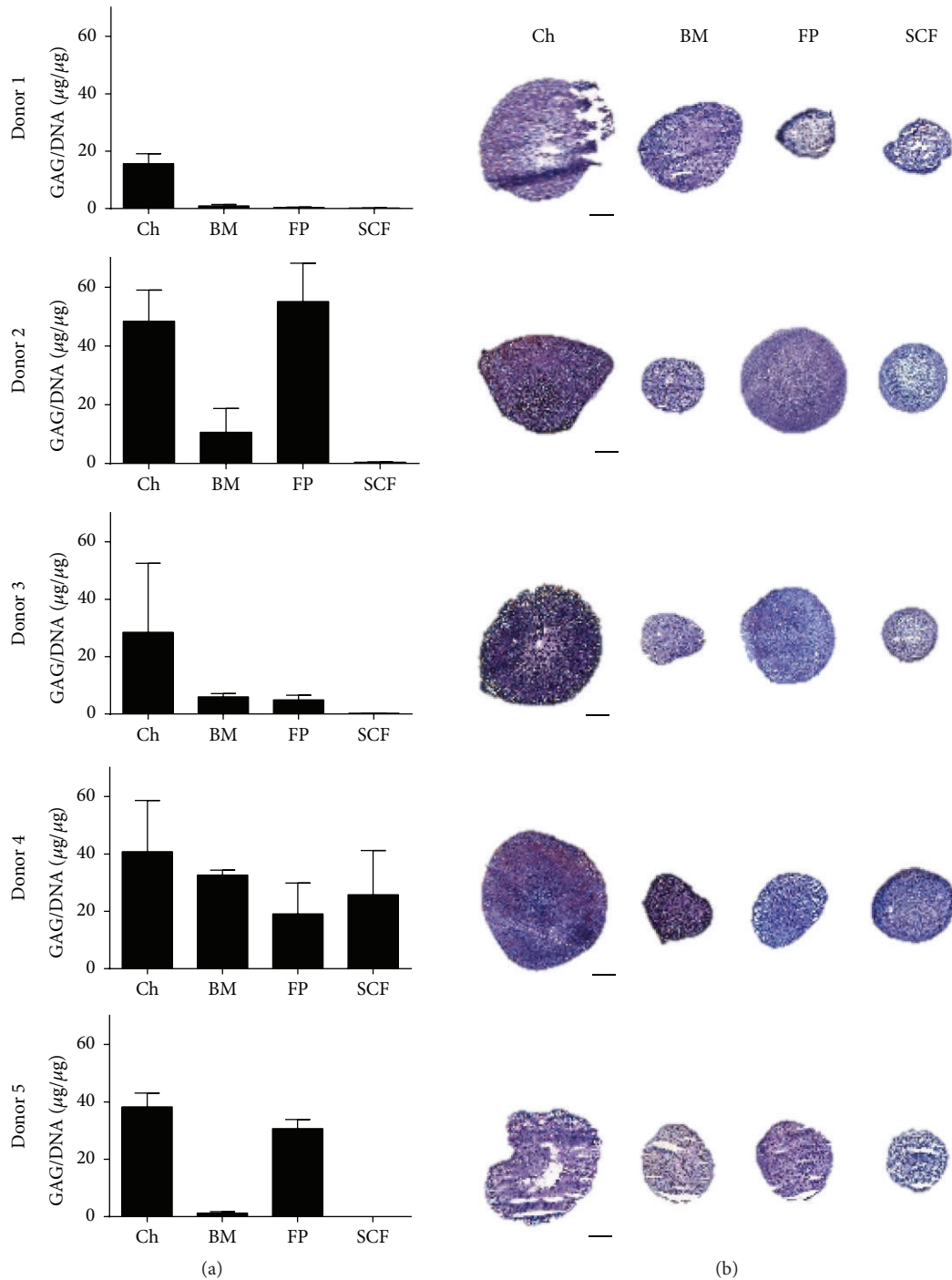


FIGURE 3: Chondrogenic assessments of pellet cultures between donors. (a) Production of GAG/DNA in pellet cultures from chondrocytes (Ch), bone marrow MSC (BM), fat pad MSC (FP), and subcutaneous fat MSC (SCF). GAGs were measured after chondrogenic differentiation using the DMMB assay and normalised to the DNA content of pellets; each donor is represented in individual graphs. Data shown are the means \pm the standard deviation of triplicate pellets. (b) Chondrogenic pellets from Ch, BM, FP, and SCF showing representative toluidine blue staining for each donor. Scale bars represent 200 μm .

($p = 0.032$ and $p = 0.030$, resp., Figure 4(a)). In terms of histological quantitation and chondrogenic score SCF-MSC scores were significantly lower than chondrocytes, BM, and FP derived MSCs ($p < 0.0001$, $p = 0.0195$, and $p = 0.0082$, resp.) and chondrocytes scored significantly higher

than BM-MSCs ($p = 0.013$, Figure 4(b)). Chondrocytes also produced the largest pellets (in terms of diameter) compared to any of the MSCs tested ($p < 0.0001$) and FP-MSC pellets were significantly larger than SCF-MSC pellets ($p = 0.008$, Figure 4(c)).

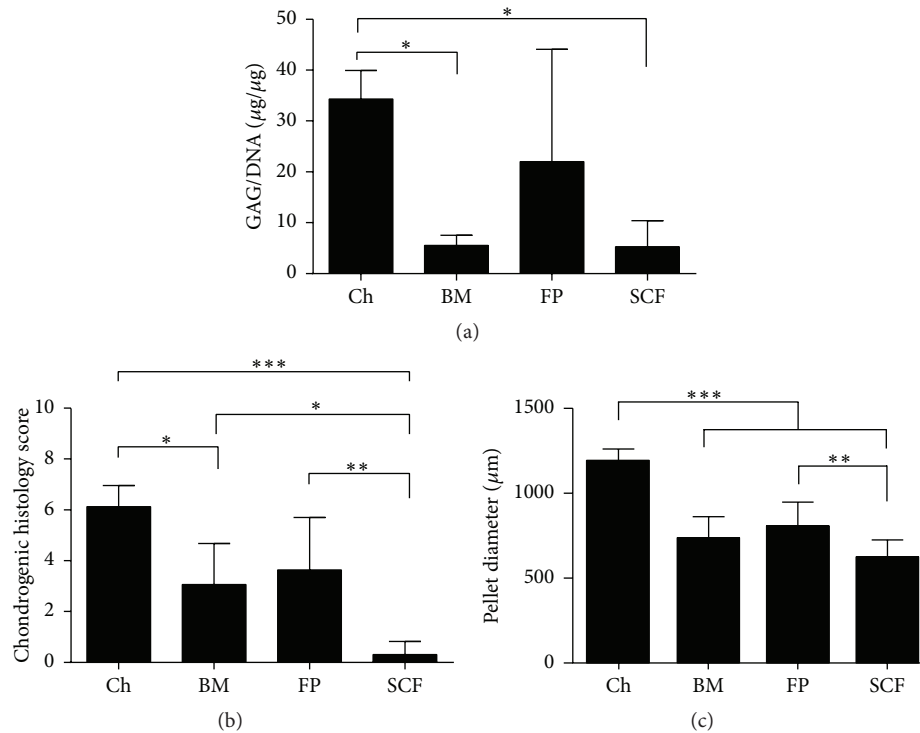


FIGURE 4: Chondrogenic assessments of pellet cultures across cell types. (a) Production of GAG/DNA in pellet cultures from chondrocytes (Ch), bone marrow MSC (BM), fat pad MSC (FP), and subcutaneous fat MSC (SCF) for all donors combined. (b) Chondrogenic histology scores for Ch, BM, FP, and SCF for all donors combined. (c) Mean chondrogenic pellet diameter (μm) for Ch, BM, FP, and SCF for all donors combined. Data shown are the means \pm the standard deviation of triplicate pellets and 5 donors for each cell population. One-way ANOVA and *post hoc* Bonferroni tests were used to test for significant differences between cell types.

3.4. Chondrogenic Potency Analyses. Multilevel modelling analysis was performed in an effort to identify chondrogenic potency predictors prior to chondrogenic differentiation. This analysis demonstrated that Alk-1 expression and CD166 immunopositivity both negatively associated with GAG quantitation in pellet cultures. However, CD49c and CD39 expression positively associated with GAG quantitation and histological score, respectively. Sox-9 expression positively associated with chondrogenic histological score, whereas expressions of the hypertrophic genes Coll X and Alk-1 were shown to negatively associate (Table 2).

Further multilevel model analysis showed that cell type (but not donor source) had a significant impact on the predictive aspect of gene expression for both of the chondrogenic assessments tested, that is, GAG quantitation ($p < 0.001$) and histological outcome ($p < 0.001$). Similarly, cell type (but not donor source) had a significant impact on the predictive aspect of cell surface marker positivity with regard to both GAG quantitation ($p < 0.001$) and histological outcome ($p < 0.001$). Using an interaction term in a multilevel model consisting only of the cell types and the variable in question, results showed that the relationship between Sox-9/Alk-1 expression and the histological outcome varied significantly across cell source ($p = 0.03$ and $p = 0.034$, resp.), which was not the case for Coll X ($p = 0.07$). The relationship between Alk-1 expression and GAG quantitation also did not vary across cell types ($p = 0.43$). In terms of immunopositivity,

the relationship between CD39 positive cells and histological outcome varied significantly between cell types ($p < 0.001$) as did the relationship between CD49c or CD166 positive cells and GAG quantitation ($p < 0.001$ for both markers).

4. Discussion

In recent years MSCs isolated from BM, FP, and SCF have been compared and contrasted extensively in *in vitro* studies [12, 13, 34–38] as alternative cell sources to the chondrocytes used in ACI. However, to our knowledge there are no studies to date that have compared the *in vitro* chondrogenic potency of these cell types together and from matched samples. In the present study, we have tested known gene profiles and immunoprofiles indicative of chondrogenic potential in a predictive model comparing chondrocytes, BM, FP, and SCF derived MSCs from 5 matched human donors. We have determined the expression of the chondrogenic genes, Sox-9, Coll II, ACAN, and FRZB, and the hypertrophy associated genes, Coll X and Alk-1, in these cell populations prior to chondrogenesis. In doing so, we have confirmed that across all of the cell populations tested, the master regulator of chondrogenesis, Sox-9, correlates with the expression of Coll II and ACAN and that the hypertrophy associated marker Alk-1 is negatively associated with Coll II expression. In addition, we have shown that there is a positive association between the expression of FRZB and ACAN, which has been

TABLE 2: Multilevel modelling.

	GAG/DNA			Chondrogenic histology score		
	Coefficient	95% CI	<i>p</i> values	Coefficient	SE (95% CI)	<i>p</i> values
Sox-9	-5.6	-11.7, 0.5	0.07	1.01	0.18, 1.84	0.02
Coll II	22.3	-7.8, 52.4	0.14	3.96	-0.16, 8.08	0.06
Aggrecan	-0.003	-0.2, 0.2	0.97	-0.019	-0.04, 0.004	0.10
FRZB	33.1	-27.4, 93.6	0.3	0.86	-7.46, 9.18	0.83
Coll X	-0.01	-0.02, 0.003	0.12	-0.002	-0.004, -0.0002	0.03
Alk-1	-9.5	-12.2, 6.7	<0.001	-0.61	-0.99, -0.23	0.003
CD49c	0.2	-0.1, 0.5	0.018	-0.04	-0.02, -0.01	0.63
CD166	-0.3	-0.5, -0.04	0.03	0.01	-0.04, 0.034	0.16
CD39	-0.02	0.01, 0.4	0.78	0.024	0.01, 0.04	0.002

Significant associations are indicated in bold.

previously reported in the chondrogenic ATDC5 cell line [39]. In terms of immunoprofile, the putative chondrogenic markers CD44, CD105, and CD271 were excluded from predictive analyses due to their uniform expression levels across cell types. CD49c, CD166, and CD39 were present on all of the cell populations examined to varying degrees and as such were taken forward into our multilevel chondrogenic potency analysis.

Following an established *in vitro* cell pellet chondrogenic differentiation procedure [12, 29] our quantitative assessment of GAG synthesis demonstrated that chondrocytes generate significantly more GAGs compared to BM-MSCs and SCF-MSCs but not FP-MSCs, with some notable variation between donors. Our findings are comparable to previous studies which have shown that chondrocytes and FP-MSCs display similar levels of GAG production and that FP-MSCs produce more GAGs than BM-MSCs [37] and donor-matched SCF-MSCs [38]. Further, our assessments for chondrogenic differentiation status in terms of GAG quantitation and histological score were significantly correlated. Chondrocyte-generated pellets consistently produced the highest scores, which were significantly greater than those formed by BM or SCF cell populations, whereas SCF pellets produced the lowest scores of all the cell populations examined. By simply measuring the diameter of pellets we have also shown that chondrocytes produced the largest pellets compared to BM and SCF derived pellets. Taken together, our chondrogenic assessments suggest that, not too surprisingly, culture expanded chondrocytes have the greatest propensity for chondrogenic differentiation *in vitro*, closely followed by FP-MSCs and then BM-MSCs, whereas SCF-MSCs consistently produced the worst chondrogenic outcome measures, regardless of the assessment used. These findings are corroborated by other studies that have reported paired comparisons between these cell types [12, 13, 34–38]. However, this is the first time, to our knowledge, that all four of these cell populations have been examined in the same study, allowing for a hierarchical chondrogenic potency comparison with the impact of donor taken into account by donor matching the samples tested.

The multilevel modelling analyses performed in this study have allowed us to explore the relationships between

putative chondrogenic potency markers (gene expression and surface marker profiles) and chondrogenic outcome based on combined data from each cell source tested, while simultaneously examining the potential influence of donor and cell type. However, we have not yet verified whether the predictive factors for chondrogenesis that we have identified for combined data are present if only individual cell types are analysed as we believe that the small donor size precludes this type of analysis in the present study. We should of course be cautious when interpreting any analyses derived from a small donor sample size and we acknowledge this as a limitation of the study. Nonetheless, our multilevel modelling has revealed that the expressions of Alk-1 and Coll X are negatively associated with chondrogenic potential in terms of histology scores and for Alk-1 expression, as well as the GAG content of chondrogenically induced pellet cultures. In contrast, Sox-9 expression prior to chondrogenesis positively correlated with histological pellet scores. Some of these gene associations match a previous report comparing FP-MSCs and SCF-MSCs [38]. The novelty of our study is that some of these chondrogenic potency gene associations hold true across all of the cell types examined in the present study. The poor correlation between the baseline (predifferentiation) expressions of the chondrogenic genes Coll II and ACAN is noteworthy and comparable to findings in other studies [40, 41]. For example, Stenberg et al. (2014) have confirmed that the transplanted chondrocyte expression levels of ACAN and Coll II in ACI had no bearing on clinical outcome [40]. Further, Cote et al. (2016) demonstrated that the genome-wide transcription profile of Coll II and ACAN (amongst other genes) did not correlate with the production of GAGs in a single cell analysis of bovine MSCs and chondrocytes. The authors attribute this finding to the heterogeneity in single cell transcriptional profiles. It is extremely likely that the gene analysis in the present study derived from heterogeneous cell populations and four very different tissue sources will vary to an even greater extent.

In addition, our multilevel analysis indicates that CD49c and CD39 immunopositivity positively predicts GAG production and histological score, respectively, in cell pellets, with no significant difference observed between donors.

Other studies have shown that CD49c positivity on chondrocytes and CD39 positivity on synovium derived MSCs are associated with increased *in vitro* chondrogenic potential [21, 27]; however, our results are the first to demonstrate these relationships across matched chondrocytes, BM-MSCs, and adipose derived MSCs. Perhaps surprisingly CD166 positivity did not indicate chondrogenic potential, as has been previously shown [24, 26]; in fact immunopositivity for this marker was negatively associated with chondrogenic assessments. One potential explanation for this finding might be that CD166 was expressed at significantly greater levels on SCF-MSCs compared to chondrocytes and BM-MSCs and that in our hands SCF-MSCs have been shown to consistently demonstrate a poor propensity for chondrogenic differentiation. Interestingly, we have demonstrated through this multicell type, donor-matched study that the source of cells significantly influences both GAG production in pellet culture and also the histological score of the pellet. In contrast, the donor had no demonstrable impact on either of the chondrogenic assessments tested, although as stated previously we must be cautious with this finding as our results are based on a small cohort of donors. Follow-up studies should be geared towards understanding the molecular mechanisms that account for the differences observed between cell populations and in the development of methods to select cells with enhanced chondrogenic potential.

5. Conclusions

We have demonstrated the chondrogenic predictive value of high levels of Sox-9 and low levels of collagen type X or Alk-1 expression as well as immunopositivity for CD49c and CD39 in a combined data analysis of chondrocytes, BM-MSCs, FP-MSCs, and SCF-MSCs. Further individual analyses on larger donor cohorts will be required to validate these findings for individual cell types before these predictive factors could be used as selection criteria prior to the transplantation or banking of each cell type in the treatment of cartilage injuries. We have also shown, using donor-matched samples, that cell type significantly influences the chondrogenic potency of the MSC sources examined in this study; we have demonstrated that MSCs sourced from the infrapatellar fat pad of the knee or bone marrow provide the “next best” alternative to chondrocytes, in terms of *in vitro* chondrogenic differentiation capacity. Further, our results have consistently shown that SCF derived MSCs have the poorest propensity for chondrogenic differentiation. These findings have important clinical implications, not only for the understanding of MSC chondrogenic differentiation capacity, but also for the development of cell therapy strategies to screen for and select potent cell types prior to application in the treatment of cartilage injuries.

Competing Interests

The authors declare that there is no conflict of interests regarding the publication of this paper.

Acknowledgments

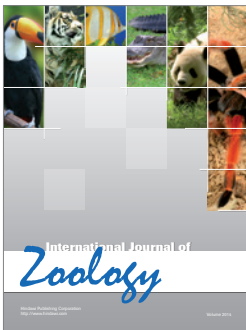
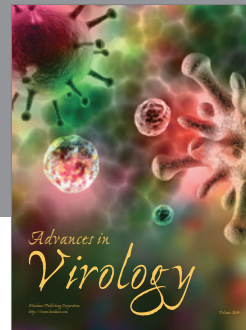
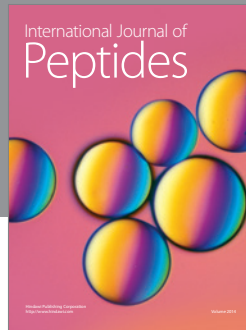
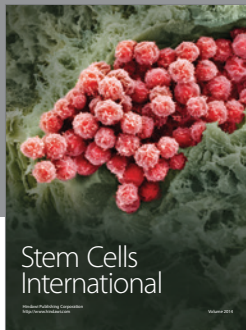
The authors are grateful to the Engineering and Physical Sciences Research Council Centre for Doctoral Training and Arthritis Research UK (Grants 20253, 19429, and 18480) for supporting this work and to Miss Jade Perry for contributing to some of the chondrogenic data analysis described.

References

- [1] M. Brittberg, A. Lindahl, A. Nilsson, C. Ohlsson, O. Isaksson, and L. Peterson, “Treatment of deep cartilage defects in the knee with autologous chondrocyte transplantation,” *The New England Journal of Medicine*, vol. 331, no. 14, pp. 889–895, 1994.
- [2] A. M. Bhoale, J. H. Kuiper, W. E. B. Johnson, P. E. Harrison, and J. B. Richardson, “Midterm to long-term longitudinal outcome of autologous chondrocyte implantation in the knee joint: a multilevel analysis,” *The American Journal of Sports Medicine*, vol. 37, supplement 1, pp. 131S–138S, 2009.
- [3] J. B. Richardson, B. Caterson, E. H. Evans, B. A. Ashton, and S. Roberts, “Repair of human articular cartilage after implantation of autologous chondrocytes,” *Journal of Bone and Joint Surgery—Series B*, vol. 81, no. 6, pp. 1064–1068, 1999.
- [4] D. B. F. Saris, J. Vanlauwe, J. Victor et al., “Treatment of symptomatic cartilage defects of the knee: characterized chondrocyte implantation results in better clinical outcome at 36 months in a randomized trial compared to microfracture,” *The American Journal of Sports Medicine*, vol. 37, supplement 1, pp. 10S–19S, 2009.
- [5] H. S. McCarthy, J. B. Richardson, J. C. Parker, and S. Roberts, “Evaluating joint morbidity after chondral harvest for autologous chondrocyte implantation (ACI): a study of ACI-treated ankles and hips with a knee chondral harvest,” *Cartilage*, vol. 7, no. 1, pp. 7–15, 2016.
- [6] H. Holtzer, J. Abbott, J. Lash, and S. Holtzer, “The loss of phenotypic traits by differentiated cells in vitro. I. dedifferentiation of cartilage cells,” *Proceedings of the National Academy of Sciences*, vol. 46, no. 12, pp. 1533–1542, 1960.
- [7] M. Schnabel, S. Marlovits, G. Eckhoff et al., “Dedifferentiation-associated changes in morphology and gene expression in primary human articular chondrocytes in cell culture,” *Osteoarthritis and Cartilage*, vol. 10, no. 1, pp. 62–70, 2002.
- [8] S. Wakitani, T. Okabe, S. Horibe et al., “Safety of autologous bone marrow-derived mesenchymal stem cell transplantation for cartilage repair in 41 patients with 45 joints followed for up to 11 years and 5 months,” *Journal of Tissue Engineering and Regenerative Medicine*, vol. 5, no. 2, pp. 146–150, 2011.
- [9] I. Akgun, M. C. Unlu, O. A. Erdal et al., “Matrix-induced autologous mesenchymal stem cell implantation versus matrix-induced autologous chondrocyte implantation in the treatment of chondral defects of the knee: a 2-year randomized study,” *Archives of Orthopaedic and Trauma Surgery*, vol. 135, no. 2, pp. 251–263, 2015.
- [10] A. Vega, M. A. Martín-Ferrero, F. D. Canto et al., “Treatment of knee osteoarthritis with allogeneic bone marrow mesenchymal stem cells: a randomized controlled trial,” *Transplantation*, vol. 99, no. 8, pp. 1681–1690, 2015.
- [11] J. L. Drago, B. Samimi, M. Zhu et al., “Tissue-engineered cartilage and bone using stem cells from human infrapatellar fat pads,” *The Journal of Bone & Joint Surgery—British Volume*, vol. 85, no. 5, pp. 740–747, 2003.

- [12] J. Garcia, K. Wright, S. Roberts et al., "Characterisation of synovial fluid and infrapatellar fat pad derived mesenchymal stromal cells: the influence of tissue source and inflammatory stimulus," *Scientific Reports*, vol. 6, Article ID 24295, 2016.
- [13] H. Busser, M. Najar, G. Raicevic et al., "Isolation and characterization of human mesenchymal stromal cell subpopulations: comparison of bone marrow and adipose tissue," *Stem Cells and Development*, vol. 24, no. 18, pp. 2142–2157, 2015.
- [14] J. Freitag, J. Ford, D. Bates et al., "Adipose derived mesenchymal stem cell therapy in the treatment of isolated knee chondral lesions: design of a randomised controlled pilot study comparing arthroscopic microfracture versus arthroscopic microfracture combined with postoperative mesenchymal stem cell injections," *BMJ Open*, vol. 5, no. 12, Article ID e009332, 2015.
- [15] A. E. Aksu, J. P. Rubin, J. R. Dudas, and K. G. Marra, "Role of gender and anatomical region on induction of osteogenic differentiation of human adipose-derived stem cells," *Annals of Plastic Surgery*, vol. 60, no. 3, pp. 306–322, 2008.
- [16] K. A. Payne, D. M. Didiano, and C. R. Chu, "Donor sex and age influence the chondrogenic potential of human femoral bone marrow stem cells," *Osteoarthritis and Cartilage*, vol. 18, no. 5, pp. 705–713, 2010.
- [17] M. S. Choudhery, M. Badowski, A. Muise, J. Pierce, and D. T. Harris, "Donor age negatively impacts adipose tissue-derived mesenchymal stem cell expansion and differentiation," *Journal of Translational Medicine*, vol. 12, no. 1, article 8, 2014.
- [18] F. Dell'Accio, C. De Bari, and F. P. Luyten, "Molecular markers predictive of the capacity of expanded human articular chondrocytes to form stable cartilage in vivo," *Arthritis and Rheumatism*, vol. 44, no. 7, pp. 1608–1619, 2001.
- [19] T. D. Schmittgen and K. J. Livak, "Analyzing real-time PCR data by the comparative CT method," *Nature Protocols*, vol. 3, no. 6, pp. 1101–1108, 2008.
- [20] M. Dominici, K. Le Blanc, I. Mueller et al., "Minimal criteria for defining multipotent mesenchymal stromal cells. The International Society for Cellular Therapy position statement," *Cytotherapy*, vol. 8, no. 4, pp. 315–317, 2006.
- [21] S. P. Grogan, A. Barbero, J. Diaz-Romero et al., "Identification of markers to characterize and sort human articular chondrocytes with enhanced in vitro chondrogenic capacity," *Arthritis and Rheumatism*, vol. 56, no. 2, pp. 586–595, 2007.
- [22] M. C. Arufe, A. De la Fuente, I. Fuentes, F. J. de Toro, and F. J. Blanco, "Chondrogenic potential of subpopulations of cells expressing mesenchymal stem cell markers derived from human synovial membranes," *Journal of Cellular Biochemistry*, vol. 111, no. 4, pp. 834–845, 2010.
- [23] T. Jiang, W. Liu, X. Lv et al., "Potent in vitro chondrogenesis of CD105 enriched human adipose-derived stem cells," *Biomaterials*, vol. 31, no. 13, pp. 3564–3571, 2010.
- [24] D. Pretzel, S. Linss, S. Rochler et al., "Relative percentage and zonal distribution of mesenchymal progenitor cells in human osteoarthritic and normal cartilage," *Arthritis Research & Therapy*, vol. 13, no. 2, article R64, 2011.
- [25] P. Niemeyer, J. M. Pestka, G. M. Salzmann, N. P. Südkamp, and H. Schmal, "Influence of cell quality on clinical outcome after autologous chondrocyte implantation," *American Journal of Sports Medicine*, vol. 40, no. 3, pp. 556–561, 2012.
- [26] C. B. Chang, S. A. Han, E. M. Kim, S. Lee, S. C. Seong, and M. C. Lee, "Chondrogenic potentials of human synovium-derived cells sorted by specific surface markers," *Osteoarthritis and Cartilage*, vol. 21, no. 1, pp. 190–199, 2013.
- [27] F. Gullo and C. De Bari, "Prospective purification of a subpopulation of human synovial mesenchymal stem cells with enhanced chondro-osteogenic potency," *Rheumatology*, vol. 52, no. 10, pp. 1758–1768, 2013.
- [28] Y. Mifune, T. Matsumoto, S. Murasawa et al., "Therapeutic superiority for cartilage repair by CD271-positive marrow stromal cell transplantation," *Cell Transplantation*, vol. 22, no. 7, pp. 1201–1211, 2013.
- [29] B. Johnstone, T. M. Hering, A. I. Caplan, V. M. Goldberg, and J. U. Yoo, "In vitro chondrogenesis of bone marrow-derived mesenchymal progenitor cells," *Experimental Cell Research*, vol. 238, no. 1, pp. 265–272, 1998.
- [30] R. W. Farndale, C. A. Sayers, and A. J. Barrett, "A direct spectrophotometric microassay for sulfated glycosaminoglycans in cartilage cultures," *Connective Tissue Research*, vol. 9, no. 4, pp. 247–248, 1982.
- [31] R. W. Farndale, D. J. Buttle, and A. J. Barrett, "Improved quantitation and discrimination of sulphated glycosaminoglycans by use of dimethylmethylene blue," *Biochim Biophys Acta*, vol. 883, no. 2, pp. 173–177, 1986.
- [32] S. P. Grogan, A. Barbero, V. Winkelmann et al., "Visual histological grading system for the evaluation of in vitro-generated neocartilage," *Tissue Engineering*, vol. 12, no. 8, pp. 2141–2149, 2006.
- [33] P. Bourin, B. A. Bunnell, L. Casteilla et al., "Stromal cells from the adipose tissue-derived stromal vascular fraction and culture expanded adipose tissue-derived stromal/stem cells: a joint statement of the International Federation for Adipose Therapeutics and Science (IFATS) and the International Society for Cellular Therapy (ISCT)," *Cytotherapy*, vol. 15, no. 6, pp. 641–648, 2013.
- [34] C. Karlsson, C. Brantsing, T. Svensson et al., "Differentiation of human mesenchymal stem cells and articular chondrocytes: analysis of chondrogenic potential and expression pattern of differentiation-related transcription factors," *Journal of Orthopaedic Research*, vol. 25, no. 2, pp. 152–163, 2007.
- [35] A. English, E. A. Jones, D. Corscadden et al., "A comparative assessment of cartilage and joint fat pad as a potential source of cells for autologous therapy development in knee osteoarthritis," *Rheumatology*, vol. 46, no. 11, pp. 1676–1683, 2007.
- [36] Y. Liu, C. T. Buckley, R. Downey, K. J. Mulhall, and D. J. Kelly, "The role of environmental factors in regulating the development of cartilaginous grafts engineered using osteoarthritic human infrapatellar fat pad-derived stem cells," *Tissue Engineering Part A*, vol. 18, no. 15–16, pp. 1531–1541, 2012.
- [37] T. Vinardell, E. J. Sheehy, C. T. Buckley, and D. J. Kelly, "A comparison of the functionality and in vivo phenotypic stability of cartilaginous tissues engineered from different stem cell sources," *Tissue Engineering—Part A*, vol. 18, no. 11–12, pp. 1161–1170, 2012.
- [38] S. Lopa, A. Colombini, D. Stanco, L. de Girolamo, V. Sansone, and M. Moretti, "Donor-matched mesenchymal stem cells from knee infrapatellar and subcutaneous adipose tissue of osteoarthritic donors display differential chondrogenic and osteogenic commitment," *European Cells and Materials*, vol. 27, pp. 298–311, 2014.
- [39] L. Lodewyckx, F. Cailotto, S. Thysen, F. P. Luyten, and R. J. Lories, "Tight regulation of wntless-type signaling in the articular cartilage—subchondral bone biomechanical unit: transcriptomics in Frzb-knockout mice," *Arthritis Research and Therapy*, vol. 14, article R16, 2012.

- [40] J. Stenberg, T. S. de Windt, J. Synnergren et al., “Clinical outcome 3 years after autologous chondrocyte implantation does not correlate with the expression of a predefined gene marker set in chondrocytes prior to implantation but is associated with critical signaling pathways,” *Orthopaedic Journal of Sports Medicine*, vol. 2, no. 9, 2014.
- [41] A. J. Cote, C. M. McLeod, M. J. Farrell et al., “Single-cell differences in matrix gene expression do not predict matrix deposition,” *Nature Communications*, vol. 7, p. 10865, 2016.



Hindawi

Submit your manuscripts at
<http://www.hindawi.com>

